Università di Modena e Reggio Emilia

Dipartimento di Ingegneria Enzo Ferrari
PhD Course "Enzo Ferrari" in Industrial and Environmental Engineering

A novel method to accelerate biodeterioration process on cool building surfaces:

experimental setup development, environmental related-aspects analysis and predictive model validation

Relatore
Prof. Ing. Alberto Muscio

Candidata
Dott. ssa Giulia Santunione

Correlatore
Prof. Elisabetta Sgarbi

XXXIV Ciclo
Anno Accademico 2020-2021

"Si può dire che l'uomo abbia condotto un esperimento di dimensioni gigantesche ed è lo stesso esperimento che la natura ha, da sempre, incessantemente condotto."

Charles Darwin

Introduzione

Il cambiamento climatico è una delle sfide più complesse a cui il mondo scientifico, e non solo, si sta dedicando data l'urgenza e la severità del fenomeno. Numerosi sono i nuovi modelli, le applicazioni e le tecnologie sviluppate e/o in corso di sviluppo per contrastare o mitigare le conseguenze del riscaldamento del Pianeta. Il sesto Report dell'*Intergovernmental Panel of Climate Change* (IPCC) del 2021 è molto chiaro nell'affermare che tale fenomeno è da attribuire alle attività antropiche. È l'uomo stesso quindi ad avere la responsabilità di agire per affrontare e contenere le conseguenze che derivano da un fenomeno di tale portata. Affinchè le azioni di contrasto alla crisi climatica possano risultare funzionali all'obiettivo, è necessario intervenire allo stesso tempo sui molteplici fattori causali. Tra questi, vi sono sicuramente gli ambienti fortemente antropizzati, ovvero le città; esse rappresentano la sorgente della maggior parte delle emissioni di gas climalteranti. Negli ultimi decenni, gli ingenti flussi migratori verso le città hanno contribuito fortemente al fenomeno dell'urbanizzazione: si prevede che circa il 70% degli esseri umani abiterà in città entro il 2050. Le alte densità abitative e produttive delle città rappresentano anche la causa dell'Isola di Calore Urbano, un fenomeno strettamente legato al cambiamento climatico. Si tratta del consistente aumento delle temperature all'interno dell'area urbana rispetto allle zone circostanti. L'isola di Calore Urbano, è causata *in primis* dalle proprietà termofisiche delle superfici urbane (coperture degli edifici e strade) che assorbono la maggior parte della radiazione solare incidente. Ciò, assieme ad altre fonti di calore antropogenico e alla mancanza di verde urbano, conduce inevitabilmente alla necessità di aumentare i consumi energetici di raffrescamento degli edifici in regime estivo. La comunità scientifica da oltre dieci anni sta investendo tante risorse nel trovare tecnologie e applicazioni che possano *ridurre* i consumi energetici e creare tecnologie quanto più *efficienti* possibile al fine del contenimento di emissioni di gas climalteranti. L'isola di Calore può essere contrastata da varie applicazioni, tra cui i *cool materials*, ovvero materiali ad alta efficienza energetica. Essi sono caratterizzati da un'elevata riflettanza solare e da un'alta emissività termica e vengono utilizzati principalmente per le coperture degli edifici contribuendo al risparmio energetico degli stessi, al miglioramento del microclima urbano e della qualità dell'aria. Tuttavia, le superfici degli edifici sono soggette a invecchiamento, dovuto al degrado chimico-fisico e allo sporcamento. Ciò altera le proprietà termofische, riducendo i risparmi per la climatizzazione estiva e la mitigazione del microclima ottenibili con i *cool materials*. Tra le cause dell'invecchiamento dei materiali vi è anche la deposizione e la crescita di biofilm, formato da colonie di batteri, cianobatteri alghe e funghi; la crescita biologica, soprattutto in climi caldi e umidi, rappresenta la problamatica maggiore del deterioramento che avviene sui materiali edili (*bioageing*).

La ricerca scientifica è da tempo fortemente impegnata nella comprensione del fenomeno di deterioramento delle superifici urbane, al fine della messa a punto

di soluzioni innovative atte a ritardare sempre di più la perdita delle performance energetiche e vincere così la sfida della durabilità dei *cool materials*. Lo stesso obiettivo è condiviso dai produttori di materiali applicati all'edilizia, che quotidianamente si trovano a dover affrontare e gestire le problematiche dovute ai processi di invecchiamento dei loro prodotti. Ad oggi la durabilità dei materiali ad alta efficienza energetica può essere verificata sottoponendo gli stessi a procedure standard di invecchiamento, le quali permettono di ottenere dati confrontabili anche se provenienti da diversi laboratori e/o siti sperimentali.

I due protocolli standard che mirano rispettivamente a riprodurre o a simulare l'insieme dei fenomeni che determinano il deterioramento dei *cool materials*, sono (*I*) l'ASTM G7, che definisce le modalità per l'invecchiamento naturale, procedura però troppo lenta per essere compatibile con le esigenze industriali; e (*II*) l'ASTM D7897, ovvero una procedura di invecchiamento accelerato in laboratorio. Purtroppo però, quest'ultimo è focalizzato sullo studio del deterioramento chimico-fisico dei materiali, senza tenere in considerazione gli aspetti legati alla colonizzazione biologica, che sono al contempo non trascurabili per definire la durabilità dei materiali stessi.

Questo lavoro di ricerca si è prefissato quindi come scopo quello di sviluppare un protocollo di prova ripetibile per accelerare la crescita di organismi su materiali *cool*, e determinarne il relativo calo in termini di riflettanza solare. La procedura sperimentale si prefigge di comprimere drasticamente i tempi di *bioageing* delle superfici, fenomeno che normalmente richiede alcuni anni per verificarsi in condizioni naturali. Il metodo è stato costruito studiando separatamente l'influenza dei parametri ambientali sulla ripetibilità del test. Sono state confrontate numerose condizioni sperimentali che sono poi state valutate per il livello di ripetibilità raggiunto. Lo strumento usato come camera di crescita è un bioreattore di tipo TIS (Temporary Immersion System). Tre tipologie di materiali *cool* sono state coinvolte: *cool asphalt shingle* (AS), *single ply white membrane* (WM) e *white paint* (WP). La procedura sperimentale di *bioaging* elaborata in questo lavoro di tesi è stata inoltre integrata con il protocollo di invecchiamento chimico-fisico già disponibile (ASTM D7897), in un'ottica di implementazione e otttimizzazzione delle procedure esistenti.

In definitiva, il lavoro svolto e i risultati ottenuti rappresentano una proposta sperimentale per completare lo studio del complesso fenomeno del deterioramento dei materiali ad alta efficicenza energetica. Tale proposta è stata formulata nell'*ANNEX*, riportato al termine della validazione interna del protocollo elaborato. Questo strumento può fornire un primo passo verso la standardizzazione di un metodo per il deterioramento accelerato delle superfici urbane *cool*; l'obiettivo finale della disponibilità di tale metodo è la possibilità di migliorare le prestazioni dei materiali *cool*, aumentandone la durabilità e quindi l'efficacia della loro applicazione come strategia di contrasto all'Isola di Calore Urbano.

Table of Contents

Abstract

Biological growth on building surfaces can be responsible of degradation of their aesthetical and functional properties. Phototrophic organisms as algae and cyanobacteria have been identified as the first ones to colonize surfaces and allow the formation of following biocenosis, where also heterotrophic bacteria and fungi are involved. Biological colonization depends mainly on climate and microclimate conditions over and all around surfaces, mainly moisture and light availability. This phenomenon is particularly damaging for solar reflective materials (cool building materials), which are characterized by the ability to reflect solar radiation in the whole wavelength spectrum and remain cooler under the sun. Cool materials represent one of the most efficient countermeasures to the Urban Heat Island effect, which causes temperatures in urban areas to be significantly higher than in the surrounding rural areas. Several standards are nowadays available to investigate natural ageing of cool materials (ASTM G7) and accelerated ageing (ASTM D7897). Unfortunately, these standards are mostly focused onto surface soiling and they do not take into proper account the presence and growth of microorganisms.

This research work was firstly aimed to develop a laboratory procedure able to reproduce biological colonization on new materials in a repeatable way, in order to quantify the loss of energy performance due to the biological growth. Another goal was to reduce the bioageing test duration, which normally requires many years through natural exposition. The novel method was build step by step studying separately the influence of different experimental parameters on biological growth then on repeatability of the test. Several setups and environmental conditions have been tested, compared and finally evaluated according to repeatability of results. The experimental device used to expose material samples to bioageing was a bioreactor - the Temporary Immersion System (TIS); three different types of commonly used roofing materials samples are considered, precisely white asphalt shingle (AS), single ply white membrane (WM) and white paint (WP). Materials samples have been characterized in terms of physical and chemical properties, before and after bioageing exposure. Furthermore, biological growth has been monitored, measured, and finally correlated to the colonization level on surfaces. Algae and cyanobacteria growth as well as bio-colonization dynamics, describe a curve which follow Avrami's law, a model previously used to simulate algal colonization process as a temporal evolution. Ancillary aspects to the bioageing phenomenon were investigated in this research: the scientific literature reports that the deposition of soiling on surfaces seems to provide a nutrient layer for phototrophic organisms, encouraging their growth; however, it has been also observed that the presence of atmospheric pollutants could inhibit both the size and

diversity of the microbial community. Hence, algal and cyanobacteria growth on soiled surfaces was here studied and compared to growth on new ones. Moreover, metabolites profile production of some algal species after their exposure to soiling mixture was described in order to outline the influence and effects of soiling solution as abiotic stress to algal cells metabolism.

This research is concluded by the proposal of an experimental protocol to induce accelerate bioageing processes on cool building materials, providing data about repeatability and strength of the method; the modularity and the application of the protocol to define bio-resistance of a surface type was finally described by Avrami's model. The application of the protocol to other cool surface types and reproducibility analysis are expected as future perspectives.

Nomenclature and Abbreviations

Nomenclature

$X_{(t)}$	Colonized Area	[%]
ρ_{sol}	Solar Reflectance	[%]
ΔE	CIE/ L*a*b* Color difference	/
Abs	Absorbance value	/
μ	Growth rate	n° cells division /day
CV	Coefficient of Variation	[%]
SD	Standard Deviation	/
U	Uncertainty	[%]
R	Repeatability	[%]
P.A.R.	Photosynthetically Active Radiation	µmol/m^2/s photons

Abbreviations

C	Carbon
Na	Sodium
Al	Aluminum
Si	Silicon
Ca	Calcium
Ti	Titanium
S	Sulfur
NaCl	Sodium Chloride
H_2O	Water molecule
FA	Fatty Acids
FAME	Fatty Acid Methyl-Ester
PUFAs	Ply-Unsaturated Fatty Acids
MDA	Malondialdehyde
BBM	Bold's Basal Medium
BG-11	Blue-Green-11 Medium
GC-MS	Gas Chromatography–Mass Spectrometry
HPLC	High Pressure Liquid Chromatography
FW	Fresh Weight
WP	Field-applied white paint
AS	White asphalt shigle
WM	Single ply white membrane
K	Surface Resistance parameter
R^2	Coefficient of determination

1. Biodeterioration of surfaces

Biodeterioration consists in the natural degradation of materials by (micro)organisms which grow and form multispecies biofilms on all types of surfaces [1], [2]. Such biofilms are complex biological systems, usually composed of multiple interacting organisms (bacteria, fungi, algae). Both outdoor and indoor surfaces are affected by this phenomenon, which constantly represents a problem to manage at different levels. It is an aesthetical and durability issue when biodeterioration occurs on historical and building surfaces [3], [4]; while it constitutes also a human health risk when a mould biofilm grows along inner walls thanks to favorable humidity and temperature conditions [5], [6]. Phenomenon of the biodeterioration of building and cultural heritage materials represents hence a high cost which includes the economic costs of cleaning, repainting and repair, as well as cultural costs because of disfigurement of historic property [7]. For its large impact on structures, biodeterioration of surfaces have gained more and more attention by the scientific community in the last decades. The word "biodeterioration" is usually applied by the Authors mainly in connection with material degradation caused by biological interactions. However, bio-colonization does not necessarily lead to physical and chemical degradation, but it could consist in a reversible color change, depending on many factors, as type of construction, location and time of exposition. Therefore, Guillitte (1995), [4] introduced the term "*bioreceptivity*" to describe the whole phenomenon of surface colonization by living organisms, considering both those characteristics affected by the colonization and those that allow colonization to take place [4].

1.1. The concept of bioreceptivity

The concept of "bioreceptivity" is referred to the "aptitude of a material (or any other inanimate object) to be colonized by one or several groups of living organisms without necessarily undergoing to any biodeterioration" [4], [8]. However, biodeterioration strongly depends on the bioreceptivity of the interested surface. Furthermore, it is important to underline that "colonization" means the harbouring, development and multiplication of living organisms on surfaces and the term excludes the simple temporary transit of animals over them. In these terms, colonization becomes a key phenomenon to know and study, in order to comprehend biodeterioration process. Indeed, "bioreceptivity can also be defined as the totality of material properties that contribute to the establishment, anchorage and development of fauna and/or flora" [4]. These properties are the intrinsic characteristic of the substrate and define the "primary bioreceptivity", which is referred to a material that has not yet been exposed to colonization and as long as its properties remain very similar or identical to those of its initial state [8], [9]. Bioreceptivity of a particular substrate is due to both its physical (porosity, roughness) and chemical (chemical

composition, alkalinity) characteristics [7]–[9]. High values of porosity and roughness have been identified as favorable features to establishment and growth on surfaces by living organisms. Porosity endures the wetness of the surface also during dry periods, helping survival of algae, cyanobacteria and others. Moreover, according with several studies [8], [10]–[12] the roughness of materials seems to be one of the most important parameters to induce colonization by organisms. Indeed, it provides many asperities increasing the physical anchorage capability of these microorganisms [13]. In particular, it has been observed that the higher the roughness is, the faster the colonization occurs [10]. Bioreceptivity is also influenced by chemical parameters. An high pH value of surface is generally correlated with the inhibition of the algal growth, which are considered among the pioneer surfaces colonizers [14]. Indeed, Manso et al. [15], [16] showed that the addition of acid compounds to cement binder stimulates bio-colonization, when compared to ordinary concrete with an higher pH level. Lastly, the presence of living organisms on surfaces depends on the chemical composition of a specific material [17]. A wide range of raw materials and compositions can be used for the production of building components, urban surfaces and cultural heritage monuments: concrete, tiles, wood, limestone, membranes, modified bitumen and more [6], [18], [19]. All their could then evolve over time under the action of colonizing organisms or other factors causing physical and chemical changes, resulting in a new type of bioreceptivity, which is defined secondary bioreceptivity [4]. Moreover, a tertiary bioreceptivity is known, that is induced by any human activity affecting the material, such as coating with biocide compound or surface polishing [4]. The complete flow of bioreceptivity processes has been reported in Figure 1. Therefore, the study of bio-colonization process of a surface should take into account all these preliminary concepts and definitions.

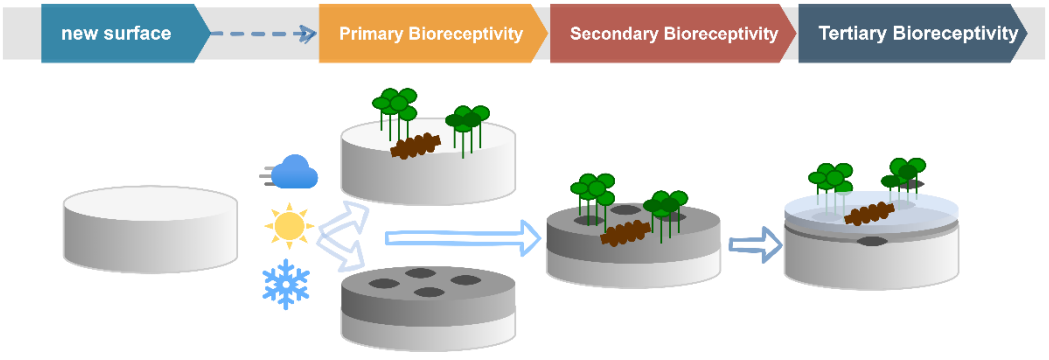

Figure 1: Primary, Secondary and Tertiary bioreceptivity occurring on new outdoor surfaces: primary one depends to the intrinsic surface's properties, the secondary occurs on physically and chemically deteriorated materials, the tertiary one occurs after polishing or coating deposition.

1.2. Fouling of building materials

Outdoor surfaces are continuously exposed to the weather elements, namely wind, sunlight, rain, hail, snow, which are added to atmospheric pollution, temperature variations and deposition of organisms. The direct and inexorable consequence is the degrade over time [1], [2]. Even the most durable materials are modified by deposition of ambient dust and debris, and may provide an opportunity for colonization by living organisms such as cyanobacteria, fungi and algae. These deleterious effects can be considered together as the ageing process which leads the outdoor surfaces to aesthetical and functional alterations [14], [18]. Surface deterioration should be therefore considered a modification of physical, chemical and mechanical properties, also due to a biological action (Figure 2) [18], [20].

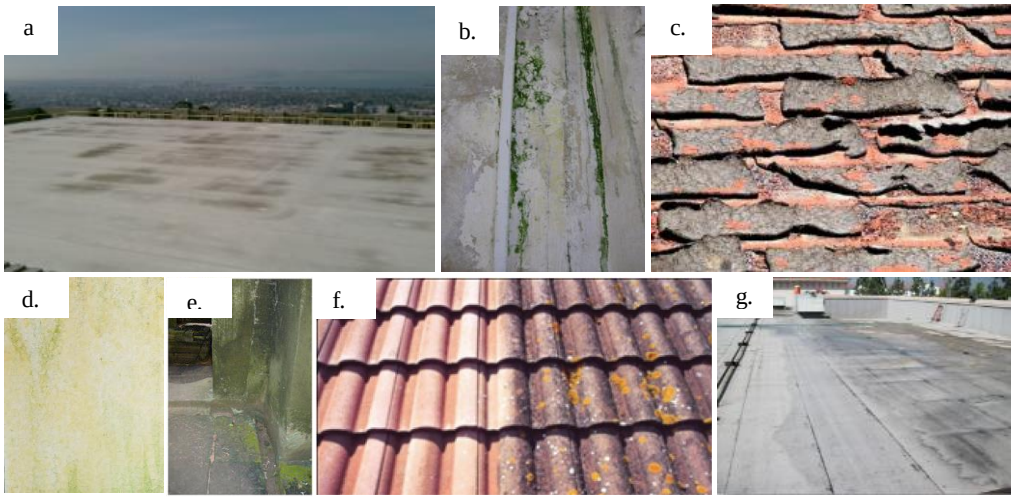

Figure 2: Evident damages on a building surface due to physical, chemical and biological deterioration: images a), d), g): soiling and biofouling on cool roofs; b) coating subject to dwindling, erosion and leaching processes [21]; c) Dark green biofilm, internal severe physical decay on asphalt shingle; e) dark green biofilm on outdoor cultural heritage structure [22]; f) roof shingle soiled by lichens and pollutants [14].

These factors superpose each to the other in the fouling process and it is not easy to distinguish or isolate among them each ageing phases in natural exposure [14].

Physical factors, which always are involved in surface ageing process, include exposure to moisture, ultraviolet (UV) radiation, wind, hail, diurnal temperature cycles. These, largely depend to the climate and microclimate conditions which are extremely variable and cannot be described as a single behavior [23]. Decay of mechanical properties is mainly due to temperature changes, either gradual or sudden (rain shower on a hot day), which cause differential thermal expansion [2], [8], [9]. Then, wind can causes vibrations of roofing materials, which lead to material fatigue and crack formation. Also large size hail causes mechanical roof damage [2]. Among physical stresses, rain provides to get moisture on surfaces, which promotes autotrophic

organism growth. Therefore an higher susceptibility to biofouling occurs in rainy regions, especially during heavy rainy seasons [24], [25]. Beside these stresses, the accumulation of soot particles, which is relatively unreactive, lead to optical and albedo changes [26]. Black carbon, air bones and particulate matter are increasing in last decades, especially in urban areas, owing to the higher incidence of environmental and anthropogenic pollution [10], [27]. Together with physical damages, chemical degradation occurs over outdoor surfaces. Firstly, reaction with atmosphere gases, as oxygen (21%) and water vapor (0.3–3%) can causes the formation of various oxides and hydroxides [2]. Moreover, combustion gases (CO_2, NO_x and SO_2) dissolve in water and form acids, which promote corrosive chemical reaction. Furthermore, polymeric materials are subjected to photo-oxidation, where chemical bonds of polymers are distrupted by UV-radiation energy [26]. During materials lifetime, physical and chemical degradation factors cause also loss of volatile constituents.

All these weathering phenomena can be even worsened by biological growth on surfaces. It is difficult to distinguish between not biological and biologically mediated weathering of materials. The two processes can occur concurrently, each contributing to the overall deleterious effects [7]. Biofilms on building facades can contain different type of living organisms, algae, cyanobacteria, heterotrophic bacteria, fungi, lichens, protozoa, and a variety of small animals (arthropods) and plants (briophyte) [9]. The presence and the development of biofilm on surfaces, as previously described, depends on intrinsic characteristics of building material and following modification which occur on them (bioreceptivity) besides the external and micro-climate conditions [28], [29]. External conditions are represented by rainfall, wind, sunlight and temperature as these determinate altogether the water availability of façade materials, an essential element to the cell metabolism [23]. The seasonal climatic conditions, which also depend on the geography position, determine moisture and light conditions on façade and define the micro-climate. This can be considered the major environmental factor in influencing bio growth [30]. If moisture is enough and if lighting and temperature conditions are suitable, colonization of the surface of new buildings can occur very quickly [18]. Also the building design and the orientation of the surface represent external factors strongly influencing bio growth. It is common knowledge that the north-facing facades, which are wetter and less sunny, get colonized faster [29]. The colonization of buildings materials by organisms worsened aesthetic and physical damages to the structures already induced by physical and chemical factors. Notably, biofilm forms variously dark-coloured patinas (with differently pigmentation depending on organisms species) on roofs, building facades or stone surfaces [13], [31]. The dark discoloration on roofs increases solar radiation absorption and consequently it influences urban temperature, contributing to heat islands occurrence (as widely described in next paragraphs). Microorganisms are also able to absorb several elements from substratum by biosolubilization, a process that involves the production of various organic and inorganic acids besides chelating agents [7], [32]. The chemical corrosion of structures is also aggravated by biomass growth, which can exerts mechanical pressure through penetration of biological communities, for example fungal hyphae, within or along

cracks and scratches [11], [33]. When roof, facades and walls which have been colonized remain untreated, environmental particles (organic or inorganic ones) might be entrapped within the entangled microbial mass, giving rise to complex crusts and patinas that are very difficult to eliminate [10].

Definitively, abiotic factors together living organisms can play an significant role in the deterioration of building materials, being responsible for aesthetic and functional damage. Hence, biological fouling represents a significant economic loss, due to the costs of maintenance and repair. For these reason, biological colonization of buildings materials has attracted great attention and concerning among civil engineering community.

1.2.1. Biofouling on building surface: microrganisms species and biodeterioration mechanism

Cyanobacteria and Algae

Algal spores, cells or fragments of algae, cyanobacteria, fungi and other organisms are transported by wind and raindrops disseminating on various surfaces. Important studies have observed that phototrophic organisms are the first ones to colonize surfaces [2], [34]–[36]. Once established, photosynthetic biocenosis (formed by green algae and cyanobacteria) permits the growth of heterotrophic bacteria, fungi and little animals, which participate in decay processes, and aesthetic or structural damages [25], [37]. Phototrophic – and chemotrophic organisms require only inorganic materials to grow and these are followed by heterotrophic (organic nutrient-requiring) organisms. Since, biofilm is strongly dependent to the moisture availability, its formation and biodiversity of materials-dwelling organisms appears to be rather wide and variously according to the climatic zone considered. However, most of the studies on natural biofilm have identified several ubiquitous *taxa* as pioneers colonizers [3], [17], [38]–[40]. They are primary algae, cyanobacteria, fungi and heterotrophic bacteria. Subsequently, also protozoa, lichens, mosses, small animals and eventually plants can be found as long as the system becomes more complex.

Cyanobacteria [41] are an ancient group of photosynthetic microbes, including about 2000 species in 150 genera, with a wide range of shapes and sizes of cells and colonies. Cyanobacteria have a variety of cell types, cellular structures, and physiological strategies, that contribute to their ecological success since they have been found in an enormous variety of habitats [42]. They do not require organic materials to grow, they are known to be resistant to intense solar radiation and are able to survive to repeated cycles of drying and rehydration [42], [43]. Because of their resistance, they are probably have the greatest ecological importance as pioneer organisms on building surfaces than any other class [44]. Cyanobacteria grow preferentially in shady situations because a reduced illumination holds the humidity; nevertheless, they have been observed in the most extreme terrestrial climates, such as hot and cold deserts. Their

growth can occur also in an endolithic microhabitat that gives them protection from intense solar radiation and desiccation [45]. Cyanobacteria capability to grow and survive under extreme environmental conditions on outdoor surfaces has been linked to the production of excrete extracellular polymeric substances (EPS) such as polysaccharides, lipopolysaccharides, proteins, lipoproteins, lipids, glycolipids [46]–[48]. These molecules represent a water reservoir and compose a matrix that binds cells together with particulate matter and allows the organisms to adhere on the surface [49]. The growth of cyanobacteria on the surfaces of buildings may lead to aesthetic deterioration, due to the colored pigments of different strains of these organisms. Under drier conditions, the biofilms are generally grey in color, whereas areas that are more humid are frequently green. Together with cyanobacteria, algae are deeply involved in the phenomenon of biodeterioration. Algae are most in evidence where atmospheric humidity is high, or the surface is damp. They have different pigments that make them variously different in color from bright blue, dark blue-green, nearly black, dark and light green and orange-red. The phylum *Chlorophyta* (green algae) engages many *taxa* involved in the colonization of external surfaces [50]. However, it is not the only phylum involved: cyanobacteria, and other algae have been found on several materials types: concrete and stones, metals, painted surfaces and plastic [36], [51]–[53]. The taxonomy of algae and cyanobacteria involved in the colonization of surfaces is wide and it depends on the environmental, climatic and the intrinsic bioreceptivity of materials. Table 1 shows the main *Genera* isolated from disfigured buildings or those that have been shown to be capable of biodeterioration.

Table 1: *Genera* of cyanobacteria and algae affecting building materials and corresponding references.

Concrete, stone, brick, mortar, limestone		
Algae	*Chlamydomonas, Edaphochlorella, Chlorococum, Haematococcus, Geminella, Klebsormidium, Neochloris, Oedogonium, Protococcus, Pseudodendoclonium, Scenedesmus, Stichoccus, Stigeoclonium, Tetracystis, Trebouxia, Trentepohlia, Bacilliariophyceae, Eustigmatophyceae, Rhodophyceae, Xanthophyceae.*	[25], [27], [33], [36], [50], [54]
Cyanobacteria	*Aphanocapsa, Aphanoteche, Borzia, Calothrix, Chamaesiphon, Chlorogloea, Chroococcus, Gloeocapsa, Microcoleus, Myxosarcina, Nostoc, Oscillatoria, Phormidium, Plectonema, Pleurocapsa, Stigonema, Synechococcus, Scytonema*	
Metals		
Algae	*Hydrogenase positive Chlorophyta*	[55]
Cyanobacteria	*Nostoc, Anabaena*	
Painted surface		
Algae	*Edaphochlorella, Chlorococcum, Eustigmatus, Pleurococcus, Stichoccus, Trebouxia, Trentepohlia, Ulothrix, Diatoms*	[53], [56]

Algae and cyanobacteria not only entail the aesthetic effect on buildings surfaces but many investigations have stressed the importance of autotrophs in the physical and chemical deterioration, especially when fed by anthropogenic pollution under moderate climates. Inorganic compounds are considered the best nutrient source for surface-inhabiting microflora: consequently, calcareous and siliceous stones, concrete, limestone, bricks and mortar are particularly susceptible to microbial attack [1], [39], [57]. As previously described, the degree of contamination strongly depends on the roughness, on the pore size distribution as well as on the alkalinity of the materials. Rough and porous surfaces are more vulnerable in facilitating attachment of both airborne propagules and accumulation of nutrient-enriching soiling materials. The biodeterioration process caused by cyanobacteria and algae has been described previously by Danin and Caneva [58], who highlight how these *taxa* contribute to the decay of calcareous stones: after the partial death of phototrophic cells, heterotrophic bacteria and fungi start to establish within the fissures, where increase internal pressure of the structure leading eventually to its detachment (spalling).

Moreover, the damage mechanism on surfaces is caused by the secretion of inorganic and organic acids by both algae and cyanobacteria, which are capable of dissolving and etching the mineral matrix [51], [59]. Biocorrosion is the name of the process induced by acids release, that solubilizes stone surfaces, due to organic

chelating agents that sequester metallic cations from stone, or to the conversion of inorganic substances by redox reactions, which form acids that etch stone and contribute to salt formation [32]. Phototrophic organisms grow also on painted surface, where are encouraged by the presence in the paint of compounds like phosphate and nitrogen, as in latex paints [53]. Mechanism of erosion on painted surfaces is due to an association between algae and lichens, whose rhizoids can penetrate masonry coatings inducing disruption and detachment of the paint film [1].

Fungi

Fungi are ubiquitous and heterotrophic organisms which metabolize the organic matter and contribute to surfaces discoloration and chemical decay through the release of acidic metabolites [37]. Besides an organic source, fungi need sufficient moisture to grow since water allows the diffusion of nutrients in their cells, for the production of enzymes, inorganic and organic acids [60]. Fungi occur frequently on paints because of their higher availability of organic carbon substrate than stone or other substrates, as reported in Table 2. The biodiversity of fungi in the urban environment is much higher than the same rock type in a rural environment. This difference can be due to the elevated organic pollution in the cities [37], [61]. Fungi contribute to biodeterioration on building surfaces because of their strong pigmentation, their acidic productions, and their hyphae growth inside the materials [51], [62], [63]. Some *taxa*, as melanotic fungi and actinomycetes, produce dark pigments that provide protection to these organism against driest periods, desiccation and hydrolytic enzymes released by some bacteria and arthropods [64].

At the same time, melanization of the cell walls is an important cause of the aesthetic biodeterioration of building surface. Chemical deterioration induced by fungi is due to the production of a wide range of acids such as acetic, oxalic, glucuronic, fumaric and citric acid [51], [62], [65], involved in the demineralization of various substrates [66]. Gómez-Alarcón *et al*. [51] and Gu *et al*. [62] indicated that fungi can produce also chelating substances responsible of the solubilization of di- and trivalents cations. Among chemical changes on concrete, George *et al*. [60] reported that surfaces exposed to *Fusarium sp.* for one year show a significant pH reduction (from 12 to 8). Fungi increase these physical damage on concrete structures by etching and extending hyphae that penetrate inside surfaces, thus resulting in an enlargement of the already damaged area and an increase in porosity [67]–[69].

Heterotrophic bacteria

Fungi and phototrophic organisms are not the only ones involved in the formation of a biofilm that reduces the durability of surfaces and structures: heterotrophic bacteria can also play an important role. Among the classes of heterotrophic bacteria, chemolithotrophic bacteria (*Thiobacillus, Nitrosomonas, Nitrobacter*) cause primarily biocorrosion of concrete and mortar, while biocorrosion of metal is overall due to and sulphate reducing bacteria (SRB), which are anaerobic [33]. Chemolithotrophic bacteria obtain their energy from the oxidation of reduced inorganic compounds such as sulphide, ammonia and hydrogen, and they use carbon dioxide as carbon source. Instead, SRB obtain energy by oxidizing organic compounds or molecular hydrogen while reducing sulphide. As other surfaces colonizers, also bacteria produce organic, inorganic acids and volatile compounds [66]. All these bacteria are particularly capable to react with metallic ions and this is the reason why they are overall implicated in biogenic corrosion of metal, rather than other substrates [47]. Biocorrosion is a result of interactions, which are often synergistic, between the surfaces, abiotic corrosion products, bacterial cells and their metabolites.

1.3. *Cool* surfaces: thermophysical properties, energy perfomance

Biological colonization of building surfaces could seriously affect materials properties and influencing their thermal or aesthetical performance. All the deterioration phenomena above described are particularly damaging for highly reflective materials applied to buildings (also called *cool materials*). Cool materials are characterized by high *solar reflectance* (also defined as *albedo*), which is the ability to reflect solar radiation in the whole wavelength spectrum (300-2500 nm) and to remain cooler under the sun [70], [71]. This property is the reason of important benefits in buildings, as well as at urban and global scales. In fact, the high solar reflectance, together with high thermal emittance, can preserve the roofing surface from summer overheating and prevent premature damaging phenomena due to thermal stress [72].

Technically, solar reflectance (ρ) is the surface capability to reflect solar radiation back to the hemisphere where the solar source is located, integrated over the entire solar spectrum, including specular and diffuse reflection components [73]. This property is the key performance parameter of cool materials [74]. The radiant flux received by some surface per unit area (irradiance) varies with varying of wavelengths in the solar spectrum, with a peak around 600 nm. The ultraviolet (UV) region holds about 5% of the energy; the visible (Vis) region contains about 44% of the solar energy, and more than 50% is irradiated by the solar source in the infrared region (IR) of the spectrum [72]. At the same time, irradiance depends on atmosphere conditions and perturbation, air humidity, and differential absorption of water, ozone, carbon dioxide, air mass and terrestrial location [72]. For this reason, to calculate solar reflectance (a number varying from 0 to 1) it is necessary using a standard spectra of solar irradiance: several standards

are available, taking into account different climate conditions, angle of incidence of the solar beam, contribution of the diffuse radiation content, etc. [74]. Thermal emittance (ε) characterizes the surface capability to reemit the previously absorbed heat away from itself [75]. It has a range between 0-1 and represents the comparative/relative emittance with respect to a blackbody operating in similar conditions. In common construction applications, the thermal emittance of a surface is usually higher than 0.8–0.85, except for those layers that are based on metallic components, for example, aluminum shingles. The thermal emittance of a roof or wall component is mainly affected by the characteristics of the layer that is exposed to the solar radiation [72]. These two thermal physical properties can preserve the roofing surface from summer overheating and prevent premature damaging phenomena due to thermal stress [72]: high albedo surfaces applied to buildings reduce indeed the energy use in a conditioned building, increasing thermal comfort in a unconditioned building [76]. High-albedo coatings limit the increase of surface temperature of a building surface (roof or walls), minimizes the corresponding release of sensible heat to the atmosphere and avoiding building overheating; as physical consequence, building energy needs are reduced in opposition to a high absorptive finishing and urban temperature results mitigated [77], [78]. The reduction of building cooling requirements during warm seasons leads to important benefits at urban and global scales, beyond to the building itself [71], [79].

Today most common cool material products are typically membranes, coatings, paintings, metal roofs, shingles, and tiles. These products and technologies are mainly developed for flat roof application, but many solutions are recently being implemented also in tilted roof surfaces [80]. Generally, reflective roofs are single ply or liquid applied coatings. Typical liquid products include white paints, elastomeric, polyurethane or acrylic coatings; a full list of cool roof materials meeting certain criteria is provided by Energy Star Roof Products (http://coolroofs.org/). The US Cool Roof Rating Council and the EU Project Cool Roofs (http://coolroofcouncil.eu/) also provide databases with information about the solar reflectance and the infrared emittance of commercial roof products.

High reflective materials, thanks to their ability to decrease absorption of the solar radiation in the urban environment, represent one of the most efficient countermeasures to the Urban Heat Island (UHI) effects, which is a phenomenon related to higher temperatures in urban areas compared to the surrounding rural or suburban areas [81], [82].

1.3.1. Urban Heat Island and its Countermeasure

Urban system increased in the last three decades and is continuing to grow rapidly due to the rising rate of population the migration of the rural population into the cities [78]. The number of urban dwellers is expected to grow to over 68% of the earth population by 2050 (ONU 2011). This fast and wide cities growth represents both benefits and penalties for the environment and for human life. On one hand, the cities symbolize and embody the place where people, coming from places affected by local

conflicts or lack of resources, can find a better life; on the other hand, anthropogenic actions are increasing very rapidly other risks, and urban citizens are ever more vulnerable. The conversion of natural environment to urban lands cause several notable perturbations to the Earth's surface energy balance [83]. High density of buildings and urban structures absorb high rate of solar radiation, and the transformation of a natural vegetation area leads to the reduction of evaporative cooling: these are generally thought to be the dominant factors contributing to the overheating of urban areas [82], [83]. Moreover, the production and release of anthropogenic heat within urban areas corresponds to an added energy input to the energy balance which further increase temperature on surfaces [84].

All these factors determine Urban Heat Island, which is well documented phenomenon, closely related to climate change: temperature in urban areas is usually several degrees higher than that of surrounding suburban and rural area (Figure 3) [81]. High urban temperatures have a strong impact on cities life, human health and on the energy consumption for cooling, raising the peak electricity demand [71], [85]. Three decades of studies on UHI tried to measure its magnitude across the world main cities stressed, and it may vary between 0.5 to 11 °C with an average value close to 4.1 °C in Asia-America and between 1°C to 10°C with an average maximum value close to 6 °C in European cities [86]. The consequences due to UHI should be added to global and regional climate change effects in order to outline and to explain the increase of frequency, magnitude and duration of extreme heat waves [87]. This synergetic effect between regional and global climate change and UHI phenomenon deteriorates even more the outdoor comfort conditions, increasing the risks of vulnerable populations. The heat-related morbidity and mortality caused by the global and local climate change is indeed highly alarming: the existing epidemiological data record that almost 60.000 persons passed away between 2000 and 2007 during 52 extreme heat events around the world [88]. Overheating which occurs in urban areas has a positive feedback pathway with the concentration of ground-level ozone and air pollutants: the rising level of these last lead to aggravate UHI, triggering a chain reaction [89]. High temperatures, heat waves and poor air quality are related to serious human health problems, affecting vulnerable people, including elders and who suffer of cardiovascular or respiratory diseases [86], [89].

To counterbalance the UHI phenomenon, important mitigation technologies have been developed and proposed. Among them, high reflective surfaces are aimed to increase the albedo of the cities, improving its thermal losses and decreasing the corresponding heat gains. Many studies have been performed in order to identify the cooling potential and the possible improvements of thermal comfort provided by cool roofs. Effects of high-albedo surfaces can be quantified in terms of 'direct' and 'indirect' contributions to ambient temperature decrease [71]. Direct effects give immediate benefits to the building that applies them, while indirect effects can be appreciated only when cool materials and other countermeasures to UHI achieve a widespread deployment. Among direct consequences, there are the energy benefits, which vary mainly as a function of the climatic conditions and the characteristics of the building.

Indoor temperatures may decrease up to 2-3°C inside the buildings while cooling loads reductions may range between 10% and 50% in summer periods [90]–[92]. In detail, it has been estimated that the application of cool roof on residential and commercial buildings on eleven high density metropolitan areas may avoid 2.6TWh saving 194K dollars [71]. Akbari et al. [93] estimate that permanently retrofitting urban roofs and pavements resulting in a net albedo increase for urban areas of about 0.1 in the tropical and temperate regions of the world would have a negative radiative forcing on the earth equivalent to offsetting about 44 Gt of CO_2 emissions [93].

Accounting for indirect effects is more difficult and the results are comparatively less certain. Nevertheless, some data estimations coming from five urban rehabilitation projects involving the combined use of reflective pavements, greenery and shading devices reported a peak and average urban temperature drop of 1.8–4 °C and 0.7–1.9 °C respectively [85]. Hence, the ability to stay cool in the sun of cool surfaces bring to air conditioning energy savings, which is directly translated into the reduction of greenhouse gases (CO_2) savings; these results establish a positive feedback pathway which may yield significant decrease of ambient temperatures [94]. These data explain how cool materials represent a real way to countermeasure urban heat island phenomenon, urban energy issues and health risks.

UHI is therefore a complex multiple-factors phenomenon, bound up with local and global causes and effects of climate changes, besides the impact on human health and environmental quality [86]. This suggests the urgent need to act on multiple sides, applying available technologies and countermeasures with the aim of "cooling the cities", and in order as well of "cooling the Earth", that has indeed become the priority challenge of 21st century.

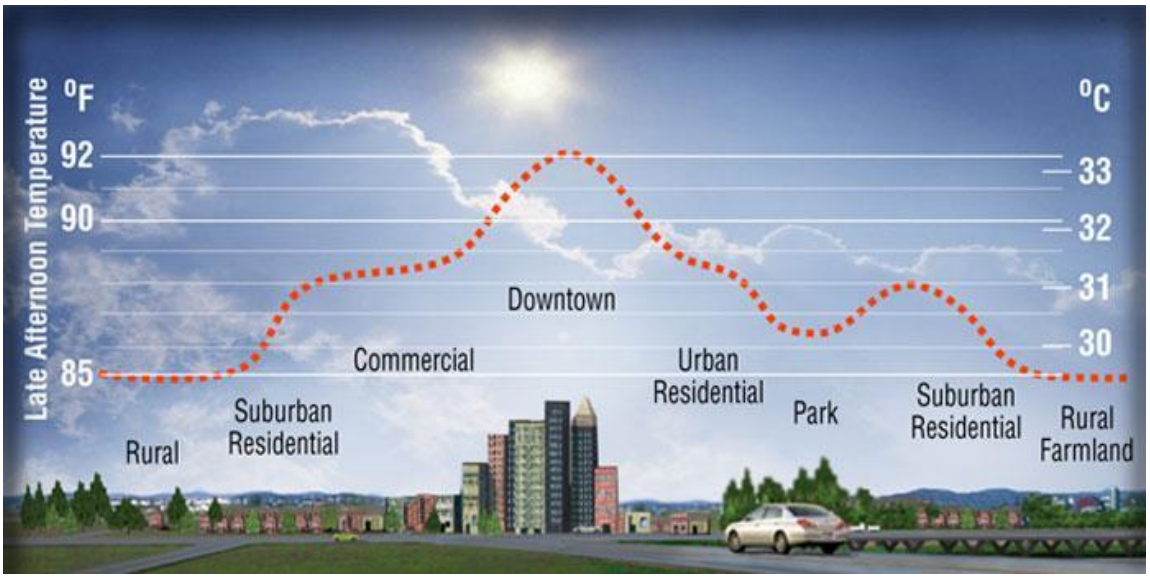

Figure 3: Urban Heat Island effect (heatisland.lbl.gov).

1.3.2. Cool Surfaces Durability issues

Highly reflective roofs can counterbalance UHI decreasing the energy required for building air conditioning. This makes cool roof highly interesting technology to help the mitigation of urban heat island and global warming. At the same time, the greatest challenge for cool materials today is not to provide enhanced performance, but to extend their durability, that is defined as "*the ability of a product to maintain its required performance over a given or long time, under the influence of foreseeable action*" [95]. The starting high albedo of a cool surface is then reduced by soiling and weathering over the time [96]. These constitute the "ageing process" to which high reflective surfaces are exposed during their lifetime, and they involve all the physical, chemical and biological processes described in the previous paragraphs. Hence, optical and radiative response of building envelope materials are affected with the passing of the time and the energy performances are reduced.

Levinson et al. [76] have studied the effects of soiling on the reflectance and solar heat gain of a light-colored roofing membrane, exposing the samples for years over some building spread across United States, trying to involve the main warm climate types regions. The results show that the high initial solar reflectance of a white membrane roof (circa 0.8) can be lowered by deposition of soot, dust, and/or biomass to about 0.6; degraded solar reflectance range from 0.3 to 0.8, depending on exposure.

The decrease of solar reflectance inevitably brings to the energy performance losses and following increase of air conditioning energy consume for the interested buildings.

It has been observed that soiling diminishes the reflectance of membranes more strongly at shorter wavelengths, consistent with the absorption spectra of black carbon and organic carbon. The study highlighted also that the most soiled samples were the ones exposed in hot and humid climates, where a biomass grew consistently on the surfaces. The same results were confirmed by other several authors: Sleiman et al. [97] have found that absolute solar reflectance losses for cool samples were 2–3 times greater in Florida (hot and humid climate) than in Arizona (warm and dry climate) on a large set of roofing sample products and Berdhal et al. [2] have described in details how the accumulation of colonies of cyanobacteria, algae and fungi are visually evident as dark stains on light-colored roofing, especially in the southeastern of United States (for example in Florida). In a second large series of studies, conducted on building materials soiling, where thousands of samples have been exposed to natural ageing and analyzed, Sleiman et al. [18] stated that microbial growth can be the main agent of roof soiling in humid climates. When largely available, water is captured and retained as moisture by roofing materials and it favors the growth of bacteria, fungi and algae. Fouling induced by biological stains is particularly damaging, due to all deterioration mechanisms described in the previous 1.2 section. Furthermore, Levinson et al. [76] have described how it would be more complicated to clean surfaces heavily interested by biofilm growth compared to other type of soiled surfaces.

Nowadays, a lot of studies investigated the potential of different technologies and biostatic and biocidal agents which could be helpful to improve the conservation of

building over time [38], [98], [99]. The first type of treatment applied to building materials to remove the deteriorating biofilm remain mechanical cleaning, which is currently often conducted before other chemical treatments. Among mechanical methods, the use of water pressure and steam system are easy to employ and widely spread. At the same time, these methods can also spread microorganisms on the substrate and are time consuming. Other methods based on the use of lasers are sometimes applied [38]. In the last ten years, the market of biocidal products is increased by more than 6% and it never knew any crisis, so it expected to grow. European commission defined biocidal a substance or a mixture applied to destroy, prevent the action or exert a controlling effect on harmful organisms by a mechanism that is not purely physical or mechanical [100]. The molecules which show the best performance in biofouling prevention are often furnished with façades or roofing coatings. Generally, they can be added as powder, solution or dispersion. Some of the mostly applied biocides are titanium dioxide, thanks to its photocatalytic oxidation power, and zinc oxide: the metal oxides have a high concentration of polar groups that act as bonding sites for the silane and siloxane components. This allows hydrophobic parts of the treatment to govern the interfacial characteristics, exerting the water repulsion from the surfaces [99], [101]. Also silver, copper, cerium salts can be applied within materials coatings in order to avoid biological growth on surfaces [102]. Some studies have also shown that the efficiency of these coatings additives is strongly dependent on the amount of biocidal particles [103]. Unfortunately, commercial and traditional biocides may be dangerous for human health and the environment, and for this reason, alternatives and eco-friendly substances or methods to halt or reduce biodeterioration are intensively searched and studied. Several natural substances, as essential oils and other substances of plant and lichen origin, have been tested as biocidal products on stone materials with some promising results [104]. These last solutions have been specifically applied on cultural heritage stones and monuments.

1.4. Cultural heritage

Besides that new building materials also stone monuments, statues and historic buildings are exposed to weathering factors, including the biological ones: also these surfaces provide a suitable substratum where different groups of microorganisms can develop [50]. Marble, limestone, travertine, sandstone and granite are the lithotypes mainly used in monument construction; several studies conducted in natural conditions if bio-deterioration suggest that bio-colonization is primarily related to the physical characteristics of the stone surface (porosity, roughness and permeability) and secondarily to the nature of substratum [105] [35]. Heterogeneous biological species have been identified by analysing the classes of organic molecules, i.e. fatty lipids, found on the surfaces, and related with the structure and the composition of the concerned tile [106]. The physical and chemical deterioration mechanisms (see section 1.2) induced by organisms on cultural heritage structures, produce aesthetical damage surface detachment, superficial losses and bio-corrosion due to the release of acids

compounds.

Biodeterioration of cultural heritage is caused by diverse communities of microorganisms, which can colonize and destroy valuable monuments and represent a severe threats for them. For this reason, it is important to assess their impact over the long term and gain comprehensive understanding. Conservation strategists are being deeply exploring by scientific community in order to limit microbial colonization and further growth if possible and preserve or restore valiant cultural heritage and monuments [107], [108]. The maintenance and restoration of cultural heritage has indeed a key role to keep high the outstanding universal value of world heritage sites. Various physical and mechanical methods have been used to fight against biological proliferation over cultural heritage; however, it is not a simple goal. Recently, new advances in biotechnology and applied microbiology provide important information on conserving cultural heritage (as well as building materials and high efficiency products) [102]. Therefore, inorganic nanoparticles have a better chance to protect cultural heritage: Silver (Ag_2O) and titanium oxides (TiO_2) are effective against biofilm formation, and nanoparticles of zinc oxide (ZnO) are effective antimicrobial agents. These compounds are the same which are involved as biocides applied to cool roofs, as described in previous section.

1.5. Interior surfaces contamination: air quality and health issues

Surfaces contamination is not only an outdoor problem: biological agents can colonize also indoor walls, representing a risk for public health [109], [110]. Indoor air pollution is a growing source of concern: the United States Environmental Protection Agency (EPA) reported that indoor air quality has an important impact on people health, since in developed countries the majority of persons spend most of their time indoors [111]. Considering energy conservation in buildings, newly constructed buildings are airtight and indoor air pollutants cannot be discharged in time, leading to the deterioration of indoor air quality [109]. This induce higher latent thermal load within thermally-insulated rooms, where unwanted and excess moisture may occur in the indoor environment as a consequence of a failure in moisture control [111]. Household air pollution is due to a complex dynamic of several compound and materials interactions: the source of contaminants can come from heating/cooling process, tobacco smoke, building and construction materials, and consumer products used for cleaning, polishing or personal care. However, another cause responsible for the approximately 21% of indoor air quality problems originate from microbial contamination, which includes a complex and highly variable populations of bacteria, viruses, fungi, small protozoa, and microalgae [112]–[114]. The indoor microbial contamination is often due to damp, which encourages the mold formation and the following formation of heterogeneous biofilm on walls and surfaces. Wherever excess moisture is available, fungi and other microorganisms start to grow, developing gradually into mold. Mold growth in a building acts as a source of indoor pollutants,

such as spores, cells, fragments of hyphae and spores, and microbial metabolites such as volatile organic compounds (VOC) and not volatile toxins [111]. Often moisture is the limiting factor for microbial growth in the indoor environment, while fungi are more tolerant of low-moisture conditions than bacteria. Some experiments indicate that spore release for some fungi can be higher under lower relative humidity [115], [116]. Then, both high and low air relative humidity or surface moisture conditions could stimulate the spread of biological agent into indoor environments. Several literature reviews describe how microbial exposure may influence the development of allergies and asthma, often also among children, which spend much of their time in an indoor environment, either at home or inside the classroom at school [112], [114], [117]. The most common genera in indoor buildings include *Aspergillus, Penicillium, Cladosporium, Eurotium*, and *Chaetomium* [118]. Among them, *Aspergillus* is one of the most common fungi, and its structure consists of foot cells, conidiophore stalks, vesicles, metulae, phialides, and spores [119]. Among microbial contaminants, fungi have been associated with adverse health effects with approximately 30% incidence rates of allergy, infection, and inflammation [109]. The infectious fungal aerosol notably increases health risks and complications to patients in the hospital environments, where the exposure to skin and respiratory inhalation could be even more dangerous [120]. The wealth of documentation regarding the health problems and diseases associated to living air pollutants (fungi spores, bacteria, viruses etc.) within the indoor environments and surfaces, gives a sense of the importance of the indoor surfaces bio-contamination.

Even though this work is mainly focused on studying the biological colonization of external surfaces, it is worthwhile to consider the bio-colonization as a general and ubiquitous issue to solve. The importance to formulate anti-bacterial, anti-mold and, at the same time, safe products for indoor surfaces has become a priority for internal coating producers, due to health related issues of these type of pollutants. Consequently, it become essential to test the resistance against biological aggression also for indoor materials. Under this point of view, the laboratory approach to study the bio-growth on materials surfaces through an accelerate way, could be even considered and crosswise applied to the internal surfaces types.

2. Ageing of building materials: state of art of available methods

The high impact of weathering and fouling processes on energy efficiency of cool building materials, as well as its consequences on indoor air quality and human health, rise the attention of the scientific community on deterioration processes of building materials. Highly reflective roofs can indeed decrease the energy required for building air conditioning, however these benefits are diminishing by soiling and weathering processes which reduce their solar reflectance [121]. The importance to win the challenge of durability for cool materials is related to the mitigation of urban heat island and to slow global warming. Hence, one of the main goals of building material producers and providers is to extend as long as possible the high energy performance of outdoor materials. It becomes then essential to comprehend in detail physical, chemical and biological deterioration dynamics and to test the resistance or the behavior of different material type to fouling processes. These industrial needs have encouraged the development of standard methods for testing and reporting the radiative properties of building products before and after the outdoor exposure.

These methods involve both Natural and Accelerated ageing procedures and have been developed by the synergic activities of many authors and with the support of the American Cool Roof Rating Council, CRRC (www.https://coolroofs.org/) and European Cool Roof Rating Council, ECRC (https://coolroofcouncil.eu/). CRRC and ECRC are two nonprofit organizations, which and are aimed to design accurate and reliable methods for evaluating and labeling the properties of the radiative surfaces (solar reflectance and thermal emittance) of roofing and exterior wall products. One of the main services provided by these organizations is the Roof Product Rating Program, a fee-for-service program that enables roofing manufacturers to have tested roofing products, labeled with information on their radiative property. In particular, ANSI/CRRC 100 describes how to cover specimen preparation and test methods for determining the initial and aged radiative properties of roofing products [122]. Moreover, CRRC has developed a database (initiated in 2005) with all the information reported by the manufacturers about solar reflectance losses after natural exposure: the Rated Products Directory. A similar database, has been done by U.S. Environmental Protection Agency (EPA), began in 2002 and it contains aged reflectance for 5397 products.

ANSI/CRRC 100 Standard defines all the requirements for field exposure of roofing products (Natural ageing standard) and for laboratory soiling and weathering of roofing materials (Accelerated ageing). Natural exposure of materials of both metallic and nonmetallic materials shall be in accordance with ASTM G7 [123]. The practice defines in detail how to expose building materials in order to test their relative durability after at least three years, as prescribed by ANSI. Specimens shall be mounted for exposure on racks in order to follow the slope to which are intended to be used. ASTM G7 outlines that exposure can be conducted in any type of climate,

recommending that results from a single exposure cannot be used to predict the absolute rate at which a material degrades because of year-to-year climatological variations. Moreover, ANSI specifies the need to simultaneously expose roofing products in three locations, representing three climate zones: hot/humid, cold/temperate and hot/dry ones. Criteria that assess the belonging to a specific climate region consider heating degree-days and cooling degree-days, determined in accordance with ANSI/ASHRAE Standard 169, and relative humidity, determined in accordance with NOAA comparative climate data (https://www.noaa.gov/).

This natural exposure procedure gives the possibility to collect highly reliable data about the radiative properties losses on aged surface. Rain, wind, solar radiation temperatures changes, soiling deposition and following chemical degradation and biological growth occur directly on outdoor exposed materials, whose durability and radiative properties losses will be verified and measured after the exposition to the real environment conditions. Even if ASTM G7 is the most realistic standard procedure to get results on aged roofing products, it presents some disadvantages, in particular for industrial needs. Firstly, natural ageing standard takes up to more years of surface exposition to the weather conditions. This time depends to the materials type and to the geographical location, which primarily influence the deterioration and biofouling rate on surfaces. However, US CRRC define a period of three-years for materials exposure, which is the applied convention reached between industry and Council. This long duration is not compliant with industrial and manufacturer's needs, but on the contrary, it represents a strong limitation for any product development and improvements. Moreover, natural ageing, and particularly bioageing, is characterized by a low repeatability; this is due to the wide variability of environmental conditions and mainly by geographical position of test site.

The high attention of the scientific community on deterioration processes of building materials recently encouraged the development of a novel laboratory accelerated ageing method, that combines soiling and weathering and simulates 3 years of outdoor exposure in three days [18]. It has been published as the ASTM D7897 Standard [124]. This allows evaluating the loss of performance of highly reflective materials in a fast, repeatable and reproducible way. A laboratory accelerated weathering device is used to simulate outdoor weathering, exposing materials to alternating cycles of ultraviolet (UV) light and moisture, at controlled, elevated temperatures. It uses fluorescent UVA-340 lamps to simulate the high energy photons in sunlight. Moisture is introduced with condensing humidity or water spray. Standard procedure ASTM D7897 also simulates the deposition on surfaces of atmospheric particles originating from windblown dust, forest and grassland fires, living vegetation, sea spray; furthermore, it reproduces deposition from human activities, such as the burning of fossil and biomass fuels. Among the atmospheric particles, black carbon soot, emitted from the burning of fossil and biomass fuels and from fires, has a strong mass absorption efficiency. The standard procedure then uses an aqueous mixture of four soiling agents to simulate field exposure [124]. The soiling agents and their concentrations have been chosen based on their respective contributions (determined

in the laboratory) to changes the solar reflectance spectra of soiled surfaces [18].

Nevertheless, experimental results show that the reflectance spectrum of samples aged by ASTM D7897 can be different from that measured on the same samples naturally aged in humid places [18], with alterations particularly evident in the visible region. In fact, the changes of appearance and solar reflectance properties of cool materials surfaces frequently are due to biofilms formation when installed in hot and humid environments. The occurrence of these alterations is not reproducible by ASTM D7897, because they are mainly due to biological growth.

2.1. Climate regions and biodeterioration

The study of Sleiman et al. [97] analyzed the initial and aged radiative properties of hundreds of products rated by the CRRC or by the Energy Star program of the US EPA and tried to explore how climate and product's features affect the loss of solar reflectance. The analyzed dataset included three years aged measurements made in three specific climates: Ohio (temperate and polluted), Arizona (hot and dry) and Florida (hot and humid). According to Köppen-Geiger's climate classification, these three ageing sites have been classified as follow:

- Arizona: "*Bwh*", Tropical and Subtropical Desert Climate: the climate is dominated in all months by the subtropical anticyclone. The atmospheric environment inhibits precipitation, making this region an extreme arid area. The average temperature for the year in Phoenix is 23.9 °C. The warmest month, on average, is July with an average temperature of 34.9 °C. The coolest month on average is December, with an average temperature of 13 °C. There are an average of 36.6 days of precipitation, with the most precipitation occurring in August with 5.0 days and the least precipitation occurring in June with 0.5 days.
- Ohio: "*Dfa*", Hot Summer Continental Climate: humid continental climate characterized by large seasonal temperature differences, with warm to hot (and often humid) summers and cold (sometimes severely cold) winters. Precipitation is relatively well distributed year-round in many areas with this climate. Most summer rainfall occurs during thunderstorms and a very occasional tropical system. It is important to note that the "humid" designation does not mean that the humidity levels are necessarily high, but that the climate is not dry enough to be classified as semi-arid or arid. The average temperature for the year in Columbus is 11.9 °C. The warmest month, on average, is July with an average temperature 24 °C. The average amount of precipitation for the year in Columbus 998.2 mm. There is an average of 104.0 days of precipitation.
- Florida: "*Am*", Tropical Monsoon Climate: the monthly mean temperatures above 18 °C in every month of the year and the variance in temperatures during the course of the year tends to be very low. The average temperature

for the year in Miami is 25.1 °C. The average amount of precipitation for the year in Miami is 1572.3 mm. There are an average of 135.2 days of precipitation, with the most precipitation occurring in August with 18.9 days and the least precipitation occurring in April with 6.4 days. (https://www.weatherbase.com/)

Results of this investigation on aged roofing materials, underline how many products suffer significant loss of solar reflectance, especially those with high initial solar reflectance. Products with very low initial solar reflectance (ρ_{sol}<0.2) tend to become more reflective as they age. The interesting evidence is that within CRRC database, absolute solar reflectance losses for samples with ρ_{sol} > 0.4 were 2–3 times greater in Florida than in Arizona; losses in Ohio were intermediate.

The analysis of the composition of material deposited on buildings reflects the main constituents of atmospheric particulate matter [125]. Black carbon and organic matter are the major components of soot particles emitted during the combustion and constituting the soiling layer, which mainly absorb sunlight over the surfaces. It has been noted that in urban soiling, organic carbon is more abundant that black carbon and this undergoes major changes on surfaces [105], [126]: the accumulation of compounds stimulates chemical transformation as photochemical oxidation, hydrolysis nitration with the reactive atmospheric species. The amount of soiling material on surfaces also depends on water availability and runoff, which to one hand promotes the particulate dissolution and surface cleaning, but to the other hand helps biofilm growth. What seems clear is that microbial growth could be the most important agent of roof soiling in humid climates. The capacity of roofing materials to capture and retain moisture in porous structures or to leach organic compounds that feed microbial colonies, stimulates the growth of bacteria, fungi and algae [18].

Complex colonies of organisms have been identified on aged surfaces in the Regions featured with hot and humid climate, such as Florida. Cyanobacteria, green algae and fungi form dark colored crusts, especially after the colonies death, due to compounds of biological origin: melanins and polysaccharides, which become persistent components of soiling thanks their resistance to photo-oxidation and degradation processes [18]. As consequence, the loss in solar reflectance is particularly evident in samples weathered in hot-humid Florida, whereas the deterioration is least marked in samples in hot-dry Arizona. Another study set in Japan, where the climate classification is "*Cfa*" (Humid subtropical), recorded a significant reduction of spectral solar reflectance in the visible wavelength range. The main cause has been granted by carbon components, considered to be derived mostly from organisms and exhaust gas [127]. Also Dornelles et al. [128] found that among surface accumulations, microbial growth is more common in humid areas. Material types which are particularly affected by loss of solar reflectance are lighter surfaces as white single ply membrane or field applied cool coatings. In detail, all field-applied coating products studied by Sleiman et al. [97] with ρ_{sol}>0.6 frequently achieved lower values of solar reflectance compared with the ones estimated by the provisional model Title 24 (http://www.energy.ca.gov/), (see section 2.3).

Definitely, biological colonization is a phenomenon which occurs overall on surfaces exposed to humid climates, bringing a series of consequences for aesthetical, structural and energy issues. At the same time, it is extremely complicated to reproduce biological growth on building material surfaces and estimate the impact on their physical properties. Indeed, as mentioned above, the presence of living microorganism on surfaces is the main reason of discrepancies observed between results obtained in laboratory and field exposure in three different climate regions [18]. The Authors compared all the solar reflectance spectra obtained after accelerate ageing (through ASTM D7897) and natural ageing (through ASTM G7) from several products. While the spectra match very well for samples exposed in Arizona and Ohio (Figure 4a), the reflectance spectrum of the laboratory-aged sample differs from that of the sample naturally aged in Florida, particularly in the visible region (Figure 4b). This last has been considered the result of absorption by microorganisms [76]. ASTM D7897 standard procedure does not provide the grow of microorganism on the surface of roofing products, hence, it is unable to gauge resistance of these products to microbial growth. At the same time, the method does not mimic all features of microbial soiling, nor extreme physical-chemical changes that occur afterwards in some materials. For this reasons, the same Authors claimed that microbial growth on roofing materials exposed in hot and humid climates can change their appearance and albedo in a way that cannot be reproduced by the developed accelerated method ASTM D7897 [18].

a.

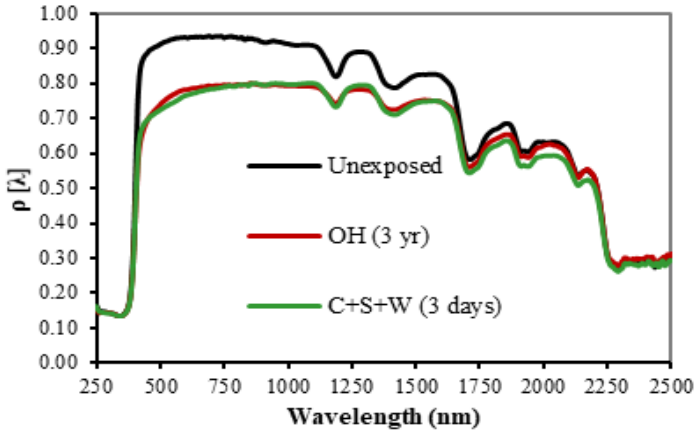

b.

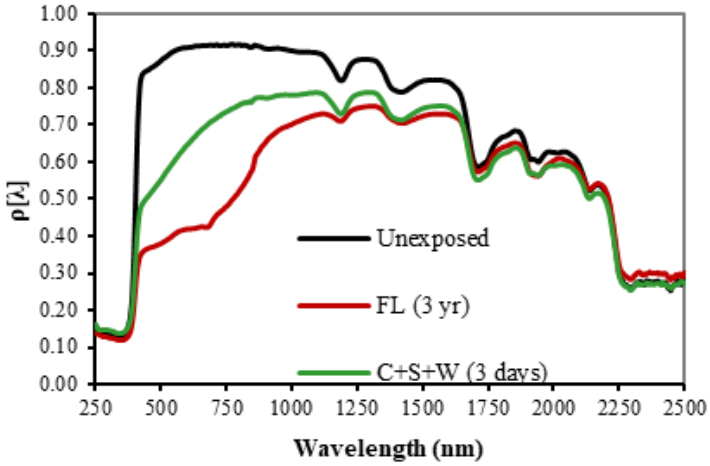

Figure 4: Comparison among solar reflectance spectra obtained on a field applied cool coating new sample (ρ_{sol} >0.82) (black spectrum), ASTM D7897 accelerate ageing (green spectrum) and ASTM G7 natural ageing in two different region: Ohio (a) and Florida (b) [18], [97].

2.2. Experimental laboratory bioageing procedures: main challenges and weaknesses

Several studies have been carried out on building facades and roofs with the aim to assess the biodeterioration effects on the building energy balance [9], [105], [126], [129], [130]. However, mainly due to the wide variability of environmental conditions, the scientific community has not yet quantitatively defined biodeterioration phenomenon. Furthermore, there is the need to develop a laboratory procedure, which takes into account biofilm growth since the available standard method (ASTM D7897) could not be reliable as building materials ageing procedure in humid regions.

Developing a laboratory approach to biological ageing may thus provide a reproducible and reliable test method to assess the long-term performance of building materials, considering changes in solar reflectance and emittance over time [131]. In fact, natural ageing processes occurring after several years, can be compressed in a very short time (weeks or months), by forcing the growth of microorganisms through a strict control on different environmental conditions, the artificial ageing [14]. Accelerated biological ageing should certainly be faster than natural processes and repeatable, two fundamental requirements of industrial research and development.

Before this work, other attempts have been made in order to setup a laboratory and repeatable procedure to induce biological colonization on building surface samples. Kultur and Turkerieri [131] weathered the specimens with an accelerated tester using radiative Xenon lamps simulating the solar spectrum range from 300 to 800 nm. However, this simulation does not take into account other environmental stresses such as moisture, wind, chemical and physical pollutants. The accelerated bioageing setup developed by Barberousse et al. [132], has been applied to accelerate microorganisms growth applying light/dark and watering cycles on the samples.

In the test facility developed by Kunzel et al. [133], for accelerated microbial growth on façade, the biological inoculation of fungi and algae were made manually by a special brush, introducing a heterogeneous way to spread biological colonies. All these studies, however, do not seem to take into account the thermal physical properties related to the building energy assessment. Moreover, they did not investigate the repeatability of the setup, that is an essential requirement to get comparable results and to evaluate the biodeterioration process among different samples and different tests.

A previous work based on the setup developed by Barberousse et al. (2007) used an accelerating bio-system, consisting in a 120 cm × 40 cm ×55 cm glass chamber (Figure 5) [20]. Samples were placed on 45° sloped stainless steel supports, which allowed the desired water runoff on the sample surfaces and thus the probability for algae and cyanobacteria to deposit and settle, starting the colonization process. Specific and controlled environmental conditions are chosen to accelerate as much as possible biological growth on building materials. In this regard, a reproducible bio-ageing protocol has been outlined and it allows a set of materials to reach an advanced bio-aged level in a short time (8 weeks). The chamber was filled with 50 liters of a liquid culture medium studied for the growth of cyanobacteria and algae, the Bold Basal

Medium (BBM). Six selected species of photoautotrophic microorganism were used: *Edaphochlorella mirabilis, Chlorella vulgaris, Klebsormidium flaccidum, Chlorhormidium sp., Stichococcus bacillaris* (green algae) and *Gloeacapsa sp.* (a cyanobacterium). The final BBM medium containing both algae and cyanobacterium was driven by the pump through the sprinkling rails, where it dropped onto the specimens and runs down, and allowing algal and bacterial cells to adhere to the specimen surface.

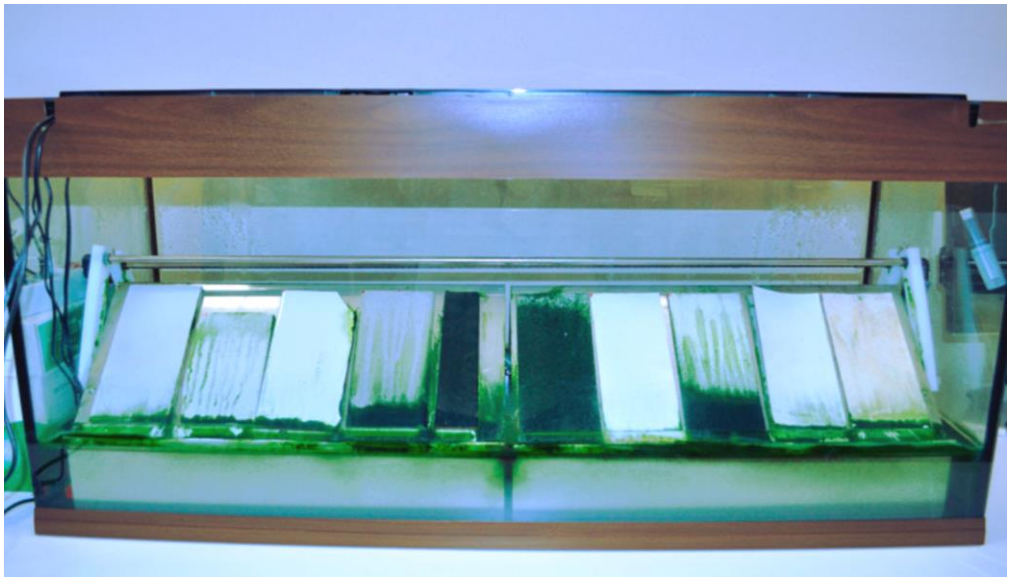

Figure 5: Accelerated bioageing set-up applied in [20]

Nevertheless the bioageing system here developed was completely automatized, and the same environmental conditions of light, temperature and relative humidity have been maintained for all the test duration, some goals remain to be achieved.

Generally, each bioageing setup previously developed raise some challenging points, which need to be solved. Firstly, the repeatability (the measure of the ability of the method to generate similar results for multiple preparations of the same samples) has not been yet investigated. At the same time, the measure of repeatability should be done on the same variable under the same experimental conditions. When the experimental variables correspond to the living organism growth, the total lack of contamination becomes a critical aspect. For this reason, a bioaging system without a sealing closing risks to be affected by external factors, adding variability to the system. Again, it is essential to ensure that the environmental conditions, such as temperature, may not be exposed to the fluctuations due to the room conditions. To ensure repeatability, exactly the same experimental step should be run across repeated tests, and this represent the first and most important challenge to reach through a laboratory bioaging setup.

The system, as well, should ensure homogeneity of colonization over the samples surfaces. The setup previously described has showed a water accumulation on the samples side, which lean to the sloped stainless-steel supports. This probably

encourages the organism dwelling over the back of each sample, compared to the resting part of sample surface. This does not provide the homogeneity of bio colonization over the whole specimen area: the result is that the covered area could be affected by a not negligible bias.

Therefore, repeatability of experimental conditions and the setup, the homogeneity of biological growth, and afterword the reproducibility in other laboratories, are the most important challenges that the following bioageing experimental setup development should face.

2.3. Previous predictive models

This thesis work is mainly focused on the development of a novel method to accelerate biodeterioration process on cool building surfaces. The whole experimental design and the aims of the work have been thought on the basis of existing building materials ageing models. The bio-colonization dynamics, indeed, has been described by Avrami's model, which provides the formulas to outline biodeterioration phenomenon over a surface. The results obtained have been then compared with the 2008 Title 24 provisional model, which can overpredict the aged solar reflectance of the product types within CRRC database [97].

Avrami's law has been developed in the form of an exponential equation by Avrami, Johnson and Melh [134]–[136]. This law has been originally used to describe the kinetic phase transformation in solids and it is based on two processes: the nucleation, which corresponds to the appearance of nuclei of a new phase, and the subsequent growth, which represents the increase in the size of these nuclei into the initial phase during time [137]. Likewise, biofouling process on building materials can be described by these two phases. Algal colonization starts with the attachment of algae on the substrate. Initially, pioneer organisms appear as small green spots, which correspond the nuclei of the Avrami's model then they grow increasing in size and forming algal filament increasing the covered extension on the material surface. Avrami's equation takes into account that the attachment and the growth of algae on surface might be affected by the porosity (p), the roughness (R), the initial pH of the surface, the chemical composition of the surface, the algae species, the algae viability, the light intensity, the temperature and the inclination of the substrate surface. However, except the material properties (porosity, roughness and pH) all other experimental parameters have been constantly fixed [138]. The colonization rate $X_{(t)}$ is calculated from the law of "nucleation" and growth previously expressed, as an exponential equation [1]:

$$X_{(t)} = 1 - e^{-K(t-t1)^n} \quad [1]$$

where the covered area $X_{(t)}$ is given as a function of time t [day]. The rate coefficient K is a parameter related to the growth rate and it is constant for each material (it depends on materials physical properties). The time $t1$ [day] represents the latency time

before a chromatic variation occurs on the material surface. The Avrami's exponent n is a coefficient which can be reasonably assumed equal to 4 in case of phototrophic growth: three dimensions represents the growth and one represents nucleation rate assumed as constant [138], [139]. In order to represent the growth process also in case of non-complete biofouling, the original Avrami's law has been improved into a modified model [139]–[141] described by the equation [2]:

$$X_{(t)} = 1 - e^{-K(t-t1)^n} * \frac{A_c}{A_t} \quad [2]$$

Where A_c /A_t indicated final covered area ratio, and expresses the percentage of covered area at the end of the growth process. *Ac* is the covered area by algae at the end of the accelerated growth test, and A_t is the total area of the sample exposed to biofouling.

The parameter *K* depends on the nucleation rate of algal cells and it is related to material properties. The modified Avrami's model, equation [2], for the biofouling modelling has been validated by several researches [139], [140], [142]. Specifically, Tran et al. [138] demonstrated that the Avrami's theory could be applied in order to simulate the colonization kinetic of mortar surfaces by algae, in an accelerated laboratory test and in order to calculate colonization rate on material surfaces, which depends in turn to material properties. These studies found that colonization rate X_t corresponds to a sigmoidal curve.

The experimental steps and results obtained through this work have been compared with the bio-colonization dynamics outlined by Avrami's laws. At the same way, solar reflectance values got at the end of the experimental trials run in this work, have been compared with the 2008 Title 24 provisional model results. That predictive formula has been designed to degrade the solar reflectance of a typical white single play membrane or white field-applied coating to an aged value:

$$\rho'_{T24} = 0.20 + 0.70\ (\rho_i - 0.20) \quad [3]$$

Where ρ'_{T24} is the overpredicted solar reflectance value according to 2008 Title 24 model and ρ_i is the starting value of ρ_{sol}. This model considers only soiling, and neglects processes such as UV bleaching and volatilization of additives. It also does not consider properties other than initial solar reflectance, such as material, roughness or spectral reflectance [97]. However it is used to predicts that soiling decreases the solar reflectance of a surface with ρ >0.20, such as a medium to light colored roof, and increases the solar reflectance of a surface with ρ <0.20, such as a black roof. Equations n° [2] and n° [3] have been involved to discuss and to interpret the results achieved in this experimental thesis work.

3. Main goals of the work

The phenomenon of biodeterioration of building surfaces has been deeply investigated when it occurs in natural conditions and over cultural heritage monuments and structures. At the same time, this phenomenon has been hardly reproduced in laboratory. Not all the previous attempts to define a procedure to expose surfaces to bio-growth through an accelerated way, have been compliant with two essential needs of both industrial and scientific world: repeatability and reproducibility. Neither the existing accelerated standard protocols (ASTM D7897) has been considered satisfactory in reproducing biodeterioration effects on materials. However, especially in hot and humid regions, the growth of biofilm on building surfaces represents an issue to solve in terms of aesthetical and energy points of view. To overcome the challenge of durability for highly reflective material products, industrial producers and manufacturers need new reliable and repeatable protocols to study bioaging through laboratory procedure in short time.

Considering these assumptions, this study is firstly aimed to develop a laboratory procedure able to induce biological colonization on new building materials in a repeatable way, in order to quantify the loss of energy, relating it with the biological growth. The study wants to build and define a setup, reproducible in other laboratories, able to test the behavior of different cool building materials exposed to biological aggression. The definition of a repeatable protocol is essential to test the resistance of different building materials to biofouling. At the conclusion of the bioaging setup development, the definition of a possible standard procedure draft has been described in the Annex I.

This first goal is strictly practicable through the reduction of the experimental test duration, which normally requires many years through natural exposition. Once the bioaging setup would be defined, this work will define the correlation between Avrami's model and the bio-growth behavior observed in this experimental study. The second goal is indeed to isolate and define the parameter *K* for each kind of involved materials. It represents the criterion, depending to the surface features, which indicates the resistance to the biological colonization for each product type. The definition of parameter *K* could be the measurement of the quality of a material against biofouling: as higher is the parameter *K*, as less resistant is that surface to biofilm growth.

Lastly, the biodeterioration of surfaces in urban backgrounds has raised a complementary view on the phenomenon: if on the one hand, the growth of organisms is a problem for the urban structures, on the other hand, atmospheric pollutants, which represent an abiotic stress for living organisms, could affect the microbial community. Thus, a third aim of this study is to understand the role and the effect of a standard atmospheric pollutants solution on the biology of phototrophic organism. After the direct exposition of green algae and cyanobacteria to the pollutants mixture, the production of metabolites has been analyzed in order to quantify the abiotic stress induced in these organisms.

4. Materials and Methods

4.1. TIS bioreactor prototype: experimental bioageing system

The experimental setup includes a bioreactor based on Temporary Immersion System (TIS), the Plantform bioreactor (Figure 6a), (http://www.plantform.se/pub/), used as bioageing chamber, where a basket with holes of 1 mm in size, placed into the chamber, holds material samples to expose to the bio-ageing process. The system consists in a sealed growth vessel made of transparent polycarbonate, with the size of 180 × 160 × 150 mm where immersion and internal ventilation cycles are regulated by two separate air pumps, each connected to a timer, as shown in Figure 6b [143]. A frame with four legs is placed above the basket to avoid the basket to rise when air pressure is applied to the bioreactor. The basket is made so that the material samples are only immersed into the liquid medium when air pressure is applied to the bioreactor: this last has three opening holes for medium supply, aeration and ventilation.

Specially designed hollow screws provided with silicone seals are fitted tightly within holes. Connected to these screws are flexible plastic Tygon tubes, with an inner diameter of 3.2 mm, and 0.22 μm polytetrafluoroethylene (PTFE) filters to ensure that the airflow in and out of the bioreactors are sterile.

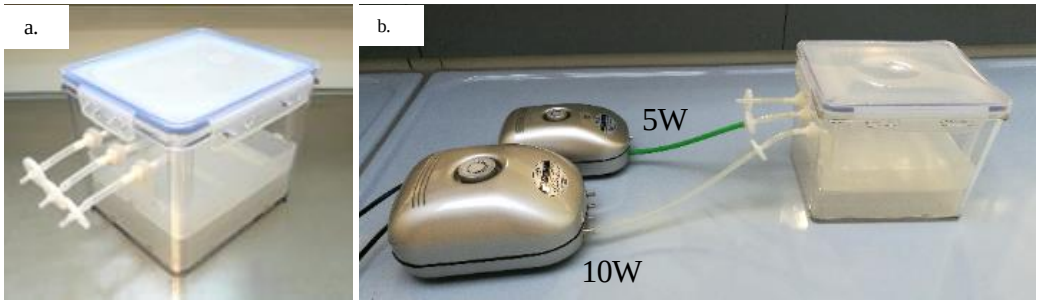

Figure 6: a) TIS bioreactor with three PTFE filters; b) TIS bioreactor linked to pumps: 5W pump introduces air through the green tube and the medium filter directly into the liquid medium; 10W pump introduces air through the white tube and the external filter into the sealed bioreactor, increasing internal pressure and pushing the air out through the third filter.

Figure 7 is a graphical explanation of immersion and ventilation cycles. Each cycle is regulated by two separate air pumps, each connected to a timer and linked with a PTFE filter through the plastic tube [143]. Material samples are placed inside TIS chamber on a plastic tray, after a biocidal treatment with UV-C rays (253.8 nm) for 30 minutes, using a UV-C Lamp placed at 80 cm over the materials surfaces. When the pressure induced by the first pump is applied to the middle filter, the nutrient solution is forced upwards and covering the material samples. When pressure is relieved, the nutrients were drained back through the internal basket [143]. In order to facilitate air

to go out from the tube connected to the middle filter an electrovalve is applied. Only material samples are immersed into the liquid medium when air pressure is applied to the bioreactor. The number and the duration of samples immersions can be set by a timer, previously configured, according to the research needs and the level of biocolonization required. Each bioreactors is autoclaved at 121 °C for 20 minutes at 1 atm before use.

This "*flood and dry*" system is able to promote a homogeneous contact between the materials surfaces and phototrophic organisms through a temporary and complete immersion of samples into the liquid medium and the following air-drying cycle.

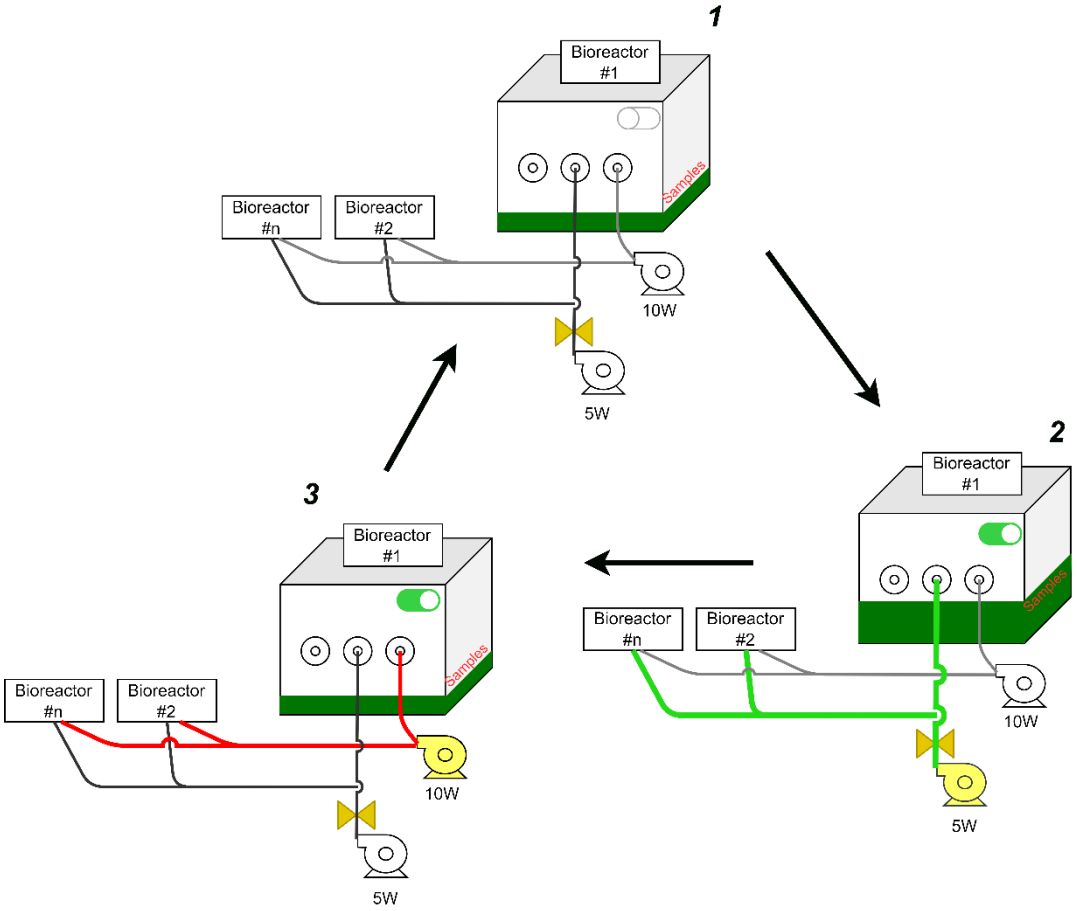

Figure 7: "*Flood and dry*" cycle run with TIS bioreactors. Step 1, *stand-by*: Each TIS bioreactor is linked with both 5W and 10W pumps through medium and external PTFE filter respectively. Pumps are off and material specimen on the tray of the bioreactor are dry; this step can last between 12 to 4 hours. Step 2, *flooding*: 5W pump is turn ON through the automatic timer; air is blown through the medium filter into the liquid (containing phototrophs organism), which raises its level submerging the specimen; this step can between 30 to 10 minutes. Step 3, *drying*: 5W pump is turned OFF, and 10 W pump is turned ON: the air is blown through an external filter raising internal pressure of the system and pushing down the liquid growth medium under specimen level; this step lasts 10 minutes. Afterwards the cycle begins again following the time schedule of the timer. One or more bioreactors could be linked to the same pumps and timers; an electro valve is applied to help the pump work.

The number and the duration of liquid medium immersion has been studied and defined from time to time through different trials. All bioreactors were maintained into a climate chamber with the 14 hours photoperiod. Light conditions have been changed across different experimental trials to define the best condition for the repeatability of the proposed bioageing protocol. Light intensity was measured in terms of Photosynthetically Active Radiation (PAR) with Delta Ohm LP471RAD probe. More details about environmental conditions tested will be provided and explained in the following sections.

Each bioreactor was filled up with 600 ml of Blue Green-11 or Bold's Basal medium liquid culture medium (PhytoTechnology Laboratories®, USA), specifically formulated for *in vitro* growth of cyanobacteria or algae respectively, depending to the species used in each trial. Media were always autoclaved at 120°C, 1 atm for 20 min after pH adjustment and before use. All the operations were performed in a laminar flow hood (Thermo scientific, MSC Advantage) in order to keep the sterility across the laboratory procedures. The culture medium was inoculated with a fixed amount of cyanobacterium or algal species, taking il from a sterile mother culture with a cell concentration range of $2x10^6$-$2x10^7$ cell/ml. Cells number at the beginning and during each experimental trial has been monitored in order to define the best starting cell concentration according to the aim of the work. Cells count was performed using the Sedgewick Rafter chamber under a light microscope (Nikon, ECLIPSE 80i 20X magnification).

4.2. Species of phototrophic organisms

Different cyanobacteria and algae species have been involved across the several experimental trials: all of them have been reported in Table 2.

Table 2: Cyanobacteria and green algal taxonomy details used during the development of experimental bioaging system.

Genus and Species	Phylum	Culture collection strain	References
Nostoc commune	Cyanophyta	https://www.ccap.ac.uk/ Code: 1453/33	[144]
Gloecapsa sp.	Cyanophyta	http://www.ccap.ac.uk Code: 1430/2	[145]
Edaphochlorella mirabilis	Chlorophyta	http://www.acuf.net/ Strain n° 038	[146]
Klebsormidium flaccidum	Charophyta	http://www.acuf.net/ Strain n° 065	[147]

Microorganisms and algal strains have been chosen according with their proved presence in urban contexts and because of their wide distribution in different types of

terrestrial environments [13], [27], [52].

As previously discussed, most of the organisms involved in the biodeterioration of building surfaces are phototrophic organisms, particularly some species of cyanobacteria and algae. Because of their resistance, they have probably a greater ecological importance as pioneer organisms on building surfaces than any other class [33], [36]. Many authors have identified the communities of cyanobacteria and algae localized at the surface of building or monuments material. Several *taxa* have been reported to colonize urban surfaces, and they have been identified through molecular analysis (DNA extraction and PCR amplification) [1], [27], [68], [148]. Phototrophic biodiversity on building surfaces can be extremely wide and it depends on the bioreceptivity of surfaces, the climate and geographical features of the area and also the microclimate on surfaces. Among the large diversity and variability of pioneer organisms, which have been isolated on natural exposed surfaces, this study selected the groups which have been most frequently found and identified in temperate or humid climates. Several papers have been checked in order to choose ubiquitous species, isolated in urban environment , on surfaces of cultural heritage, building roofs and walls [7], [13], [14], [27], [36], [50], [149]. Two *genera* of cyanobacteria have been selected: *Nostoc* and *Gloeocapsa*, often reported by authors as subaerial particles which settle down on surfaces and provide the organic source to the following more complex biocenosis, formed by heterotrophic organisms (as fungi) [150]. *N. commune*, moreover, creates macroscopic colonies in natural habitats with filaments embedded in a matrix of extracellular polymeric substances (EPS), mainly polysaccharides [46]. These seem to give to cyanobacteria an important role in the stabilization of cells in the air-dried state, inhibiting the fusion of membrane vesicles during desiccation and acting as an immobilization matrix for secreted enzymes, which stay fully active after long-term air-dried storage [47], [48]. The production of EPS by *Nostoc* genus seems to be essential to protect the organism itself from a range of physical as well as biological stresses. These biological features make *N. commune* a great candidate to apply it to experimental bioaging system: the group is widely spread across different ecosystems and climatological areas, it is highly resistant to abiotic and biotic stresses thanks to EPS production and extremely adaptable to *in vitro* conditions. *Gloeocapsa* species have been isolated on several painted surface in urban areas [30]. *Edaphochlorella mirabilis* and *Klebsormidium flaccidum* have been often involved in previous research works concerning the biodeterioration process for their common presence on building facades [36], [132], [151]. *E. mirabilis* is a unicellular alga belonging to the Division Chlorophyta, while *K. flaccidum* is a filamentous pluricellular alga which belongs to the Division Charophyta; this last is also studied for its high resistance to UV radiation [152]. Both chosen algal species are able to live into freshwaters, wetlands and soil ecosystems; furthermore, they have showed a high capability of reproduction rate in *in vitro* conditions thanks to their high adaptability. Generally, criteria applied for species selection have been the following [151]:

- *representativeness*: the chosen species are regularly quoted in the literature;
- *growth rapidity*: the selected species are able to develop rapidly in favourable conditions;
- *easy-growing in liquid culture*: the selected algal species are easy to homogenize in liquid culture, that has allowed to control the quantity inoculated into supports.

4.3. Biological growth and analysis

Biological growth parameters have been monitored during the total duration of each experimental trial, according to different quantification methods. Cyanobacteria and algae growth rate into the liquid medium was estimated by measuring absorbance, cells number count, pigment concentration and biomass weight. A rate of liquid culture was collected from each bioreactor at different time during the trial and used to monitor biological growth. Absorbance (Abs) was measured with UV-Vis Spectrophotometer (Jasco, V-730) reading 1 ml of culture medium at 750 nm, according to Chioccioli et al. [153]. Absorbance measurement at 750 nm is widely used to monitor algal growth, being inexpensive and reliable: it avoids the absorption of light by cellular pigments (chlorophyll and carotenoids) and it is treated as a pure light scattering measurement [153]. The growth rate (number of cell division per day) was calculated applying the following formula:

$$Abs750 = [\ln Abs_1 / \ln Abs_0]/(t1 - t0) \quad [4]$$

where t_1-t_0 represent the considered time range and Abs_0 and Abs_1 are the values read at 750 of liquid growth medium at t_0 and t_1 respectively.

The total pigments extraction was performed in order to measure organism's growth within the unit of liquid medium and to correlate it to the fraction of the colonized area on the samples. A fixed amount of liquid culture medium was drawn every three days; biomass was then collected through a filtration apparatus on 47-mm-diameter membrane, made of mixed esters of cellulose, with pores of 0.45 μm . Fresh biomass was then weighted with an analytical scale (Kern, d=0.1mg) into pyrex tubes prepared for total pigments extraction according to Lichtenthaler (1987) [154]. All prenyl pigments, as chlorophylls and carotenoids, are fat soluble compounds that can be extracted from water-containing cells by organic solvents such as acetone, methanol or ethanol [154]. 100% of absolute acetone was used as extraction solvent: 1 ml of solvent was added to the biomass, the mixture was grinded and vortexed to homogenize it for 30 minutes (BioSan mini-shaker). Then, the tubes were centrifugated at 5000 rpm for 5 minutes (Thermo scientific, SL 8R) and the supernatant was recovered into a second tube. Two following extractions have been run in order to extract as many pigments as possible. Then, all the supernatant fractions were mixed and the absorbance measured with UV-Vis Spectrophotometer . The equation used to determine chlorophyll *a* and *b*, and total carotenoid concentration are based on the specific absorption coefficients in

absolute acetone, according to [154]:

$$Chl\ a = 11.24A_{661.6} - 2.04A_{644.8} \quad [5]$$

$$Chl\ b = 20.13A_{644.8} - 4.19A_{661.6} \quad [6]$$

$$Chl\ a + b = 7.05A_{661.6} + 18.09A_{644.8} \quad [7]$$

$$C\ x + c = \frac{1000A_{470} - 1.9C_a - 63.14C_b}{214} \quad [8]$$

Where:
Chl *a* = is the amount of chlorophyll *a* (µg/ml of biomass extract solution)
Chl *b* = is the amount of chlorophyll *b* (µg/ml of biomass extract solution)
Chl *a*+ *b* = is the sum amount of chlorophyll *a* and *b* (µg/ml of biomass extract solution)
C *x*+ *c* = is the amount of total carotenoids (µg/ml of biomass extract solution)
A = absorbance reading at specific $\lambda_{(nm)}$values.

4.4. Building material products

Three types of solar reflective materials for building surfaces have been involved in this investigation (Figure 8):

- factory-applied single ply cool white membrane (WM)
- white asphalt shingle (AS)
- field-applied cool white paint (WP)

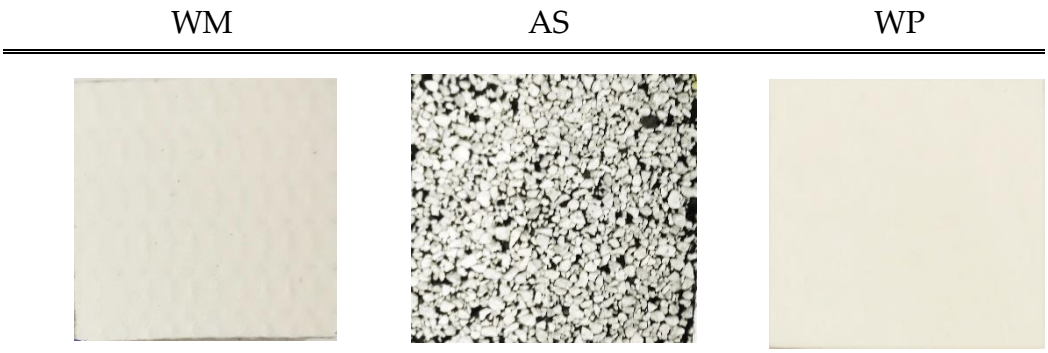

Figure 8: Building material samples used across all the experimental trials: new samples (before each type of deterioration process) of factory-applied single ply cool white membrane (WM); white asphalt shingle (AS); field-applied cool white paint (WP).

These materials have been chosen because widely applied to new buildings, representing the most common types of cool materials applied in the urban context (https://coolroofs.org/directory).

Most of the experimental trials have been run using these type of materials; each specimen involved has come from the same industrial batch, in order to reduce as much

as possible the variability among specimen surfaces under analysis. Each sample was 4 cm x 4 cm sizes and each of them was placed on the tray into the bioreactors before to be submitted to the bioageing treatment, according to the experimental setup schedules.

4.4.1. Characterization of building materials

Material characterization was performed on each sample surface before and after the bio-ageing test measuring Solar Reflectance (ρ_{sol}) and color changes (ΔE).

Solar reflectance was assessed through both instruments UV-Vis-NIR Spectrophotometer (Jasco V-670) equipped with an integrating sphere, according to the ASTM Standard E903 [155] and Solar Spectrum Reflectometer (Device&Services, SSR version 6), according to the ASTM C1549 [73]. UV-Vis-NIR Spectrophotometer was applied to measure randomly new samples and in some cases to analyze the spectrum of aged ones, in order to understand which part of solar spectrum was mainly affected by the biological colonization. Solar reflectometer was used to analyze ρ_{sol} before and after bioageing procedure of *all* specimens involved in *all* trials. Therefore, the results presented in the next sections correspond to ρ_{sol} measured according to ASTM C1549, if not otherwise specified. Beam normal spectrum E891BN spectrum is currently the most utilized standard for calculation of ρ_{sol} and it is employed via ASTM E903 and also into ASTM C1549 [156], [157]. A largely used hazy sky air mass 1 (AM1GH) is provided by the ASTM E891 standard [158]. Measurements performed with spectrophotometer were carried out over the 300-2500 nm wavelength range, with a spectral resolution of 5 nm. Reflectance measurements were calibrated by a Spectralon reference sample (Labsphere, SRS-99). Solar reflectance results are the average spectral distribution of the reflectivity of the sample. The integral values of solar reflectance were calculated by averaging the spectrum of the surface reflectivity (ρ_λ) measured in the range from 300 to 2500 nm spectrum of the solar irradiance ($I_{sol,\lambda}$), that is of the global solar radiation over a horizontal plane with air mass = 1, Equation [9] [74], [157].

$$\rho_{sol} = \frac{\int_{300}^{2500} \rho_\lambda I_{sol,\lambda} d\lambda}{\int_{300}^{2500} I_{sol,\lambda} d\lambda} \quad [9]$$

Solar reflectometer has been employed since after bioageing of surfaces, where biological colonization shaped different color regions on samples. Indeed, biofilm grown on uniform cool surfaces may turn them into variegated ones and the measurement of ρ_{sol} according to ASTM C1549 is preferred [73]. In this case, since the involved specimen have 4 cm x 4 cm size, which is an area similar to the measurement head of the instrument, ρ_{sol} was averagely calculated on all sample surface area for each measurement point.

Moreover, color changes induced by biofilm were also assessed in terms of L*a*b*

values, measured on both new and treated samples using a Colorimeter (PCE-CSM 3) according to UNI EN ISO11664-4 (CIE 1976). ΔE values were calculated by means of Equation [10]:

$$\Delta E = \sqrt{(L_1^* - L_2^*)^2 + (a_1^* - a_2^*)^2 + (b_1^* - b_2^*)^2} \quad [10]$$

Colorimetric method was sometimes applied to quantify the microbial growth on surfaces, especially when phototrophic organisms, such as algae, cyanobacteria and lichens are involved. This is a quick and nondestructive technique to estimate biomass and microbial activity based on color measurement [24][159].

Image analysis on each treated sample was performed using the ImageJ® software, and the area fraction covered by biofilm was thus calculated. The images were recorded by digital camera (Nikon 5000D) under the same conditions of light intensity. The 'K-Means-like' method is used to gather similar pixels of the image into sets, as found in previous works [160]. This method allows to identify *k*-clustering (gathering of the pixels into *k* classes) through criteria of nearness (color zones), where the number of pixels in each class can also be quantified. In this way, greenish pixels representing algae or cyanobacteria are grouped separately from the gray ones of not colonized zones. Figure 9 shows an example of image processing by the clustering method (Color Segmentation plugin) with separation into three classes: pixels corresponding to biological growth have been accurately separated from white background. Since organisms involved in this research work came from different species, their growth on surfaces showed different color intensities of the colonized area, which can also express a non-homogeneous density of organisms. For this reason, color clustering separation identified three or more classes on each sample, considering the aspect of the colonization. After the iterative process of putting the pixels into classes, each class is assigned one interval of gray level. The different pixels percentages for the classes matching colonized zones were added. The percentage obtained is the proportion of the slab area that is colonized. Colonization area percentage obtained at time *t* was indicated as $X_{(t)}$.

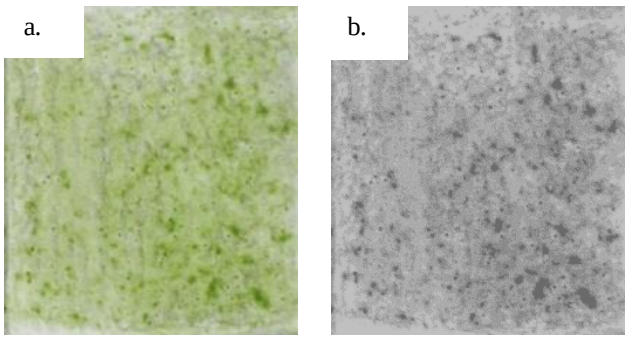

Figure 9: '*K*-Means-like' method applied on WP bioaged sample (a): colonization spots have been processed through *k*-cluster colors and the covered area fraction has been calculated (b).

Other physical and chemical parameters have been studied and measured on new products to have a detailed description of their starting features. In details, the

following properties have been analyzed: thermal emissivity (ε) using TIR-100 emissometer according to UNI EN ISO 15976 Standard [161], roughness measurements adhering to EN 10049:2013 are carried out by means of a DIAVITE DH-5 stylus tester. Five measurements per sample were recorded both for thermal emissivity and surface roughness for statistical reasons. The standard deviations (SD) was estimated from the five measurements. Micro-morphological analysis using a Scanning Electron icroscope (SEM, Oxford Instruments, XL-30) and semi-quantitative chemical analysis on surface composition through the Energy Dispersive X-ray Spectroscopy (X-EDS SEM system, Oxford INCA-350). The mean porosity values (%) of materials were provided from previous characterizations and materials producers datasheets [20]. All the physical and chemical features have been reported in Tables 3 and 4.

Table 3: Physical features of involved product specimen at t0 (before each ageing procedure). Porosity was determined according to EN 1062-3 and it is virtually zero on polymeric tiles (WM) and painted polymeric ones (WP). Asphalt shingle (AS) tile porosity was not determinable.

	Thermal emissivity [%]	**Roughness** [μm]	**Porosity** [%]
Single ply membrane (WM)	90±0.5	6.83±0.9	<0.05
White paint (WP)	89±0.4	10.90±0.3	<0.05
White asphalt shigle (AS)	87±0.6	30.39±2.2	ND

Table 4: Semi-quantitative analysis of surface elemental composition on WM, WP, and AS. Data are expressed as mean weight percentage of three sites of interests on each surface.

	C [%]	Na [%]	Al [%]	Si [%]	Ca [%]	Ti [%]	S [%]
Single ply membrane (WM)	90.0	/	/	9.8	/	/	/
White paint (WP)	82.5	/	1.9	2.1	8.2	5.3	/
White asphalt shigle (AS)	65.8	3.2	1.8	15.8	2.3	8.9	1.2

4.5. Statistical analysis

The experimental data were statistically analyzed through T-student test and the Analysis of Variance (ANOVA) considering a confidence interval of 95% (*p-value*<0.05). Siegel-Tukey test has run in order to compare different experimental setups and find out any significant differences among repeated trials. Correlation analysis and R^2 calculation have been applied to establish the correlation between biological growth and colonization area rate. Statistical elaborations were performed with Past3 Software. Standard deviation (SD) and Coefficient of Variation (*CV* %) among repeated trials were calculated as defined into UNI ISO 11095:2010:

$$SD = \sqrt{\frac{\sum(X - \mu)^2}{N}} \quad [11]$$

$$CV\ (\%) = \frac{SD}{\mu} * 100 \quad [12]$$

Where:
SD= Standard deviation of measurements
CV = Coefficient of Variation
X = a single measure value
μ = relative mean of measurements
N = number of samples

The statistical tests and analysis run in this work are necessary to the repeatability assessment.

The physical parameter used to calculate the repeatability and the following uncertainty of the bioageing method purposed is the solar reflectance, the main property to evaluate the energy efficiency of cool surfaces. According to ASTM E177 [162], repeatability is the precision determined from a multiple test results conducted under the identical conditions by a single, well-trained operator using one set of equipment [18]. It is a means for quantifying the uncertainty in the observed difference between identical samples submitted for analysis to a single laboratory. The repeatability limit (*R%)* is applied to assess repeatability. According to the not statistical interpretation of this value, *R%* is the maximum differences between two test results obtained under specified conditions, and it can be attributed to the test method precision. Repeatability coefficient is calculated as:

$$R(\%) = 2.77\ x\ CV_p \quad [13]$$

where 2.77 is a constant value obtained by multiplying the inverse of the standard normal cumulative distribution for a confidence interval of 95% (which is k=1.96) by the square root of 2, as some Authors have been considered for ageing experimental setup evaluation [18], [162]. The repeatability coefficient is a precision measurement which represents the maximum value below which the absolute difference between two repeated test results may be expected to lie with a probability of 95%. The 95% confidence interval is the range of values that contains the true mean of the values at 95% of probability. CV_p is the average of the coefficients of variation for each of the three products: it is a statistical measure of the relative dispersion of data points in a data series around the mean [163]. CV_p is also considered as a simple standard measure of uncertainty of ecosystem variables [164]. Uncertainty (U) of measurement is defined by ISO 15189 as '*a parameter associated with the result of a measurement that characterizes the dispersion of values*' or, by the International Vocabulary of Metrology (VIM) - Basic and General Concepts and Associated Terms (VIM, item 2.26) as a '*non-negative parameter characterizing the dispersion of the quantity values being attributed to a measurand*'. The Evaluation of Measurement Data - Guide to the Expression of Uncertainty in Measurement (usually referred as the GUM) provides general rules for evaluating and expressing uncertainty in measurement [163].

The measure of uncertainty is given by the amount of errors around an average value of a data set: in other words, U is the best estimate of how far an experimental data might be from the "true value".

Since this is an experimental work, where the "true values" of solar reflectance on bioaged specific surfaces (WM, AS, WP) are not available, U has been calculated considering the distance of repeated measurements from the average values. According to the previous definition, the lower is the value of U, the more accurate is the method. One of the first goal of the work, is the development of a *repeatable* bioageing protocol, then the evaluation of bias become a critical aspect to assess the effectiveness of the research. Considering the high variability of a system that entails the biological factors, the objective of the work is to achieve the threshold of 10% of uncertainty and to get a maxuimum R coefficient of 10%. It means that experimental setup and experimental data will be considered acceptable when U (%) and R (%) values will be below than 10%: if they will be higher, it means that the system could not be assess as repeatable.

4.6. Experimental design

The experimental work has been organized in three main chapter, as shown in Figure 10 (green boxes): *Development, Definition and Application* of the accelerated bioaging procedure, the topic of the entire study. The first section, the *development* of a repeatable procedure, involves the main number of the experimental trials (I-IV), since it explores several numbers of possible experimental setups and environmental conditions. After the first trial, the following ones have been designed considering the previous trials achievements and results. In this way, each trial has been useful to implement, step by step, the bioageing setup, in order to reach the best solutions and conditions. The different environmental factors or experimental variables, which have been studied primarily in each trial, have been claimed (yellow boxes): these are chosen in each case always considering the previous trial outcomes. Once the acceptable repeatability threshold has been reached, and verified through three repeated test, the biodeterioration procedure has been defined. Collected data about the bio-colonization trend have been then compared with Avrami's model to define *K*-parameter and find out the resistance criterion of each material product. Finally, the experimental bioageing setup has been applied running the same procedure on building material samples previously treated with biocidal coatings.

These three main sections have been enriched with other side-researches (red boxes): the first one has the aim to study the influence of soiling mixture, used to mimic the pollutants deposition on urban surfaces, on green algae growth. The determination and quantification of specific secondary metabolites produced by algae and cyanobacteria, could contribute to understand the effect of abiotic stress. The second side-test is represented by the natural ageing exposition of the same material products involved in the laboratory trials. Since the natural ageing has a minimum duration of three years, it is currently ongoing. However, preliminary data obtained until here have been elaborated and compared with those obtained with accelerated experiments, in order to understand if any time-correlation would be possible.

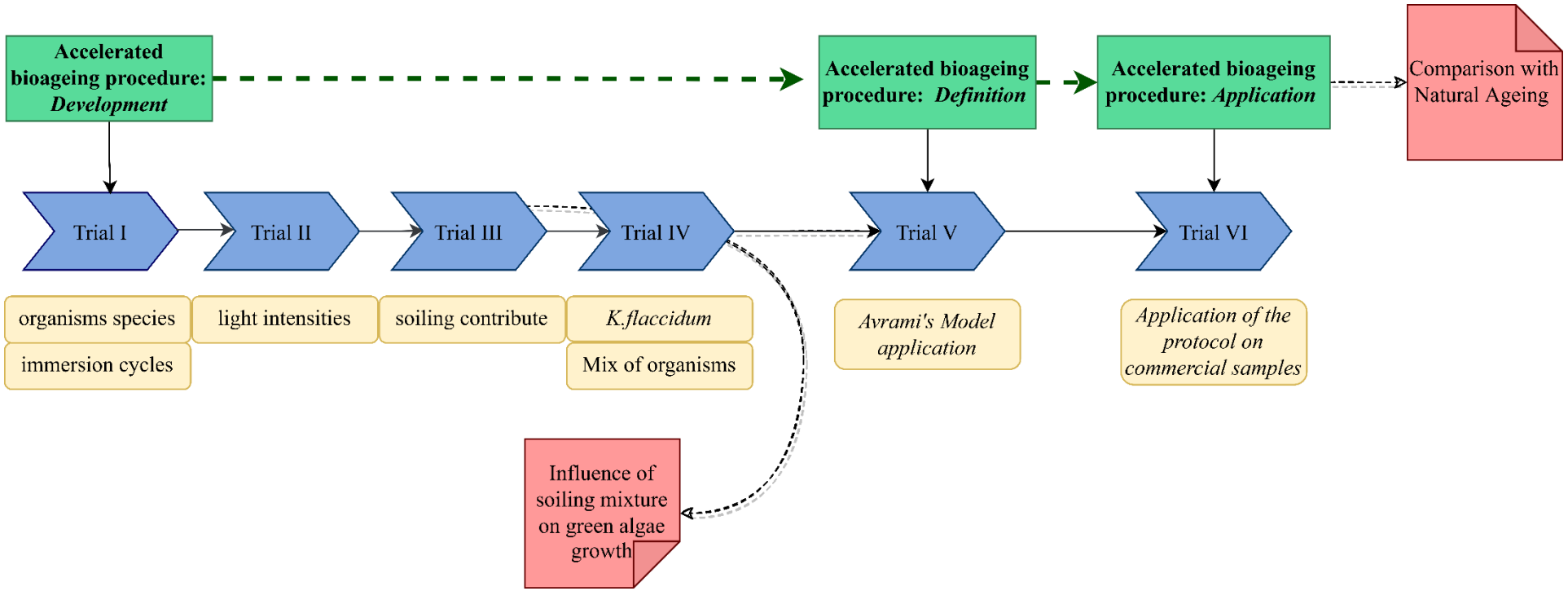

Figure 10: Experimental design of the entire research work. Green boxes are the "red-line" sections: Development, Definition and Validation; each section involves one or more Trials (blue boxes); two other side-researches have been involved in this thesis (red boxes).

5. Experimental Trials

5.1. Trial I – *Development* of accelerated bioageing procedure: immersion time and organism species

The first trial run in this research work has been essential to understand which environmental factors mainly influence the growth of phototrophic organisms into the bioreactor. Trial I describes the preliminary setup studied in this research design: each trial has been useful for TIS bioreactor system optimization and definition of the final procedure. Two essential experimental variables have been studied in the following tests: duration and intensity of samples exposition and organism species to involve.

Materials and methods

Trial I considered two types of building materials: Asphalt shingle (AS) and white single ply white membrane (WM). TIS bioreactor, described in section 4.1, was applied as bio-ageing chamber. After sterilizing procedures previously described two samples for each type of material have been put into each bioreactor, filled with liquid culture medium and inoculated with phototrophic microorganisms. One species of cyanobacterium and one species of green algae have been considered in order to compare their eventually different behavior during the colonization process, *Nostoc commune* and *Edaphochlorella mirabilis*, inoculated separately in thebioreactors. Each bioreactor was filled with 600 ml of BG-11, at the concentration of 1.68 g/L (BG-11, PhytoTechnology Laboratories®, USA) or 600 ml of BBM at the concentration of 0.705 g/L (Bold's Basal Medium, PhytoTechnology Laboratories®, USA), depending on species inoculated: *N. commune* in BG-11 and and *E. mirabilis* BBM. Sulfuric acid (1ml/L, 0,1%) was added to BBM, then pH was adjusted to 5.5–5.7 before autoclaving. An inoculum of 10 ml from sterile mother culture, at starting cell concentration of 2x107 cells/ml for cyanobacterium species and 3x106 cells/ml for green alga species, was added into each bioreactor. This first investigated bioageing setup was planned as showed in Figure 10: TIS system has been scheduled to run 4 immersions of 10 minutes per day. TIS bioreactors were put into a growth chamber (Biolog, AG-System) at 23±1°C under cool white fluorescent light (light intensity, 30 – 90 μmol/m2 s), and a 14-h photoperiod. Total bioageing procedure lasts three weeks and it was run in triplicate. The decrease of solar reflectance and colorimetric values on bio-aged samples have been measured before and after bioageing procedures as described in 4.4.1 section. Colonized area on each sample was calculated at the end of three weeks of trial, according to K-Means like method. In this trial I, data about the growth of cyanobacterium and green alga have not been collected.

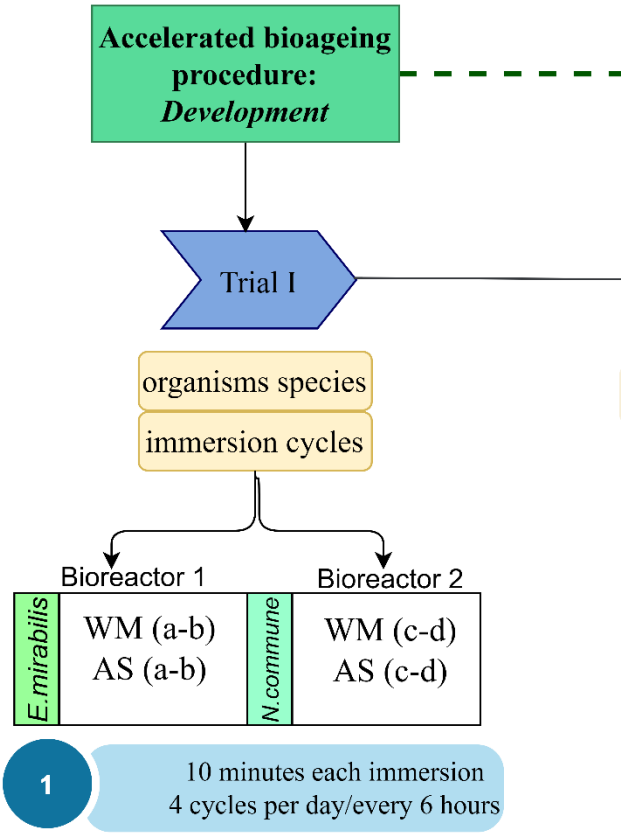

Figure 11: Trial I experimental details: 2 bioreactors were prepared in each test, one of them was inoculated with green alga *E. mirabilis* (two specimens of each product type are involved, named a-b); while the second one was inoculated with cyanobacteria *N.commune* (two specimens of each product type are involved, named c-d).

Results

The images of the samples at the end of bioageing treatment have been reported in Figure 12, where both cyanobacterium and green algae colonization were presented. *N. commune* and *E. mirabilis* seem to settle down and grow on surfaces creating areas of different shapes, especially observable on WM samples. *E. mirabilis* forms small and spread circular colonization areas, while *N. commune* was more homogenously distributed on the surface. This could be related to the different cells aggregation and colonies form between the two species: the green alga has spherical cells which are grouped together; cyanobacterium forms multicellular filamentous colonies [165].

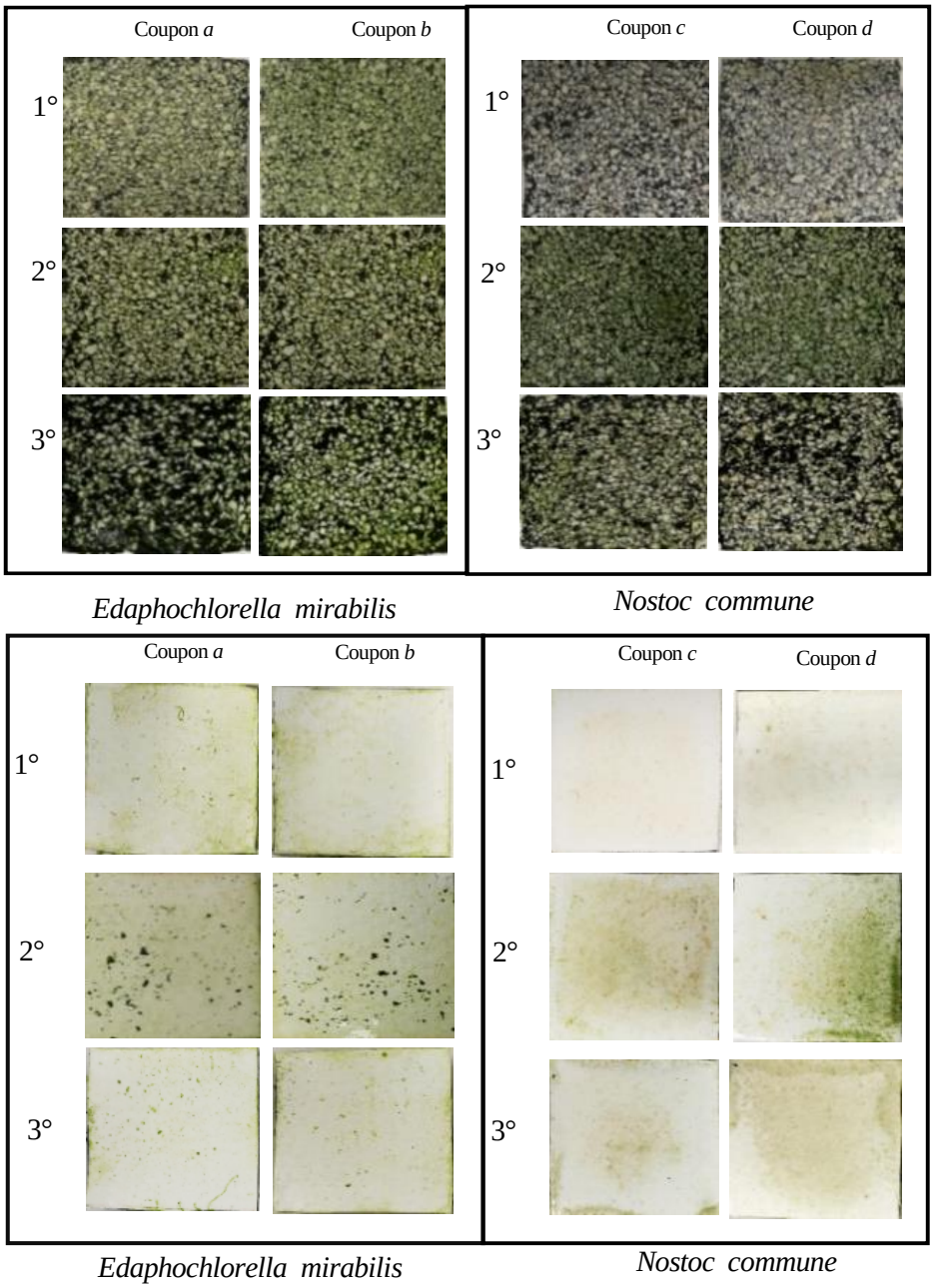

Figure 12: Images of building material specimens after 3 weeks of laboratory bioageing trial into TIS bioreactor system. Samples are shown in clusters by material type: asphalt shingle (AS) and white single ply membrane (WM) and according to the two organism species: cyanobacterium *N. commune* and green alga *E. mirabilis*. Two samples for each material type (*a,b* and *c,d*) are shown.

Colonized areas on all samples were measured through to *K*-Means like method applying the *Color segmentation* plugin provided by ImageJ; the area covered by different species have been compared through T-test statistical analysis (Figure 13): the colonized area ($X_{(t)}$) by *N. commune* on WM sample type was significantly higher than area covered by *E. mirabilis* (*p-value* <0.05). A significant difference was not observed on AS samples, where the growth of two different species did not show variability (*p-value* >0.05).

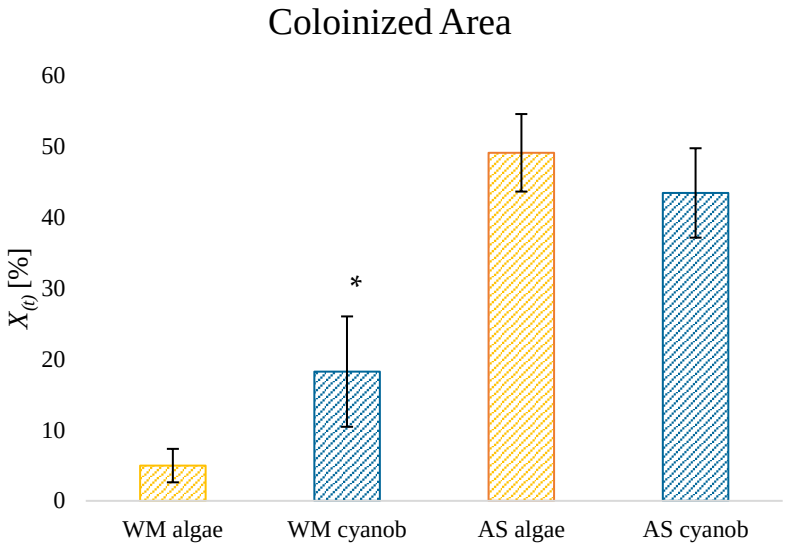

Figure 13: Mean colonized area percentage ($X_{(t)}$) over WM and AS material samples. The results are the mean calculated over 6 coupons from the same material type and the same organism species used as colonizer: two coupons aged into each bioreactor for 3 repeated test; SD is shown.

Differences in colorimetric values (ΔE) values are reported in Figure 14. While for WM samples, six coupons have been considered, this was not possible for AS samples, where only 4 coupons were involved in statistical analysis since 2 of them have been damaged (the ones from the third test). T-test did not underline any significant differences among ΔE; this may be due to high standard deviation obtained within repeated tests.

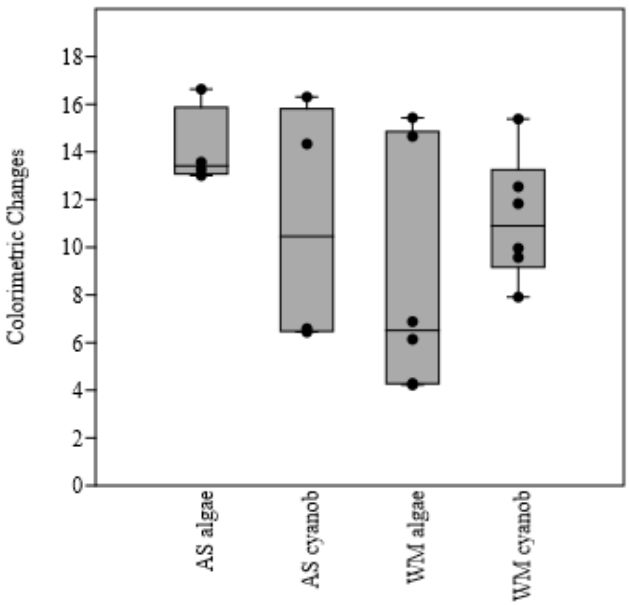

Figure 14: Boxplot of ΔE values obtained over WM and AS samples. Distribution of data corresponds to ΔE obtained over 6 samples for WM and over 4 samples for AS; SD is shown.

Solar reflectance decrease was higher on AS samples compared with WM samples and this is coherent with the size of colonized areas. Not significant differences (*p-value*>0.05) in $\Delta\rho_{sol}$ have been found between AS colonized by *N. commune* and that one colonized by *E. mirabilis.* These two microorganisms seem inducing a similar average solar reflectance decrease: 5.7%±1.4 and 7.0%±2.2 respectively. However, standard deviation among repeated tests was too high to get an adequate repeatability. Solar reflectance decrease on WM samples highlights a different pattern: *N. commune* colonization provided a significantly higher $\Delta\rho_{sol}$ compared with *E. mirabilis* one: 5.8%±0.7 and 3.2%±0.5 respectively (*p-value*<0.05) (Figure 15).

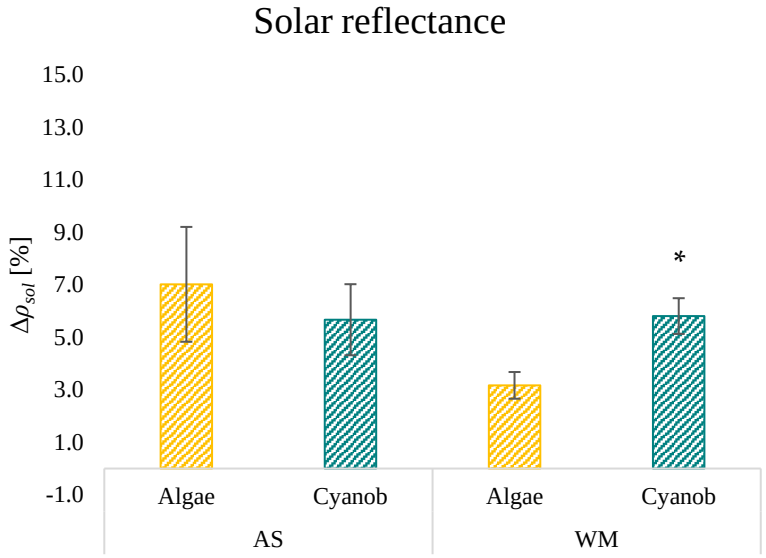

Figure 15: Mean decrease of solar reflectance (% $\Delta\rho_{sol}$) obtained over WM and AS material samples. Data correspond to the average of 6 samples for WM and 4 samples for AS; SD is shown.

Discussion

This first experimental trial has considered separately two different microorganism species. Achieved results were heterogeneous and outlined some first considerations about this first experimental procedure. Different species have provided different colonization rates on surfaces, and this is in agreement with previous researches as [151] where various results in the growth of Chlorophyceae and Cyanophyceae have been obtained. Specifically, the only significant data from this first setup underlined that *N. commune* seems to induce a considerable level of biological colonization on WM samples, compared with *E. mirabilis.* On the contrary, this last did not cover a significant area on materials, neither solar reflectance decreases. AS resulted highly susceptible to biological colonization, considering the high percentage of covered areas obtained on all aged samples. However, other factors could have influenced the repeatability of the experimental setup, as immersion times and light intensity. As described in section 4.5., the repeatability coefficient was evaluated considering the mean CV_p of final ρ_{sol} values

achieved on products involved through different organisms' colonization. Statistical results showed that the variability is too high to consider this first experimental setup acceptable: CV_p was 19% and the calculated uncertainty overcomes the target of 10%. The high variability is probably due to the different light intensity since repeated trials are exposed randomly to different flux of photons into the growth chamber. This environmental factor, indeed, seems to deeply influence the biological growth into the bioreactor medium and on surfaces [166]–[168]. It is known that cyanobacteria, for example, have several environmental drivers, such as water temperature and irradiance: light intensity is a particularly important factor of the growth for cyanobacterial blooms and their growth patterns respond to different light intensities via morphological and physiological changes [169]. Cyanobacteria and ubiquitous species of micro algae as genus *Edaphochlorella* have been adapted to respond to different radiation intensities (depending on the climate and micro-climate conditions of a specific geographical area) [44], [170].

Intensive radiation could represents an abiotic stress source for phototrophic organisms, which are induced to change their metabolites production, also increasing their antioxidants compounds production, as carotenoids or other pigments classes [1], [171]–[173]. The capability of the organisms involved in this study to change their metabolites production and their growth rate depending on external light conditions represent then the starting point of the next experimental trial (Trial II) run in this work. Hence, different light intensities have been applied to bioageing system and studied separately, in order to isolate the best irradiance for the experimental purpose. This first trial showed also how *E. mirabilis* and *N. commune* could differently behave and colonize surfaces: *N. commune* reveals higher rates of colonized areas (on WM samples) and induces a higher decrease on solar reflectance (on WM samples) compared with *E. mirabilis.* Besides these observations, *N. commune* is largely applied in laboratory works on biodeterioration of surfaces [151] and widely descripted as one of the ubiquitous organism in urban environments and surfaces worldwide [22], [34], [36], [44], [149]. Cyanobacteria are considered the pioneering inhabitants in the colonization of environmental surfaces as stones [27], [50], painted surfaces [53] and other building materials [36]. Furthermore, cyanobacteria are assessed as the most important colonizers since they are not dependent on any organic source of carbon and are very resistant to environmental changes [149].

These evidences has led this research to focus the biodeterioration process only on cyanobacteria, restricting the experimental variables to just one phototrophic organism species: *N. commune,* which is the only involved in the next experimental trial, where different light intensities are studied. The last observation about this first trial is about the number of immersion and ventilation cycles: four cycles allow the organism to adhere on the surfaces. However, the spots and colonies grown on materials resulted yellowed colored, in particular cyanobacterium ones. This could indicate that the cells growth occurred under abiotic stress [171], [173]. For this reason, more cycles have been scheduled in the following trial in order to provide more air exchanges to help and to optimize the organism growth.

5.2. Trial II - *Development* of accelerated bioageing procedure: the influence of light intensities on *N. commune* growth

Different irradiance values have been considered for TIS bioreactors exposure in this second experimental trial, in order to understand better which light intensities would be the optimum to achieve a more homogenous biological growth for repeatability purposes. As other studies have already underlined, the light regime under which cyanobacteria, and in this case *Nostoc* genus, should be taken into consideration because it affects the biomass growth and metabolites production [166]. Indeed, varying light intensity and photoperiod pigment production changes, resulting in phycobiliprotein, such as phycocyanins or carotenoids accumulation depending to low or high light intensity applied respectively [167]. For cyanobacteria, different pigments accumulation or metabolites production becomes an essential parameter to keep under control in order to achieve replicable colonization rates and comparable changes in physical and optical properties. Figure 16 shows the technical details of Trial II.

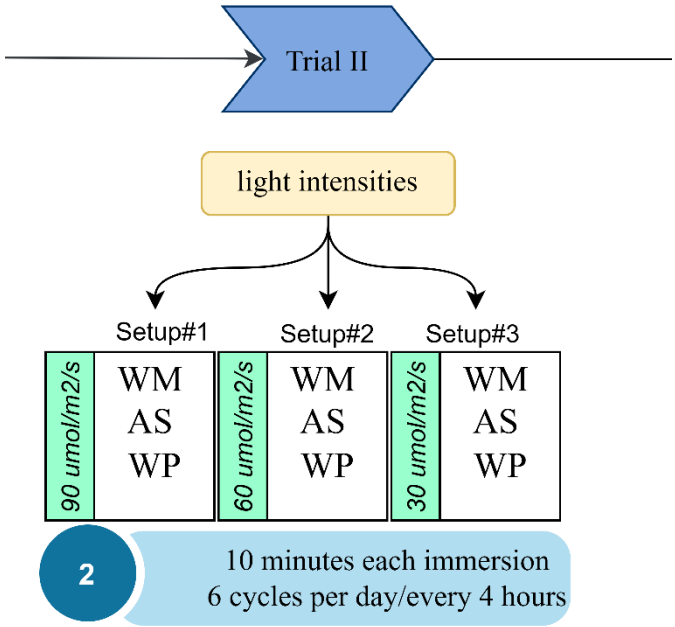

Figure 16: Trial II experimental details: 3 bioreactors were prepared in each test, each of them was exposed to a different light intensity. Setup#1: 90 µmol/m²/s; setup#2: 60 µmol/m²/s, setup#3: 30 µmol/m²/s. Three material types have been involved (WM, AS, WP) and two coupons for each type have been insert into each bioreactor. Six "flood and dry" cycles were scheduled every day.

Materials and methods

Temporary Immersion System bioreactors were used as bioageing device, filled with 600 ml of BG-11 liquid culture medium, at the concentration of 1.68 g/L. Sterile culture medium was inoculated with *Nostoc commune*. The inoculation was made with 10 ml of *Nostoc commune* of sterile mother culture, at starting cell concentration of $2x10^7$ cells/ml. The mother strain was grown in BG-11 medium and kept at 24±1°C into the incubator (AG System, Biolog-Lux). TIS bioreactors were maintained in a growth chamber at 24±1°C, under cool white fluorescent light, and 14h photoperiod. Three different light intensity conditions, measured in terms of photosynthetically active radiation (PAR), were applied to identify which one provided the best condition for the growth of cyanobacterium and the repeatability of the procedure:

1) setup#1 is set to 90 μmol/m²/s of photons;
2) setup#2 is set to 60 μmol/m²/s of photons;
3) setup#3 is set to 30 μmol/m²/s of photons.

Immersion and ventilation cycles were scheduled as showed in Figure 14: TIS system has been scheduled to run six immersions lasting ten minutes per day: immersion times have been extended with respect to the previous trial. Here, three types of solar reflective building materials were involved: a factory-applied single ply cool white membrane (WM), white asphalt shingle (AS) and a field applied cool paint (WP), as described in section 4.4. After the exposure to UV-C ray for 30 minutes each side, two coupon for each material type have been input into each bioreactor.

A complete test lasted three weeks and each setup type has been run in triplicate to get statistically significant results. The results about solar reflectance decrease, biological colonized area fraction and colorimetric values were reported in next paragraphs.

Results

Different light intensity conditions of setup#1, setup#2 and setup#3 resulted in not-negligible macroscopic differences among the three material types and among repeated trials results, as shown in Figure 17. Indeed, different dark green patches occurred on the surfaces in correspondence of the colonized areas. Generally, the biological growth had a significant bloom, and the most part of material samples have been interested by an intense cyanobacterium colonization. All setup types provided significant differences (*p-value*<0.05) among repeated trials in terms of colonized area. Setup#1 got the lowest average variability in terms of percentages of covered surface: 17.9±9.3% on WM; 36.2±21.2% on WP, and 65.0±11.0 on AS, even if it remained high.

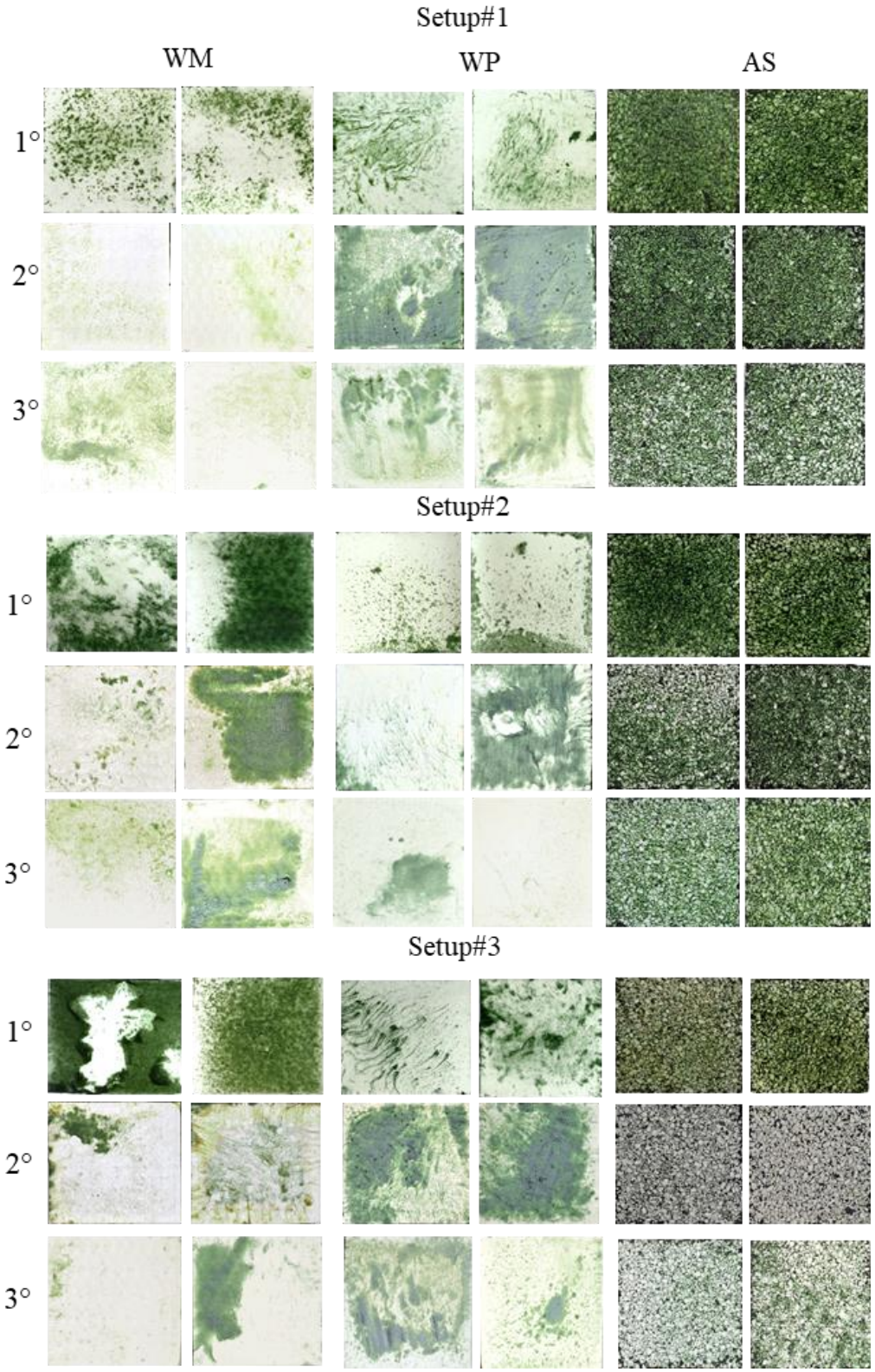

Figure 17: Images of samples after three weeks of laboratory bioageing exposure through three different setup: #1, #2, #3. Samples are shown in clusters by type: asphalt shingle (AS), cool single ply membrane (WM), and field applied cool paint (WP); images of all repeated tests have been reported and two coupon for each material have been processed during each trial.

The changes of the solar reflectance ($\Delta\rho_{sol}$) between new samples (t0) and after 3 weeks of bioageing exposure (t1) were averagely lower for asphalt shingle (AS) samples and higher for white paint (WP) and single play white membrane (WM). Mean results about $\Delta\rho_{sol}$ from setup#1 have been shown in Figure 18. Specifically, mean $\Delta\rho_{sol}$ got under 90 µmol/m²/s was 9±1% on AS samples, 11±5 % on WM and 24±6 % on WP samples. Coefficient of variation have been calculated among the values of relative aged solar reflectance. *CV* was quite high for each material types and did not ensure the repeatability of the results, in particular *CV* from setup#2 and setup#3 overcame always 10% for WM and WP; while for AS was 7%. The uncertainty of setup#2 and #3 was always higher than 10%, achieving even the 30% on WM product type. However, setup#1 (90 µmol/m²/s of photons as light growth condition) has provided the lowest *CV*% among setups in term of the bioaged solar reflectance: *CV* calculated on AS was 3.6%, 9.1% on WP and 7.1% on WM. The value of *U* on repeated test run through setup#1 were 14% and 18% for WM and WP respectively, while it remained under 10% for AS. Despite of setup#1 showed some improvements to statistical analysis of collected data, the uncertainty values could not consider the procedure repeatable, in particular for white samples: variability was very significant on WM and WP specimens. The statistical analysis underlined the effects of little light intensities changes in the variability of phototrophs growth.

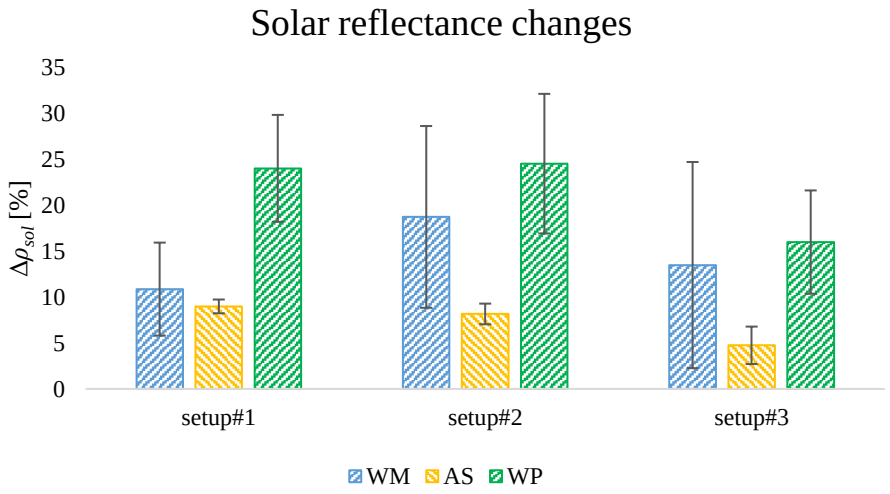

Figure 18: Mean decrease of solar reflectance (% $\Delta\rho_{sol}$) for setup#1, setup#2 and setup#3. All material types (AS, WM, WP) are shown. Data are the mean of six coupon: two coupon run in three repeated test. SD are shown.

Results about colorimetric changes had a trend similar to solar reflectance one: ANOVA highlights significant differences among ΔE values among repeated trials (*p-value* <0.05) within the same material type, with the exception of setup#1 run on WM sample where *p-value* was 0.1. This means that the difference in colorimetric values was negligible on bioaged WM samples run through setup#1. Considering setup#1, highest mean ΔE values were achieved on WP samples, where the decreases of solar reflectance was deeper. ΔE values obtained were 37.9±13.2, 31.7±6.5 and 17.9±9.9, measured on WP, AS and WM bioaged samples, respectively.

Discussion

Results of experimental Trial II have highlighted how biological colonization dynamics on surfaces is highly variable and it remains hardly repeatable through laboratory procedures. Beyond the intrinsic variability of biological growth, repeated trials run through different setups has signed that also small changes in light conditions can influence the microorganism growth and consequently the surface colonization. Despite the hard challenge to make repeatable a highly variable phenomenon as the growth of phototrophic organisms, this trial gave some considerable findings and results. The experimental conditions defined through setup#1 seems to provide better environmental conditions compared to the other tested light intensities. Nevertheless, the differences of solar reflectance and colorimetric values on most of the bioaged samples were significantly distant within repeated tests. These data underline how it is strictly necessary to optimize and carefully define and manage each single environmental parameter to study bioageing on surfaces through a laboratory protocol. The lower values of $\Delta\rho_{sol}$ and ΔE on AS samples, despite of the highest colonization area percentage compared to other studied materials types, depends on the lower starting solar reflectance value on new AS sample, which was 0.3±0.01, compared to the initial values measured on WM and WP samples, which were respectively 0.82±0.01 and 0.88±0.02.

Analyzing all the reflectivity spectra obtained on bioaged samples, it is evident that the abatement of reflectance mainly occurs in the visible waveband (Figure 19 a,b,c). A similar shape of the spectra was also found after natural ageing by Paolini and Zinzi [174]. The bioaged spectrum from white single ply cool membrane (WM) returned to its original shape between 1200 and 2500 nm (near Infra-Red region, NIR), as well as between 300 and 400 nm (UV region), and almost no variation has occurred in those wavebands. While, WP (field applied white paint) and AS (asphalt shingle) showed a shifted spectrum in NIR waveband. In particular, the AS spectrum was higher on bioaged sample, probably due to a bleaching effect on granules caused by the repeated flood and dry cycles. Instead, WP samples presented an opposite situation: the NIR spectrum was lightly shifted down, probably due to yellowed pigmentation that appears on the surface after the biological growth. The same reduction of reflectance in this spectrum waveband is a symptom of physical degradation, as described by Paolini et al. [174], a sign that the phenomenon of biodeterioration is occurring. *N. commune* did not colonize homogeneously the surfaces, covering different percentages of the whole area. Colored patinas widespread on surfaces have been already observed and widely described on building and monument surfaces in external environment [34], [52], [175]. These biofilm depositions have been identified to be the causes of remarkable modification on new surfaces, inducing aesthetic damage and losses in physical performances [1], [176]. In particular, white surfaces are mainly affected by green or dark colored colonies that severely induce a decrease in solar reflectance [129], [174].

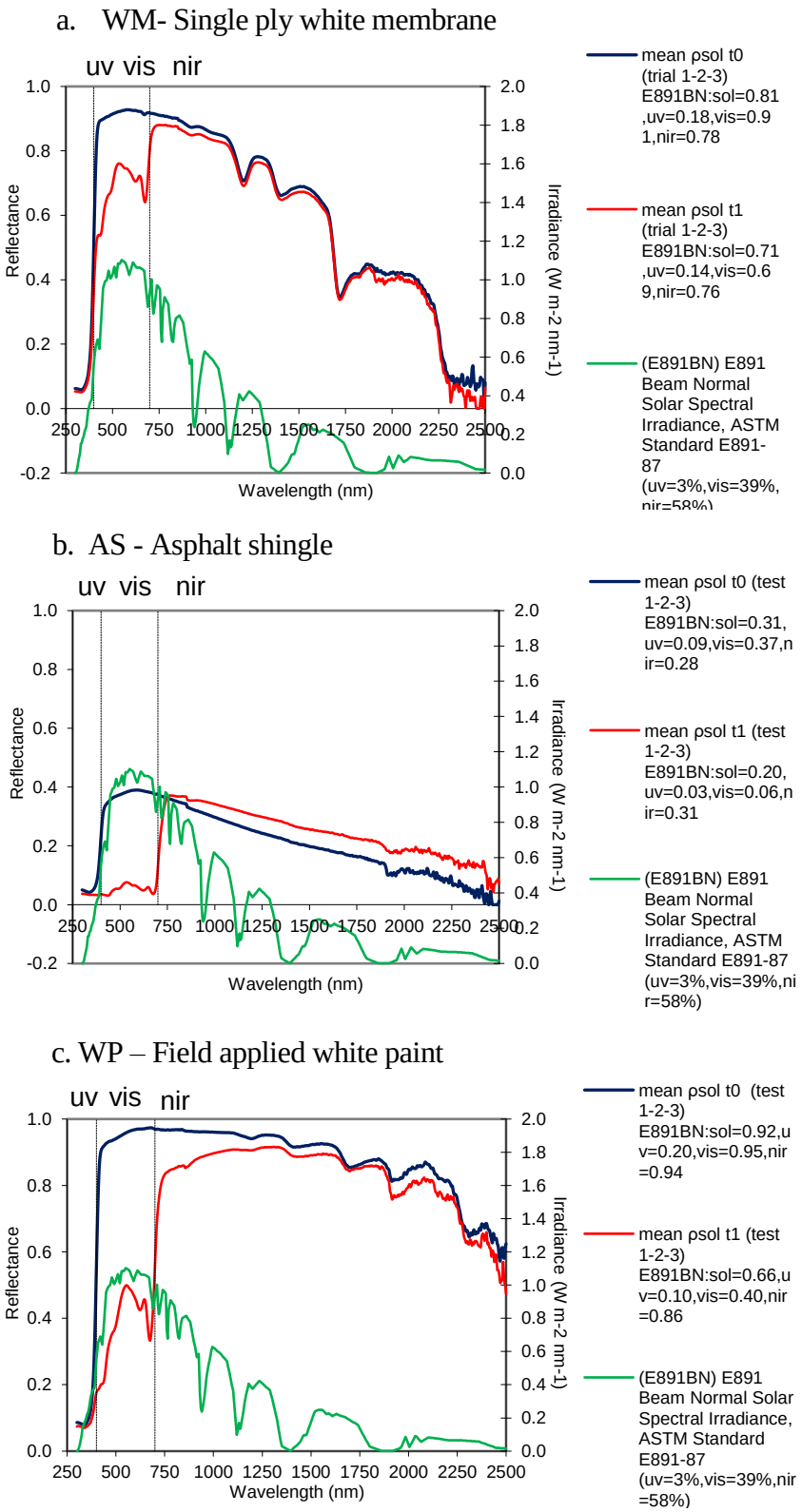

Figure 19: UV-Vis-NIR spectral charts of mean reflectivity on new samples (t0 - blue line) and on bioaged samples (t1 - red line). Data are the mean ρ_{sol} measured after three repeated tests on six coupon for each product: a) WM, b) AS; c) WP. All the spectra came from setup#1 and have been acquired by UV-Vis-NIR Spectrophotometer (Jasco, V-630).

The decrease in solar reflectance was eventually correlated with the colonized area, in order to understand if any possible cause-effects relationship could be hypothesized. This correlation has been defined for all sample types. Results have been reported in Figure 20: a positive correlation (R^2) between $\Delta\rho_{sol}$ and percentage of colonized area exists for WP and WM material types, where always $R^2>0.8$. Differently, AS did not show the same trend between the colonization rate and the decrease in solar reflectance: $R^2<0.6$ indicates a weak correlation. This was due to the lower initial ρ_{sol} values, which is not subjected to a sharp ρ_{sol} decrease in case of green covering.

The positive correlation found on white products, highlights the importance to take into account a potential biological colonization when surface properties of building materials are estimated.

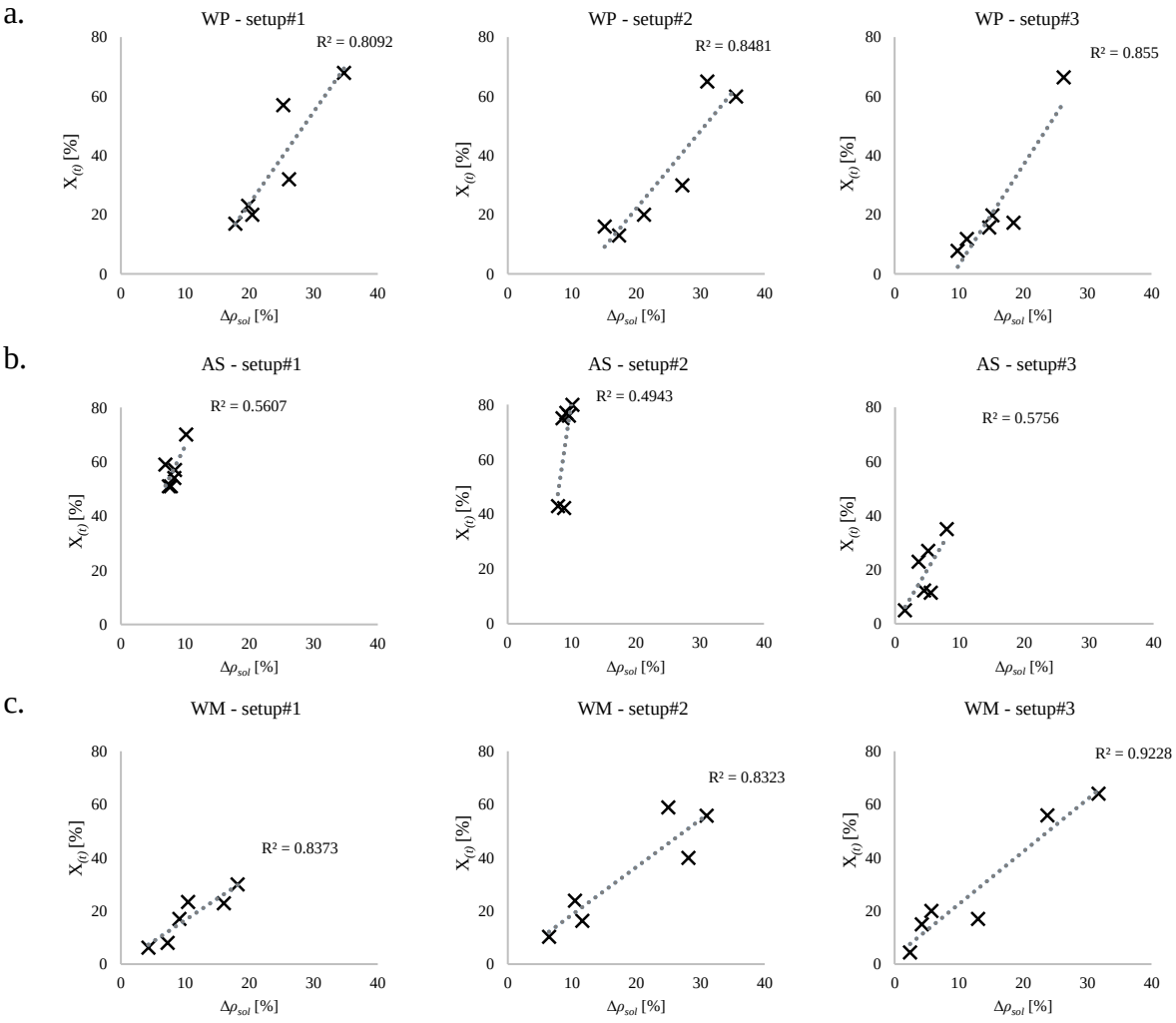

Figure 20: Linear correlation and related R^2 values between change of solar reflectance ($\Delta\varrho_{sol}$) and percentage of $X_{(t)}$ by cyanobacteria. a) WP cluster ; b) AS cluster; c) WM cluster. All data are means of three repeated tests.

The hypothesis formulated to explain the high variability of biological growth and their heterogeneous colonization rate on surfaces regards the position of lights source

into growth incubator. The ability of light regime to affect cyanobacterium growth is already proved by other authors [166], [169]. Thus, next experimental trials have been implemented through the management of light suorces, achieving the same intensity over each point into the growth chamber.

5.3. Trail III - *Development* of accelerated bioageing procedure: Could soiling influence biological growth on surfaces?

The previous Trial II showed how light setting and its management is a critical point for the development of an accelerated bioageing procedure since the biological growth variability mostly depends on lights availability and intensity. Many Authors have analyzed the influence of different light intensities on cyanobacteria and algae growth and their metabolites production: many studies identified a range between 60 and 200 μmol/m²/s photons as the optimum to cultivate these types of organisms [169], [177], [178]. Then, a mean light intensity of 100 μmol/m²/s of photons was applied in this experimental Trial III, according with scientific literature. Moreover, the chosen light intensity is very close to the light irradiance of setup#1 of the previous Trial II, which is resulted better than the other ones in terms of repeatability (90 μmol/m²/s).

A second goal was here discussed: the bioageing procedure applied on new cool material samples was applied in series with the soiling procedure of ASTM D7897, in order to mimic a complete process of cool materials deterioration. The aim was to study the effects of biocolonization on the same samples previously exposed to 'standard' (accelerated) soiling deposition [124]. Some findings, indeed, proved that the deposition of atmospheric particulate matter on surfaces stimulates microbial growth [179], [180]. Soil, dust or organic particles which have been deposited and accumulated on built surfaces can represent the concept of surfaces secondary bio-receptivity as described in [181]. Samples may be interested by dust and atmospheric matter deposition; subsequently, microorganisms settle down on surfaces and their growth can even be encouraged by organic and inorganic pollutants, which supply growth substances [21], [25]. Some studies have showed that the first visible biological development begins generally after about one year of exposure, when the dust and particulate matter layer has been deposited on surfaces [13], [174], [181].

Thus, Trial III wanted firstly to study the repeatability of the bioageing procedure applying a light intensity of 100 μmol/m²/s, changing the position of light source in order to uniform the photons emission. The second purpose was to induce fast biological colonization on samples previously aged through Standard method ASTM D7897. The attempt was to reproduce, through the accelerated procedure, the whole soiling process, which includes deposition of atmospheric black carbon, dust, and organic or inorganic particulate matter, as well as the growth of microscopic organisms. This trial has been divided in two following Phases: the physical and optical properties changes obtained on soiled samples (Phase II) have been compared with the results obtained on new samples (Phase I) in order to discuss the influence of soil deposition on biofilm growth, already observed in literature. Figure 21 shows how the tests of Trial

III have been scheduled according to the claimed aims.

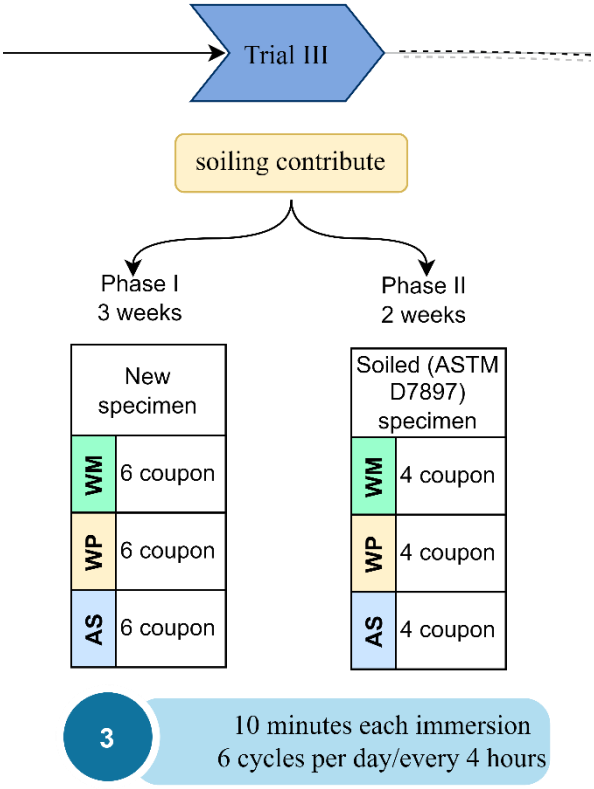

Figure 21: Trial III experimental details. During phase I, *new* material samples have been exposed to bioageing procedure for three weeks: one bioreactor for each product type with six coupon were involved. In phase II, *soiled* material samples have been exposed to bioageing procedure for 2 weeks: one bioreactor for each product type with 4 coupon were involved. Three repeated tests are run for each phase.

The influence of soiling mixture on biological growth has been studied in a sided trial (explained din Section 5.4.1).

Materials and methods

Trial III was composed by two following phases: in the first one (Phase I), bioaging procedure was run on *new* samples and in the second phase (Phase II), the same procedure was applied on *soiled* samples, for a different exposure time. The experimental protocol here applied was an implantation of the previous one, even if some features were maintained unaltered. TIS bioreactors were placed into a different growth chamber (Frigor Box, model 900 AT) at 24±1 °C and exposed to 14h of photoperiod. 600 ml of BG-11 liquid medium was prepared as nutrient solution for the growth of *N. commune*. Six immersion cycles per day were run, lasting 10 minutes each. The whole duration of each test was three weeks for Phase I and two weeks for Phase II and it was run in triplicate. Three bioreactors were prepared within each test, one for each material type (WM, AS, WP); each bioreactor contained six or four coupon of the same material type, depending on the Phase, as showed in Figure 21. Light source was a LED lamp (3F Linda LED 12W L660), set at 100 μmol/m²/s photons. Light source was placed over the bioreactors, so that beams can diffuse homogenously over the samples (Figure 22).

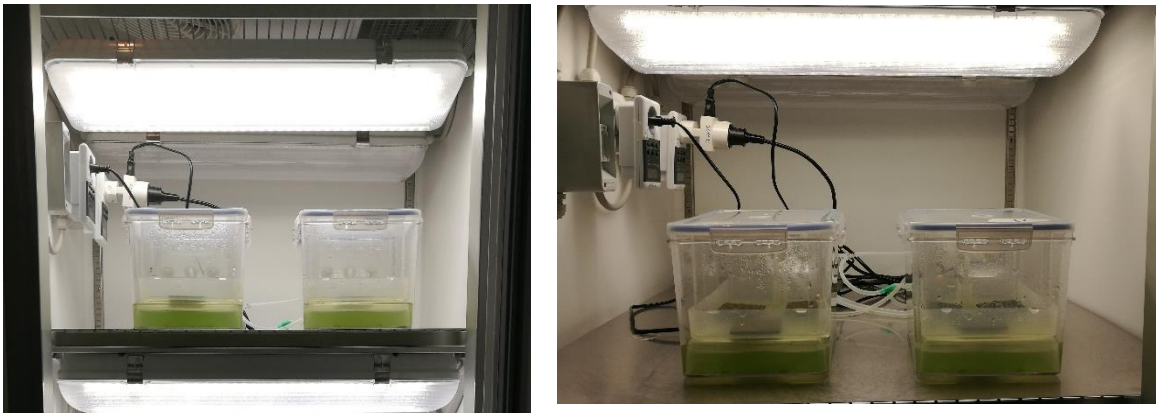

Figure 22: the internal shelves of growth chamber, Frigor Box, model 900 AT, equipped with LED lamps, emitting 100 μmol/m²/s photons. The position of LED lamps, placed in the central part of the upper part, made them able to spread the light uniformly. Some TIS bioreactor are showed in one of their possible disposals; behind them, pump system is placed.

During Trial III, both biological growth and physical parameters of samples surface were measured and monitored. Some samplings were performed at regular intervals of days during each experimental test. Sampling days were named t0-t1-t2-t3-t4-t5-t6, where t0 refers to the starting day of procedure (and identify the properties of materials before bioageing) and t6 refers to the last day of the test (in Phase I, while in Phase II, samplings have been stopped at t4). During each sampling day, one different material coupon was picked up to measure solar reflectance (ρ_{sol}), colorimetric changes and the fraction of colonization area, this last according to image analysis. Besides the material coupon sampling, a rate of liquid medium was sampled at each sampling day to quantify biological growth during the test. Biological growth was evaluated through biomass weight and pigments extraction for the absorbance measurement. Pigments extraction and quantification from cyanobacteria biomass was performed according to method described in section 4.3 of this work. The progressive concentration of pigments could be considered as an indirect measurement of growth into the liquid medium [182]: it could be then correlated with the colonized area and with the decreasing of solar reflectance. Collecting data about bioageing level across the duration of the test allowed building a progressive "*bioageing scale level*" where the colonization dynamic occurring on each material type was measured by collecting physical and biological data through time. High attention was paid to the repeatability of the test procedure: at the end of three repeated tests, the repeatability limit (*R*%) and uncertainty have been calculated.

Soiling procedure

In the second phase of the Trial III, the same experimental procedure described in the previous paragraph was applied also to *soiled* samples. WM, AS, WP coupon have been firstly exposed to soiling agents as disposed by [124]: black carbon soot, mineral dust, salts and organic acid, mixed in an aqueous suspension, as described in the ASTM D7897 Standard (ASTM International PA 2015). In details, dust is a solution of 0.3±0.02 g/L of iron oxide powder (purity ≥99 %, CAS: 1309-37-1; Sigma Aldrich) and 1±0.05 g/L of two natural clays, montmorillonite K10 and nanoclay hydrophilic bentonite, CAS: 1318-93-0; Sigma Aldrich), CAS: 1302-78-9; Sigma Aldrich). Inorganic salt solution contains a mixture 0.3 ± 0.03 g/L of sodium chloride (NaCl, CAS: 7647-14-5), 0.3 ± 0.03 g/L of sodium nitrate ($NaNO_3$, CAS: 7631-99-4) and 0.4 ± 0.03 g/L of calcium sulfate dihydrate ($CaSO_4 * 2H_2O$, CAS: 10101-41-4). Organic acids solution was prepared using humic acid (CAS: 1415-93-6) at 1.4 ± 0.05 g/L concentration. Soot was reproduced by a surrogate commercially available self-dispersible carbon black (Aqua-Black 001: Tokai Carbon Co., Ltd5); the concentration was 1.37 ± 0.05 g/L. Firstly a separate solution was prepared for each soiling agent. Later, the four soiling solutions or suspensions described above were combined to get a single soiling mixture, applied on surfaces to simulate the fouling material which occurs in urban contexts. The soiling mixture has been poured into an air-pressurized spraying tank (Figure 23), equipped with an air pressure gauge, maintained at 20psi. The vessel was connected with a tubing to a brass spraying nozzle that includes a strainer to minimize clogging. The soiling solution has

been homogeneously sprayed on coupon samples by means of a specifically developed soiling apparatus, calibrated to spray 8 ± 1 mg/cm² of wet soiling mass on each sample, according to ASTMD D7897 Standard (ASTM International PA 2015). Afterwards, soiled samples, here named WMs, ASs, WPs, were exposed to two weeks of bioageing treatment, as described above.

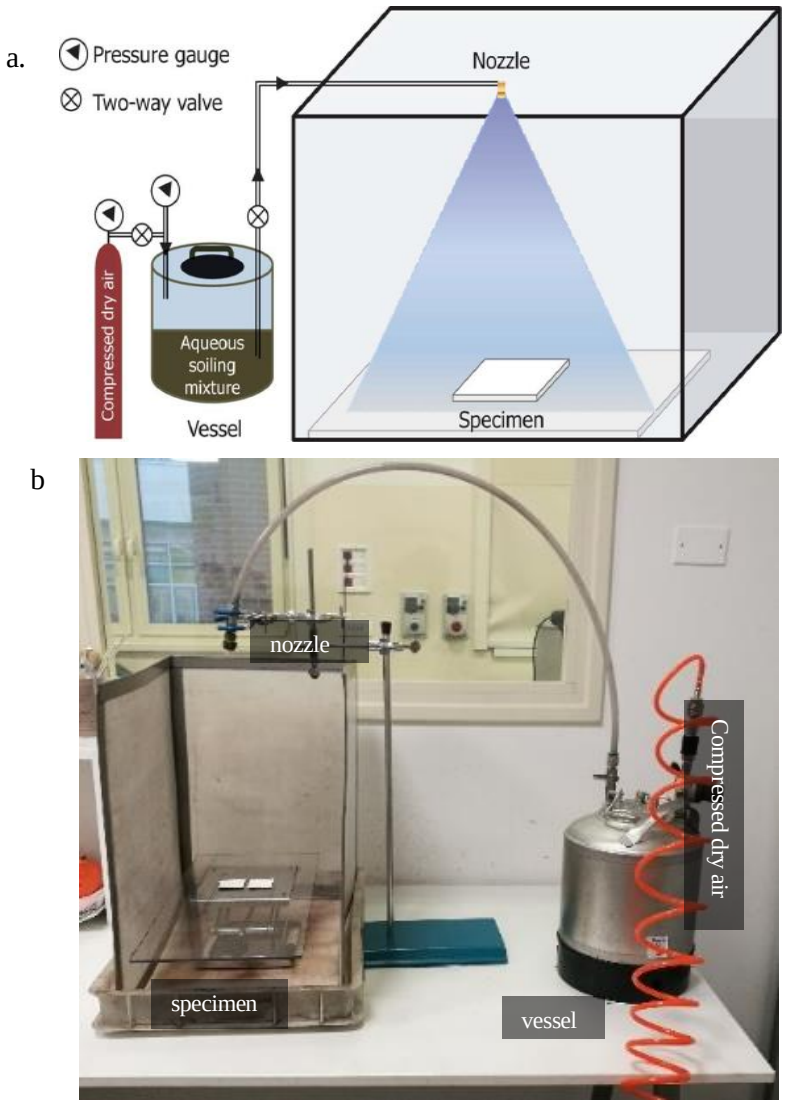

Figure 23: *a*) Apparatus used for laboratory soiling of roofing materials, designed by ASTM D7897 Standard [124]; *b*) Soiling apparatus applied in this work, equipped with each element shown in *a*).

Results - Phase I: Colonization rate on new samples

The progressive samplings of material coupon and growth medium have been carried out at regular intervals during the experimental trials and it has allowed to get a bioageing scale on surfaces. As shown in Figure 24 (a, b, c), the colonized area on the first coupon sampled (after 3 days from the starting of bioageing exposure) remained

meanly very low in all materials: 3±2% for WM and WP, 3.3±1.5% for AS. Then, colonization rate has started to increase and have a bloom during the second week of the trial (7th - 14th day): here the average of covered area fraction calculated on different materials was: 35.0±8.7% for WP, 48.3±11.4% for WM, and 49±9.6% for AS. At the end of the third week of exposure (21st day), the growth level on surfaces of the sixth coupon was mostly variable and irregular, indeed standard deviation results higher: 43.7±14% on WP, 56.3± 10.7% on WM, and 56.7±12.1% on AS (Figure 25). While on WP and AS biological colonization seems to grow progressively through time, this was not always true on WM specimens. Figure 25 shows that t5-coupon had a lower growth compared with t4-coupon, even if t5-coupon has been exposed 3 days more than t4-one. This underlines higher variability of colonization dynamic on single play white membrane.

a. WM – Single ply white membrane

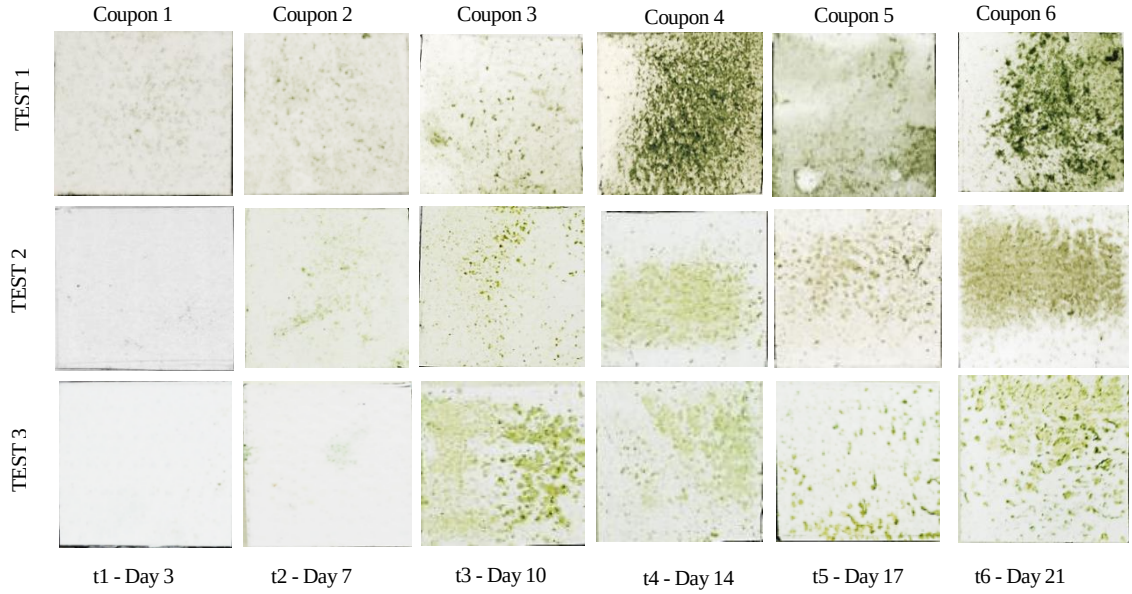

b. AS – Asphalt shingle

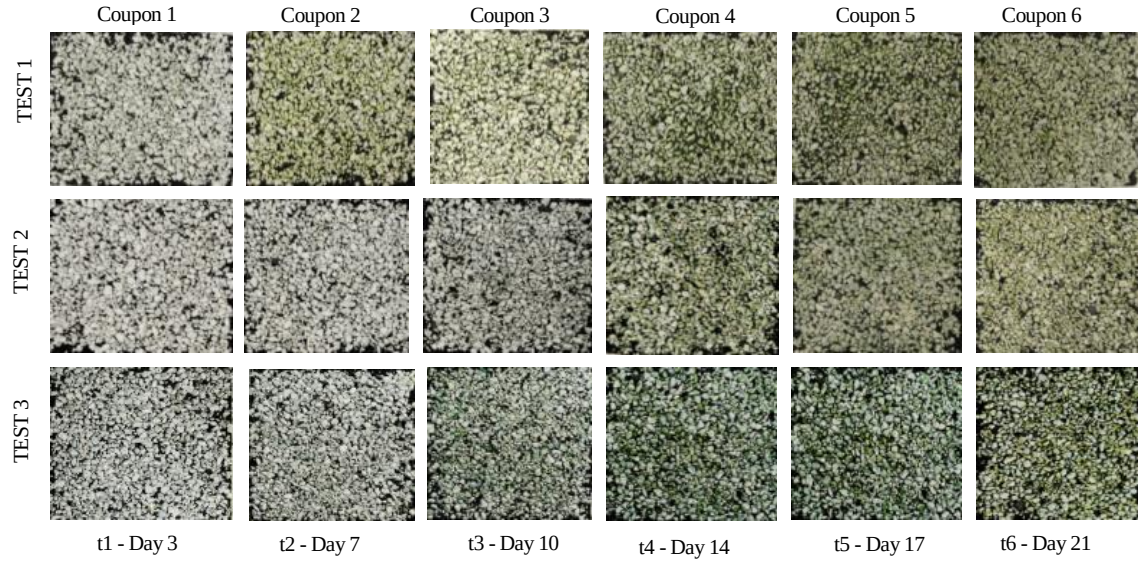

c. WP – Field applied white paint

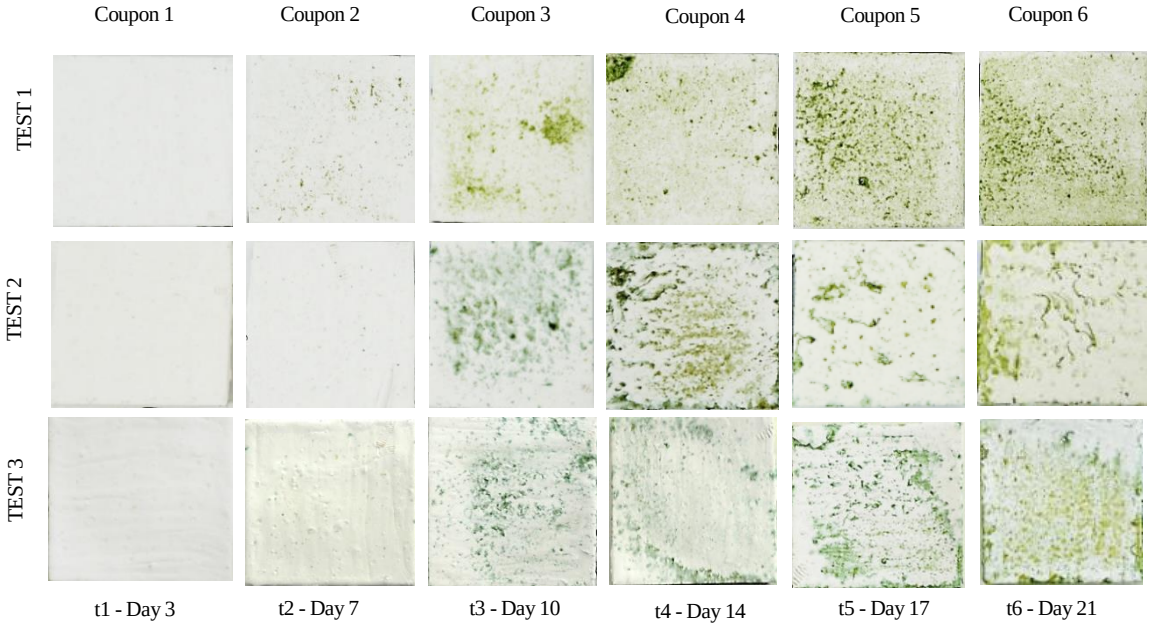

Figure 24: Progressive colonization rates (X_t) on building material specimens, during three weeks of bioageing procedure. Each coupon corresponds to a sampling day; t1-t2-t3-t4-t5-t6 are the six sampling performed across each repeated test. Covered area rates grow with the passing of time on Single ply white membrane samples (a), asphalt shingle samples (b) and white paint samples (c).

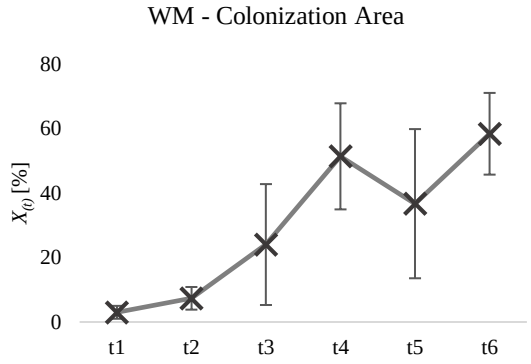

a.

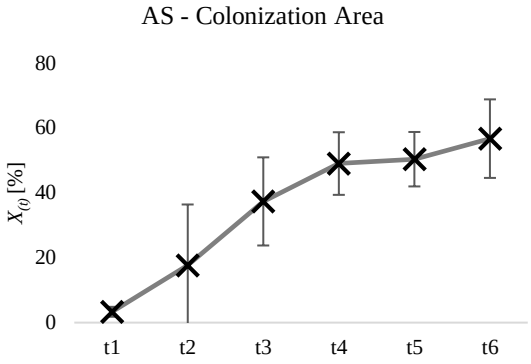

b.

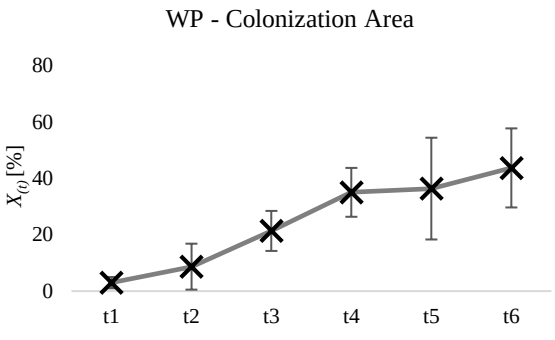

c.

Figure 25: Mean percentages of colonized area ($X_{(t)}$) during phase I repeated test; the analysis was perferomed through the image analysis software (ImageJ). Six sampling have been performed (t1-t2-t3-t4-t5-t6). SD is shown.

Solar reflectance trend followed the colonized area one, having a ~3% of decrease after 3 days on all materials, then the loss in solar reflectance became higher with the passing of the time, achieving their maximum between day 14th and day 21st (Figure 26). Specifically, the greater decrease occurred on WM samples, was 15.2±12.1% (at day 14th), 5.9±1.2% on AS and 11.3±3.5% on WP samples (at day 21st). Standard deviation among three repeated trials remained under 2% on AS material type, but not on WM and WP samples. Notably, WM presented high standard deviation on t4, t5, t6 specimens. The assessment of repeatability was performed through coefficient of variation, evaluated using data about final (t6) coupon. Results have showed that *CV* ranged from 4% to 10.3 %, with an average of 6% (*CVp*). The uncertainty was 12.6% and the repeatability criterion was 17.4%, which is still too high since the observed difference overcome the significance threshold set at 10%.

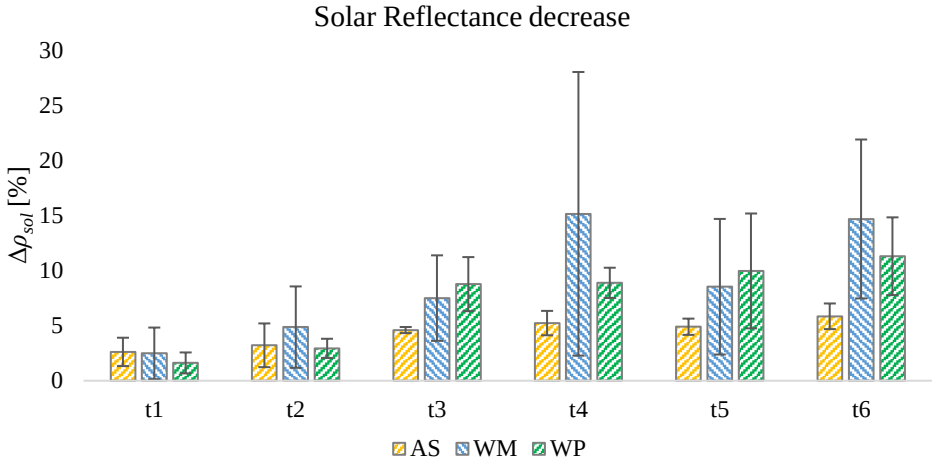

Figure 26: Progressive solar reflectance decrease ($\Delta\rho_{sol}$ %) obtained on each product type (WM, AS, WP) during the three weeks of bioageing exposure. Data are the mean values of three repeated tests. SD is shown.

Colorimetric measurements have been reported in Figure 27 and underline how the changes increase gradually until the day 14th, where ΔE values were 11.8±3.0, 26.2±18.9 and 12.8±6.2 for AS, WM, and WP respectively. Colorimetric values on WM samples show the highest variability after bioageing procedure, as already observed for solar reflectance changes. Generally, ΔE values did not follow the same trend on different product types: AS did not show any further significant increased value, while WM and WP have variable results. It must be noted that standard deviation outlined high variability on colonized WM and WP surfaces especially during the last week of test (from 14th to 21st day).

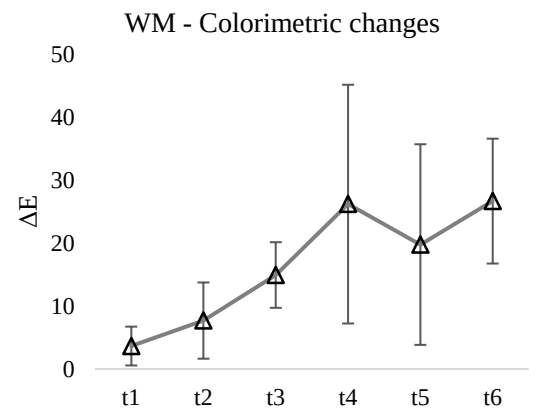

a.

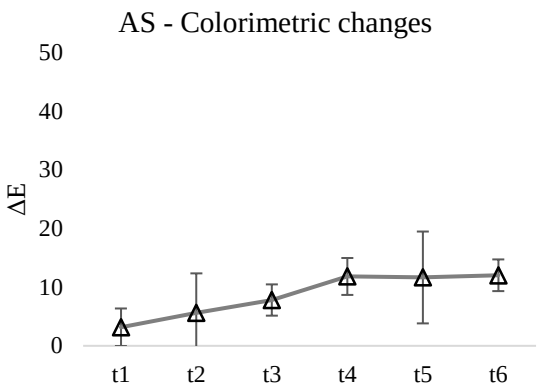

b.

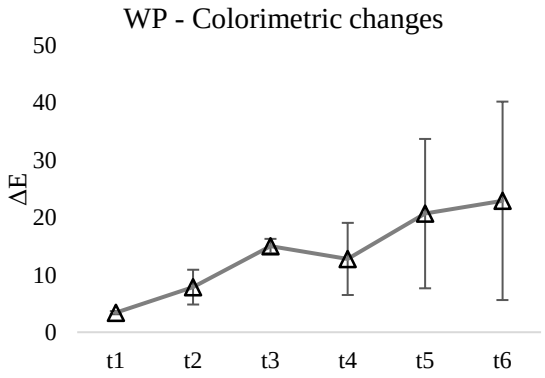

c.

Figure 27: ΔE values obtained on WM (a), AS (b) and WP (c) specimens sampled progressively during t1-t2-t3-t4-t5-t6. SD calculated on three repeated test are shown.

The growth of Cyanobacteria into the liquid medium allowed biofilm formation on samples surfaces. The mean cells concentration at the beginning of each test was $8x10^2$ cells/ml within the liquid of each bioreactor. After 21 days of growth, mean final concentration was $2x10^4$ cells/ml. Figure 28 reports mean biomass weight during the tests. The first days (3°-7°) are known as "lag phase", where a delay initially happens due to the presence of nonviable cells in the inoculum or physiological adjustments in nutrient concentration or culture conditions, as described by [183]. It continues to the "exponential phase", where cells grow and divide as an exponential function of time, as long as mineral substrates and light intensity are saturated a linear phase. Then, stationary phase, where the growth remains constant (14°-17°). In this experimental trial, a second exponential phase (17^{th} - 21^{st} day) occurred after the stationary one. During the decline phase (not shown) the decrease in the concentration of nutrients and/or accumulation of toxic waste products leads to microorganisms' death. Statistical analysis (ANOVA) run on biomass data, did not show significant differences (*p-value*>0.05), as demonstration that the experimental setup guarantees repeatability in terms of algal growth within the medium of different bioreactors.

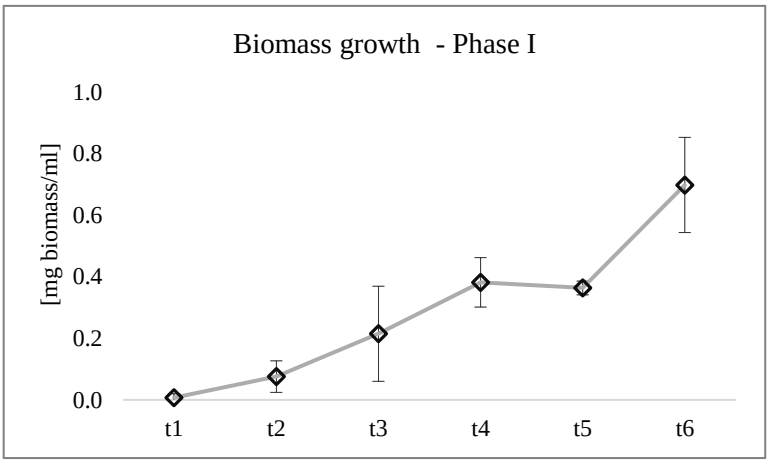

Figure 28: Weight of biomass produced by *N. commune* per unit (ml) of liquid growth medium during the entire duration of experimental test (t1-t2-t3-t4-t5-t6). Mean values and SD of three repeated test are shown.

Results - Phase II: Colonization rate on soiled samples

Results obtained within phase I have highlighted that biological colonization on surfaces seems having a higher variability from the 14th day of exposure, probably due to the first and mild biomass growth plateau observed (Figure 27). The variability in terms of solar reflectance and colorimetric changes after the day 14th of exposure has encouraged the review the test duration. Hence, phase II has been stopped at day 14th. Firstly, as shown in Figure 29 (a, b, c), *N. commune* has colonized all samples nevertheless the soiling layer. As the previous test, the colonized area on the firsts coupon sampled (after 3 days from the starting of bioageing exposure) remained meanly low in all involved materials, even if the standard deviation calculated on three repeated tests was high: 13.3%±6.1% for AS_s, 8.1%±12.1% for WM_s and 7.2±10.3% for WP_s. Final mean values of colonized area percentage achieved at the end of this soiling + bioaging procedures, were 42±6.9%, 58.7±1.7% and 54.7±9% for AS_s, WM_s, WP_s respectively. The variability was particularly high on WM_s specimens, where SD related the colonized area fractions remained high along all samplings times (Figure 30). It is important to underline that *N. commune* biomass seems turn the surface color through the passing of time. This phenomenon was perceivable especially on white samples (WP and WM), where pigmentation appeared yellowing, as confirmed by pigments extraction and analysis (Figure 31).

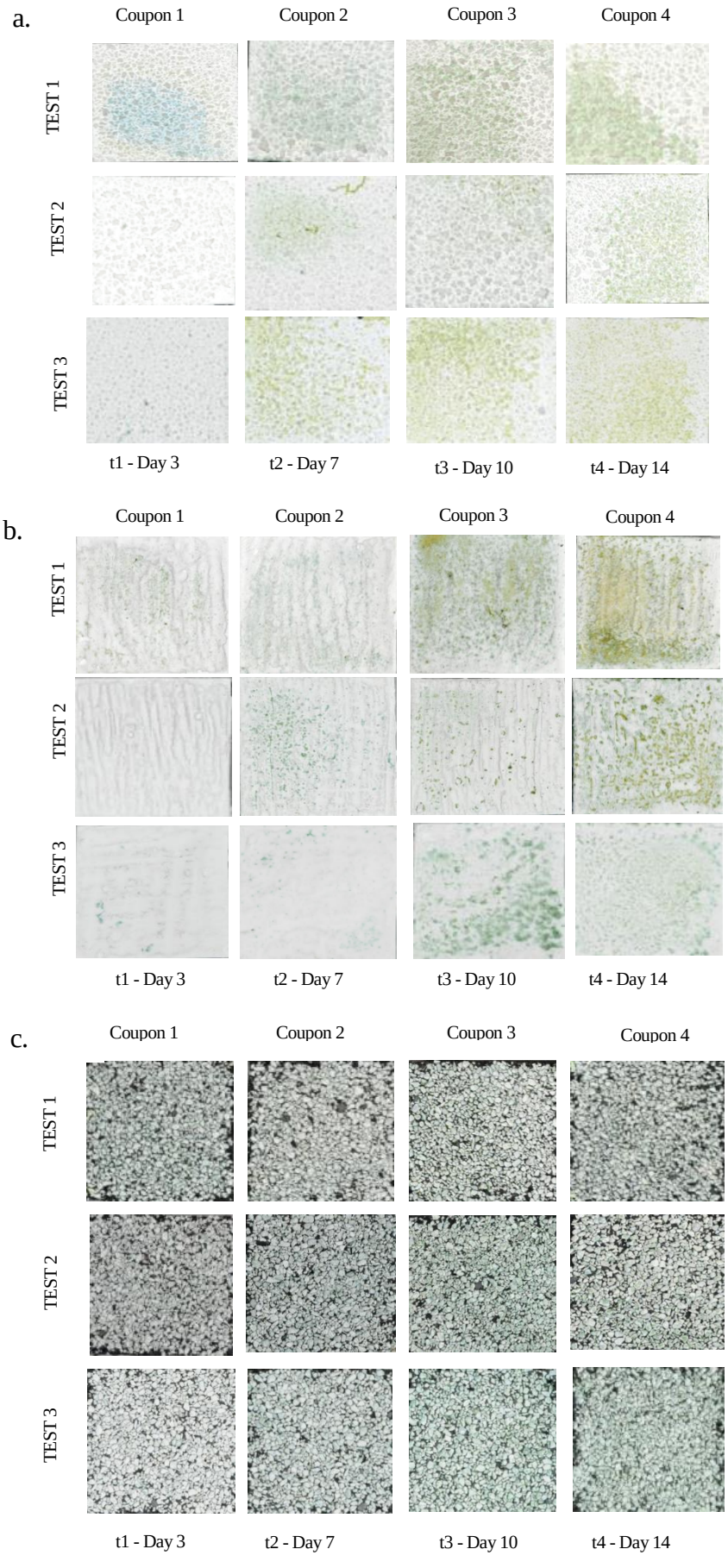

Figure 29: Phase II: Progressive colonization rates on soiled material specimen, during two weeks of bioageing procedure. Each coupon corresponds to a sampling day; t1-t2-t3-t4 are the four samplings performed across each repeated test.

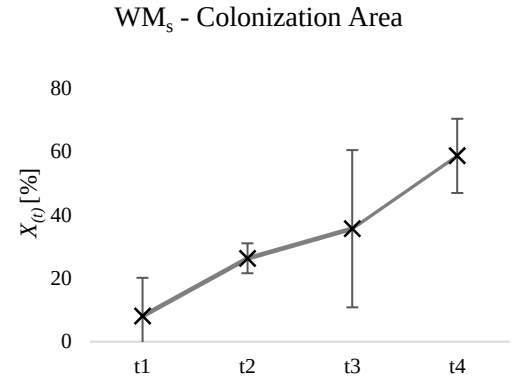

a.

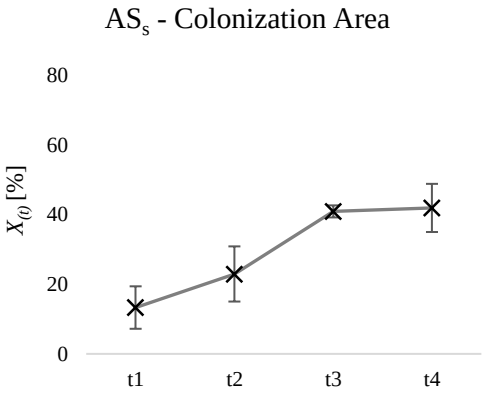

b.

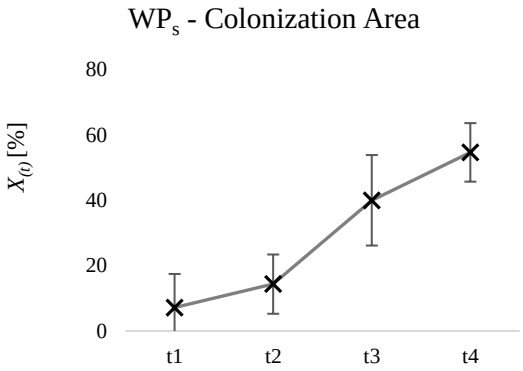

c.

Figure 30: Mean percentages of colonized area during phase II repeated test, evaluated through image analysis software (ImageJ). Four samplings have been performed (t1-t2-t3-t4). SD is shown.

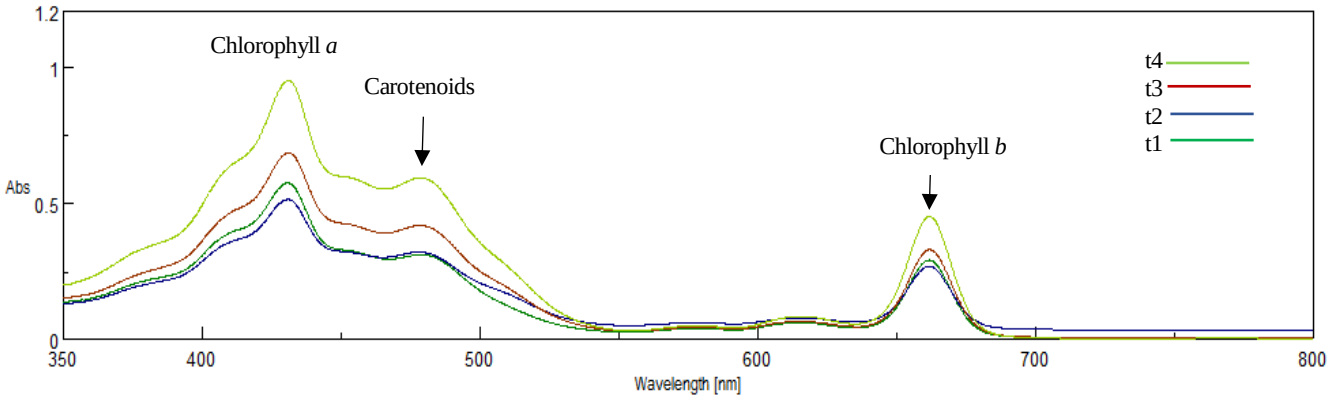

Figure 31: Main groups of pigments during progressive extractions (t1-t2-t3-t4). Absorbance of extracts containing chlorophylls and carotenoids from *N. commune* biomass is shown.

Solar reflectance decrease of phase II was measured after both soiling treatment and biological colonization. Differently form phase I, most of solar reflectance changes have been occurred averagely just after 3 days of bioageing exposure (t1), in details $\Delta\rho_{sol}$ data were 2.15 ± 0.7% for ASs, 17.3 ± 3.7% for WMs and 18.2±3.5% for WPs. The final

values (t4) of solar reflectance decrease were 3.5± 0.5% for AS_s, 22.1±1.3% for WM_s and 26.1±8.1% for WP_s (Figure 32). This means that between 62-79% of total solar reflectance decrease was primarily due to soiling deposition; then, biofilm was responsible for the remaining 38-21% of solar reflectance decrease observed in these tests. Standard deviation among three repeated tests was under 2% for AS_s and WM_s, but not for WP_s, where it was over 8%. CV_p calculated among final ρ_{sol} achieved on different materials has an average of 5%, while the uncertainty slightly overcame the 10% threshold: it was 10.9%. The repeatability coefficient then was 15.1%. Also in this case, the statistical error related to the repeatability was still too high since the observed differences overcome the significance threshold set at 10%. The highest variability in terms of solar reflectance difference among repeated tests took place on WP soiled samples.

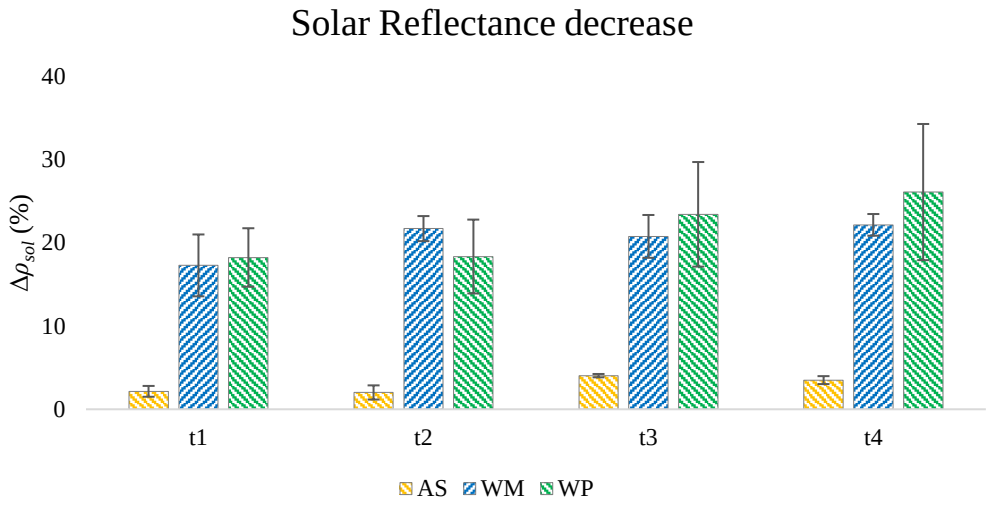

Figure 32: Progressive solar reflectance decrease ($\Delta\rho_{sol}$ %) obtained on each product type (WM_s, AS_s, WP_s) during the two weeks of bioageing exposure of phase II. Data are the mean values of three repeated tests. SD is shown.

Colorimetric changes trend line was not sharp along the exposure time (Figure 33). This trend corresponds to solar reflectance decrease one, where most of changes were due to soiling deposition; then, biological colonization worsen physical and aesthetical performances. ΔE values at day 14th were 8.9±1.4, 25.4±6.5 and 26.9±6.1 for AS, WM, and WP respectively. T-student test between colorimetric mean values got on bioaged new and soiled specimens at comparable exposure time (t4), has gained significant difference (*p-value* <0.05) only on WP product, but not on AS and WM ones, where a higher variability did not make significant repeated data.

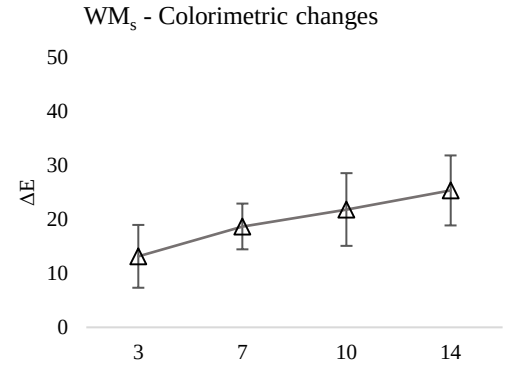

a.

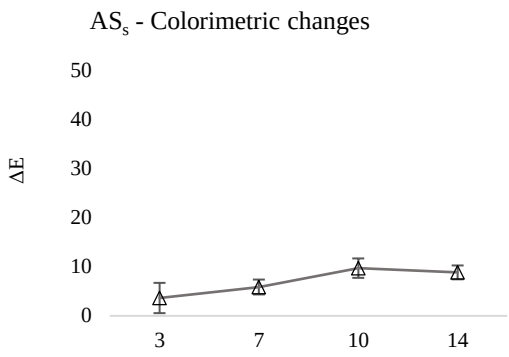

b.

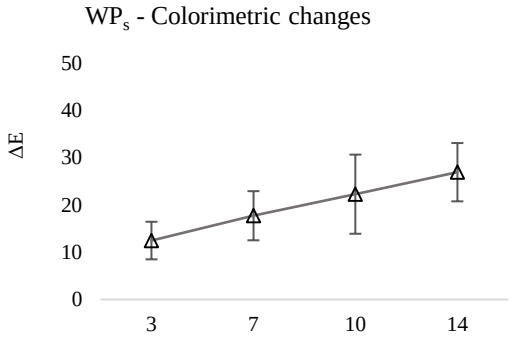

c.

Figure 33: ΔE values obtained on WM_s (a), AS_s (b) and WP_s (c) specimens sampled progressively during t1-t2-t3-t4. SD is calculated on three repeated test.

N.commune growth during phase II within TIS bioreactor was shown in Figure 34. It presented a lag phase during the first three days, then the biomass started to increase more intensively and reached its peak at the end of the test, at day 14th. Stationary and decline phases have not been reached by the cyanobacterium during these repeated test.

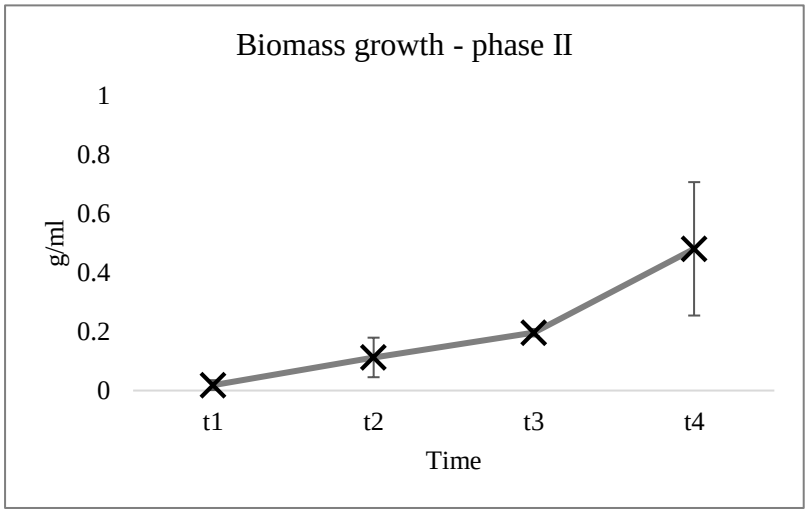

Figure 34: Weight of biomass produced by *N. commune* per unit (ml) of liquid growth medium during the entire duration of experimental test (t1-t2-t3-t4). Mean values and SD of three repeated test are shown.

Discussion

Experimental Trial III, composed by phases I and II, has applied the light intensity of 100 µmol/m²/s photons according to the optimum amount of PAR for cyanobacteria growth in literature. The lamps have been placed in order to provide homogenous light diffusion around each TIS bioreactors. Cyanobacterium biomass data have demonstrated that the light intensity provided an adequate PAR amount to ensure *N. commune* growth into bioreactors. Statistical analysis compared biomass production from phase I and phase II and not significant differences were emerged (*p-value*>0.05) until the end of the second week of bioageing. This suggests homogeneity of biological growth across repeated trials keeping steady environmental conditions. Uniformity in cyanobacterium growth was also confirmed by the pigment extraction and quantification, presented in Figure 35. Total chlorophyll *a* and *b* and total carotenoids have been calculated according to Lichentaler's formulas n° [5], [6], [7], [8] [154] and data showed that no statistical differences exist between both type of pigments produced during phase I and phase II in the same period time (*p-value*>0.05). Moreover, Figure 35 marked as both groups of pigments have increased their concentration per unit of liquid medium during the test. The increase of chlorophylls was an indirect indicator of the cyanobacteria cells growth; the increase of total carotenoids could also be the cell signaling response to the rising oxidative cellular stress during the experimental procedure [184].

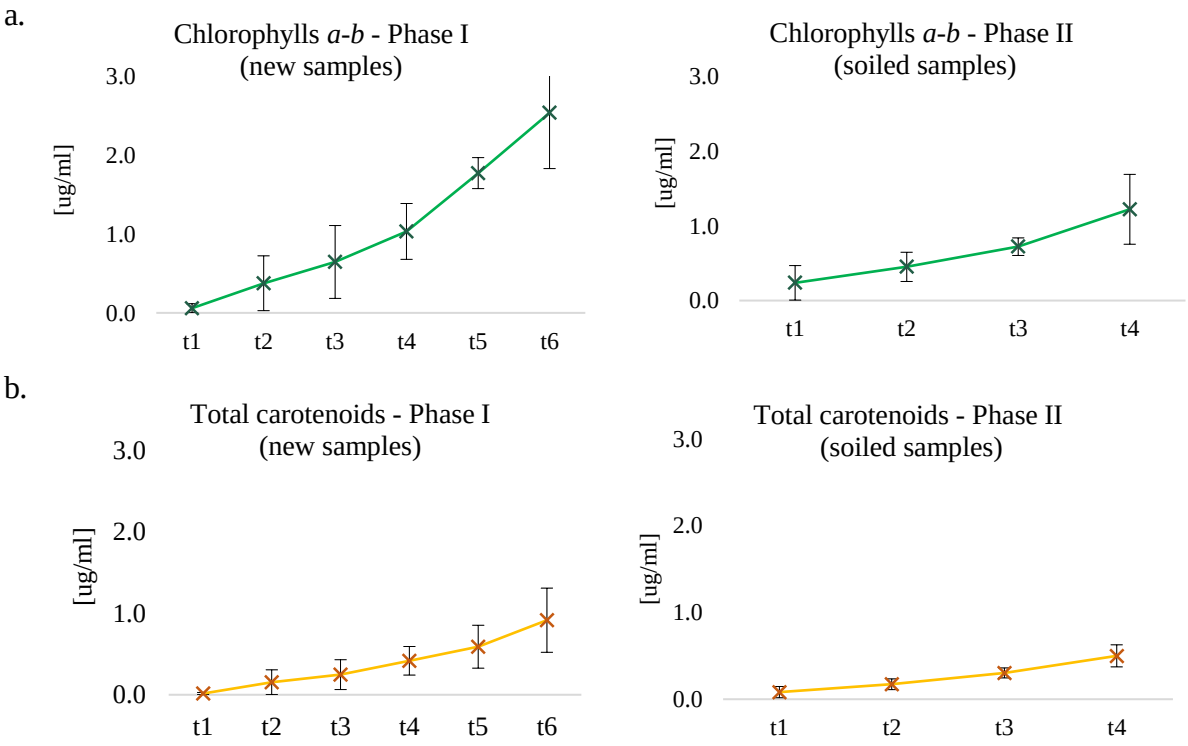

Figure 35: Pigments production from cyanobacterium *N. commune* during Trial III experimental tests. a) Total amount of chlorophyll *a* and *b* produced during phase I and phase II and their SD from repeated test are shown. b) Total amount of carotenoids produced during phase I and phase II and their SD from repeated test are shown. Results are the mean of three repeated test of the three bioreactor run in each test (AS, WM, WP).

Growth curve of phase I indicates a first stationary phase after day 14th; growth trend was confirmed also during phase II, where growth rate per day [185] was calculated using absorbance data obtained during each sampling day (Figure 36), applying equation n°4. Growth rate identified the beginning of stationary phase in the last interval time (t3-t4 which corresponds to 10th-14th days). Previous works which have developed accelerated bioaging setups, did not monitor algal or cyanobacteria growth rate neither through absorbance level or biomass weight [151], [176], but Blanc et al. [160] used pigments extraction to quantify biofilm formation on surfaces. However, this research collected more data about biological growth to provide a great tool for studying the fast response of microalgae to sudden change of the environmental conditions.

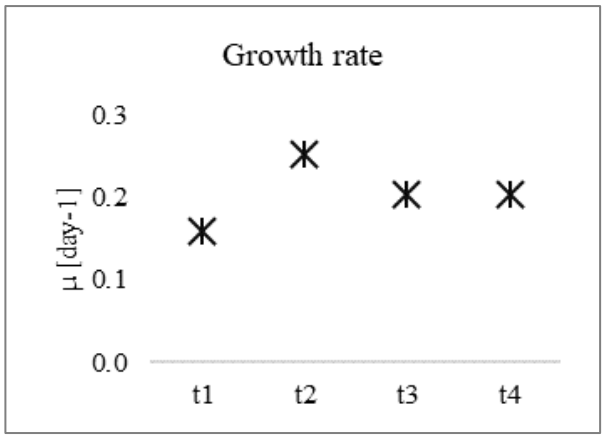

Figure 36: Growth rate [μ]: it is the mean growth rate among three repeated bioaging test run on soiled specimens. It indicates the rate of cells number increase per each unit of time (day).

The critical analysis of data about colonization area fraction, solar reflectance decrease and colorimetric values from phase I, have underlined higher variability in the last week of bioageing exposure. Specifically, biofilm formation on surfaces did not follow a linear trend after the 14th day, as observed on all types of materials (Figures 24, 25): the standard deviation resulted considerably high after t4 in phase I. Neither solar reflectance decrease (Figure 26) had a linear trend after day 14th: maybe due to lower biological growth on surfaces, in some cases $\Delta\rho_{sol}$ resulted lower on t5 and t6 samples than t4 (Table 5). High heterogeneity during the last week of phase I was described also by high standard deviation got on ΔE values (Figure 27). Irregular data about colonization and physical performances obtained during the last week of phase I, represented one of the reason, together with the analysis of biomass growth, to anticipate the stop of each test in the following phase II at day 14th instead of 21st.

Table 5: Comparison of mean decrease of solar reflectance between phase I and phase II results. Presented data are the mean of three repeated test for each phase run on each product type (asphalt shingle, white paint and single ply white membrane). All the results obtain at each sampling time are presented (t1, t2, t3, t4, t5, t6). SD is shown.

	Mean $\Delta\rho_{sol}$ [%]					
	AS phase I	AS$_s$ phase II	WP phase I	WP$_s$ phase II	WM phase I	WM$_s$ phase II
t1	2.6±1.3	2.2±0.7	1.6±1.0	18.2±3.5	2.5±2.3	17.3±3.7
t2	3.3±2.0	2.0±0.9	2.9±0.9	18.3±4.4	4.9±3.7	21.7±1.5
t3	4.6±0.3	4,.0±0.2	8.8±2.5	23.4±6.3	7.5±3.9	20.8±2.6
t4	5.2±1.1	3.5±0.5	8.9±1.4	26.1±8.1	15.2±12.9	22.1±1.3
t5	4.9±0.7		10.0±5.2		8.5±6.2	
t6	5.9±1.2		11.3±3.5		14.7±7.2	

Statistical comparison among colonization area obtained on new and soiled samples did not get statistical significant difference (*p-values*>0.05) on any product type and for any sampling time. Results have been reported on Table 6. This apparently means that soiling layer on samples surfaces wouldn't increase significantly biological growth on them, even if previous studies underlined how urban particulate deposition could provide nutrients to microflora growth [13], [181]. The influence of soiling to biological growth is not a easily valuable phenomenon due to huge variability of species involved and their several way to interact with surfaces and respond to urban abiotic stress. Caneva et al. [54] analyzed in details biological communities growth and variations on urban surfaces in Rome (Italy) considering climatological data and air pollution data across two decades: scientific findings describes that the less favorable climatological conditions together with increasing air pollution caused the reduction of biodeterioration phenomena during XX century.

Air pollutants caused a biodiversity reduction with the disappearance of the most sensitive species, such as many lichens; at the same time, this evidence underlines how more resistant species among algae, cyanobacteria, fungi could still survive in favorable microclimatic conditions forming large populations [54]. Other Authors outlined that the presence of atmospheric pollutants which can interact and react with urban surfaces (as sulfur dioxide and hydrocarbon compounds) inhibit both the size and diversity of the microbial community [40]. The interaction and influence phenomena among urban air pollutants, soiling deposition and autotrophic organism populations response is extremely wide because depends to climate, microclimate, biological species and physical and chemical features of surfaces [186]. The detailed comprehension of these phenomena and the description of causes-affects relationship are not among the topic of this study. The first interest of this research is indeed to define a repeatable protocol able to consider biological colonization of cool surfaces fouling factor, which is not adequately considered in existing protocols [124]. For this reason, the laboratory procedure under development has applied the standard soiling solution, which is formulated by [18] as average of compounds responsible of spectral and solar reflectance losses on aged sampled in three specified locations, as CRRC specified.

Results from Trial III did not found any significance in terms of increased colonization area on soiled and not-soiled cool surfaces. This means, firstly, that soiling deposition had not a biocidal effect on cyanobacterium and even more, it did not seem to influence negatively *N. commune* growth. This was a reasonable result for the scope of the work: it is possible to consider the standard soiling mixture compliant with biological growth without having an inhibiting effect of biofilm. At the same time, biological growth on final soiled samples (t4) showed a more homogeneous colonies distribution, compared with growth on new samples at t4. This was deduced by solar reflectance and ΔE values, which have a smaller standard deviation on soiled samples compared with new ones. Uniformity in organisms colonies distribution is necessary requirement to reach expected results regards repeatability of procedure, as already highlighted in previous works by [20], [133], [160], [176].

Table 6: Comparison of mean colonization area fraction ($X_{(t)}$ %) between phase I and phase II results. Presented data are the mean of three repeated tests for each phase run on each product type (asphalt shingle, white paint and single ply white membrane). All the results obtained at each sampling time are presented (t1, t2, t3, t4, t5, t6). SD is shown.

	$X_{(t)}$ [%]					
	AS phase I	ASs phase II	WM phase I	WMs phase II	WP phase I	WPs phase II
t1	3.3±1.5	13.3±6.1	3.0±2.0	8.1±12.1	3.0±2.0	7.2±10.3
t2	17.7±18.7	23±7.9	7.3±3.5	26.3±4.7	8.7±8.1	14.3±9.1
t3	37.3±13.6	41.0±1.7	24.0±18.7	35.7±24.8	21.3±7.1	40.0±13.9
t4	49.0±9.6	42.0±6.9	51.3±16.4	58.7±11.7	35.0±8.7	54.7±9.0
t5	50.3±8.4		36.7±23.1		36.3±18.0	
t6	56.7±12.1		58.3±12.7		43.7±14.0	

Statistical comparison between ρ_{sol} data obtained from phase I and phase II have been performed in order to evaluate if soiling deposition may significantly influence biological growth in this experimental procedure and then evaluate its contribution to loss of physical performances. First remarkable consideration was that soiling layer significantly increase (*p-value*<0.05) the loss of solar reflectance on white cool materials (WP and WM), since the beginning of bioaging procedure (t1) (Figure 37 a,b). The same did not occur on AS material, where solar reflectance decrease after bioageing exposure seems comparable on new and soiled samples (37c). All $\Delta\rho_{sol}$ results at the end of the second week of bioageing were presented in Table 5.

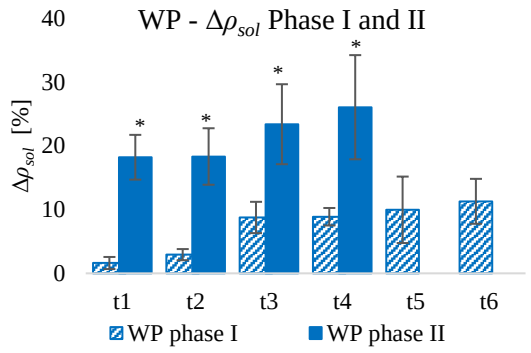

a.

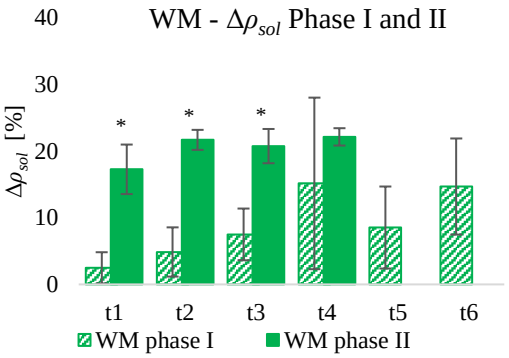

b.

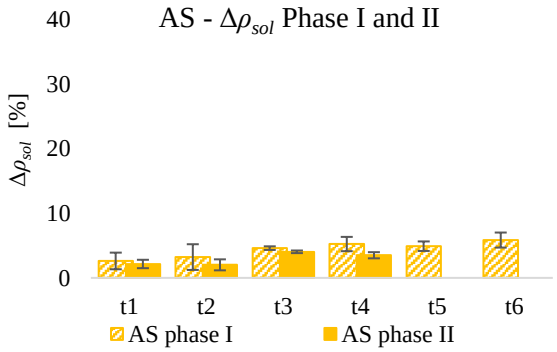

c.

Figure 37: $\Delta\rho_{sol}$ comparison between phase I and phase II on WP, WM and AS product. Data are the average of three repeated test and are expressed in percentage; SD is shown.

Loss of solar reflectance on soiled samples was similar to some previous research where cool materials have been exposed to natural ageing according to ASTM G7 [187]. Paolini et al. [188] have describe that cool membrane with starting solar reflectance of 0.80, lost mainly 0.24 after three years of natural exposure in Milan (Italy). While the mean losses observed in this experimental Trial III were in the order of 0.22 for single ply white membrane and 0.26 for white paint coating, both after soiling and bioageing exposure (phase II). These data have been compared with three years aged samples data available by CRRC database (https://coolroofs.org/directory) and reported by Sleiman et al. [18]. The CRRC's Rated Product Directory has initiated in 2005 and contained aged ratings for 1357 products as of April 2011. CRRC database reported an average solar reflectance decrease of about 17-18% for single ply white membranes and field applied (which have a starting ρ_{sol}> 0.80) after three years of natural exposure. Asphalt shingle lost about 5%, as it has been observed in this work. CRRC database has been built considering natural aged samples data as average loss at the three CRRC exposure sites (Ohio, Florida and Arizona). Considering only data from Florida exposure site, where the hot and humid climate stimulate biological growth, the brightest membranes lost 0.24±0.15 [97] of ρ_{sol}, which was a similar loss obtained through phase II of bioagieng setup of this work (Table 5). Bioageing procedure presented in this Trial associated with soiling deposition, seems to provide aged data comparable to ones achieved at hot and humid climate zones, as Florida. As described

by [18], reflectance spectrum of the laboratory-aged sample differs from that measured on naturally aged samples in Florida (Figure 4b, here reported): abatement of reflectance was evident mainly in the visible region, as occurred also on samples from phase II of this trial, where both soiling deposition and biofilm have occurred on surfaces (Figure 38).

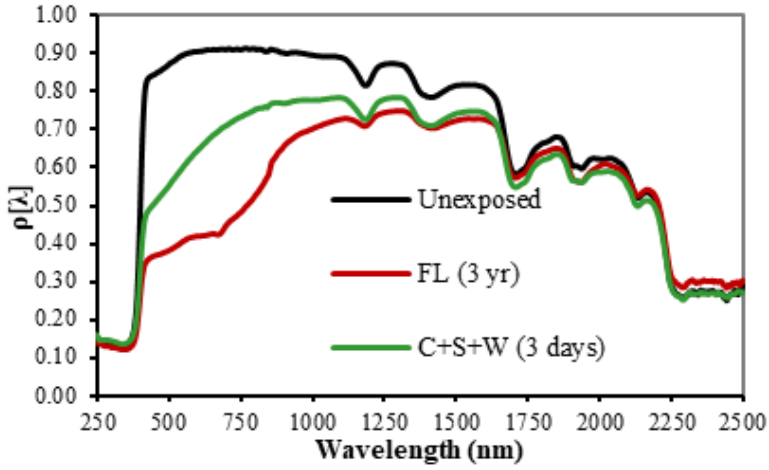

Figure 4b: Comparison among solar reflectance spectra obtained on a field applied cool coating starting ρ_{sol} > 0.80 on new sample (black spectrum), ASTM D7897 accelerate ageing (green spectrum) and ASTM G7 natural ageing (red spectrum) in Florida [97][18].

Comparison between spectra presented in Figure 38 clearly shows the variation in solar reflectance in the visible region, due to the biological growth, as spectrum from phase I underlines (Figure 38a). Moreover, as [18] deeply described, it was recognizable the variation across whole spectrum due to soiling mix, where black carbon in particular is the responsible of solar reflectance absorption. Specifically, black carbon reflectance absorption decreases as much as wavelength increases [188].

Comparison with Title 24 model (http://www.energy.ca.gov/), designed to predict the degrade of solar reflectance of a typical white single-ply membrane or white field-applied coating [97], was run on WM and WP, which are the two products fully compliant with the Title 24 requirements, but also on AS product since the staring ρ_{sol} >0.2. Figure 39 presented these data. Notably, not negligible differences exist among $\Delta\rho_{sol}$ got from bioageing test and theoretical $\Delta\rho'_{24}$ (calculated through Title 24 model) on white products (WM_s, WP_s); but not the same was observed on AS_s samples, where the distance between experimental data and estimated ones were much lower. These evidences were linked with the type of building material products and its starting ρ_{sol} values: when the solar reflectance has high values (>0.70) on new sample, its decrease was usually greater. Moreover, $\Delta\rho_{sol}$ achieved through experimental test were always higher compared to the estimated ones and this is consistent with the deeper decrease in the visible region of the spectrum when it is interested by biofilm growth in hot and humid climates [18].

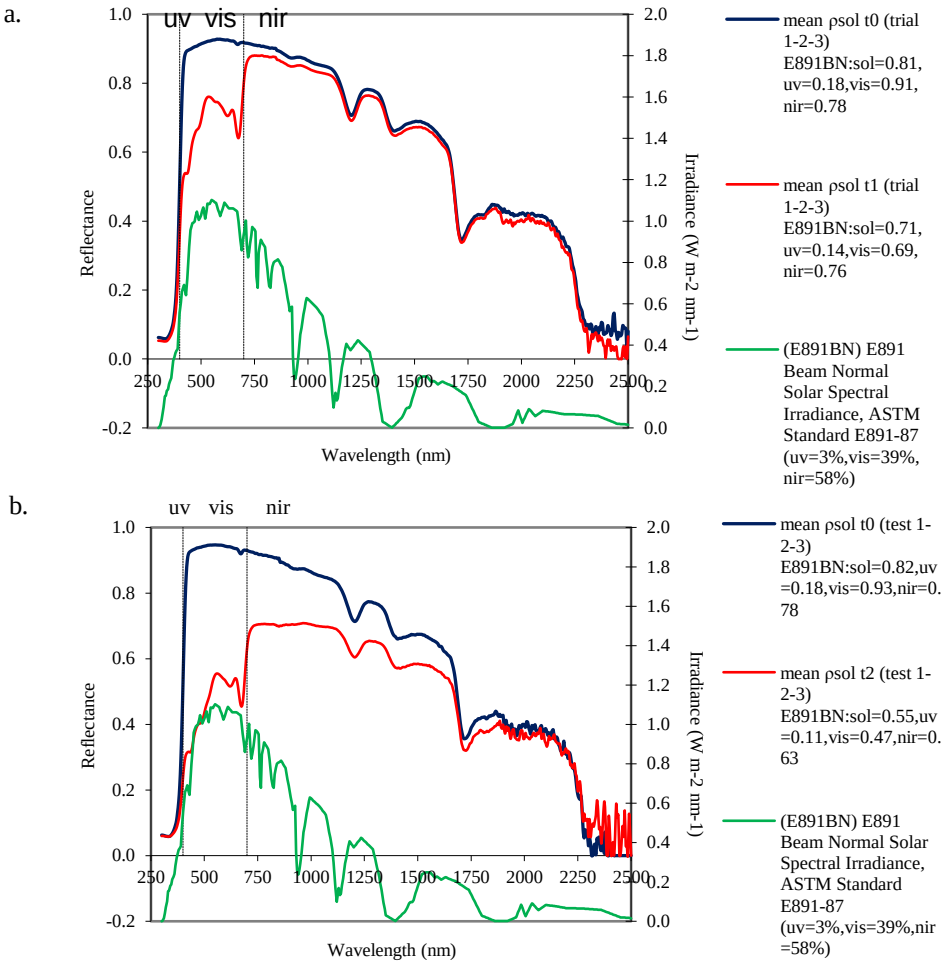

Figure 38: Reflectivity spectra (300-2500 nm) on single ply white membrane (WM): a) before and after bioageing process and b) before and after soiling deposition + bioageing process. Blue spectra are t0, obtained on new sample, red spectra are t1 obtained with phase I (only bioageing) and t2 obtained with phase II (soiling+bioaging). The spectra have been acquired by Spectrophotometer UV-Vis-NIR (Jasco, V-630).

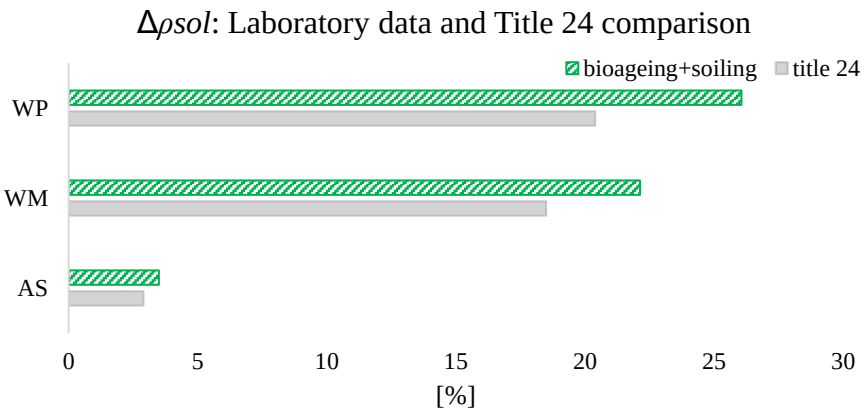

Figure 39: Mean solar reflectance decrease comparison between results achieved after phase II (soiling+bioageing) on WM, WP and AS and results of estimated solar reflectance decrease according to Title 24 model.

The correlation (R^2) between the $X_{(t)}$ and the changes in solar reflectance ($\Delta\rho_{sol}$) results was improved, comparing to the previous Trial II. Figure 40 (a, b) reports data about R^2, which was always > 0.5. R^2 values were slightly higher when samples were exposed to bioageing treatment without soiling (phase I), since biofilm was the only fouling agent in those tests. This confirms that the investigated thermophysical property of surfaces could be heavily affected also when subjected only to biocolonization process. Covered area and the changes in solar reflectance seems to be more positively correlated in case of WP samples than AS and WM. This evidence was due to greater reliability of results obtained on this surfaces type, such as indicated by the lower standard deviation (then the lower coefficient of variation). In agreement with other studies, microbial growth seems to represent a not negligible agent of roof soiling in humid climates. At the same time, the statistical comparison between biofouling results obtained on soiled and not soiled samples highlights that ρ_{sol} worsen more when samples have the soiling layer, while biocolonization rate is not particularly affected or stimulated by the standard soiling mix. Nevertheless, these outcomes will be validated and discussed in the next trial.

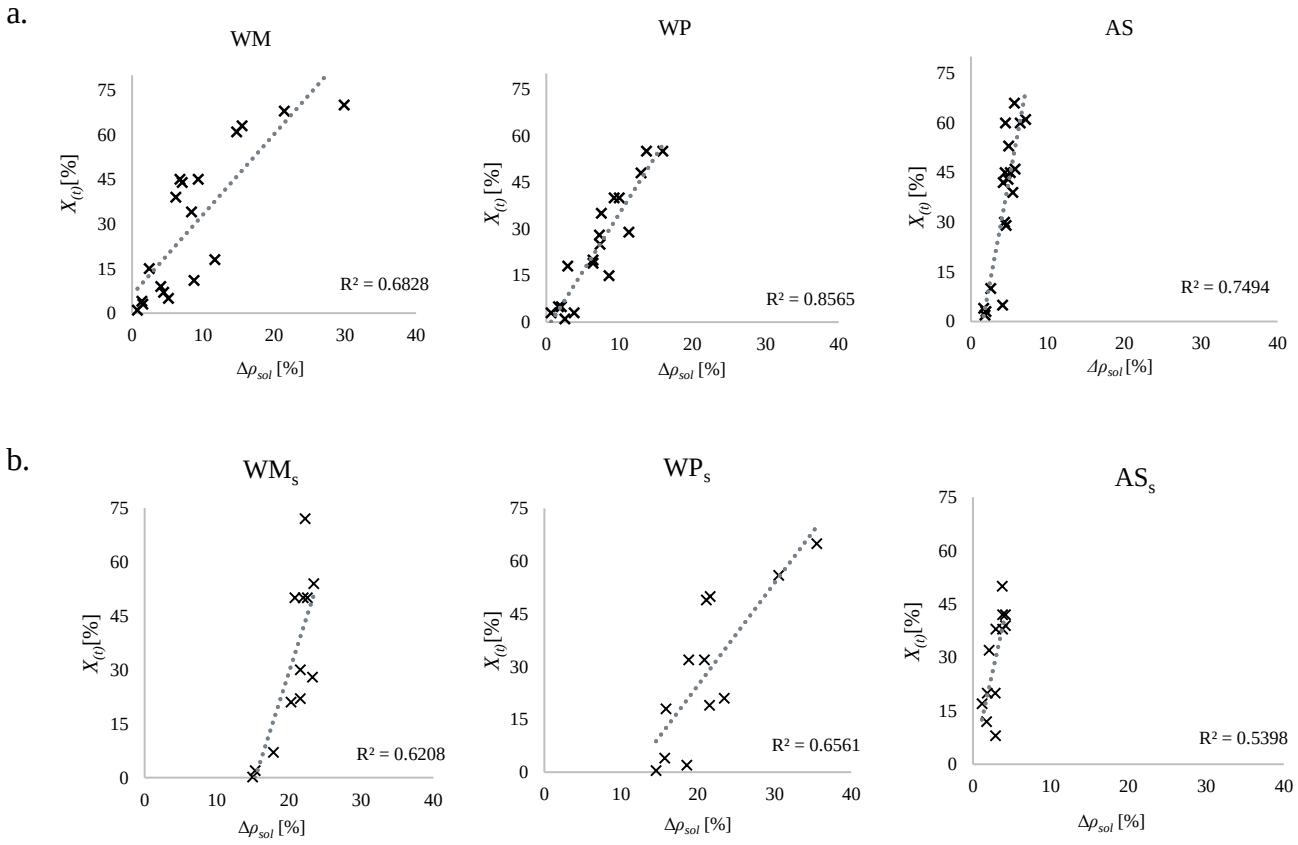

Figure 40: Correlation between $\Delta\rho_{sol}$ and colonized area (X_t %) on building materials: WM, WP, and AS from two different phases: a) data from phase I and b) data from phase II.

Setup applied in Trial III used only a cyanobacterium species *N. commune* as organism to promote surfaces biodeterioration. The repeatability and the uncertainty obtained through this setup is resulted better than the previous one, eventually thanks the use of a different growth incubator and light system. However, uncertainty values (12.6% and 10.9% for phase I and phase II respectively) was not enough to consider the procedure suitable to evaluate the biological growth on building materials as a preliminary standard protocol and to apply the same procedure to gauge the resistance of surfaces to biofilm growth. Then, other implementations on the setup will be applied and discussed in the next Trial.

5.4. Trial - IV Development of accelerated bioageing procedure: the involvement of other species of phototropic organisms

Trials II and III have been carried out with cyanobacterium species Nostoc commune, after a first trial, which has involved also the green alga species Edaphochlorella mirabilis. N. commune is chosen because it represents an ubiquitous organism detectable in urban environments and surfaces worldwide [151]. As previously cited, cyanobacteria extracellular polysaccharides (EPS) may enhance adhesion of microorganisms to the surface, thereby facilitating the corrosive action of the cells to solid substrates [49]. This contributes to adhere to surfaces and starts to form the first layer of biofilm which afterwards grows through the adhesion of other organism species (algae, fungi, lichens etc.). These reasons have driven the choice to select Nostoc genus to develop bioaging procedure here discussed. The development of a setup apparatus, which involves biological variability, needs to be as simple as possible to limit at the most the influence of ambient conditions and the fluctuations due to several variables. Choosing only one species in very firsts phases of the protocol development, allows analyzing the growth of a single species without any other biological interference. In this case, the species of a pioneer organism might describe the first steps of bio-settlement on material surfaces. At the same time, the involvement of just one organism species (*Nostoc commune*) represents also one of the weaknesses of Trial III. Even if, its presence has been recognized by several external biodegradation studies, and even if it belongs to the group of pioneer organisms, it could not entirely represent the biological colonization of building surfaces that are promoted by several groups of organisms. Given that, environmental factors have been optimized (ageing chamber, lights intensity, immersions times, test duration), on Trial IV other phototrophic organism species were involved. This in order to improve the procedure and to make it closer to natural exposure, at least in terms of coexistence of several species on the same surface. All the existing literature on the topic is indeed concordant to the identification of the wide biodiversity found on naturally exposed surfaces (facades, walls, roofs, monuments etc…) [23], [69], [189].

Hence, the experimental bioageing setup has been here implemented introducing other species in order to assess if any improvements would be possible according to the

aims of this work. The involvement of different species has been studied on both new and soiled samples to evaluate the influence of soiling on biofilm formation. Indeed, previous Trial III allowed achieving some experimental encouraging results regarding the soiling effects on biocolonization: soiling deposition on surfaces did not significantly increase, neither decrease, colonized area on surfaces. In the further Trial IV the experimental procedure run on soiled samples was compared again with the same procedure run on new samples in order to discuss the soiling contribution to bio-growth. According to previous data collected on biomass growth (Trial III, phase I) and high percentage of covered area after 14 days of bioageing, Trial IV has been stopped within two weeks. This has been assumed as fulfilling achievement, especially according to the need to shorten time of biological degradation process, discussed in section 2. Figure 41 presents the technical detail of Trial IV.

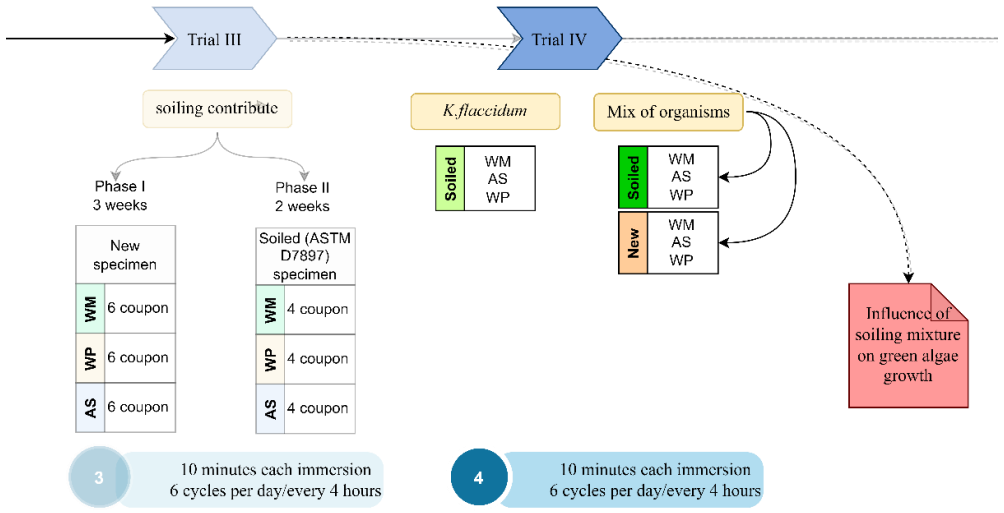

Figure 41: Experimental details of Trial IV: two batch of species (the green alga *K. flaccidum* and a group of cyanobacteria and algae) have been applied to accelerate to bioageing procedure. Setup involving the group of organism has been tested both on soiled samples and on new samples. Each bioreactor contained three specimen, one from each material product (AS, WM, WP) and each test has been run in triplicate. At the end of Trial IV, a further test has been carried out to study the culture solution as the source of abiotic stress for algal metabolites productions.

Materials and methods

Trial IV used two different batch of organisms to colonize the samples. The first test (named *soiled K*), run in triplicate, has used *Klebsormidium flaccidum*; the second test (named *soiled MIX*), always run in triplicate, has involved a group of different species: two green algae (*Edaphochlorella mirabilis, Klebsormidium flaccidum*) and two cyanobacteria (*Gloeocapsa sp., Nostoc commune*). In these two tests, sample surface has been previously soiled according to the same procedure described in section 5.3. Then, a third test applied the same setup and procedure (named *new MIX*) where same

material products have been exposed on accelerate bioaging without being previously soiled. Single ply white membrane (WM), white paint (WP) and asphalt shingle (AS) are involved also in Trial IV. One coupon for each material type was inserted into each bioreactor (Figure 40) and each test was run in triplicate. The complete duration of the test lasted 14 days, as previously identified as a better exposition time. Bold's Basal Medium was used as liquid growth medium for each TIS bioreactor, since it has been identified as more appropriate nutrient source for green algae (*Chlorophytae*) and *Gloeocapsa sp*. [190]. *N. commune*, as well, can grow well in BBM medium since it is no strict demanding species [191]. 600 ml of BBM were prepared for each bioreactor, according to producer's recommendations: final concentration was 0.705 g/L and pH adjusted at 6.6, after the adding 1 ml/L of sulfuric acid 0.1%. The medium was autoclaved at 120°C, 1 atm, for 20 minutes before use.

In the first test, the culture medium was inoculated with 20 ml of *K. flaccidum* (K test). The mother strain was grown in BBM medium and kept at 24±1°C into the incubator (AG System, Biolog-Lux). In the second test and third tests (MIX test), 5ml for each considered species (*E. mirabilis, K. flaccidum, Gloeaocapsa sp., N. commune*) were inoculated into the liquid medium in order to have a final inoculum of 20 ml in each bioreactor. Cells concentration at the beginning of test (t0) were different in these two cases: 30 cells/ml are averagely counted into *K* bioreactors and 200 cells/ml into *MIX* bioreactors. This difference did not affect the uniformity of trial starting condition: indeed, as shown in Figure 42, *K. flaccidum* cells were considerably bigger than other species cells. Despite of the starting number of cells was distant between these two tests, the value of absorbance read at 750 nm resulted very similar among bioreactors, ranging from 0.03 to 0.07. The number of cells have been counted also during each sampling time: t1, t2, t3, t4, which correspond to day 3, day 7, day 10 and day14 respectively. Beyond the number of cells, biomass weight was collected and absorbance of liquid medium has been analyzed through UV-Vis spectrophotometer (Jasco, V700) at each sampling time. Then, the calibration curve has been built in order to determine the concentration of cells using the absorbance values in the following trials (Figure 43). The calibration curve underlined some mild difference between the concentration of the two batch of species used into the bioreactors: *K. flaccidum* reached an higher Abs value with a lower cells number compared to the *MIX*. This could be explained again through the cells dimension (Figure 42): in particular, cyanobacteria cells are considerably smaller than *Charophyta* ones and this could influence the optical density of the growth medium.

In this Trial, the colonization area on the specimen exposed to the accelerated bioageing procedure were monitored during the test. At each sampling time, the images of the surfaces were acquired through Nikon D5000 camera to be evaluated with image analysis. Moreover, at each sampling day, a rate of liquid medium was collected to carry on with pigments extraction.

Instead, solar reflectance and colorimetric changes are analyzed just at the beginning (t0) and at the end (t4) of each test. Growth incubator is the same than Trial III and it has been kept at 24±1°C with 14 hour as photoperiod. Light intensity was set at 100 μmol/ m^2/s of photons.

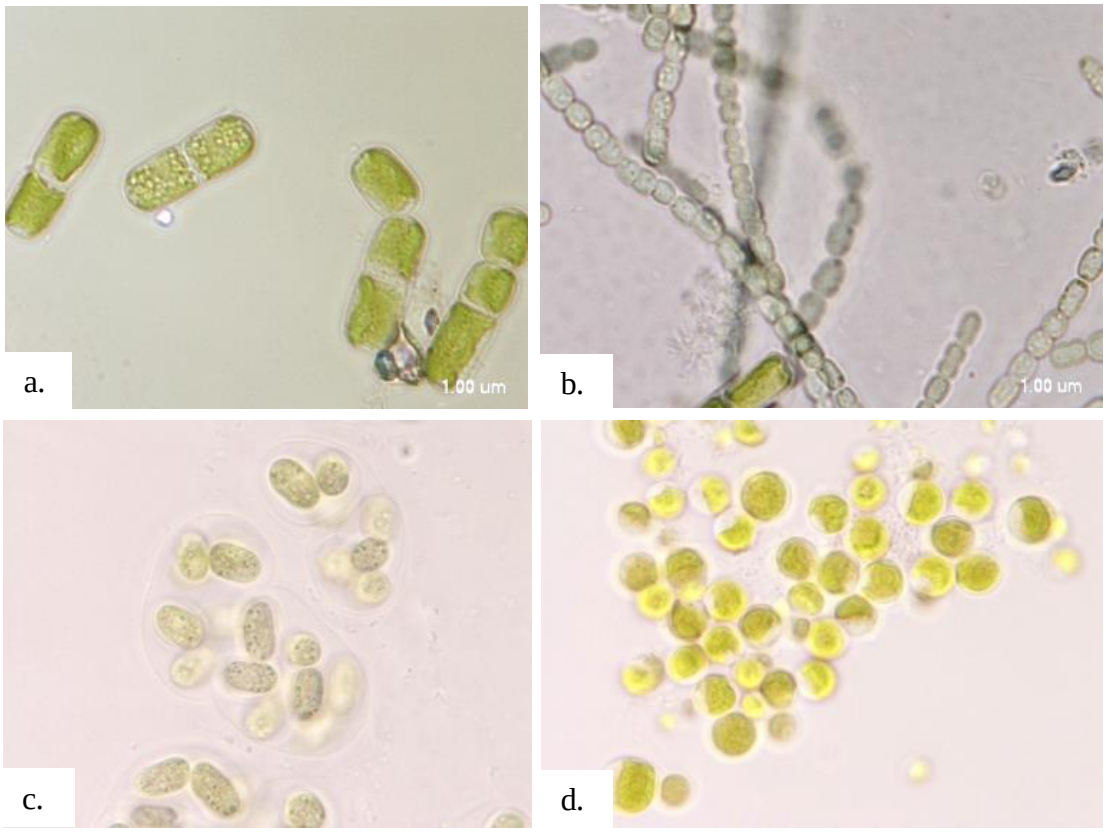

Figure 42: images from light microscope (Eclipse, mod. 80i; lens: CFI planapo VC 100x oil, Nikon instruments) of *K.flaccidum* cells (a), *N.commune* (b), *Gloecapsa* sp. (c). *Edaphochlorella mirabilis* (d). Magnification 100X.

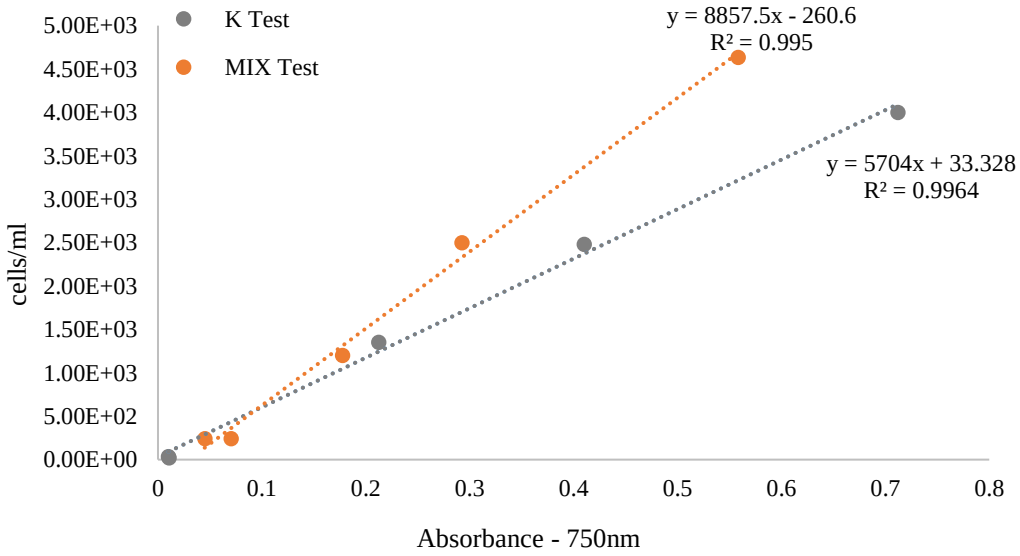

Figure 43: Calibration curve based on the number of cells and absorbance measurement (at 750 nm). Two batches of species are used to build the two curves: *K. flaccidum* for "*K* test" and two cyanobacteria (*N. commune* and *Gloeocapsa sp*.) and two algae (*K. flaccidum* and *E. mirabilis*) for "*MIX* test"

The first test was run with green alga *Klebsormidium flaccidum* chosen on its representativeness among urban phototrophs and ease of growth into liquid culture [23]. *Klebsormidium* is one of the most widespread taxa of microcharophytes in the world, ranging in distribution from polar to tropical regions [192]. Moreover, some detailed observations and surveys on the subaerial algal flora of urban environments in Europe, revealed that species of *Klebsormidium* are widespread in urban habitat too [193]. These algae are a common occurrence at the base of old walls and on the concrete between paving stones and produce large green patches at sites characterized by high humidity. Beyond *K. flaccidum*, other species were inoculated in the second and third tests of Trial IV as further implementation of the experimental procedure. Among the several microbiological and algal species involved in natural bioageing [14], some ubiquitous green algae and cyanobacteria have been selected, in view of their fast and relatively undemanding growth conditions [20]. Most representative species able to colonize building surfaces and responsible of bioageing, according with previous studies [27], [30], [36], [51], [194], have been chosen.

Results

Colonization rates obtained on *soiled K* test, *soiled MIX* and *new MIX* test after 14 days of exposure showed a pretty higher uniformity compared with previous trials. In Figure 44 (a, b c), images of surfaces at the end (day 14th) of the test are reported. In most cases, biological growth was distributed over soiled and new coupon surfaces homogenously. Also in this case, it seems that the presence of soiling layer on surfaces was not affecting the growth of involved organism species. This was particularly evident comparing *soiled MIX* and *new MIX* results. Colonized area $X_{(t)}$ achieved on each coupon is reported in Figure 45. Growth curves on surfaces marked a slower colonization on specimen without the deposition of soiling layer (*New MIX*), since the $X_{(t)}$ was always above the two *soiled* test (*K* and *MIX*). This was true during the experimental tests on all material types, but not in the final stage of the procedure (t4), where the difference became not significant (*p-value* >0.05) on WM and on WP. Instead, the colonization rates on AS achieved by the *MIX* of organisms on new and soiled specimens resulted significantly different (*p-value*<0.05). Results of $X_{(t)}$ on single ply white membrane achieved within the same test type were more variable than the other products. This behavior has been already found in Trial III, where the mean $X_{(t)}$ results on WM had a high standard deviation. The lowest $X_{(t)}$ value occurred on AS exposed to *Soiled MIX* tests, where the mean colonized area fraction was 63.7±3.1%. This lower percentage of surface area interested by biofilm growth was well perceivable by samples images (Figure 44b) and it was confirmed by colorimetric results (Figure 46). All the other final colonization rates have overcome 70% and $X_{(t)}$ for WP and WM was statistically higher (*p-value*<0.05) when the biofilm was formed by the group of species (*MIX* tests) than only *K. flaccidum* (*K* test). The comparison of biofilm grown on soiled and new specimen confirmed what has been found in the previous Trial III: soiling mix did not significantly contribute to promote phototrophs growth on surfaces.

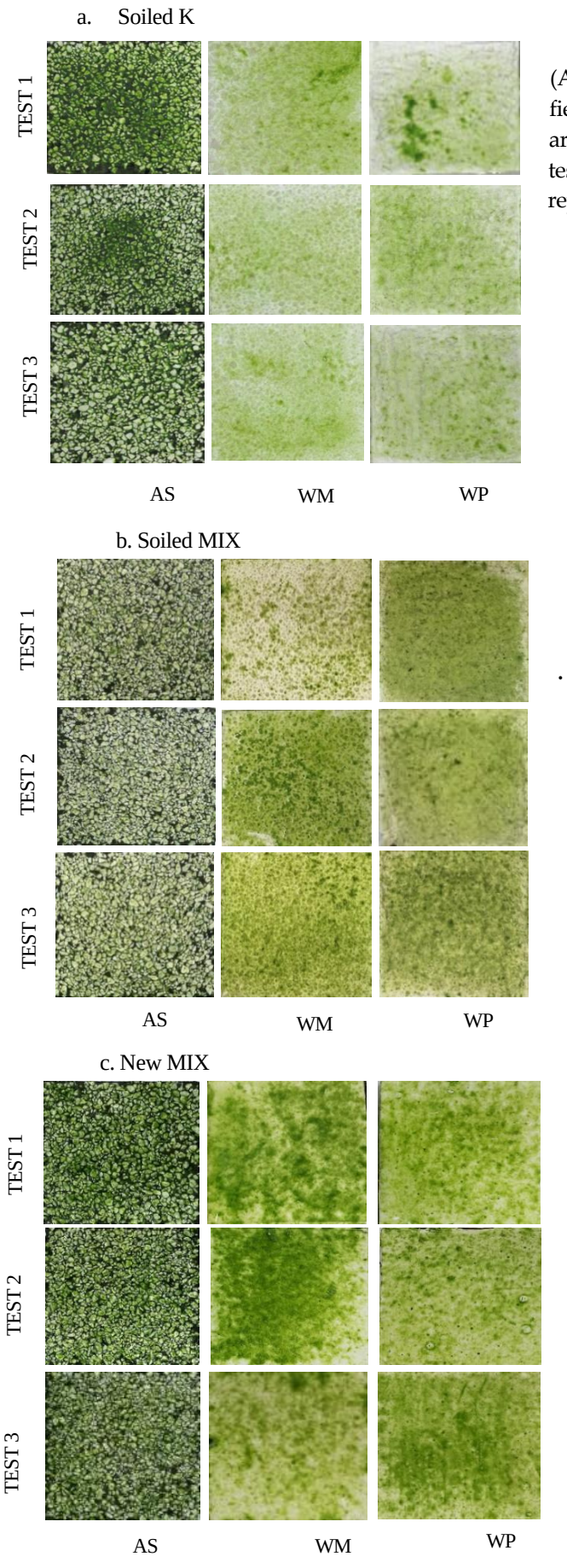

Figure 44: Images of asphalt shingle (AS), cool single ply membrane (WM), and field applied cool paint (WP); final images are shown (t4): a) *soiled K* tests, b) *soiled MIX* test and c) *new MIX* test. Images of all repeated tests have been reported.

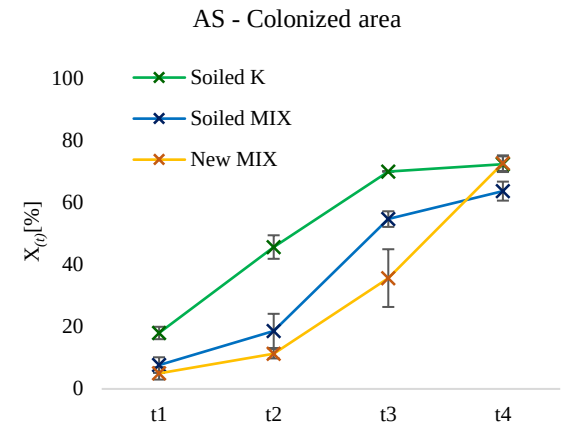

a.

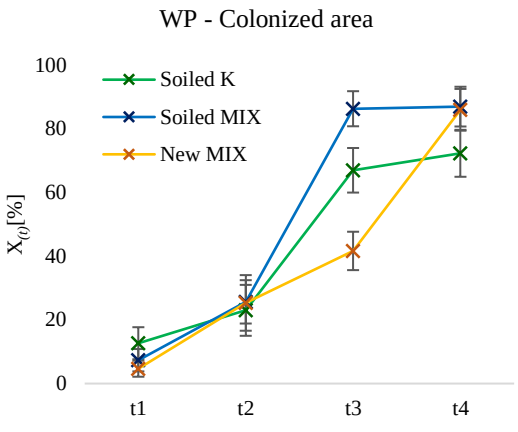

b.

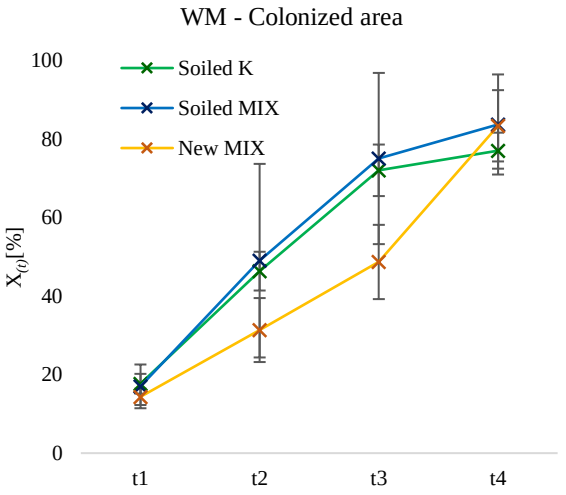

c.

Figure 45: Percentages of colonized area ($X_{(t)}$) achieved on each material type (AS, WP, WM), at each sampling time (t1-t2-t3-t4). *Soiled K*, *Soiled MIX* and *New MIX* test type have been compared. SD of three repeated test is shown.

No significant differences (*p-value*>0.05) have been found for the final values of colorimetric changes among three test types, *Soiled K*, *Soiled MIX* and *New MIX* on white samples (WP and WM). On the contrary, asphalt shingle (AS) has given different results: ANOVA test reported not negligible differences (*p-value*<0.05) among the three setup types: *Soiled K* gains the highest ΔE values, followed by *New MIX*. Standard deviation was generally low, a part for WM material, where some larger discrepancies emerged among repeated test. These results have a behavior similar to colonization rate one. Hence, ΔE values obtained through Trial IV confirmed that the soiling solution deposition on surfaces did not influence biological growth neither in negative nor positive way. Also ΔE achieved on AS surfaces, indeed, were clearly not due to the presence of soiling, rather than the colonized area values. Where $X_{(t)}$ was higher, colorimetric changes were highly dependent on biofilm covering, even if the surface has been previously soiled; vice versa, where $X_{(t)}$ did not reach high percentage (over 70% and more), soiling can significantly affect colorimetric changes.

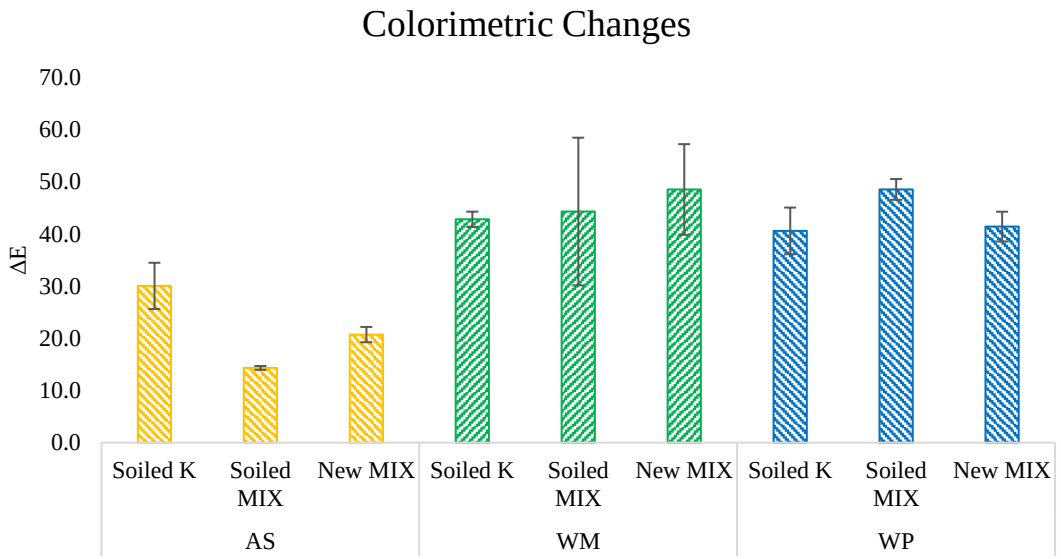

Figure 46: Colorimetric changes (ΔE) obtained after two weeks of different bioageing setups: *Soiled K*, *Soiled MIX* and *New MIX*. Average results and their SD on each product type (AS, WM, WP) have been shown. Different letters indicate significant differences among values *p-value*< 0.05.

Solar reflectance decrease on white samples, WP and WM, was particularly high in all cases (*Soiled K, Soiled MIX* and *New MIX*), due to the deep rate of colonization, which covered most part of surfaces (Figure 47). However, the decrease of ρ_{sol} resulted significantly lower (*p-value*<0.05) on AS and WP samples coming from *New MIX* setup compared with the two *Soiled* ones. In addition, $\Delta\rho_{sol}$ values on WM were lower on samples which were not previously soiled before bioageing, but in this case the difference was not statistically significant (*p-value*>0.05), may due to the higher SD. In detail, $\Delta\rho_{sol}$ on WM was 30.1±0.6 %, 29.7±6.2 %, and 23.6±4.3% for *Soiled K*, *Soiled MIX* and *New MIX* respectively. $\Delta\rho_{sol}$ on WP was 34.5±1.4%, 36.0±0.8% and 21.8±2.3% always on *Soiled K*, *Soiled MIX* and *New MIX* respectively. Hence, the decrease of solar reflectance seems generally greater when the surface was previously soiled even if the biofilm cover the most part of it. Dark color of soiling solution deposition had always a strong effect on physical properties of a surface, especially for ρ_{sol} [26]. The $\Delta\rho_{sol}$ achieved through Trial IV were quite greater on WP and WM samples than the decreases observed within Trial III, since the biological growth resulted stronger. The application of more species as pioneer organisms appeared more effective on biofilm formation compared to the application of just one species of cyanobacteria (*N. commune*).

Solar reflectance final values have been used to calculate the mean Coefficient of Variation to evaluate the repeatability of each setup run in this Trial. CV_p were 8.6%, 13.9% and 10.8% for *Soiled K, Soiled MIX* and *New MIX* test respectively. These values describe the distribution of final solar reflectance value around mean value, underling how, in case of *Soiled K* test, it was slightly more uniform compared with the other two test. However, the only considerable difference regards WM values, which resulted mainly susceptible to variability when submitted to biodeterioration procedure, as

already showed in previous results. Consequently, the uncertainty was lower than 10% case of *Soiled K* setup and *New MIX* where it was 6.2% and 7.8% respectively; it remained on the threshold of 10% for the *Soiled MIX* (*U*=10.1%).

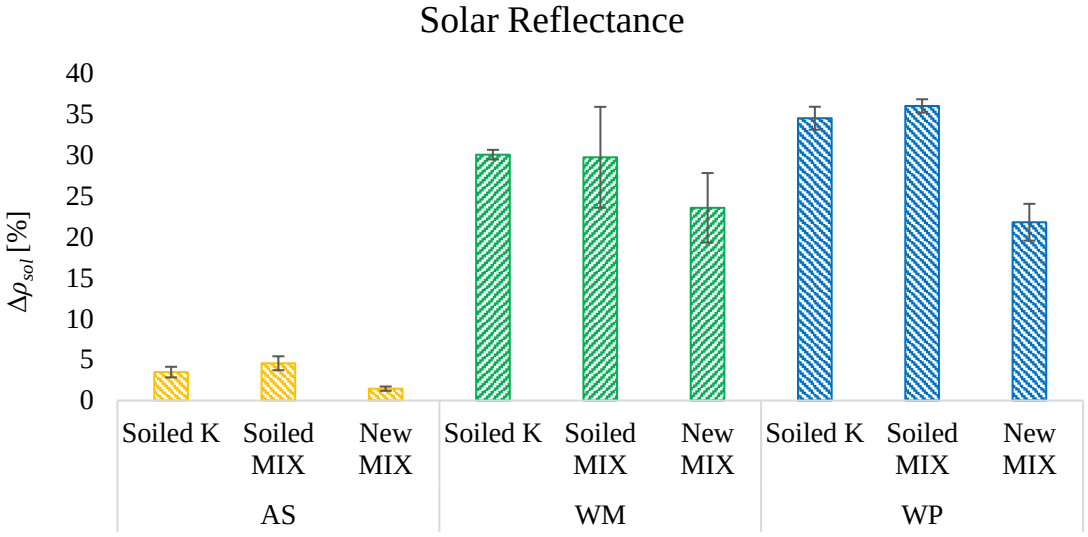

Figure 47: Mean solar reflectance decrease and SD on the three building materials products: comparison among the three setup types: *Soiled K, Soiled MIX* and *New MIX*. In "Soiled" setups, each specimen has been previously soiled with a standard solution; while the "New" setup expose specimen directly to bioageing procedure, equipped with a group of pioneer algal and cyanobacteria species.

Biological growth has been monitored through the measurement of liquid medium absorbance (Abs at 750nm). Figures 48 and 49 report the relative results, where also growth rate has been calculated according equation n°4. No significant differences (*p-value*>0.05) emerged among the setup bioreactors until time *t4*, when *K. flaccidum* achieved a marginally higher absorbance compared to the mix of organisms into the "Soiled" bioreactor (0.69±0.06 and 0.56±0.04 respectively). Observing the biomass growth curve, it should be highlighted the typical algal growth phases: at the beginning there is the "lag phase" (t0-t1), where prevails adaptation of the organism instead of their growth; then it starts "exponential phase", where a sharp and fast growth occurs, (t2-t4). The other phases were not shown. Growth rate, which identifies the number of cells division per day, remained lightly lower into bioreactor inoculated with *K. flaccidum* (Figure 49). This was also confirmed by the cells count (Figure 43), which marks as the number cells of *K. flaccidum* remained considerably smaller compared with cells number from different species. This could be explained by the greater dimension of *K. flacciudm* cells (averagely 10 μm), as reported by [147]. Other autotrophic organisms inoculated into *MIX* bioreactors, have smaller dimension cells, within the range 1-5 μm. For this reason, growth rate and cells number may result mildly greater where more organism species have been used.

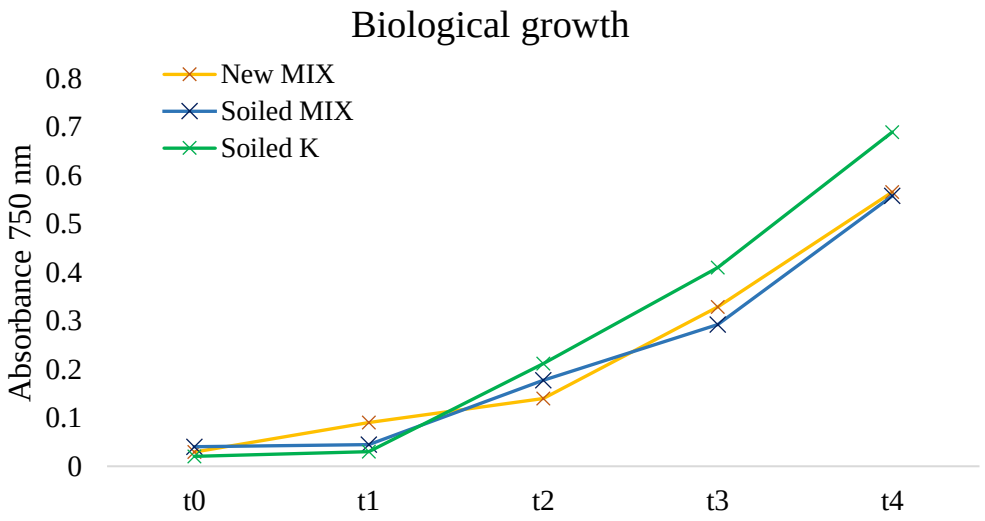

Figure 48: Biological growth into each bioreactor type during the complete test duration: t0 correspond to the starting time and t4 correspond to the 14th day of bioageing exposure. Absorbance values have been measured through UV-Vis spectrophotometer at 750 nm; data are the average of three repeated test and SD is shown.

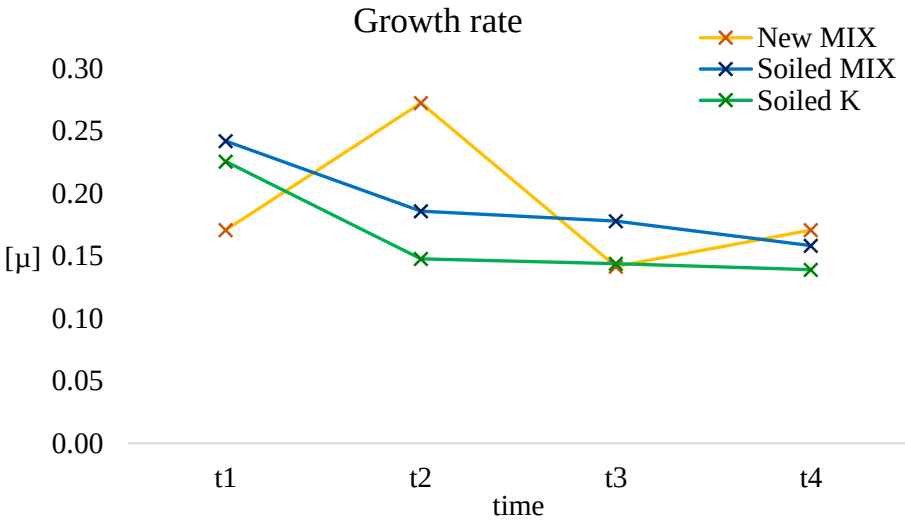

Figure 49: Growth rate [μ] for each bioreactor type (*Soiled K, Soiled MIX* and *New MIX*) during the complete test duration calculated among three repeated bioageing test. It indicates the rate of cells number increase per each unit of time (day).

Discussion

Data about uncertainty were below the threshold of 10% in two setups run into Trial IV: *Soiled K* and *New MIX* ones. *U* calculated on the final solar reflectance obtained on surfaces in the final stage of each test was in detail 10.1%, 7.8% and 6.2% for *Soiled MIX*, *New MIX* and *Soiled K* respectively.

Several considerations deserve to be examined in details comparing these and previous Trials results. Firstly, biofilm colonization rates achieved by two different phototrophs species used individually (*N. commune, K. flaccidum*) were statistically different (*p-value*<0.05) among them. This underlines the extremely wide fluctuation among algae or cyanobacteria species capability to form biofilm on surfaces. Moreover, this was largely described when surfaces are exposed to natural exposition [22], [149], [165]; however, results here obtained have confirmed the variability of bio-dynamics even when all environmental factors were strictly optimized and set within a thin range of values. *N. commune* and *K. flaccidum* have been chosen thanks their representativeness among ubiquitous organisms involved in biodeterioration of surfaces. While *Nostoc sp*. could not guarantee a satisfactory repeatability among repeated tests, *K. flaccidum* appeared to gain a more uniform biomass production among different run tests, which makes possible a higher homogeneity among colonization rate. Growth variability of *Nostoc* species could be linked to its deeply high sensitivity to light intensities [166], [167], [169], [177]: also small variations in light radiation (10 μmol/s/m^2) could stimulate cyanobacterium to different pigments and proteins production. Thus, this created different colored patinas on biofilm on surfaces, and resulted in different growth rate depending on small light variability (which can be represented also by the intrinsic variability found into the growth incubator).

These arguments and evidences led the research to avoid just one single species in this bioageing standard procedure development. Involving more pioneer species allows the starting experimental conditions to get closer to natural ones, where surfaces colonization generally initiates with a wide variety of phototrophs [28].

It is important to remind that the aim of this work was not the reproduction of what exactly occurs in nature on surfaces: this was already assumed as a unrealistic scope due to the extremely fluctuant conditions across urban cities and much more on urban surfaces, exposed to complex physical, chemical and biological interactions [126]. What is fundamental here is to establish specific laboratory conditions able to optimize and accelerate biological growth on materials; at the same time, this work wanted, overall, define which experimental conditions are able to get repeatable results in terms of biodeterioration. The first application to this finding would be to test the resistance to biological growth of building material, especially cool building materials. For all these reasons, it was assumed that involving more organisms species into experimental setup could better to recreate the bio-colonization dynamics which occur on outdoor surfaces, without the claim to mimic what exactly happens in nature, otherwise unrealistic to reproduce. Introducing two cyanobacteria species, considered as pioneer organisms by several studies [144], [175], [181], and two algal species, has permitted to achieve a biofilm from different organism types, which have different pigments production, different growth rate and different deposition dynamics: this has brought to a mixed final biofilm, created by more contributors, as occurs on naturally exposed surface [34], [180].

Observations on colonized area on samples at the end of the procedure (t4) denoted a significant difference only on AS samples (*p-value*<0.05) between *Soiled K* and *Soiled MIX* setup, while on white materials (WM, WP) $X_{(t)}$ remains similar. Comparing

colonized areas among three repeated tests where only soiled samples where used from Trial III and Trial IV (Figure 50), some findings can be highlighted. Colonization carried out by *N. commune* was significantly lower (*p-value*<0.05) than the one supplied by *K. flaccidum* or the mix of organisms on all materials types. This probably depends to the type of organism and not to biological growth rate into liquid medium. Some differences during biological growth were emerged only in the very first time interval of growth (t0-t1); then, the growth reached similar values, and no significant distances have been signed among these three repeated tests at the end of the exposure (Figure 51).

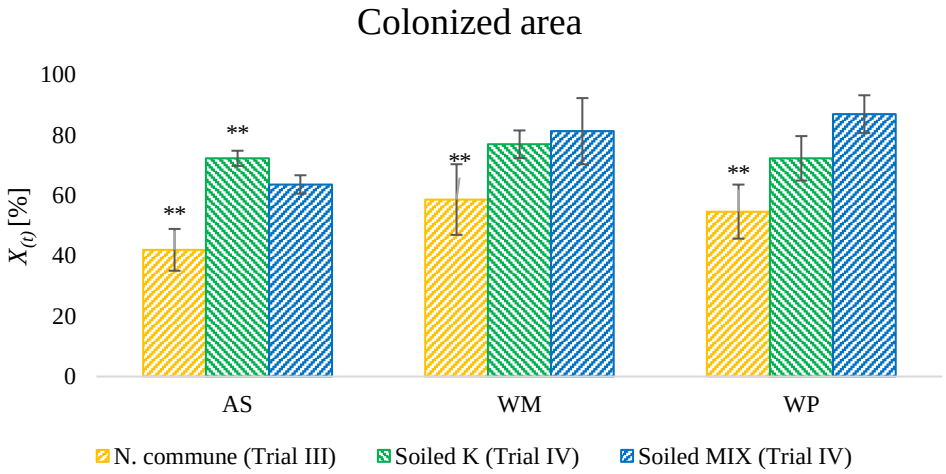

Figure 50: Comparison among colonized area fraction obtained after bioageing procedure on previously soiled samples. Mean $X_{(t)}$ data and SD of three repeated test from three setup types are shown: bioageing test of Trial III, Phase II, run with cyanobacterium *N. commune* (yellow bars); bioageing test of Trial IV, *Soiled K*, run with *K. flaccidum* (green bars) and bioaeging test of Trial IV, *Soiled MIX*, run with a mix of four organism species (blue bars).

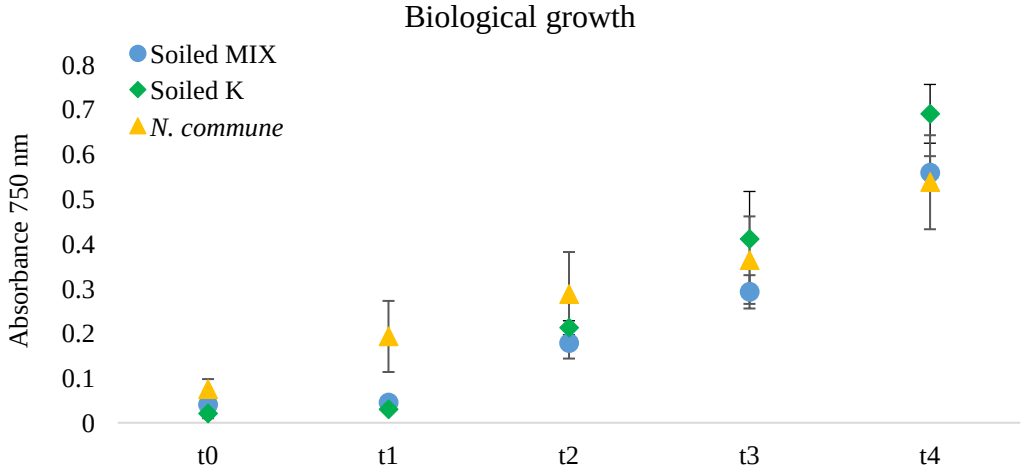

Figure 51: Comparison of mean absorbance values of liquid growth medium measured at 750nm during three bioageing test which involved only soiled samples. Test from Trial III, phase II, run with cyanobacterium *N. commune* (yellow serie); test from Trial IV, *Soiled K*, run with *K. flaccidum* (green serie) and bioaeging test of Trial IV, *Soiled MIX*, run with a mix of four organism species (blue serie).

The monitoring of colonization rates during bioageing procedure in Trial IV has allowed collecting data of covered area achieved in each time interval considered (t1, t2, t3, t4). This has permitted to study the deposition dynamic on a same surfaces during two weeks experiment. Colonization rates have been correlated with biological growth data (absorbance values of liquid growth medium measured at 750 nm). The aim was to know of any relationship among biological growth into the medium and colonization rate on surfaces exists. All data collected through the three tests (Soiled K, Soiled MIX and New MIX) have been evaluated and the results analysis are shown in Figure 52 (a, b, c). Data showed that positive correlation between absorbance and covered area fraction exists (in all cases R^2 >0.65). The linear relationship was greater for WP samples compared with WM and AS: cool paint is indeed the product which presents the lowest variability in term of biocolonization levels during these tests. Analyzing in details the correlation data batches (Figure 52), it should be evidenced that when samples reach almost 50% of bio-colonized surfaces, absorbance value at 750 nm was higher than 0.2 in at least 68.2% of the times. This means that, when biological growth achieved a specific value, this was highly correlated with a considerable (>50%) colonized area fraction. These observations could be useful in order to standardize the bioageing experimental method and in order to extrapolate data about biodeterioration level considering biological growth into the experimental setup.

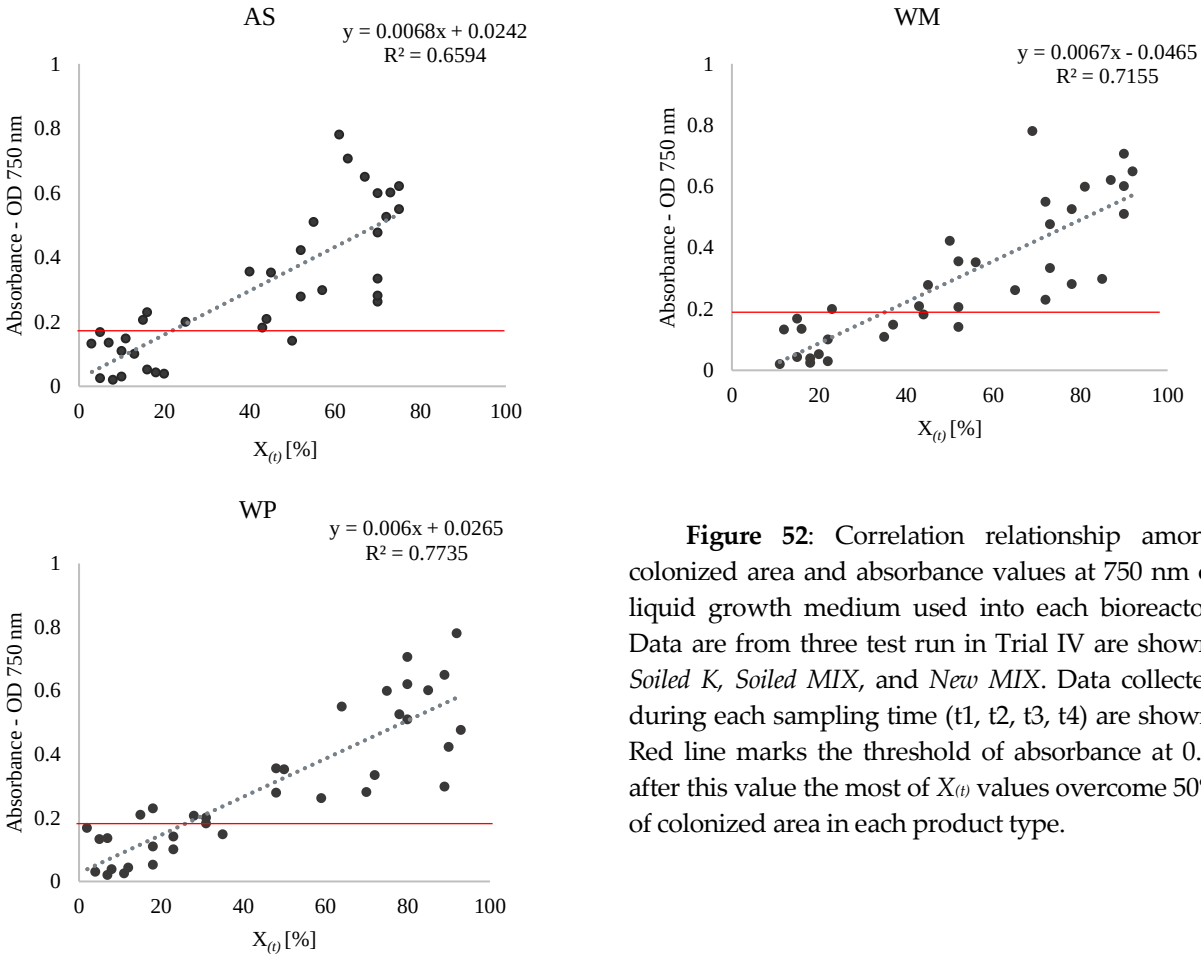

Figure 52: Correlation relationship among colonized area and absorbance values at 750 nm of liquid growth medium used into each bioreactor. Data are from three test run in Trial IV are shown: *Soiled K*, *Soiled MIX*, and *New MIX*. Data collected during each sampling time (t1, t2, t3, t4) are shown. Red line marks the threshold of absorbance at 0.2; after this value the most of $X_{(t)}$ values overcome 50% of colonized area in each product type.

Solar reflectance decrease achieved on single ply membrane (WM) and on-field applied cool paint (WP) through *Soiled K*, *Soiled MIX* and *New MIX* have been compared with Title 24 [97]. This analysis indicated that experimental $\Delta\rho_{sol}$ was greater than over-predicted value through the model when the surfaces samples have been soiled (Table 7). In detail, $\Delta\rho_{sol}$ got on previously soiled samples (*Soiled K* and *Soiled MIX*) were greater than $\Delta\rho_{sol}$ values obtained on not soiled samples (*New MIX*). The distance among experimental and theoretical values was considerable for *Soiled* setups, while it was smaller when *New MIX* bioageing setup is considered. Similar observations and considerations have been concluded also after Trial III, where the ρ_{sol} decrease after the growth of cyanobacterium *N. commune* on soiled surfaces was major than the Title 24 estimated values. The obtained experimental values could be considered as possible losses in hot and humid climates, as Florida. Sleiman et al. [18], [97] described as microbiological growth could represent the major agent of roof soiling in humid places. It is important to underline, indeed, that CRRC site-resolved database reported that absolute solar reflectance losses for samples with ρ_{sol} >0.4 are 2–3 times greater in hot and humid climates (like Florida) than dry climate zones (Arizona, Ohio). In these cases hence, provisional aged solar reflectance could not correctly be over predicted by Title 24 model, which underestimates $\Delta\rho_{sol}$ in hot and humid regions [105], [195]. For these reasons, experimental data and setup here obtained could represent a useful tool to take into consideration microbiological growth among roofing products soiling factors, in particular when they are applied in liable regions (hot and humid climates).

Table 7: Comparison among theoretical (estimated by Title 24 model) Δρsol values and the experimental data obtained at the end of the three bioageing procedures: Soiled K, Soiled MIX and New MIX.

		$\Delta\rho_{sol}$ - [%] Experimental	$\Delta\rho_{sol}$ - [%] Title 24
WM	Soiled K	30.0	18.5
	Soiled MIX	29.7	
	New MIX	23.6	
WP	Soiled K	34.5	20.4
	Soiled MIX	36.0	
	New MIX	21.8	
AS	Soiled K	3.5	2.9
	Soiled MIX	4.6	
	New MIX	1.5	

The assessment of repeatability showed a satisfactory improvement of Trial IV compared the previous Trials; in particular, two setups run in Trial IV fully achieved and even drop the acceptance uncertainty threshold of 10% set in this work: *Soiled K* test and *New MIX* test. The first mentioned test was the bioageing procedure run inoculating the liquid growth medium with just one algal species: *K. flaccidum* and involved only soiled specimen; the second one used four species of phototrophs and did not apply the soiling layer. As discussed before, the use of just one species should

be avoided towards the development of a bioageing standard procedure. Indeed, the biofilm features and colonization dynamics could be deeply dependent to the single species chosen and the results in terms of material resistance to biodeterioration risk to be not reliable. The application of more organisms together ensure a more homogenous biological growth within the liquid medium and consequently on the surfaces: a group of species could be more capable to face any environmental condition and produce a more uniform response in terms of cells density and pigments production, compared to just one type of organism. Within a mix of species, a possible temporary stress effect on the metabolism and growth for one of them could be compensate by the other ones, ensuring a homogenous growth during the experimental duration test even if one species would be affected by an abiotic stress [66]. Furthermore, involving more pioneer species allows the starting experimental conditions to get closer to natural ones, where surfaces colonization generally initiates with a wide variety of phototrophs [28].

One of the critical aspects of the setup hereby realized was that it promoted a very fast microorganism attachment on sample surfaces. Colonization rates indeed overcame 50% of total area after just 10 days of exposure (t3). This is a strength point considering the aim to accelerated the bio-dynamics on building samples; at the same time it could represents a challenge since one of the experimental needs is a detailed description of all the biodeterioration process. This very limited experimental duration makes tough the accurate analysis of the biological growth on samples. Moreover, the same results in this short time was never reached by no one other accelerated bioageing setup previously studied: all the available setups contemplated laboratory exposure to bio-growth for months [137], [138], [151], [168]. TIS bioreactor provided a modularly number of immersion/ventilation cycles, keeping the specimen completely flooded for ten minutes, than air cycle helps to bring liquid medium below samples level and encourage their drying. Nevertheless, TIS bioreactor is a sealed growth chamber, and air humidity rate inside reached saturation point during bioageing test. Increasing the number of immersion cycles, wetting time on surfaces increase as well. Since water availability on surfaces stimulate biological growth, number of immersion cycles could positively influence and even accelerate surface colonization. Hence, number of immersion cycles has been reviewed in the next Trial, always in a view of a mild deceleration of bioageing process.

Previous Trial III, where the same setup experimental conditions have been run on both new and previously soiled samples, did not get significant differences (*p-value*>0.05) in biofilm colonization area on surfaces (Table 6). Also the images analysis from Trial IV did not mark the soiling deposition as factor which remarkably contribute to enlarge or reduce colonization areas, especially on WM and WP products. Hence, results from Trial IV constitute a further evidence that the biological growth is not remarkably influenced by the presence of standard atmospheric pollutants solutions. At the same time, available literature has mixed views on this topic, as earlier described. While [180] supported that the deposition of atmospheric particulate matter promotes microbial growth, other researchers found that air pollution suppressed the total community of microorganisms, which included fungi, in the biofilms growing on gravestones in Massachusetts, USA [40], [196]. What seems clear is that the interactions

among microorganisms and pollution would depends, again, by many aspects link to nature of pollutants, organisms species and climate region [168]. Regarding experimental needs, results from both Trial III and IV showed that standard soiling mix should not affect biological growth on surfaces; however, it could influence solar reflectance losses.

Given all these considerations, the next bioageing Trial (described in section 5.5) has used only the mix of organisms as liquid medium inoculum since it was evaluated more representative than just one species to induce biological aggression effects. This choice was moreover considered by the most part of accelerated setup developed by other authors [20], [140], [142], [160], [196], [197]. Since the biological growth over the surfaces seems to be not affected by the soiling layer during these experimental tests, the next Trial used not previously soiled building material specimen.

The *Development* phase of accelerated bioageing procedure might be considered as concluded through Trial IV. The next Trial V on building materials is the "*Definition*" Trial, the one that collected and applied all the experimental and environmental conditions developed in order to build and confirm the final accelerated biodeterioration procedure.

However, before going on to Trial V, an entire section has been dedicated to study the effect on algal cells metabolism of soiling solution, considered as an abiotic stress source. The environmental-related aspects of atmospheric pollutants deposition on urban surfaces have been then investigated studying some metabolites algal production in response to stress exposure.

5.4.1. Abiotic stress on algae: study of soiling solution effects on their growth and metabolism

This thesis work was primarily focused on the study of biocolonization phenomenon, which is part of surfaces fouling as broadly described in sections 1 and 2. In urban environments, microflora species settle down on surfaces, previously soiled by atmospheric pollution and other sources of particulate matter such as dust [40], [198]. Some research works studied the influence of atmospheric pollutants on microbial community ecology, demonstrating how biofilm is inhibited on both size and diversity [40], [195], [199]. These outcomes have provided new insights into the effects of abiotic stress (as urban pollutants) on living organisms. Airbone particles originate from windblown dust, forest and grassland fires, living vegetation, and sea spray, as well as from human activities, such as the burning of fossil fuel; these last in particular represent a global issue for public health [200]. Starting from these assumptions, this part of the work wanted to study the influence of atmospheric particles on phototrophic organisms, which can be found in urban environment. Several works have investigated how certain environmental conditions and abiotic stress (as UV radiation, high-low temperature,…) influence and stimulate cyanobacteria or green algae metabolites production in order to overcome and acclimatize stress conditions [172], [201]. Carbonaceous particles and other pollutants, which are released into the air and settle down on surfaces, fully represent a source of abiotic stress on cells growth.

The aim of this part of the work was to analyze the cellular response of some ubiquitous green algae when they are exposed to soiling agents. An aqueous mixture of four soiling agents (as described in section 5.3), which simulates atmospheric pollution compounds [124], was applied as algae growth medium. During their growth, then, algal cells were exposed to soiling mixture, which represents the abiotic stress source. Microalgae show great adaptability towards the abiotic stress factors and produced valuable metabolites. This study then analyzed the metabolites production of two algal species after their exposition to the standard soiling mixture already applied by ASTM D7897 [124]. An abiotic stress could induce oxidative stress, caused by Reactive Oxygen Species (ROS) accumulation within cells, which induces in turn algal cells to produce valuable secondary defensive metabolites with antioxidant potential to compensate for this imbalance [173].

Photosynthetic organisms are especially vulnerable to ROS since the reduction of molecular oxygen along the electron transport chain results in superoxide anions (O^{2-}) [202]. Increased levels of ROS in microalgae can damage nucleic acids, proteins, lipids, and damage signal transduction. Lipids and membranes are vulnerable to lipid peroxidation caused by ROS, which produces in turn highly reactive molecules as aldehydes (i.e. malondialdehyde, MDA), that can further damage proteins, amino acids, and DNA structure [203]. Thus, the production of antioxidants by algae is essential to reduce severe cellular damages caused by ROS. Algae have evidenced the capability to induce an antioxidant defense system consisting of enzymatic and non-enzymatic protection to mitigate organelle damage instigated by ROS [173]. Among the antioxidant metabolites produced by algae against environmental stress there are polyunsaturated fatty acids (PUFAs), pigments, in particular carotenoids e phenolic compounds [201], [204]. PUFAs are notably interesting molecules since are known for their cell-protective and repair properties [205]. Thus, in this study, oxidative stress products (MDA) and antioxidant molecules (PUFAs and pigments) were extracted from algal cells grown into soiling mixture in order to identify and quantify their production and evaluate oxidative stress induced by the exposition to soiling solution.

Material and methods

Algal species chosen for this study were *Edaphochlorella mirabilis* [146] and *Klebsormidium flaccidum* [147], both selected because they are low demanding species and adapted to live on land and urban surfaces; for this reason they were species certainly exposed to soiling agents. Two types of growth medium have been prepared: *control medium* involved was BBM, the liquid medium already used in previous trials and considered as the common optimum substrate to algal growth; BBM was then added to soiling solution, which represent the source of abiotic stress applied (*treated medium*). Soiling mix was prepared according to [124] and used with a dilution 1:50 (v/v). Final solution was dark in color and it constitutes a screen for light absorption by phototrophic organisms. This solution represented *treated* samples (Figure 53).

a. b. c.

Figure 53 : a) TIS bioreactor filled with *control* BBM medium inoculated with *E. mirabilis*; b) TIS bioreactor filled with *treated* medium (BBM + soiling mix) 1:50 (v/v), inoculated with *E. mirabilis*; c) TIS bioreactor, top view on treated medium.

TIS bioreactor system has been modified and adapted according to the requirements of this experimental trail: no trays were used into the sealed vessel. A pump blowed the air through the central filter, which was linked with an internal tube, which reaches the liquid (Figure 53c). The pump was activated automatically by a timer, 6 times per day, for 10 minutes each. Bioreactors were kept at the same light and temperature conditions (24±1°C) into a growth incubator (Biolog Lux, AG-System). Six bioreactors were prepared for each experimental test: 1 *control* and 2 *treated* bioreactors for each algal species studied were involved as summerized in Table 8. 500 ml of growth medium solution have been inoculated with 25 ml of sterile mother culture.

Also in this case, bioreactors and culture medium has been sterilized (autoclaved at 120°C, 1 atm, for 20 minutes) before the algal inoculum. This has allowed avoiding biological contaminations, which could compromise algal growth and invalidate the test. Each test lasted three weeks and it has been run in triplicate.

Table 8: Bioreactors names and algal species involved in each test. The abbreviation for each sample is shown.

Edaphochlorella mirabilis		***Klebsorbidium flaccidum***	
Control	CC	Control	KC
Treated sample 1	T1C	Treated sample 1	T1K
Treated sample 2	T2C	Treated sample 2	T2K

During the experimental test, algal growth has been monitored through biomass dry weight and absorbance analysis. A rate of algal biomass has been harvested on cellulose esters filter plates (0.22 μm pores), then dried with N_2 and weighted. Absorbance at 750 nm has been determinate with UV-Vis Spectrophotometer (Jasco V-730) [153]. Data were collected weekly and growth curve has been outlined from t0 values (which is the first day of test) to t4 (final day). At the end of three weeks, all liquid medium was filtered with vacuum flasks and all algal biomass was collected on hemicellulose filter plates (Figure 54). About 30 ml of liquid medium were filtered to get a satisfactory biomass amount on each plates. The following metabolites extraction

and analysis has been performed using the biomass collected on several plates for each bioreactors.

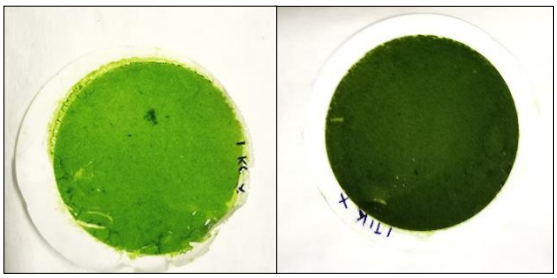

Figure 54: Algal biomass collected on hemicellulose filters: a) control (green) growth medium and b) treated (dark green) growth medium.

MDA extraction and analysis

Malondialdehyde (MDA) was secondary metabolite product of the oxidation of polyunsaturated fatty acids, was considered a useful index of general lipid peroxidation [206]. Peroxidation of lipids in membrane and biological systems could be estimated by thiobarbituric acid-reactive-substances (TBARS) assay, which is able to analyze and quantify the concentration of MDA. The extraction of MDA from algal biomass was performed according the protocol described by [206]. Approximately 0.2 g of fresh weight (FW) of algal biomass was homogenized with inert sand in 2 ml 80:100 (v/v) ethanol: water. Then, 2 ml of acid solution including trichloroacetic acid (TCA) at 20.0% (w/v) and 0.5% thiobarbituric acid (TBA) were added to each sample. Samples were then mixed vigorously, heated at 95 °C in a block heater, for 25 min, cooled, and centrifuged at 3000 g for 10 min. Absorbance was read with Spectrophotometer (UV-Vis, Jasco V-730) at 532 nm, and adjusted at 600 nm. Malondialdehyde equivalents were calculated with the following formula [207]:

$$MDA\ equivalents\ \left(\mu\frac{mol}{ml}\right) = [(A_{532} - A_{600})/155] \quad [14]$$

Where 155 is the molar extinction coefficient for MDA.

Fatty acids extraction and analysis

Fatty acids (FA) extraction from algal biomass was carried out following Folch Method and next modifications [208]. This protocol used a chloroform: methanol 2:1 (v/v) solution together with saturated NaCl solution, which allows the samples separation into two distinct phases: the polar one (upper layer) and the lower lipophilic phase, which contains fatty acids (Figure 55).

Figure 55: Two-phases fatty acids extractions: polar phase is the upper layer and the lower phase contains fatty acids. Two algal species FA extraction are shown (*K.flaccidum* on the left and *E. mirabilis* on the right).

After the lipid extraction, the whole amount of triglycerides have been trans-esterified in order to detect and identify them through Gas Chromatography Mass Spectrometer analysis. Trans-esterification is performed adding a basic solution (KOH, 2M). After a vigorous mixing and centrifugation (3000g, 10 minutes), fatty acid methyl esters (FAME) were obtained. This specific transesterification method is widely used in the analytical field [209]. They have been identified and quantified with Gas-Chromatograph (GC, HP 6890 Series) coupled with mass spectrometer (HP 5973 Mass Selective Detector) as already described by [210]. FAME analysis were run according to the procedure described by Montevecchi et al. [210]: "Splitless" method was applyed during GC analysis. Peaks were identified by comparing the retention times and mass spectra of pure standards (Supelco 37 Component FAME Mix, Merck) and by comparing the mass spectra with those ones present in libraries focused on fatty acids methyl esters (Fame db23.l and Fame dbwax.l; Agilent Technologies). Quantification was performed using the internal standard (nonadecylic acid methyl ester, 1% exane). Fatty acids were expressed as mg/100 mg algal biomass.

Pigments extraction and analysis

Pigments have been extracted through three following step applied to algal biomass using three different solvents as already described by [211]. Firstly, 20mg of fresh algal biomass has been suspended in 2 ml of ethanol absolute, then shacked for 30 minutes, and centrifuged for 10 minutes at 4000g to separate pellet and liquid phase. These operation was repeated other two times changing the solvent: after ethanol, the biomass residue was suspended into 2 ml of acetone, and lastly into 2 ml of exane. After the last extraction, the entire supernatant (which is the sum of ethanol, acetone and exane) was concentrated using gaseous N_2: the organic extract was then recovered and accurately weighted. Lastly, all the amount of pigments extract was suspended into acetone and subjected to pigment analyses. Pigments separations, detection and quantification were performed through High Pressure Liquid Chromatography (HPLC). Main standard solutions were used for calibration and validation of HPLC method: Chlorophyll *a* and *b* (*Chls*), Lutein (Lut), and β-Carotene (β-Car) standards were purchased from Sigma-Aldrich s.r.l (Milan, Italy). Standard stock solutions are prepared in acetone, except for *β*-Car that is dissolved in absolute ethanol. All the pigments contained into the samples were quantified by reverse phase HPLC (PU 4180,

Jasco Europe Srl, Cremella, LC, Italy), equipped with a carotenoids C30 column (YMC, Europe), 250x4.6 mm, set at 25 °C. The auto sampler AS-4050A was coupled with an isocratic pump: the different compounds have been separated isocractically and quantified using UV/Vis detector (4070 UV/Vis detector) at the wavelengths of 450nm and 600 nm. Two mobile phases were used: Phase A=MeOH/MTBE/H_2O (81:15:4) (v/v/v); Phase B= MeOH/MTBE/H_2O (6:90:4) (v/v/v). The analysis method started with 100% of phase B, then phase A gradually increased its concentration through a linear gradient of until the 66.6% of phase A and 33.3% of phase B in the first 60 minutes. Then, the last 15 minutes of analysis, the method used 100% of phase B again, for a whole duration of 75 minutes for each sample. The flow rate was 1 ml min^{-1}. The peaks identification and quantification has been performed on UV–Vis spectra obtained at 450 nm since it was seem the best absorbance λ for these pigments types according to chromatographic analysis [212]. Peaks identification and attribution was performed comparing retention time (RT) of pure standard solutions. Pigments were quantified by HPLC, using an external calibration curves for β-carotene, chlorophyll *a*, chlorophyll *b* of five concentration levels. Pigments contents are quantified and expressed in μg of pigment on mg of algal biomass (FW). Results have been analyzed running ANOVA and T- student test to compare repeated data set using PAST3 software.

Results and discussion

Algal biomass curve was reported in Figure 56, where dry weight is collected during the experimental trails. Algal biomass amount meanly produced at the end of three weeks growth was 1,43 ± 0.94 mg/ml and 1.10 ± 0.96 mg/ml for *control* samples (*E. mirabilis* and *K. flaccidum* respectively); and 1.20 ± 0.94 mg/ml e 0.85 ± 0.75 mg/ml for *treated* samples (*E. mirabilis* and *K. flaccidum* respectively).

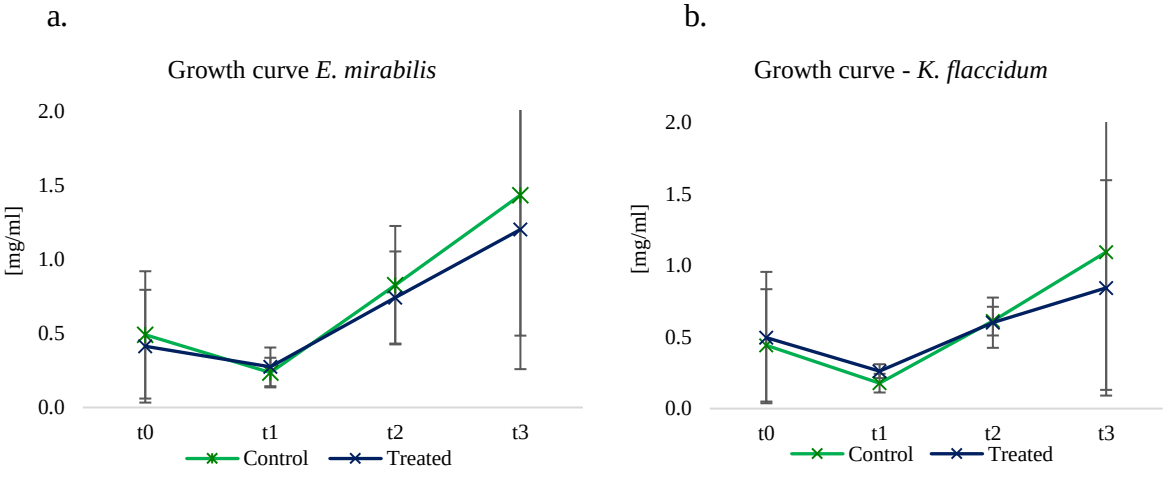

Figure 56: Growth curves of fresh biomass produced by *E. mirabilis* (a) and *K.flaccidum* (b). Data are collected on sampling days 0, 7, 14, 21 which correspond to t0, t1, t2, t3. Values are the mean of three repeated trials and SD is shown.

The growth curves had a similar trend: both algal species presented a slight growth

decrease during the first week, which corresponded to "lag phase". This could be due to algal adaptation response once the organisms have been inoculated into bioreactor. Then, biomass production started to increase until the end of the third week. There was not significance difference between *treated* and *control* samples regarding biomass production (*p-value*>0.05). However, these results had a remarkably high standard deviation, mainly due to the very low amount of FW collected on filters. The small quantity of biomass increased the standard error on the weight measure. Even if soiling mix absorbs part of light radiation, compromising light transmission to phototrophic cells, algae can activate specific metabolism pathways which make them possible to tolerate abiotic stress [172]. This has highlighted that the soiling solution did not inhibit algal growth. This was consistent with previous results achieved in this study already observed on soiled material surfaces: the standard soiling mixture was compliant with biological growth and it did not have inhibiting effects on biofilm. As other authors have already underlined, soiling could cause a reduction to most sensitive species population [54]; however, algae and cyanobacteria could still survive thanks to their highly tolerant metabolism [13], [172]. Following results describe metabolites production as response of algal cells exposed and grown to soiling mixture.

Higher MDA levels emerged on treated samples of both algal species studied, but only into *K. flaccidum* MDA production was statistically higher into treated samples compared to control ones (*p-value*<0.05). Treated samples of *K. flaccidum* produced 80,7% of MDA more than control samples (0,38 ± 0,06 μg/g compared to 0,21 ± 0,09 μg/g respectively). MDA production on treated samples of *E. mirabilis* recorded a lighter increase of 7,5% compared to controls: 0,25 ± 0,21 μg/g compared to 0,23 ± 0,05 μg/g (Figure 57). Higher values of MDA found into algal biomass exposed to soiling solution, even if the increase was not always significant, denoted the rise of lipid peroxidation, which was the marker of stress action on living cells. *K. flaccidum* and *E. mirabilis* had the ability to activate some response mechanisms to tolerate the abiotic stress induced by soiling solution [201].

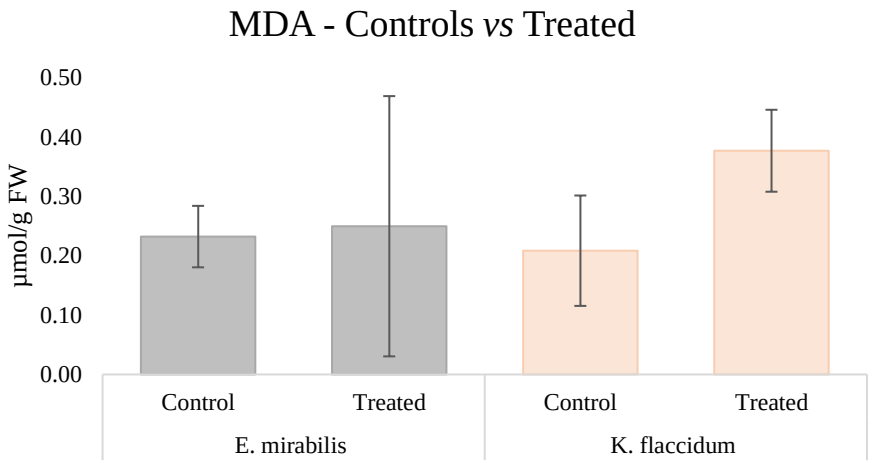

Figure 57: Malondialdehyde production (μmol/g FW) by *K. flaccidum* and *E. mirabilis* after three weeks of growth into soiling solution and into control medium. Values are the mean of three repeated test, where two treated samples and one control sample are included into each test. SD is shown.

Soiling solution did not affect considerably the total amount of lipids on both algal species. *E. mirabilis* lipid content indeed was averagely 0.27±0.12 mg lipid /mg of fresh biomass and 0.24±0.12 mg lipids/mg fresh biomass into control and treated samples respectively; *K. flaccidum* produced 0.15 ±0.10 and 0.26± 0.12 mg lipid content /mg fresh biomass on control and treated samples respectively. T-student test run to compare these results did not highlight any significant differences (*p-value*>0.05).

Analyzing in detail fatty acids profile (Figure 58 a,b), it was possible to observe that the most abundant FA was C:16 in both algal species. Among the unsaturated C:18 series, C18:3, and C18:2*α* represented some of the most abundant FA species found in these algal species. Furthermore, the increase of linoleic acid (C18:2) (*p-value*<0.05) and palmitoliec acid (C16:2) (*p-value*<0.1) in treated samples of *E. mirabilis* was significant according to statistical analysis. Mean gain of PUFAs C18:2 and C16:2 from *E. mirabilis* was in line with previous findings by [213] which underlines how *Chlorophytae* mainly contain C16 and C18 FA species with 0–4 double bonds. Lipid production by *K. flaccidum* showed averagely a decrease of percentage content of C:16, and other C:18 PUFAs (C18:2, C18:1), even if these decline was not significant due to high standard deviation (*p-value*>0.05). A remarkable difference was achieved by C18:1*cis* and C:14 which increaseds significantly into *K. flaccidum* cells grown into soiling solution. C18:1*cis* content into control samples achieved meanly 0.6±0.2 mg/100 mg total lipid content, while into treated samples its production was 2.9±1.0 mg/100 mg total lipid content. Other FAs were not showed in Figure 58 because only small percentages have been detected into investigated samples. Interesting fact is that most of these traces of FAs have been found only in treated samples and most of them were PUFAs, as reported in Table 9.

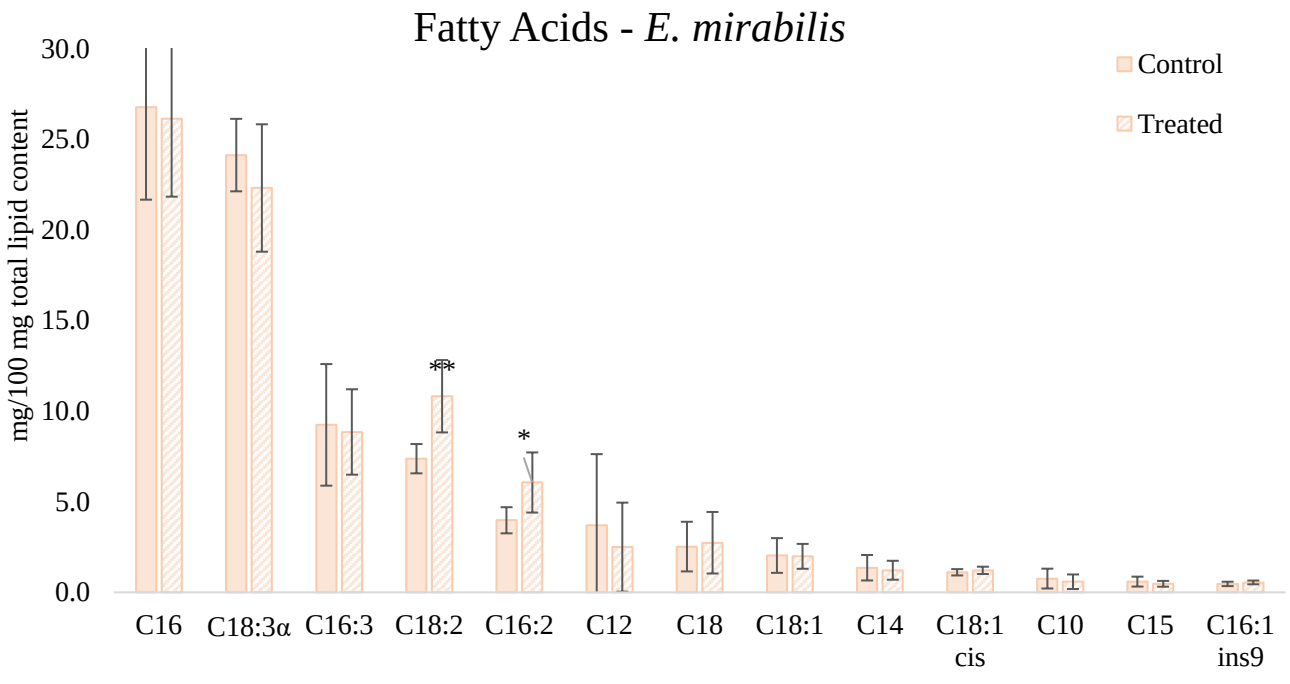

a.

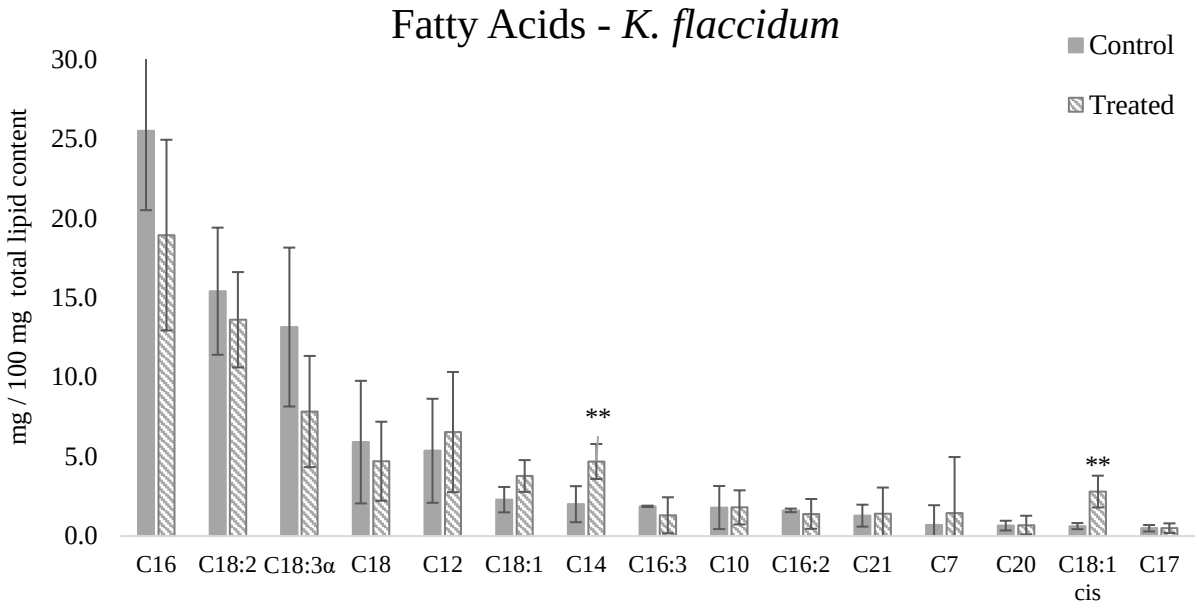

b.

Figure 58: Fatty acid production by *E. mirabilis* (a) and *K. flaccidum* (b) species: mean data about control and treated samples of three repeated test and relative SD are shown. Data are expressed in percentage on total lipid content (mg of FA/100 mg lipid content). Statistically significant difference between control and treated samples have been evidenced with * (*p-value*<0.1) or ** (*p-value*<0.05).

Table 9: Trace content (%) of single fatty acids on total lipid content in treated samples. Results are shown according to the algal species.

E. mirabilis		***K. flaccidum***	
Fatty acid	**%**	**Fatty acid**	**%**
cis-10-Heptadecenoic a.	0.009	C14:1	0.06
C22:2	0.035	cis-10-Heptadecenoic a.	0.03
		C18:3 1γ	1.02
		C18:2 (trans, trans)	0.12
		cis-11-Eicosenoic a.	0.13
		C20:2	0.04
		C24:0	0.04

The lipid accumulation, and in particularly, the increase of specific PUFAs (linolenic acid, palmitoleic and C18:1*cis*) recorded here after the exposition to soiling mix, was a common algal response to abiotic stress [172]. Paliwal et al. described that the polyunsaturated lipid gain could be a consequence of the light radiation reduction, which corresponds to one of the stresses effect of soiling solution.

An example of chromatograms of pigments extraction is shown in Figure 59. Each

peak identified a different pigment type or class; compounds were identified on the base of combined information from chromatographic elution through the C30 column and chromatography profile of standards run at known concentration. The position and of the pigments' macro-categories (xanthophylls, chlorophylls and carotenoids) have been reported into chromatograms profile. Each group involved more than one single molecule, which have been chromatographically separated; however, it was possible to identify and quantify only the compounds whom the specific standard was available during the analysis. *Chlorophyta* and *Charophytae,* the two belonging phylum of the algal species involved in the study, presented primarily chlorophyll *a* and *b* [212], and its derivative compounds as photosynthetic pigments. However, carotenoid were also always produced from these organisms even if they were quantitatively lower than chlorophylls, and their respective rate was 1:7,7 and 1:9,5 for control samples *E. mirabilis* and *K. flccidum* respectively. These data could be comparable to the ones available in literature regarding pigments rates into green algae [212]. The differences among carotenoids and chlorophylls seems to rise into treated samples, where the rates *carotenoid:chlorophylls* were 1:9,4 and 1:14,3 for *E. mirabilis* e *K. flaccidum* respectively. Chlorophyll *a* was the most abundant pigment in both algal species: its production was not notably affected in *E. mirabilis,* but only in *K. flaccidum* where it resulted statistically higher in treated samples (*p-value*<0.05) (Table 10). Statistical analysis did not highlight any other discrepancy between controls and treated samples (*p-value*>0.05). Again, the standard deviation is often very high: the wide variability of results has been linked to the small biomass amount submitted to extraction and following analysis.

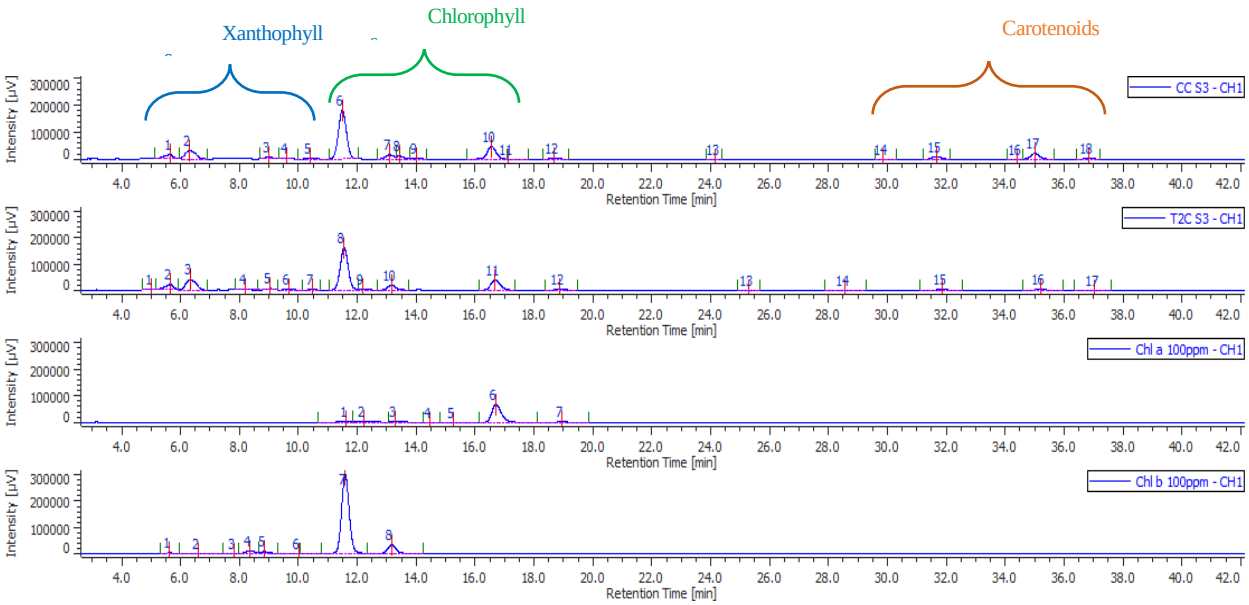

Figure 59: Chromatograms obtained by HPLC analysis: Xanthophyll, chlorophylls and carotenoids extract from *E. mirabilis* are shown (CC is a control sample, and T2C is a treated sample). Chlorophyll *a* and *b* pure solution have been run as standard at 100ppm concentration. Peak identification and characterization are given in Table 10.

Table 10: Average of pigments species concentration into control and treated samples of *E. mirabilis* and *K. flaccidum*. Retention time of each pigment peak and its SD is shown. All data have the SD calculated on three repeated trials. ** indicate significant results (*p-value*<0.05)

		[ug pigment/mg algal biomass]			
	RT ± SD	*E. mirabilis*		*K. flaccidum*	
		control	treated	control	treated
Chl *b*	11.48±0.41	11.5±4.8	7.7±1.5	9.0±3.4	10.3±0.2
Chl b*x*	13.08±0.36	7.3±3.1	5.6±2.1	9.2±9.5	8.4±2.5
Chl *a*	16.54±0.42	58.5±12.6	45.0±7.9	18.4±12.9	40.8±6.0**
β-Car	34.97±0.37	7.0.0±2.5	6.1±0.8	4.4±1.6	6.3±1.2

On concluding, soiling solution applied as growth medium for *E. mirabilis* and *K. flaccidum*, has some noteworthy effects on these algal species cells metabolism. However, growth data underlined that the standard mix of pollutants has not any inhibiting impact on algal cells division, as already observed in natural exposure and conditions [50], [181]. MDA and some specific PUFAs production denoted the influence of soiling on cells peroxidation level, which is a marker of stress factors effects. At the same time, these organisms showed the capability to respond to the changing environmental factors by modulating their metabolites as adaptation behavior already reported by several studies [184]. No great difference have been recorded in pigment production, where only Chl *a* concentration significantly raised into *K. flaccidum*. This could be interpreted as the capability of these algal species to respond and adapt to abiotic stress; at the same time it should be considered that the scarce algal biomass availability represented a not negligible limiting factor, which makes the results hardly repeatable. Increasing growth medium volume and extending the experimental test duration may be a way to harvest a bigger amount of algal biomass as future implementation of this study.

Beyond the detailed secondary metabolites production, one of the main evidence of this trial is the ability of studied algal strain to grow into a standard atmospheric pollutants and particles solution. This is consistent with the results achieved through accelerated bioaging Trial l III and Trial IV run on soiled building material. The exposure to this kind of abiotic stress did not affect in a substantial way these urban organism growth, as already noted by other studies [69].

5.5. Trail V - *Definition* of Accelerated bioageing procedure: Avrami's Law application and modelling of the experimental results

The mix of species applied within Trial IV has given improved results compared with other setups, then it was considered more reliable to describe a representative bio-colonization dynamics. Hence, Trial V has been focused on the repeatability of the accelerated bioageing setup using TIS bioreactor and the mix of phototrophs as colonizers. The algal colonization as temporal evolution was here studied day by day in order to monitor and describe the kinetic process which occurs on surfaces [29]. The following tests have been constantly monitored, and biological growth and colonization rate on surfaces were measured daily.

This way brought to obtain experimental values of daily colonized area ($X_{(t)}$). Considering Avrami's model described in section 2.3 and the equation n° [1], *K* factor, related to material properties, became the evaluation parameter to indicate the capability of the material product to resist to biological colonization. Since $X_{(t)}$ can be determined experimentally by image analysis, the value of *K* (dependent variable) could be determined by least square methods. It was estimated applying least squares regression [16] in order to achieve the best fit for normalized experimental data ($X_{(t)}^{exp}$) by minimizing the sum of the squared residuals (*S*) of points from the plotted curve, using the formula:

$$S = \sum(y_i - \hat{y}_i)^2 \qquad [15]$$

Where: $(y_i - \hat{y}_i)$ is the difference between the normalized observed value (y_i) of colonized area $X_{(t)}$ and the value predicted ($\hat{y}_i$) by the model. By using the expression of $\hat{y}_i$, *S* was minimized and *K* was estimated for each material. Then coefficient of determination R^2 was calculated applying the following formula:

$$R^2 = 1 - \frac{\sum(y_i - \bar{y}_i)^2}{\sum(y_i - \hat{y}_i)^2} \qquad [16]$$

y_i are the observed values, $\bar{y}_i$ is their average value and $\hat{y}_i$ are the predicted values of $X_{(t)}$.

The following experimental tests have been planned in order to apply the environmental conditions which previous trials have indicated as the best according to bioageing requirements to reach the acceptable uncertainty criterion (10%). Experimental results were then modeled to Avrami's theory [138]–[140], which has been indicated as the law able to correctly reflect the biofouling process and colonization rate under accelerated laboratory growth conditions. The correlation analysis (R^2) between experimental colonization curve ($X_{(t)}$) and the model curve has

been performed in order to evaluate the application of Avrami law to this bioageing procedure. Once the correlation has been defined, the resistance parameters (*K*) of each building material product has been calculated. Bioageing procedure developed in this work found its final definition through Trial V (Figure 60); the final procedure has been reported also in Annex I.

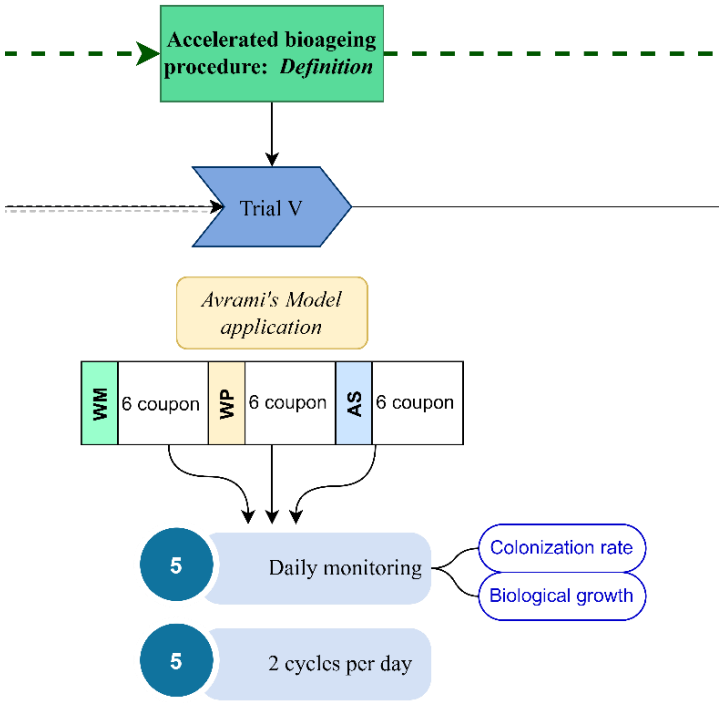

Figure 60: Trial V experimental details. Three bioreactors were prepared in each repeated test, one for every material product: WM, WP, AS. Six coupon were inserted into each bioreactor. Biological growth and colonization area fraction were monitored daily; two immersion-ventilation cycles were run every day and the bioaging procedure lasts three weeks.

Materials and methods

Among all the parameters and environmental variables tested and discussed before, Trial V has selected only the ones that achieved effective results with respect to the research's goals. All the details and experimental conditions applied in Trial V were summarized in Table 11.

Table 11: list of the environmental and experimental conditions for Trial V.

Bioageing holder	TIS bioreactor
Growth incubator	Frigor Box, model 900 AT
Growth temperature	24±1°C
Ligh intensity over each bioreactor	100 μmol/m²/s photons – LED lamps
Immersion cycles	2/day – 10 minutes immersion +10 minutes air
Photoperiod	14 hours/day
Organisms species	Mix of 4 phototrophic organisms: *Edaphochlorella mirabilis, Klebsormidium flaccidum, Gloeocapsa sp., Nostoc commune*
Initial cells concentration	3x10²±50 cells/ml
Starting Absorbance	0.03-0.07
Liquid medium	600 ml BBM – pH 6.6 – 0.705 g/L
Material samples	AS – WM – WP
Sample surface	Not soiled (new)
Test duration	3 weeks

The number of immersions-ventilation cycles has been lowered from six to two per day. Two cycles per day had the aim to slow the dynamic of biologic attachment ensuring a more accurate daily monitoring (without compromise the process of acceleration of biofouling with respect to natural ageing phenomenon). The modification of number of samples immersions wanted also to verify the scalability of the setup. The increasing or decreasing of immersion times would speed or decelerate the deposition of biological colonies on surfaces, depending on surface's resistance itself, which was an independent variable. The velocity of biofilm formation on outdoor surface was due to the climate and micro-climate conditions. So, depending to climatological features of the specific region where the building product would be used, its biological aggression resistance could be tested through a modular accelerate bioageing procedure. However, it should be considered the results achieved by Trial III, run with six cycles per day, where colonization rate has demonstrated a high variability after the 14th day of bioaging exposure. For this reason, a less intensive bioageing exposure was applied on studied samples (two "*flood and dry*" cycles instead that six) and, overall, a strict and accurate monitoring activity on biological growth was performed from the start to the end of the procedure. As the previous trials, each TIS bioreactor was prepared with 600 ml of BBM at 0.705 g/L and adjusted at pH 6.6. A mix of four species of algae and cyanobacteria formed the inoculum (see Table 11) and the starting cells concentration has been carefully set measuring the Abs value of liquid

medium after the biological inoculum. The starting measurement of absorbance was assumed as a critical point since it could influence the repeatability of the whole following biodeterioration process. This was the reason why the starting absorbance value was set within the range 0.03-0.07 and all the bioreactors must record a value included in that range. The achievement of this range by Abs measurement could be considered as a "calibration" of bioageing system, before starting the procedure. The reduction of immersion-ventilation cycles, hence, should reduce the velocity of biological colonies on the samples with the aim to monitor more accurately the process. At the same time, the whole duration of each test was overextended to three weeks in order to follow and to study the biological growth for a longer time and get a more detailed knowledge of the phenomenon. Image analysis on surfaces and liquid medium absorbance have been measured every day in order to build the growth and biofouling curves. Likewise Trial III, six samples for each material types were exposed to bioageing within the same TIS bioreactor. Beyond daily measurements, solar reflectance and colorimetric changes were analyzed at regular intervals of days toward coupon samplings (named t1-t2-t3-t4-t5-t6). Three bioreactors were prepared for each material product (WM, AS, WP) in the same manner of the previous ones.

Results

Complete final results achieved by three repeated test are shown in Figure 61 (a, b, c). Progressive images have been reported, but not for every sampling day. Final colonization rates (21st day) seem similar among the repeated tests and among the materials type, since most of the surfaces appears covered by biofilm; however, something different occurred during the exposure, in particular between 3rd and 14th day, approximately. During the central days of biodeterioration process, the deposition and the growth of algae and cyanobacteria had faster or slower rates according to the product types. On WM, for example, the "lag" phase referred to surface colonization appeared longer than WP. This could be eventually due to the physical features of the materials, as the higher roughness of WP, which encourage the establishment of the organisms.

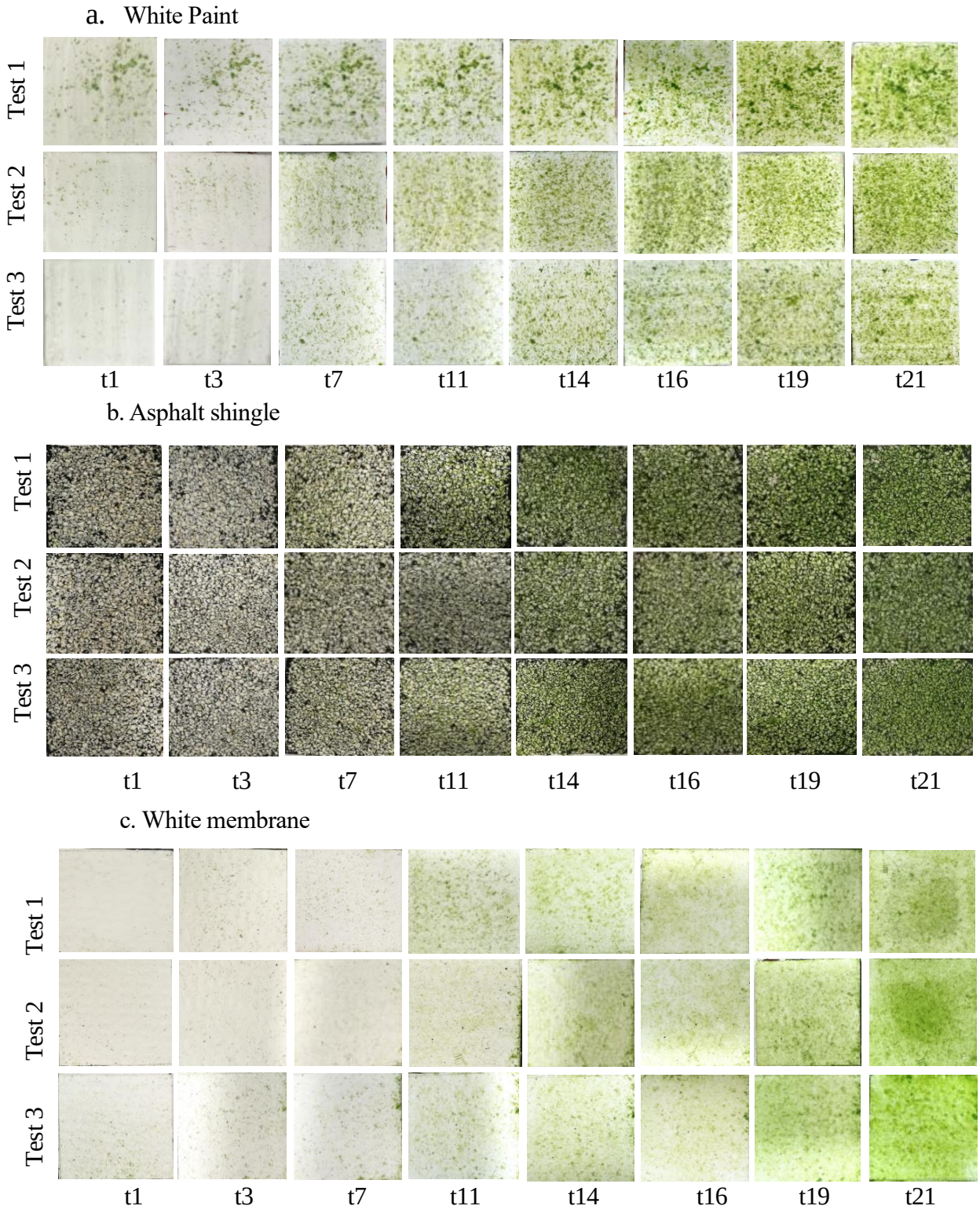

Figure 61: Progressive colonization on building material specimen, during three weeks of bioageing procedure. Even if the image analysis was made every day, only some of the collected pictures have been reported. Each coupon corresponds to a sampling day; t1-t3-t7-t11-t14-t16-19-t21 and these images are coming from the coupon n° 6, the one which is remained under bioageing exposure from the beginning to the end. Covered area rates increased with the passing of time on Single ply White Paint samples (a), Asphalt Shingle samples (b) and White Membrane samples (c).

Daily monitoring of colonization rate and biological growth has allowed to build the curves showed in Figure 62. Absorbance readings at 750 nm outlined a complete growth curve, where lag (1st-7th day), exponential (8th-17th), stationary (18th-20th) and the beginning of decrease phases (21st) can be recognized across the whole duration of experimental test. Even if the biological trend was the same across the repeated tests (as the low standard deviation underlines), absolute values of absorbance at 750nm were different among materials bioreactor types. In details, AS bioreactors reached higher values than WM and WP bioreactor, which did not show significant differences (*p-value*>0.05). The distance among these values were not due to the specific material product: considering all the previous trials, they did not have any particular influence.

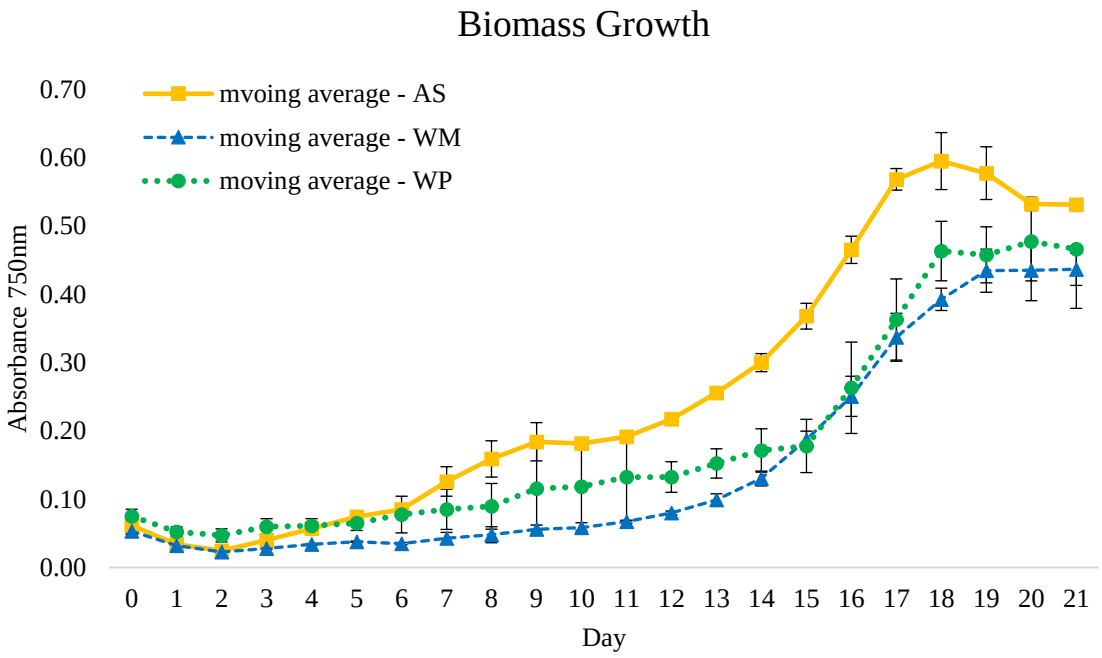

Figure 62: Algae and cyanobacteria growth medium absorbance (read at 750 nm) through the whole duration of bioageing test (0-21st day). The results are the moving average (among three values) of three repeated test and SD is shown. WM and WP did not show significant differences (*p-value*>0.05), while the biomass growth into the liquid medium appears higher into AS bioreactors (*p-value*<0.05).

Data suggested again that the $X_{(t)}$ have progressively increased with the proceeding of organisms growth into liquid medium (Figure 63). It should be noted that during lag phase (1st – 7th), colonization rate remained meanly low (above 20%) for all material types (AS-WM-WP). Then, as soon as exponential phase has started, $X_{(t)}$ begins to raise faster (8th – 17th); then, covered area seems to achieve a plateau (18th – 21st) since the covered area fraction stopped to grow. In this trial, colonized area after 21 days on WP samples was 82.7± 3.1%, compared to WM and AS where it was 81.7±0.6 and 78.7±1.5% respectively. Statistical test ANOVA have underlined that there was not significant difference among WP, WM, and AS final values of $X_{(t)}$. Even if during the procedure, the colonization rates had a different behavior, in the last phase of exposure (the last

three days), surfaces achieved a similar and remarkable covered area (*p-value*>0.05).

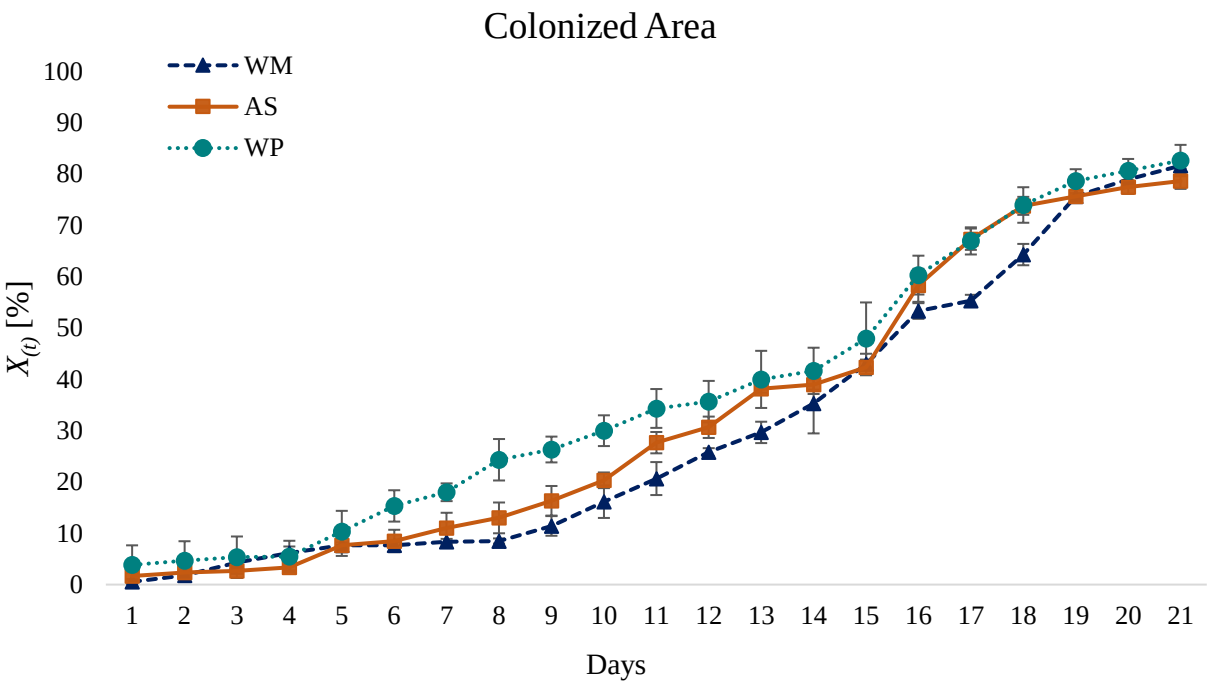

Figure 63: $X_{(t)}$ measured day by day for three weeks on each material type (AS, WP, WM); SD of three repeated test is shown.

One of the most important result of Trial V was about the repeatability of the procedure. *R* (%) was obtained considering the final measurements of solar reflectance after three repeated tests for each samples product involved in the study. As showed in Figure 64, $\Delta\rho_{sol}$ after 21 days of bioageing exposure was 24.5±2%, 21±2.9% and 3.4±0.9% on WM, WP, AS respectively. Standard deviation among repeated test remained low in all analyzed cases: coefficient of variation calculated was 3.5%, 3.9% and 2.6% for WM, WP and AS respectively. Consequently, CV_p was 3.3%, then the relative uncertainty profile was always 6.7%. The repeatability coeffiecient, which represents the experimental repeatability limit of the experimental procedure, was 9.2%. Calulating the absolute difference of ρ_{sol} between two repeated test, the repeatability limit has been always observed. However, the low variability found among the repeated test mostly depends to biological growth into TIS bioreactor system, and this is an intrinsically variable phenomenon, in nature, as well as under laboratory conditions.

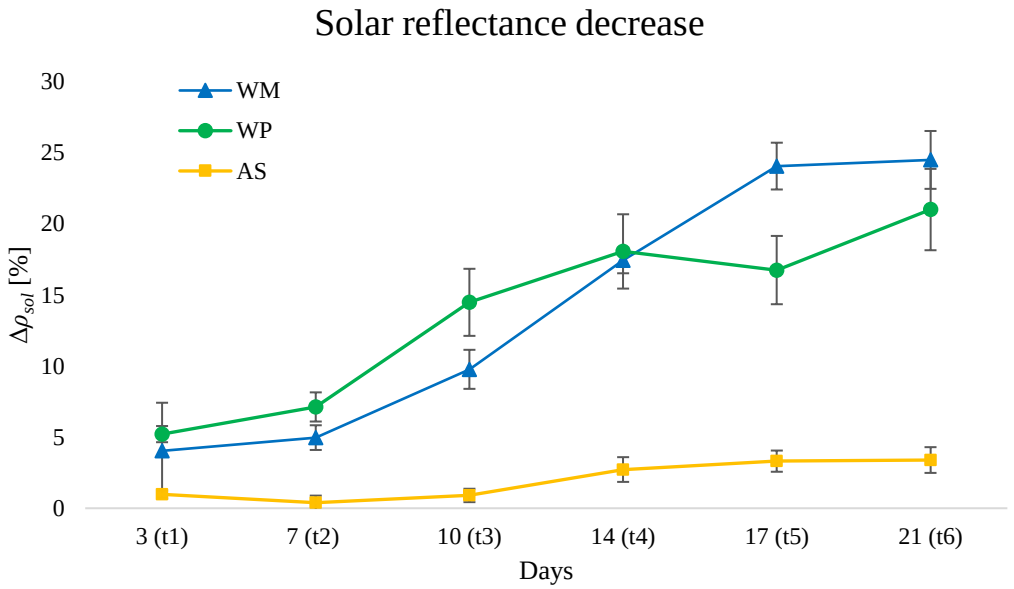

Figure 64: Progressive mean solar reflectance decrease and relative SD achieved through three repeated test. ρ_{sol} measurements have been collected during the sampling days (3rd ,7th,10th, 14th, 17th, 21st).

ΔE values of Trial V followed $\Delta\rho_{sol}$ trend (Figure 65): colorimetric changes on AS were significantly (*p-value*<0.05) smaller than WP and WM. Specifically, ΔE values after 21 days of bioageing exposure were: 47.6±8.3, 40.8±6.3 and 23.9±5.6 for WM, WP, and AS respectively. Similar results have been recorded at the end of Trial IV, on surfaces WM and WP colonized by the mix of organism. Comparison among ΔE values obtained through this last and the previous trials was presented in Table 12. ΔE values after the bioageing procedure run with the mix of organisms (Trail IV and V) were statistically distant from results obtained with Trail III, phase I, where the only organism used as colonizer is the cyanobacterium *N. commune*. This comparison has been performed only among specimen which were not been previously soiled; however it should be reminded that the test duration and the number of immersion cycles of Trial V were different from the other ones.

It is possible to hypothesize, observing these findings, that the color changes depend to the organism species responsible of biological deposition, beyond the covered area. This has been already observed in other case studies [31].

Table 12: Comparison among ΔE values achieved after Trial III (Phase I, using only *N. commune*), Trial IV (considering only the new samples) and Trial V. Mean values and SD of three repeated test are shown.

	AS	**WM**	**WP**
Trial III	12.0±2.7	26.6±9.9	22.9±17.3
Trial IV	20.7±1.5	48.5±8.6	41.4±2.9
Trial V	23.9±2.6	47.6±8.3	40.8±6.3

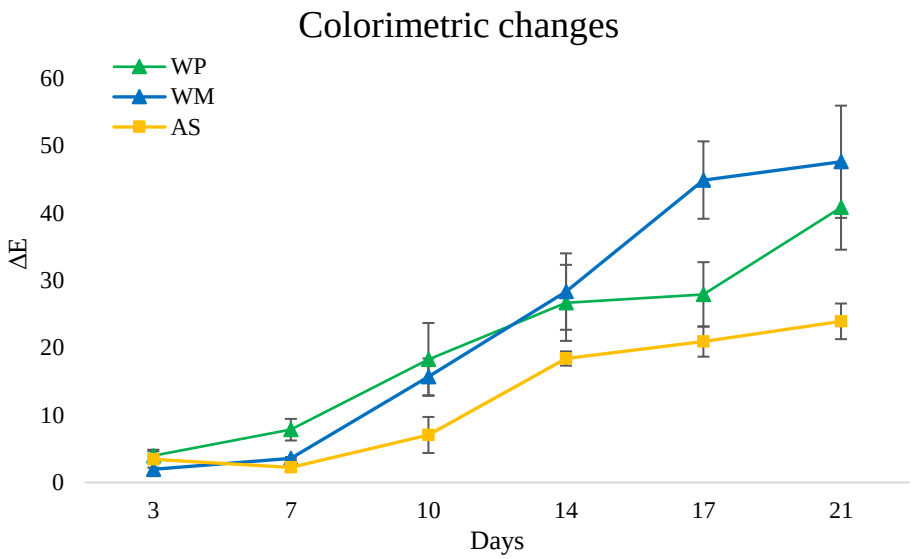

Figure 65: Mean colorimetric changes (ΔE) and SD occurred on WM, WP, and AS samples during the three weeks of bioageing exposure. Data are referred to the 3rd ,7th,10th, 14th, 17th, 21st sampling days.

Discussion

Repeated results achieved from the accelerated bioageing setup run in Trial V did not overcome uncertainty threshold enforced by the goal of this study. The average uncertainty of the procedure, evaluated through the calculation of *CV* on each bioreactor type, was 6.7% and it never overcame 8%. This result was reached using solar reflectance final values collected over each specimen after 21 days of exposure. Moreover, the uncertainty was calculated applying ρ_{sol} values collected during 14th and 17th sampling day (namely t4 and t5 respectively): *U* % was always below than 9%, and the repeatability yield always below 10%. Other parameters have been considered to evaluate the repeatability of the procedure, in particular colonization area. Final coefficient of variation (CV_p) calculated using final $X_{(t)}$ values was 5.9%, within the established threshold (10%). Also in this case, mean *U* % weighted on three repeated trials for three material types was below 10%, specifically it is 4.2%. Considering *U* % calculated on a single material sample, the highest *U* % was on cool white paint, since variability on final results was greater ($X_{(t)}$=82.7±3.1, *CV*=3.7). However, uncertainty of the method should be calculated on several materials types in order to define the reliability of the method regardless the material type. These results suggest, firstly, that an adequate repeatability was observed not only at the end of the bioageing procedure here arranged but also at partial outcomes. Then, the repeatability was fulfilling (within the established threshold of 10%) in terms of both solar reflectance decrease and biological colonization surface rate. Biological aggression reached by reproducing the accelerated bioageing setup according the same experimental parameters listed in Table 11, has achieved a reliable repeatability at different partial times of the procedure. The achieved uncertainty values means that if identical samples are submitted to the same

laboratory, running the same accelerated procedure, 95% of the time the observed difference should fall within the uncertainty criterion of 10%. Standard deviation obtained on mean final solar reflectance values for each material type was always within 3%. This results is comparable with standard deviation achieved by Paolini et al. according to accelerate ageing standard ASTM D7897 [95], even if those results could not reproduce biological deposition, otherwise involved in the present work.

The analytical observation of collected results underlines some interesting correlations. Primarily, the linear correlation between solar reflectance decrease ($\Delta\rho_{sol}$) and colonized area percentage ($X_{(t)}$) exists and it has a stronger correlation factor (always $R^2>0.80$) compared with R^2 obtained through Trial III ($0.68<R^2<0.85$). The relationship among colonization rates and solar reflectance changes showed in Figure 66, confirms how biological growth could be decisive into physical fouling process [121], and it leads to visible stains on roofing in particular in humid areas [2]. Furthermore, this suggest that it would be possible to develop, though more studies and data, a predicting model to obtain the solar reflectance decrease knowing colonization area rate.

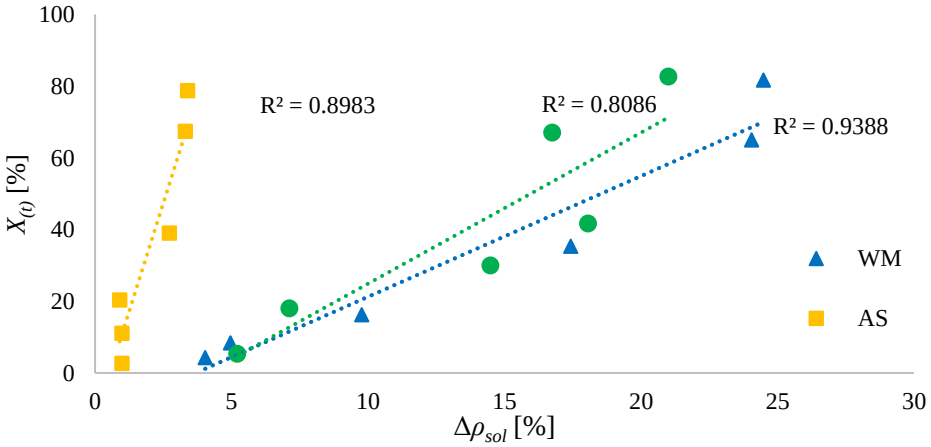

Figure 66: Correlation relationship between $\Delta\rho_{sol}$ (%) measured during six progressive samplings and colonized area $X_{(t)}$ (%) calculated through image analysis every day. Data shown are the mean of three repeated test over three product materials: WM, WP, and AS.

Linear correlation (R^2) among the liquid growth medium absorbance (read at 750 nm) and covered area was 0.955, 0.879, and 0.940 for AS, WP and WM respectively. These values highlight a positive correlation between biological growth into liquid medium and colonization rates. Data analysis have identified again the same relationship between the two parameters: when the colonization rate on surfaces reached 50% of total area, the absorbance value was always equal or higher than 0.2 (Figure 67). This consolidates the behavior already found in Trial IV, where the 68.2% of samples presented a substantial colonization (>50%) after 0.2 of Abs at 750 nm. However, this output should be only considered as relative to the accelerated bioageing procedure here proposed. The 50% of colonization rate over whole areas was reached after 15-16 days from the beginning of this bioaging exposure, which had a starting cells density of $3x10^2$ cells/ml and used four organisms species (belonging to cyanobacteria

and green algae taxa).

All these findings were strictly related to the experimental conditions applied to this specific accelerate bioageing procedure. The previous Trials run in this work are the evidence that the biological growth could be extremely variable despite it occurs under controlled laboratory conditions. It depends on starting cells/density, light intensity, and species involved and other several parameters as nutrients concentration, presence of any abiotic stress. Then, the repeatability could only be assumed when a strict control of *every* parameter, which could influence the bio-growth, is defined within accurate ranges and monitored. At the same time, these outcomes are important to define precisely each step of the accelerated bioageing protocol which represents the final goal of this work, and it is featured in Annex I.

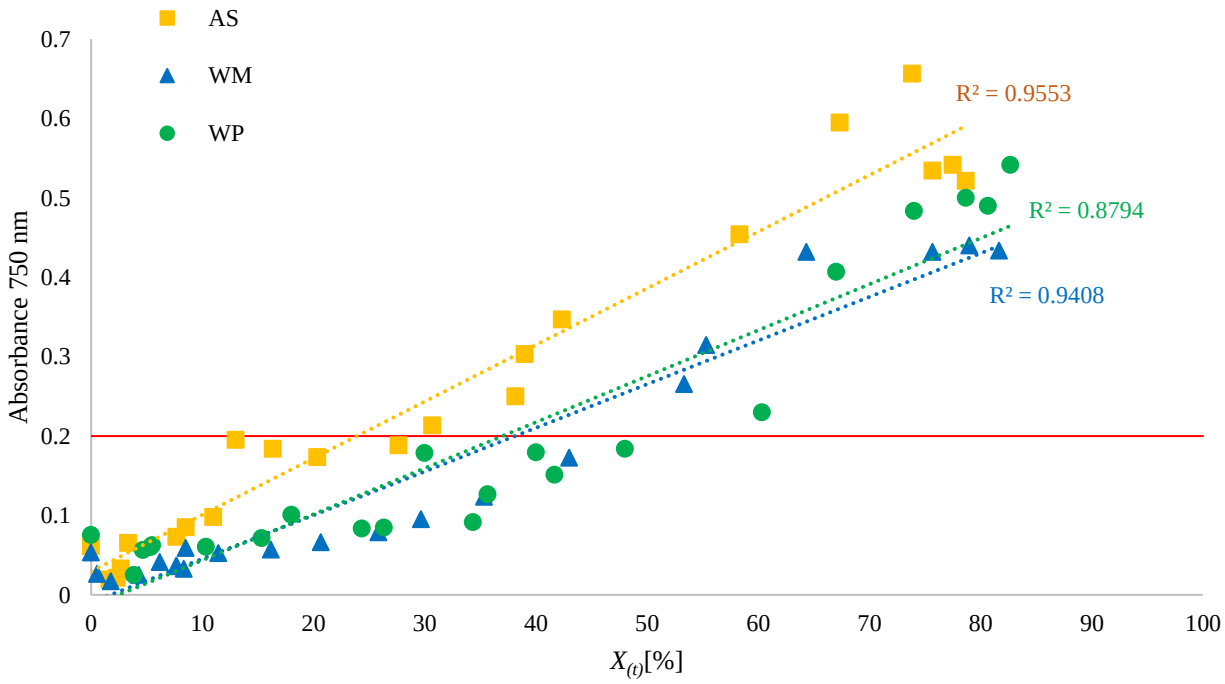

Figure 67: Correlation relationship among $X_{(t)}$ and Abs750 of liquid growth medium used into each bioreactor. Mean results of three repeated test on WM, AS, WP are shown. Data have been collected every day for the whole test duration (three weeks). Red line marks the threshold of absorbance at 0.2; after this value, most $X_{(t)}$ values overcome 50% in each product type.

Accelerated bioageing setup here implemented is not focused on the mechanism of organisms attachment influenced by physical features of the surface. However, the procedure was able to define the progressive and final colonized area X_t thanks to daily monitoring of colonization rate measured by image analysis. Experimental $X_{(t)}$ curve found on each material type, is a sigmoidal function, and this is in line with previous investigations [137], [138]. Moreover, it should be underlined that the colonization rate trend has an asymptotic behavior in last days on all type of specimens (WM, WP, AS). Given that, this work has applied Avrami's model to calculate *K* parameter according the equation n° 2 and n° 16: the least squares regression was used to minimize the difference between experimental colonization rates (X_t^{exp}) and predicted one (X_t') assuming *K* as the group of surface variables on which biofouling depends. According to the best-fit method, *K* values were 2.12E-05, 3.2E-05, 2.92E-05 for samples WM, WP, and AS respectively. Latency time t_1 was the same as for all the products, since after the first day, some algal spots compared on all types of surfaces. Parameter *K* did not differ significantly among the products, however WP has a slightly higher one. Considering that *K* depends to surface intrinsic features, WP has a greater starting roughness compared with WM but lower compared to AS. However, AS contains greater amount of titanium which has a biocidal effects when coupled with oxygen [12], [98], [99]. Besides that, algal growth depends to several substrate characteristics; the influence on bio growth of some of these, as pH, are not well known yet [13], [181]. Quagliarini et al. [137] have evaluated the effect of environmental temperature and relative humidity on algae biofouling that often occurs on porous and rough fired brick surfaces, modelling Avrami model under different environmental conditions. That study has found some *K* parameters by the same scale order to the ones estimated in this experimental study (E-05). Even if the study of Quagliarini et al. has applied Avrami model on bricks, their experimental setup is completely different to the one developed in this study. Parameter *K*, which allows to define if Avrami model is able to predict biofouling, is highly dependent to the laboratory conditions and the way to induce biological growth [137]. Then, parameter *K* here calculated should be considered related to the protocol here developed and presented; they are not absolute values. This being known, more studies are needed to evaluate biological resistance of more building products according to this accelerate and repeatable method.

Once the parameter *K* has been found according the best fitting among experimental (X_t^{exp}) and predicted (X_t') colonization rates, R^2 between these two curves – experimental and estimated- has been calculated. The minimum R^2 was equal to 0.879 (WP), while R^2 is 0.973 for WM and 0.962 for AS, denoting that predicted data satisfactorily fitted the experimental ones in case of WM and AS, almost enough for WP. In Figure 68 (a,b,c) it was possible to appreciate the overlapping between the analytical curve and the experimental values of $X_{(t)}$: higher values of R^2, better fit between the curves was observed. These results about reliability were in line with other results from literature where the same model has been applied [138], [140], [141]. The observed phenomenon of colonization rates obtained was able to catch the results predicted through Avrami's model, which has been deeply verified in previous works on laboratory biofouling procedures [137]–[139], [141].

a.

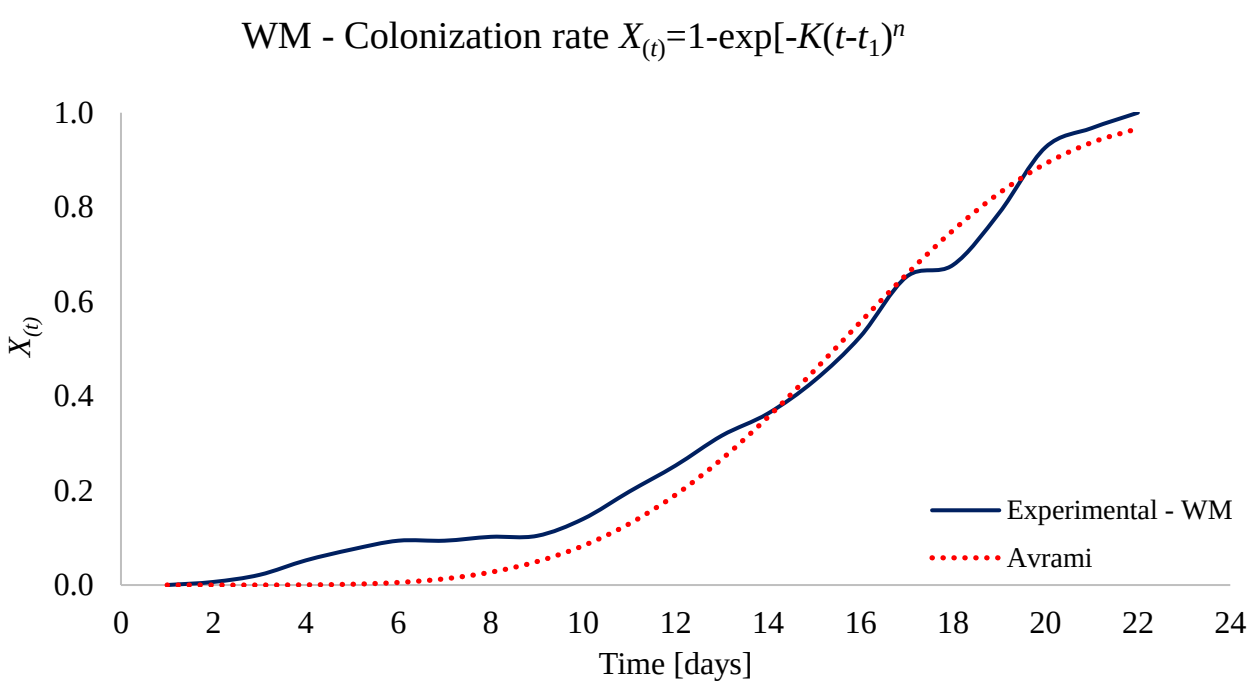
WM - Colonization rate $X_{(t)}=1-\exp[-K(t-t_1)^n$
1.0
0.8
0.6
0.4
0.2
0.0
$X_{(t)}$
0
2
4
6
8
10
12
14
16
18
20
22
24
Time [days]
Experimental - WM
Avrami

b.

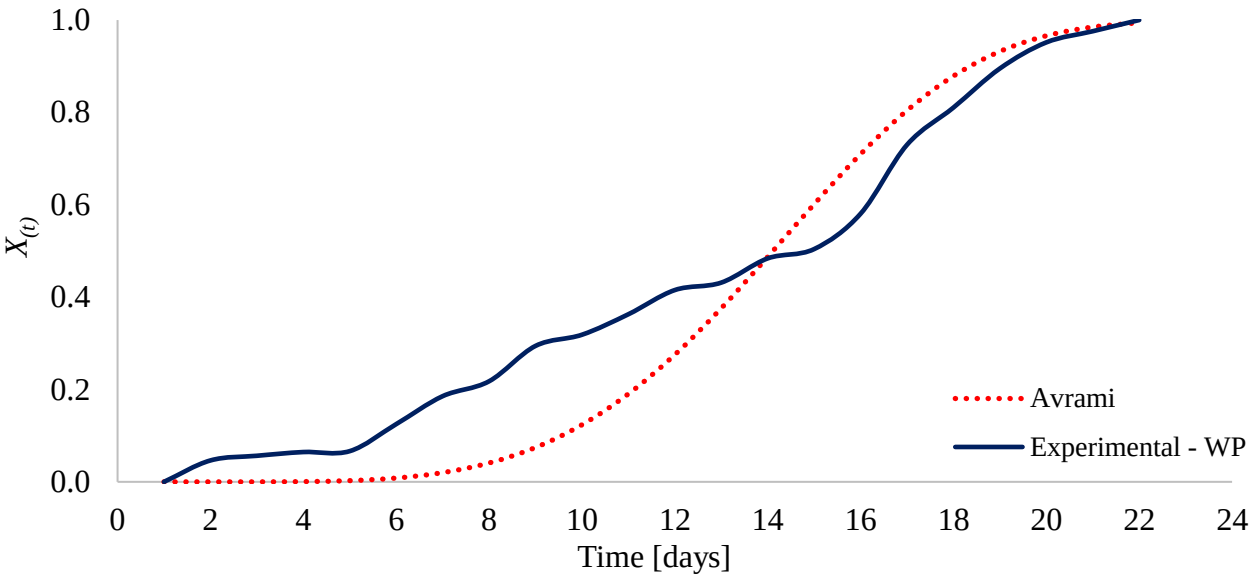
WP - Colonization rate $X_{(t)}=1-\exp[-K(t-t_1)^n]$
1.0
0.8
0.6
0.4
0.2
0.0
$X_{(t)}$
0
2
4
6
8
10
12
14
16
18
20
22
24
Time [days]
Avrami
Experimental - WP

c.

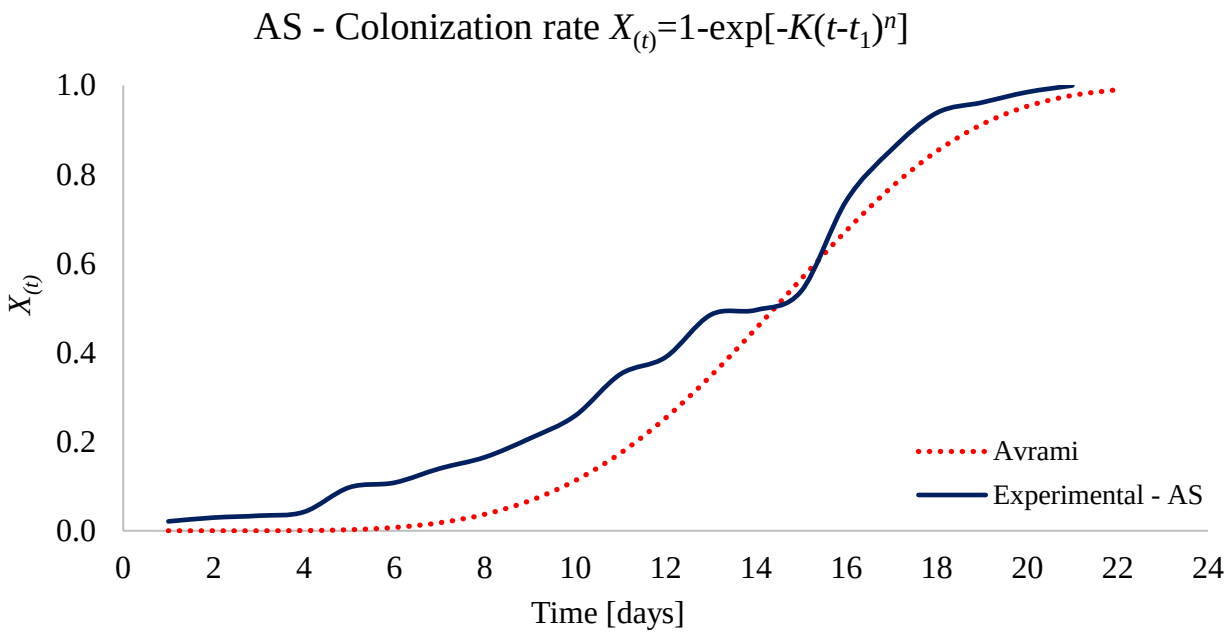

Figure 68: Experimental and predicted colonization rate (X_t^{exp} *and* X_t') by Avrami law, for each product time studied: WM (a), WP (b) ans AS (c). The sigmodial curves are expressed in function of the time (days).

Trial V applied a list of experimental and environmental conditions developed and implemented according to the previous findings. Statistical data about three repeated test, mark that a satisfactory repeatability threshold has been achieved. ANOVA and CV_p calculated on final solar reflectance results or colonization rates did not underline any significant differences among repeated test on the same product type (*p-value* is always>0.05). The accurate analysis of biological parameters permitted to admit some growth ranges, which become a kind of "calibration requirements" to comply in the accelerated bioageing procedure definition, as described in Annex I.

The function fitting among experimental and Avrami's model $X_{(t)}$ curves, describes how the accelerated method proposed is able to reproduce the growth phases of algae and cyanobacteria already observed in nature [214], [215], but in an accelerated way. The application of the model to experimental data, enables to estimate the best value of parameter *K* which is an indicator of the resistance to biodeterioration of the surface type. Single ply white membrane (WM) appears the surface most durable against the biomass growth, since its *K* values was the lowest among the investigated ones. These observations find its confirmation in the analysis of the colonization rate curve of WM: exponential phase of $X_{(t)}$ started with a delay compared to the other two products. After 9 days of bioageing exposure, $X_{(t)}$ on WM was ~11%, while on AS and WP was ~16% and 26% respectively; during the 13th day, $X_{(t)}$ reached ~29% on WM, while on AS and WP it sketched to ~38% and 40% respectively. Even if the final area covered by the mix of algae and cyanobacteria species achieved similar fractions over the three product, the timing and the way to reach that rate was different. Parameter K could be considered as the measure of the sum of the physical and chemical features of the surfaces which make a surface less or more durable versus biological agents.

5.6. Trial VI - *Application* Trial: Application of accelerated bioageing procedure on building material treated with antialgal products

Results obtained through the development and definition Trials shall be considered functional to the draft of "Proposal of Standard Practice for Laboratory Biofouling of Roofing Materials to test their resistance to biological aggression", as detailed in Annex I. The same protocol described in the draft proposal, has been applied to some building material products (specifically Asphalt shingles) previously treated with biocidal or biostatic coatings. These building products, which usually are not included among cool materials, are largely applied to industrial buildings [216]. Shingles are exposed to biological growth which raise concern since it accelerates fouling and deterioration processes [3]. One of the main challenges of roofing materials manufactures is to make a product able to resist against the fast soiling and biodeterioration processes. According with this aim, which has inspired the whole work here presented, Trial VI wanted to apply the accelerated bioageing procedure on commercial products. The goal was to compare the colonization rates eventually occurred among the materials treated with different antialgal coatings and the referring standard, where any biocidal coating has been added on surfaces. This test should work as an example of application trial of the experimental protocol, verifying its capability to test the resistance to biological aggression of a material product, which is thought to inhibit bio-growth. Among the expected results, there is a lower colonization over antialgal surfaces compared with the referring samples (Figure 69).

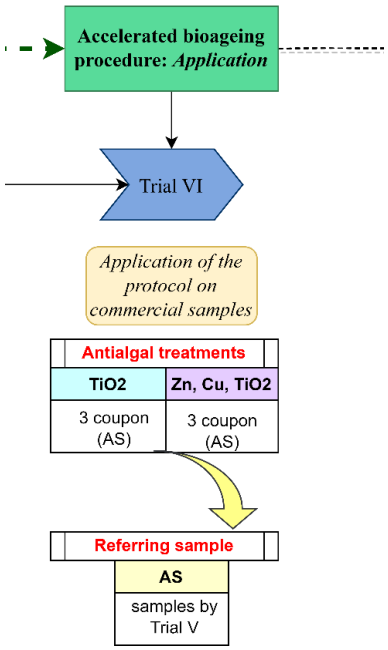

Figure 69: Experimental details of *Application* Trial VI: accelerate bioaging setup has been applied to asphalt shingle commercial products, previously treated with antialgal coating. Results are compared to colonization rates achieved on AS sample not previously treated.

Materials and methods

Sample products involved in this trial are commercial asphalt shingles presented in Figure 70. Bitumen single layer plus a single layer of granules, previously treated with biocidal compounds and antialgal treatment, composed these asphalt shingles samples. Specifically, the treatments performed on granules were:

- Sample A: Mix of Copper (CuO), Zinc (ZnO) oxide and Titanium dioxide (TiO_2);
- Sample B: Titanium dioxide (TiO_2) plus hydrophobic treatment on granules.

The application of these compounds were part of the strategies to prevent algal fouling of building surfaces. These are aimed towards the decrease of the bioreceptivity, as shown by some authors [12], [98]. They demonstrated that TiO_2 or ZnO nanoparticulate additives are able to reduce significantly biofouling intensity and surface coverage when compared to the control treatment.

This has been attributed mainly to the photo-induced breakdown of microorganisms. Among the antialgal treatments, several evidences and factors indicate that TiO_2-based products are ones of the most feasible and useful solution in the field of preservation of building surfaces: titanium dioxide is considered the most efficient photo-catalyst readily available [98], [99], [142]. Photocatalysis can decompose most of the organic and inorganic pollutants in contact with coated surface under ultraviolet (UV) irradiation, causing a depollution effect too [217]. Chemical photocatalytic effect could be even more effective when applied in synergy with other biofouling prevention strategists, as hydrophobicity. A hydrophobic surface may decrease the bioreceptivity of a material thanks to reduction of water ingress, the low affinity for polar molecules (as extracellular polysaccharides) and reduction of roughness. These series of effects hinders the growth of microorganisms, decreasing biofilm attachment [218].

Sample A: Asphalt Shingle treated with CuO, ZnO and TiO_2

Sample B: Asphalt Shingle treated with TiO_2 and hydrophobic treatment

Figure 70: Commercial asphalt shingle samples involved in Trial VI: sample A and sample B, subjected to two different anti-biofouling treatments.

Three coupons of the same material type have been inserted into the same TIS bioreactor in order to get repeated results. Bioreactors have been prepared exactly as described in the last Trial V (and as it reported in Annex I). Each bioreactor has been previously autoclaved at 120°C, 1 atm, for 20 minutes and filled with 600 ml of sterile BBM. Each samples side has been exposed to 30 minutes to UV-C lamps before starting the test. The liquid growth medium was inoculated with a fixed amount of four phototropic organisms species mother cultures: *Gloeocapsa sp*. and *N. commune* for cyanobacteria and *K. flaccidum* and *E. mirabilis* for Chlorophytae, The inoculum volume was adjusted in order to have a starting absorbance value within the range 0.03-0.07, read at 750 nm. This corresponds to 100-500 cells/ml as estimated from absorbance and cells count correlation shown in Figure 43. As already underlined, it was extremely important to keep constant every experimental factor and condition within defined tolerance ranges in order to ensure a repeatable setup. Thus, two immersion cycles per day of 10 minutes each, followed by 10 minutes of air input were run to each bioreactor. The test lasted 21 days. During the test, growth medium absorbance (with UV-Vis Spectrophotometer) and colonization rates analysis (through image analysis) have been performed at specific time intervals (t1-t2-t3-t4-t5-t6). Final images have been captured through stereo microscope and a digital camera (Photonic PL3000 and Nikon SMZ800 respectively) in order to get magnified images (10X). Stereomicroscope allowed observing the details, distinguishing better the colonized area over the granules from the background of asphalt shingle surfaces. In this way, ImageJ software, which applies K-Means like method, had a higher accuracy. For statistical purpose, five magnified images (5mm x 7mm size) on each samples have been used to calculate the colonization rate (Xt). Then, the final $X_{(t)}$ value for each product type has been statistically assessed through the mean and SD of five magnified images on each coupon of sample A and sample B. Colorimetric differences between new and bioaged samples have been also analyzed with Colorimeter (PCE-CSM 6).

Results and discussion

Some stereo microscope captures on final colonization rates were shown in Figure 71, where it was included also a magnified imaged of referring sample (AS, Trial V). Despite of antialgal coatings and treatments, algae and cyanobacteria succeed to grow on both samples surfaces. The fraction area covered by biofilm at the end of 21 days of bioageing was summarized in Figure 71. Nevertheless the bio-growth occurs on all type of surfaces, it should be highlighted that sample B presented the lowest average of colonization rate (25.6±6.1 %) compared with sample A (40.6±6.6 %) and referring standard AS (78.6±1.5 %). The monitoring on biological growth has been carried out during the test, analyzing the absorbance of liquid growth medium at specific interval day (t0-t1-t2-t3-t4-t5-t6) into each bioreactor. All gained data were showed in Figure 72: it is worth to mark that biological growth into liquid medium fully satisfy the expected results, already obtained through Trial IV and V, where the final absorbance value falled within the range 0.5-0.8. These data means that the mix of organism species have a comparable growth with the one observed through the same setups run before. At the

same time, the biological growth did not exhibit any sign of stress due to the antialgal product contained into the coatings. These outcomes about the expected growth is essential to consider reliable the following results. Statistical analysis (ANOVA and Tuckey Test) have found significant differences among each of the three groups of repeated samples A, B and AS (*p-value* <0.05). These data denote, first, the capability of antialgal treatments to prevent partially algal growth on surfaces. The treatments were not able to avoid biological deposition on surfaces, since they partially have been covered by organism colonies. More in detail, it could be hypothesized that B type treatment (TiO_2 dioxide plus hydrophobic treatment) was more effective that type A treatment (Mix of CuO, ZnO, TiO_2) for their purpose, while both of them seems to have a lightly positive effectiveness against biofouling compared with not treated referring sample. Since the amount of TiO_2 in the coating applied to different samples (A and B) was the same, the enhanced anti biofouling effect of treatment type B may be due to the synergic consequence of photocatalytic and hydrophobic effect. TiO_2 coatings have been becoming more and more widespread during last years since they seem to be among the best effective treatment to keep the various substrates self-cleaned and to prevent the formation of biofouling [131]. However, some recent researches have pointed out that the efficiency of these coatings is strongly dependent on the substrate itself (i.e.: porosity and roughness), and its interplay with other bio-growth prevention strategists [129], [207], [208].

Results of Trial VI pointed out at least two levels of considerations. Firstly, the accelerated bioageing setup, developed through this thesis work, has been successfully run on other types of commercial building material samples. Results on biological growth observed during the test were comparable with the ones obtained during Trial V. This could represent an indicator of the repeatability of the setup itself, when the physical parameters on surfaces are not comparable (as solar reflectance, colorimetric values and colonization rates). Furthermore, $X_{(t)}$ data underline that antialgal treatments have a partial effect to contrast the biocolonization under accelerate bioageing procedure. Between the two of them, the coating containing only TiO_2 seems to exert a stronger effect compared with the mix of metal dioxides. Despite these results, more trials are requested to confirm these first findings.

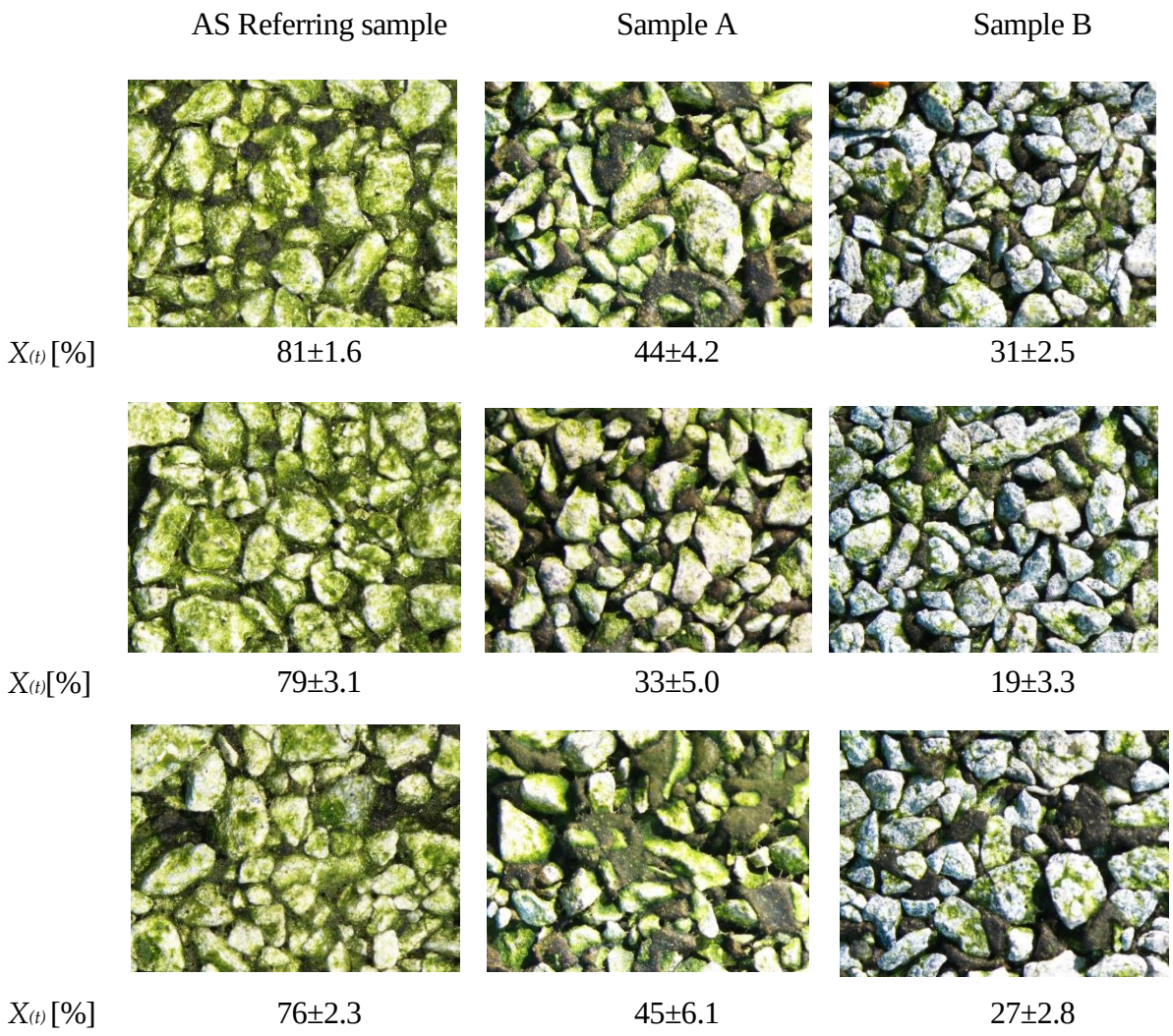

Figure 71: Magnified images (10X) on Sample A (mix of CuO, ZnO, TiO_2), Sample B (TiO_2 plus hydrophobic treatment) and referring sample (AS without any treatment) after 3 weeks of laboratory bioageing tests. Three coupon of the same type are inserted into each bioreactor; $X_{(t)}$ has been calculated processing five captures from stereo microscope on each coupon and calculating the mean on all collected captures on three coupon.

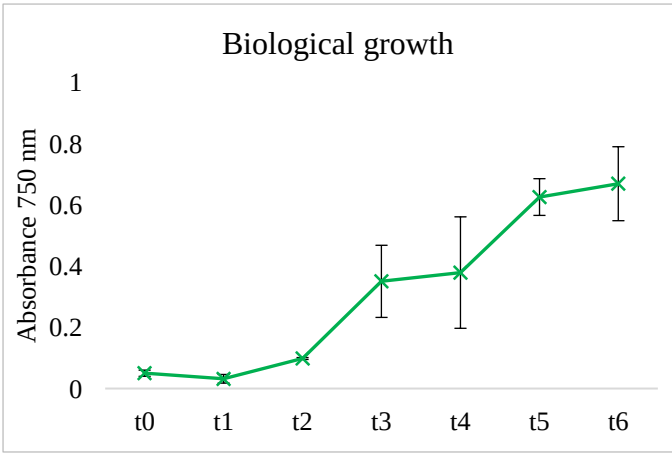

Figure 72: Mean absorbance of liquid growth medium during the complete test duration: t0 correspond to the starting time and t6 correspond to the 21st day of bioageing exposure. Absorbance values have been measured through UV-Vis spectrophotometer at 750 nm; data are the average of two bioreactors and SD is shown.

5.7. Natural ageing of building material: is a time-correlation possible?

Natural exposition of materials in a specific geographical place remains one of the most reliable way to understand the durability of a product and to study its fouling processes due to outdoor conditions, in that precise place. However, the durability of materials under natural exposures can be very different depending on the location because of differences in ultraviolet (UV) radiation, time of wetness, temperature, pollutants, and other factors. Therefore, it cannot be assumed that results from one exposure in a single location will be useful for determining relative durability in a different location [123]. This represents one of the functional reason why natural exposition it is not always a practicable way to study the performance durability of a building material product. Some researchers have already claimed that natural exposure in hot and humid climates, lead to a strong biological aggression on surfaces; while marine environments cause a strong chloride contamination due to the marine aggressive atmosphere [18], [57], [219]. For these reasons, exposures in several locations with different climates which represent a broad range of anticipated service conditions are recommended to know the average behavior of a product in outdoor conditions [123].

Furthermore, results from a single exposure test cannot be used to predict the absolute rate at which a material degrades because year-to-year climatological variations. Several years of repeated exposures are needed to get an "average" test result for a given location: natural exposition needs a lot of time (at least 3 years) which often is in conflict with industrial demands. These aspects would make the natural exposition across different geographical and climatological locations, highly expensive and hardly feasible for the manufacturers. Moreover, new building materials, innovative technologies should be able to keep pace with the ever changing needs of the costumers and, overall, with the ever changing environmental conditions in urban context, also due to climate change [79]. For these reasons accelerated methods to study the durability of materials have been (or are being) developed.

Even if this work was firstly focused on the development of an accelerated bioageing procedure, the same material products involved in the laboratory protocol have been subjected also to the natural exposition, according to ASTM G7. The aim was to collect data about the change of physical performance when the same WM, WP and AS products were exposed to real outdoor conditions in order to investigate if any possible time relationships between laboratory and natural expositions effects would be assessable.

Materials and methods

Material specimens have been exposed at the *Test Farm* placed in Modena, precisely at the following geographical coordinates: 44.670248 N; 10.983461 E. Test Farm is a test site equipped with two exposure racks, which are panels for test specimens fixtures (Figure 73). Exposure racks (Q-LAB ®) have been located in a cleared area, so that there is no shadow on any specimen when the sun's angle of elevation is greater than 20° [123]. Since specimens should be exposed at different orientations or "exposure angle" in order to simulate end-use conditions of the evaluated materials, the exposure rack was positioned so that an angle of 5° from the horizontal. However the slope comes from ASTM G7, some Authors [95] have underlined how the difference in soiling between low-sloped (~5 degree) and flat roofing applications (1.5-2%) cannot be ignored. Nevertheless, it has been chosen 5° slope to be compliant to the ASTM standard. This is the position which typically receives the highest levels of solar radiation during mid-summer and it is used to test materials that would normally be used in horizontal or nearly horizontal applications [123], as the product tested in this study. The frame is made be anodized aluminum measuring 366 cm x 168 cm x 10 cm. They have been assembled and mounted on two legs 100cm high. Each panel base has five panel flaps, which could be adjusted to fit various size of test specimens. All the specimens have been attached to an exterior grade plywood, which forms the substrate to sustain the samples. A meteorological station (Davis, Vintage Pro 2) recorded environmental and climatological data of test farm (air temperature, relative humidity, total solar radiation, rain volume). The same material products exposed to accelerate biological procedure have been exposed to natural ageing: single ply white membrane (WM), field-applied white membrane (WP), and white asphalt shingle (AS). A sampling every 3 months has been planned for the three following years, then 24 specimens for each material type have been exposed (Table 13). The exposure has started in September 2019 (t0) and it is on going. Each sample has been analyzed before the exposure, measuring solar reflectance (with Solar Reflectometer, SSR 6) and colorimetric values (with PCE-CSM 3). Then, two samples of the same type have been drawn at each sampling time, analyzed measuring solar reflectance and colorimetric changes. The natural ageing test is currently in progress and it will finish in September 2022.

Table 13: Sampling schedule during the three-years natural exposure placed in Test Farm, Modena. Data of sampling in *italics* have been already collected and processed, and relative results are presented in following paragraphs. At each sampling time, two specimen of each material products are drawn and analyzed. The sampling in *italics* have already been analyzed, data from samplings in **bold** are still in the processing phase.

Sampling code	***t1***	***t2***	***t3***	***t4***	***t5***	***t6***	***t7***	***t8***	**t9**	**t10**	**t11**	**t12**
Month - year	*Dec 19*	*Mar-20*	*Jun-20*	*Sept-20*	*Dec-20*	*Mar-21*	*Jun-21*	*Sept-21*	**Dec-21**	**Mar-22**	**Jun-22**	**Sept -22**

Figure 73: a) WP, WM and AS specimen at the starting day of the natural exposure (t0); 24 specimen for each material type have been exposed; b) Q-Rack (anodized aluminum frame) positioned with an angle of 5° from the horizontal. The exposure is going on at the *Test Farm*, placed in Modena.

a. b.

Results and discussion

Some preliminary data on samples are shown in Figure 74. It is important to note that on t6 sampling specimens, some biological strain started to appear on samples surfaces. Then biological material has been scraped and isolated into liquid medium in order to observe living cells under optical microscope.

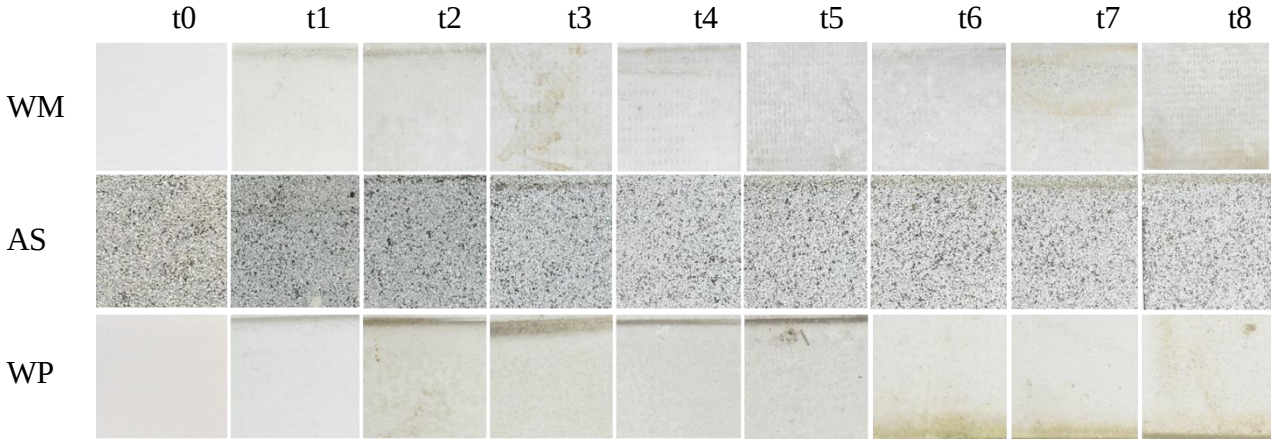

Figure 74: WP, AS, and WM samples details, naturally exposed at Test Farm and sampled every three months. The exposure has started in September 2019 (t0) and the last processed sampling is from September 2021 (t8). The study is not yet complete, since one more year of exposure is needed to complete requirements described in ANSI/CRRC S100 [122].

Progressive solar reflectance changes underlined that most of the decrease occurs within the first 6 months of natural ageing (Figure 74), which corresponds to wintertime, when building heating systems are operating. The yield of solar reflectance

decrease after six months (sampling t2) was 15%, 4% and 26% on WM, AS, WP respectively. As already observed on cool membranes or coatings by Paolini et al. [128], [174], [220], the first winter season represents the period where the greatest drop in solar reflectance occurred. Also Miller et al. [221] recorded an higher falling of solar reflectance during the first year of exposure, even if it continued to slightly drop also past two years of weathering. Partial data of natural exposure marked how after t4 (which correspond to 12th month after starting natural ageing), solar reflectance did not undergo to further remarkably falls: while asphalt single (AS) and field applied paint (WP) seem to keep a linear trend, single ply membrane seems to be more liable to intrinsic variability. WM showed higher variability also after some accelerate biological ageing exposition (Trial III, IV).

The maximum losses observed were in the order of ~30% of the initial value after 24 months of natural exposure and occurred on field applied paint. The average loss on single ply reflective membranes (with a ρ_{sol} t0>0.8) was 20-25%. These values overcame the average ρ_{sol} decrease obtained by other authors [60], [79], on field applied coatings and reflective membranes after natural ageing. Solar reflectance losses on asphalt shingle (about 5%) was instead comparable to previously published data. It should be noted that, experimental data here presented regard the changes in ρ_{sol} after 24 months of natural ageing in Modena; the test is currently running, then these are preliminary data and could not be the object of a complete final discussion.

Colorimetric changes follow the same trend of solar reflectance on each product type: it is clear the positive correlation between ΔE and loss in ρ_{sol} (Figure 75). After the first winter season (t6), ΔE were 16.14±3.3, 1.5±0.8 and 23.27±5.1 on WM, AS and WP respectively. As soon as colorimetric changes were getting higher, also solar reflectance undergoes to a rising drop; moreover, after 12th month (t4), ΔE appeared to be stabilizing. Nevertheless, these were not the definitive results. More considerations on colorimetric values are worth of a deeper analysis.

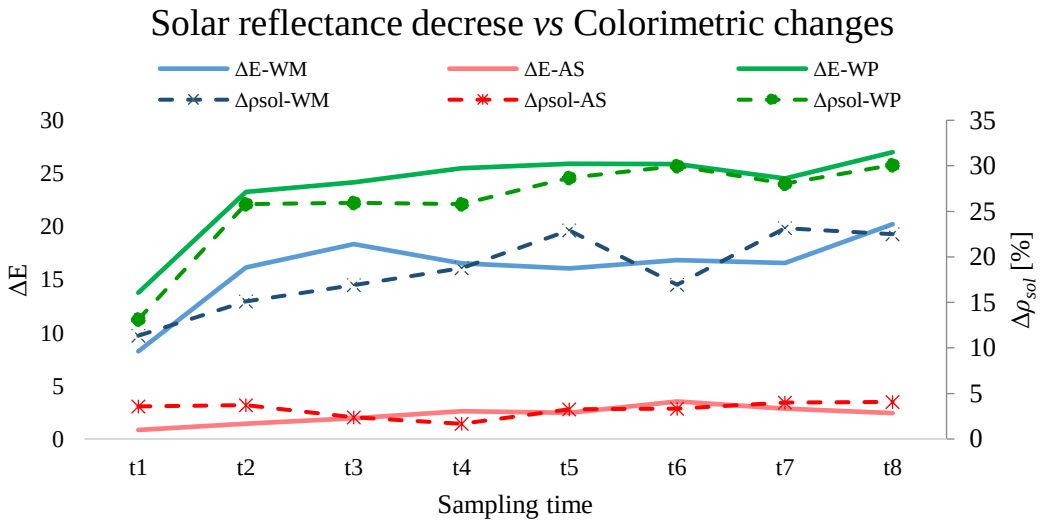

Figure 75: Comparison between ΔE and loss in ρ_{sol} (%) on progressive aged samples exposed at Test Farm in Modena. Results are the mean of repeated measurements performed on two specimen.

Data on colorimetric values obtained through natural ageing have been compared with data coming from Trial IV of accelerate bioageing setup, where both soiling and bioageing procedures have been applied inoculating the mix of organisms on each specimen surface (Figure 76). After 24 months of natural exposure the Δa^* and Δb^* values on the white samples (WM, WP) had a stronger change than the same parameters on asphalt shingle (AS). WM and WP surfaces became darker (brown-grey) after the first year. Red/green coordinates variation (Δa^*) presented a deeply different behavior between natural and laboratory exposed surfaces: in first case, Δa^* has increased by approximately +10/15, while negative values (-5.4, -14.0, -13.0) were recorded for AS, WP, WM respectively after accelerate bioageing. Substantial distance (*p-value*<0.05) has been found also for Δb^*, that indicates yellow/blue coordinates: accelerate bioageing got significantly higher Δb^* values (+10.2, +32.3, +31.2 on AS, WP, WM respectively) compared to natural ageing. This fact is mainly due to the greening over samples exposed to laboratory bioageing, while there was no visual evidence of significant growth of phototrophic (green) organisms on specimen surfaces aged under natural conditions.

Even if any noteworthy biofilm colonization has been observed on surfaces, some green spots of biomass start to be visible after 18 months after the starting of exposure (t6). These biological formations are visible primarily along edges of field applied paint edges, and can not be measured as a proper bio-colonized area. It is known that biofilm formation on surfaces is a phenomenon which become considerably appreciable and damaging after at least 2.5/3 years of natural exposure [7], [180], [221]. As described by Viles et al. [180], during the first year of exposure air-borne cyanobacterial and micromycetes spores, undetectable by human eye, produce a conditioning film important for further colonization. As soon as the surface is exposed for a longer period, a more developed and a more adapted community develops [180]. All these previous observations indicate how it could take long time to study the biological formation on building surfaces and test their resistance to living organisms. Furthermore, climatological conditions deeply influence biological growth: the study completed by [221], set in Tennessee where the climate is very wet and warm, found that the parameters that most strongly influence the decrease in membrane reflectance are relative humidity, average daily temperature change, time, and the number of rain days. All these parameters promote and stimulate the growth of biomass [221].

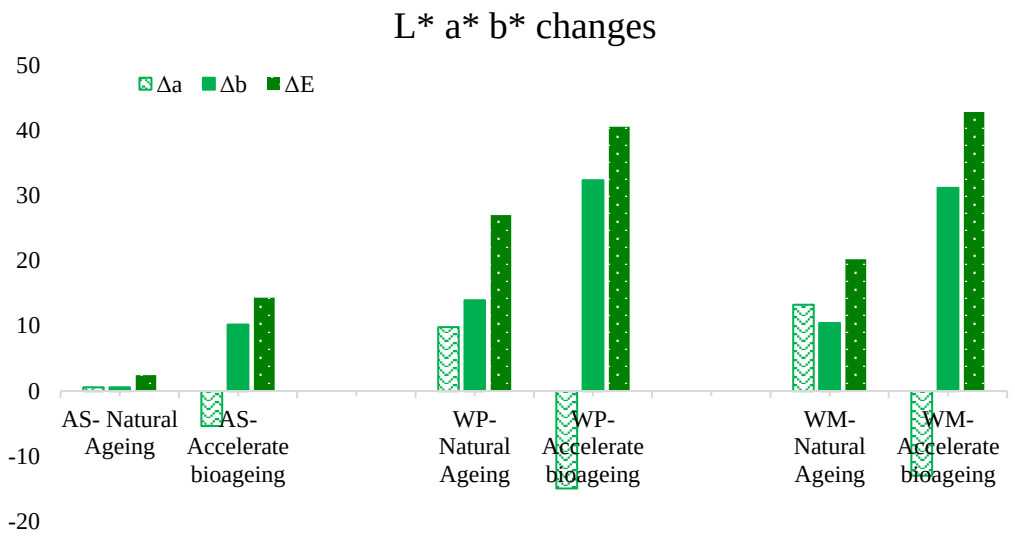

Figure 76: Comparison between natural ageing and accelerated laboratory bioaging (Trial IV): Red/green (Δa*), yellow/blue (Δb*) and ΔE colorimetric changes occur on AS, WP and WM samples.

The climate, which characterizes the city of Modena, in Emilia Romagna region (Italy), is the typical climate of Po Valley, with hot summer and cool winter. This climate is described by the Köppen climate classification as *Cfa* [222]. The city is affected by the strong urbanization, which is responsible of dust and pollutant depositions; moreover, thanks to the observation and data collection by Geophysical Observatory of Modena and Reggio Emilia University (founded by Duke Francesco IV d'Este) it has been possible to measure and describe the climate changes impact on climate in Modena. The analysis of several temperature indices, for all the period 1861–2010, showed for example that frost days are decreasing while tropical nights are increasing [223]; at the same time the precipitation trend has shown a general tendency to decrease over the last 50 years [223], [224].

These data may bring to a climate shift in Modena in the next future, according to the worst emission scenario outlined by IPCC, becoming *Csa* (from fully humid to summer dry) [225]. All these findings can explain the reason why the sample under natural ageing exposition in the city of Modena had no developed a strong biofilm on their surfaces. Climate conditions, characterized by wide temperature difference among season and long dry period, did not provide until now a complete colonization by organisms. Despite this, some green/dark spot have been identified on WP samples in particular. Biological material has been harvested through scraping, than cultivate in laboratory in order to analyze it. Collected biomass has been observed at optical microscope (Eclipse, mod. 80i; lens: CFI planapo VC 100x oil, Nikon instruments) under magnification of 100X. The genus *Klebsormidium* could be identified among the organism grown on samples exposed at Test Farm placed in Modena (Figure 77b). The species which belong to this group are characterized by filaments of cylindrical or beadlike (doliform) cells [147]. Also filamentous cyanobacteria are observable in figure 77c, but it has not been possible to recognize the species. These findings support the selection of the *Klebsormidium* genus and a filamentous cyanobacterium as *Nostoc spp*.

into the laboratory procedure: the species, due to their broad dissemination, are easy to find in urban environment.

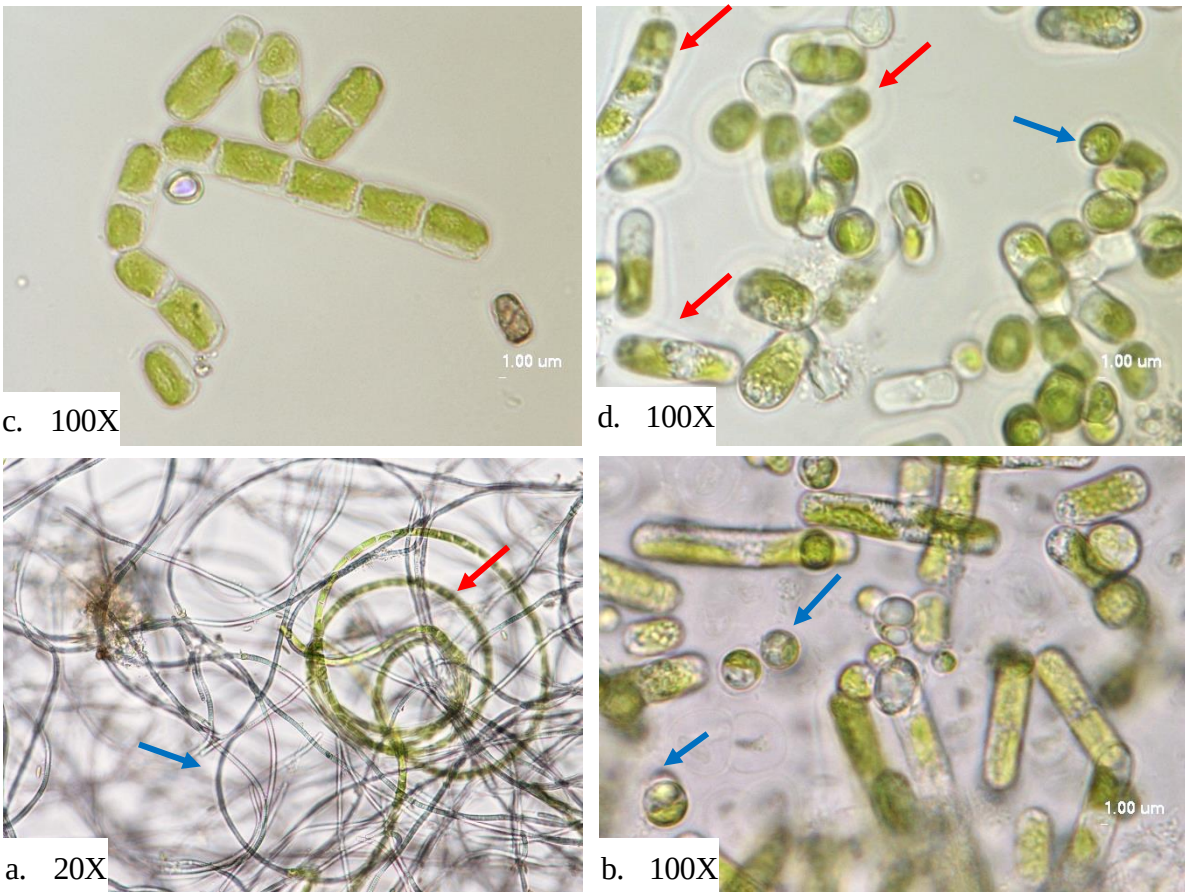

Figure 77: Images from optical microscope (Eclipse, mod. 80i; lens: CFI planapo VC 100x oil, Nikon instruments): a) *Klebsormidium flaccidum* from pure culture cells; b,c,d) algal and other organisms cells grown on WP sample exposed to natural ageing in Modena; red arrows marks *K. flaccidum* identified cells; blue arrows indicates possible cyanobacterium filamentous or other species.

Since the natural exposition is still on going, it is not yet possible to get final remarks about time correlation between natural ageing and the accelerated bioageing setup here presented. Nevertheless, some partial considerations could be evidenced. Comparison among final reflectance got on bioaged samples and naturally aged ones has been reported in Table 14.

Table 14: $\Delta\rho_{sol}$ [%] data obtained after three weeks of accelerated bioageing and after different timeframes during the outdoor natural exposure at the Test Farm placed in Modena. Results are the mean of three repeated test in case of accelerate ageing, and the mean of five measurement on two specimen for the natural ageing. SD is shown.

	Natural ageing		**Accelerated bioageing**	
		$\Delta\rho_{sol}$ [%]±SD		$\Delta\rho_{sol}$ [%]±SD
WM	*21 months*	23.2±3.5	*3 weeks*	24.5±2.0
AS	*18 months*	3.3±0.2	*3 weeks*	3.4±0.9
WP	*12 months*	25.8±1.4	*3 weeks*	21±2.9

The decrease in solar reflectance obtained after three weeks of laboratory accelerated bioageing according to the setup defined in section 5.5, had similar results (*p-value*>0.05) to ρ_{sol} decrease obtained through natural ageing currently on going. The three different material types, however, have achieved this similarity, in very different times of natural exposure. Indeed, while WP reached over 25% of $\Delta\rho_{sol}$ after just 12 months, WM got the ~23% after 21 months. The discrepancy between the natural exposure times and the laboratory bioageing ones to achieve similar ρ_{sol} decrease values, did not make possible a time-correlation between the two ageing methods. In particular, colorimetric analysis has signed a considerable ΔE differences on natural aged and laboratory bioaged surfaces. This last, contributes to modify the solar reflectance spectrum, overall on visible interval (Figure 78), while solar reflectance spectra measured on natural ageing samples shown a lowering across the whole spectrum.

These findings were in line with the ones already described during the setting of ASTM D7897 test method. The contribution of black carbon lowered the reflectance of the white single-ply membrane across the entire solar spectrum: soot and dark, inorganic particulate matter are compounds highly represented in the urban and industrial atmosphere, as the city of Modena shows to be. The distance between solar spectrum measured on new WM and the natural age (after 21 months) samples was so far, since the drop of ρ_{sol} regarded both visible and near-infrared regions. The spectrum coming from the accelerate bioageing had "only" a deep drop within the visible region, while the IR region seems to maintain its highly reflectance performance. Even if the solar spectra between the two different ageing methods showed very distant shapes, results about the changes of solar reflectance $\Delta\rho_{sol}$ (%) were similar. WM samples exposed to the strong biocolonization compressed their ρ_{sol} losses within the Vis-region, which correspond to the 42.8% of the entire solar irradiance; while natural aged samples showed a lower drop of solar spectrum, but it was spread also through the Near-IR region, which contemplated over the 50 % of solar irradiance.

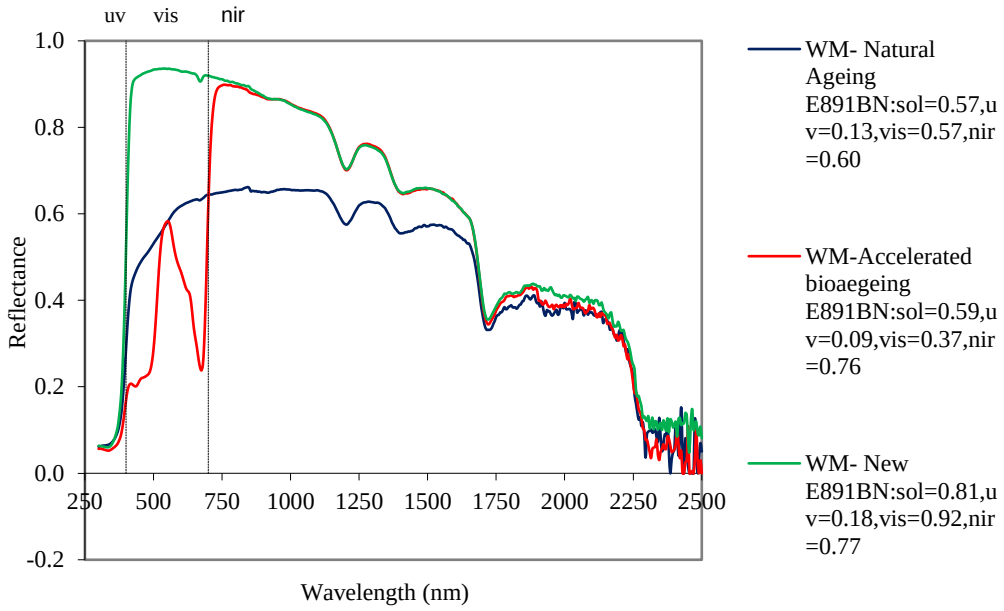

Figure 78: Reflectivity spectra (300-2500 nm) on single ply white membrane (WM) after two different ageing methods. Blue spectrum is a mean of three measurements on WM sample after 21 month of natural ageing in Test Farm, placed in Modena. Red spectrum is a mean of three measurements on WM samples after the bioageing process (sample coming from Trial IV, where a mix of organisms has been applied). Green spectrum is from a new WM sample, before each type of ageing process. The spectra have been acquired by Spectrophotometer UV-Vis-NIR.

Then, until now, results from natural ageing currently on running in Modena, would not seem be reproduced by laboratory conditions, which encourages a considerable biogrowth on surfaces. It should be considered, as well, that climate which interests the city of Modena in Emilia Romagna region, is not classified as hot and humid, but it is under the temperate climates according the Köppen climate classification [222]. Observing a cool surfaces obtained after the natural ageing in Florida, [18], [97], it is easy to notice a similar covering rate by organism with the samples bioaged in laboratory (Figure 79). Even if the colonization level has reached the most area of the sample on both specimen, the color of biofilm was very different: the great difference is due to the biodiversity and the age of the organism grown outdoor compared to the ones grown into TIS bioreactor. It is known that on natural environment, microbial biofilms favors the adherence of airborne particles (dust, pollen, spores, carbonaceous particles from combustion of oil and coal), giving rise to crusts and dark patinas [21]. The black pigmented patinas, at the same time, could derive from melanin producers as fungi (*Alternaria, Ulocladium, Cladosporium* genera) or death algae cells. The production of melanin by fungi and the meristematic development allow them to survive in stressed environmental conditions like low humidity and high sun irradiation [226].

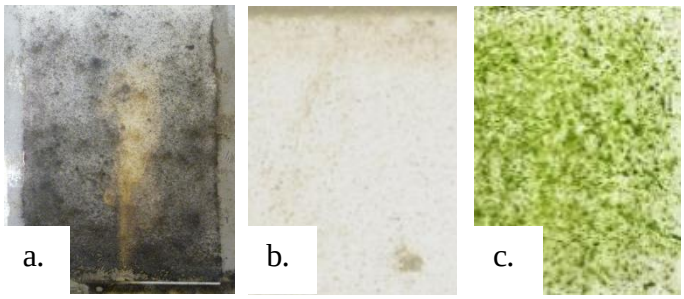

Figure 79: Images from three different Ageing trials: a) cool building sample naturally aged for three years in Florida, biological growth is highly visible; b) field applied cool coating (WP) naturally aged in Modena, after 24 months of exposure, biological growth has started on sample edges; c) field applied cool coating (WP) after three weeks of accelerated bioaging setup.

6. Final Discussion

This study has developed a laboratory bioageing procedure to study the biocolonization and biodeterioration dynamics on building surfaces, especially on solar reflective materials. A new device has been applied: Temporary Immersion System bioreactor. The most innovative aspect introduced by TIS bioreactor to the investigation of accelerated biodeterioration test is the possibility to expose the entire building samples surfaces to a homogenous growth medium inoculated with phototrophic organism.

The structure of the bioreactor and its particular system of air pimps, allow the uniform exposure of the material specimen to algae and cyanobacteria. The same volume of liquid growth medium, where organisms cells are continuously mixed and spread by the air flow from pump, encounters each surface at the same time within the bioreactor. Then, each exposed surface has a similar probability to match a phototroph colony. However, these algae and cyanobacteria colonies do not have the same possibility to grow over different material surfaces: everything depends to their bioreceptivity [13]. Intrinsic features of the surfaces, including physical and chemical characteristic, could lead the following bio-deposition and bio-deterioration process: their intensity would depend to the ability of each surface to resist to biological aggression. The measure of the capability to resist to biofouling is calculated applying Avrami's model, which could simulate the colonization kinetic of building surfaces by algae, in an accelerated laboratory test [138]. This work used the experimental data collected about colonization kinetics ($X_{(t)}$) to estimate *K* factor (from equation°1), which described the surfaces features, and represents their capability to resist against biofouling. *K* factor has been calculated for the three material types involved in this study: single ply white membrane (WM), asphalt shingle (AS) and field-applied white paint (WP). It was estimated applying least squares regression (equation n°16) by minimizing the sum of the squared residuals (*S*) of points from X_t^{exp} plotted curve. The analysis of *K*, has indicated WM the most resistant product type against biological colonization, since it had the lowest *K* values compared to the other ones. This behavior could be confirmed by experimental results. In the "*developing*" Trials (I-IV), WM showed the most variable behavior, obtaining often a high standard deviation among the physical changes of aged surfaces through repeated test. The high variability has not been found in the "*definition*" Trial (V), where the biological deposition and growth on WM samples surface showed a delay compared to the other products. The WM sigmoidal curve, which describes the colonization kinetics, had a different tilt, underlying a lag in the exponential phase, which seems starting at day 10th on WM, and day 6th on WP and AS.

At the same time, single ply white membrane showed a higher variability on solar reflectance and colorimetric changes when exposed to natural ageing. Magnified images captured on WM and WP samples after 21 months of natural ageing, showed some differences: the area fraction covered by particulate matter, pollutants and

biological colonization was considerably higher on WP than WM (Figure 80). Thus, the physical features of single ply white membrane seem to perform better versus biodeterioration processes according to the results of both natural and accelerated ageing run in this work.

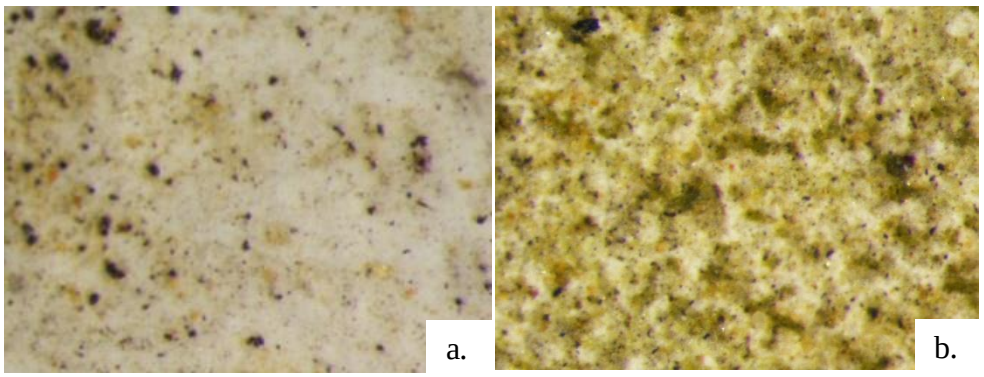

Figure 80: Magnified images (10X) on WM (a) and WP (b) samples, after 21 months of natural ageing in Test Farm, placed in Modena. Images have been captured with stereo microscope (Photonic PL3000 and Nikon SMZ800).

It would be useful to involve, in the future works, other cool material types in this accelerated bioageing setup in order to test and compare more materials and to get a database, which collects the measure of the surface's ability to resist against biological aggression. This should become an interesting instrument for industrial manufacturers, providers and costumers, which would find data on biological resistance of building products.

One of the most critical aspect of the entire study here described is the study of repeatability of the bioaeging setup. According to the aim of the work, indeed, the purpose was to develop an experimental method able to accelerate the biodeterioration on material surfaces, in a repeatable way. The draft protocol here proposed is the result of a series of repeated tests, which have investigated several experimental conditions. Among these, the best one in terms of repeatability of biological growth and surface colonization, have been selected. The main challenge of the work was been to make repeatable (minimizing the distance among identical analysis) the bio-growth phenomenon on material surfaces. The variability which characterizes the biofouling, has been widely described in natural conditions, and at the same time it has been considered unrealistic to be reproduced into a laboratory [66], [227] due to the unlimited outdoor variables which can influence phototrophic organism lives and growth. The employment of TIS bioreactor allowed creating a sealed and sterile growth chamber where possible contaminations would be avoided as much as possible and where a strict monitoring of environmental parameters could be carried out. The experimental design followed in this work, has envisaged the construction of a final laboratory bioageing setup through the study of the influence of each experimental parameter or condition involved.

Thus, several Trials have been scheduled in order to study separately the influence of different variable factors: the number of "*flood and dry*" cycles over the specimen and the difference of bio-colonization dynamics between a green alga species (*E. mirabilis*) and a cyanobacterium (*N. commune*). It was been necessary to isolate just one pioneer species (*N. commune*) in the first steps of the study in order to understand its response to the different laboratory conditions. The light intensity has been one of the most critical aspect to manage. Trial I and Trial II, indeed, have revealed that also little variations in the photons amount emission could elicit such diverse physiological response by cyanobacterium cells, and this makes not compliant the laboratory procedure with the repeatability requirements. For this reason, the introduction of a growth incubator, able to provide the same light intensity over all bioreactors, has represented an essential turning point of the research. It is also worthwhile noting that the starting algae and cyanobacteria cells concentration represents another critical parameter to manage.

The calibration of the liquid growth medium absorbance become a necessary step to ensure homogenous starting conditions. For this purpose, the calibration curve between cells number and the optical absorbance read at 750 nm allowed to identify the Abs range within which the bioageing should starts in order to get a repeatable growth rate and a repeatable colonization rate. Ji et *al*. [228] and Li et *al*. [229] have reported that both biomass production and biofilm growth could be modified by varying the inoculum density at the early stages of biofilm development, which in turn may affect biomass and compounds production. The monitoring of cells concentration might be of great help to rapidly standardize the starting biological operational factors. This work has set an initial growth medium Abs range of 0.03-0.07, which should be observed into TIS bioreactor afterwards the mix of species inoculum. Considering the four species involved, the absorbance range corresponded to $3x10^2 \pm 50$cells/ml. Depending to the starting cells concentration, the total duration of the procedure has been reviewed during the protocol development, and finally defined as three weeks. These two experimental conditions are strictly correlated each other and this work has identified the ranges which prove an acceptable repeatability.

The uncertainty (%) calculated on bioaged solar reflectance resulted coming from setup of Trial IV and Trial V was greatly improved from the previous ones (Figure 81). The uncertainty coefficient of 10% predefined as the last acceptable threshold, was not fulfilled by the Trials II and III setup (red points), overcoming the 30%, while it started to be improved by Trial IV (blue points), which ranging within ~10% to ~20%, and finally Trial V (green points) results remain always below 10%.

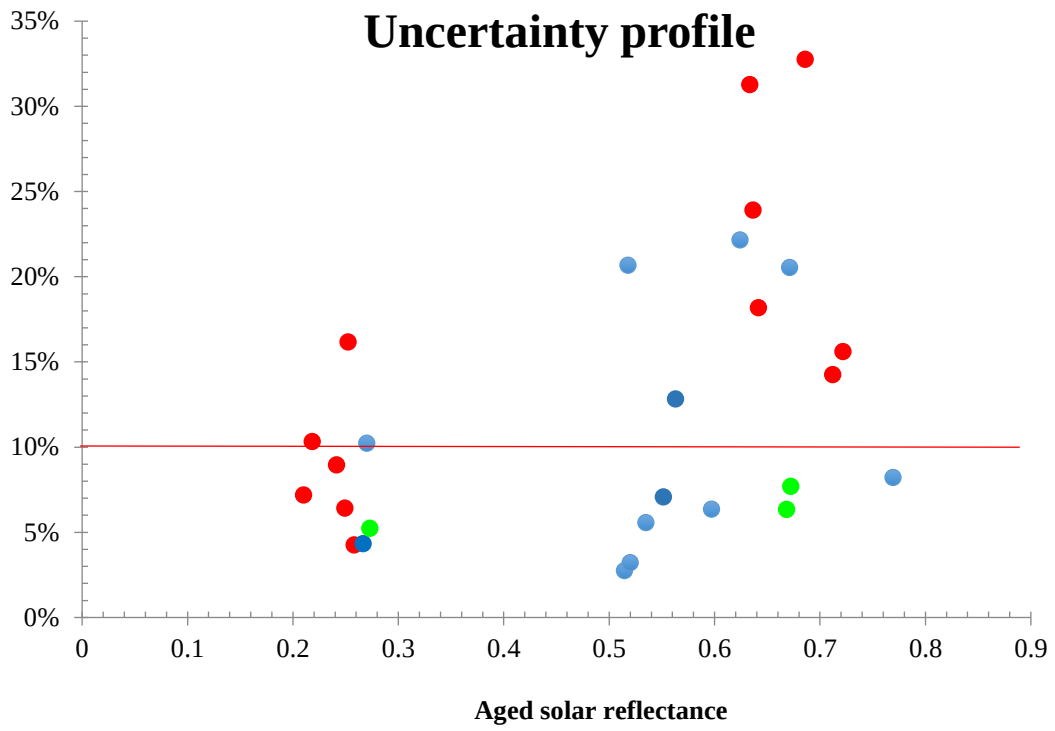

Figure 81: Uncertanty profile of Trials II and Trial III (red points), Trial IV (blue points) and Trial V (green Trial). The uncertainty is calulcated considering all the final values of solar reflactance over the repeated bioaged samples. The uncertainty threshold of 10% is shown with a red line.

The analysis of coefficient of variation (CV_p) on data obtained during the *definition* Trial (Trial V), included both solar reflectance and colonization rates results, in order to study the repeatability across the different physical parameters. In this case, final repeatability coefficient *R* (%) calculated on repeated solar reflectance values was 9.2%, while *R* (%) of covered area fraction was 5.8%. This means that the absolute difference between two repeated test results is expected to lie below the error of 10% with a probability of 95%. This has been verified through the absolute difference of $X_{(t)}$ and ρ_{sol} recorded on each repeated test of Trial V.

Trial III and Trial IV analyzed in details the influence of soiling layer on biological colonization of surfaces. The soiling solution applied in laboratory studies, was intended to mimic the mix of atmospheric particulate matter and other pollutants or compounds normally retained on urban contentext [18]. Berdhal et al. [3], [26], have described that environmental dust and dirt represent a solar reflectance and aesthetical's factor of degradation. These understandings represented the first steps that have driven the ASTM D7897 Standard development, which included the soiling solution within the accelerated ageing process to estimate the change of thermophysical properties (in particular solar reflectance) after three years of outdoor exposure [124]. The ability to measure and to take into account, through accelerate methods, the soiling deposition over building surfaces was essential to evaluate their physical and enrgy decay. In this regard, the design of this thesis work has rising a key question: *could soiling deposition influence biological growth on surfaces and biodeterioration process*? In

natural environment, the effects of soiling deposition over microroganism growth, has been described as the cause of both biodiversity reduction and, at the same time, the expansion of most resistant species population of algae, cyanobacteria and fungi [54], [106]. This work has also analyzed algal secondary metobalites production (as fatty acids, pigments and the products of oxidative stress), after their direct contact with soiling soilution (see section 5.4.1). The results have revelead light signs of abiotic stress on algal metabolism, since some poly-unsaturated fatty acids significantly change their cells concentartion in treated samples (linoleic acid and palmitoleic acid). Other evediences [149], [230], [231] made certain the influence of the mix of pollutants and organic or inorganic atmospheric particles on surfaces phototrophic colonizers, overall during long timeframes. However, *what happens to biological colonization process on soiled surface when it occurs in a laboratory and accelerated setup*? Considering the approach of the entire work, where every single experimental factor is studied seprately, the knowledge about the soiling influence has been an important issue. All the comparisons between colonization rates ($X_{(t)}$) achieved on soiled and new building material samples did not mark any significant difference (*p-value*>0.05). Data from both Trial III and Trial IV (Figure 82) were consistent to the hypotesys that biological growth was not remarkably influenced by the presence of standard atmospheric pollutants solutions over the samples. These evidences should be contextualized: in this specific experimental and accelerated setup, soiling deposition is not a factor which substantialy contribute to enlarge or reduce colonization areas during this laboratory procedure.

Giving that the presence of soiling layer should not affect biological growth on surfaces, the final version of bioageing protocol (described into ANNEX I) does not involve the soiling on specimen preparation.

However, this does not preclude the possibility to introduce the soiling deposition over the samples, and maybe all the entire ASTM D7897 standard procedure, before to submit the building specimen under bioageing setup. The repeatability of the procedure should not be affected by previous tretatment described by the standard protocol, already avaliable to compress three years of outdoor exposure to three days. Conversely, the purposed accelerated bioageing protocol would deserve future investigations, where it could be run afterward the ASTM D7897 entire procedure. In this way, the sum of soiling (deposition of atmospheric black carbon, dust, and organic and inorganic particulate matter), weathering (moisture, ultraviolet radiation and temperature cycles) and the not negligible microbial growth, could be reproduced into laboratory through a fast procedure.

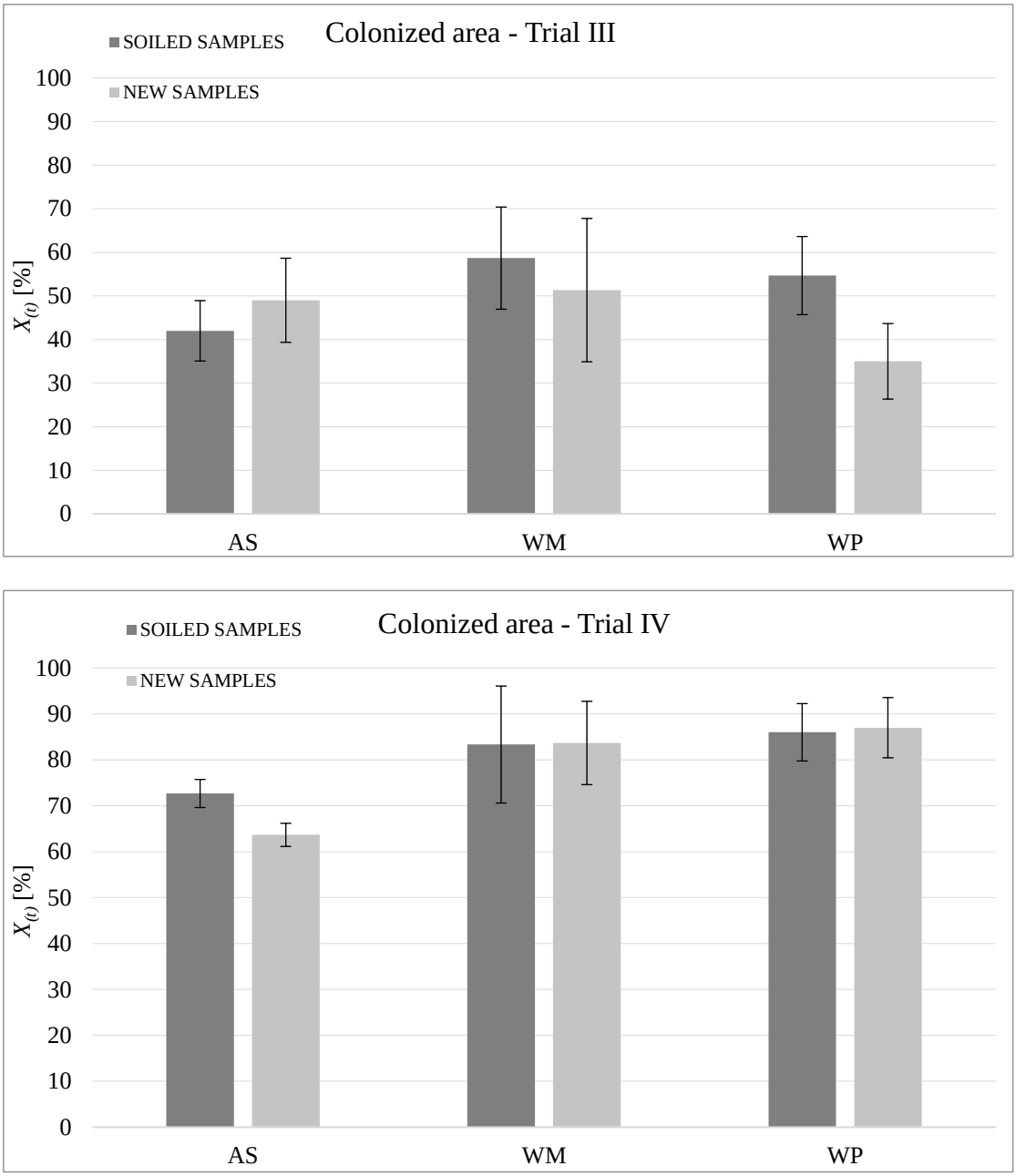

Figure 82: Colonized area ($X_{(t)}$ %) between previously soiled samples and new samples at the end of Trial III (a) and Trial IV (b). Data are the mean of three repeated test for each material type and SD is shown.

7. Limitations

The outcomes of the entire work present some limitations, mainly due to the limited timings and limited experimental spaces: this has led to take some choices, which represent at the same time limitations of achieved results. These are listed below.

Number of cool roofing products – This research has carried out the study about biocolonization, and the following biodeterioration, on three products, which represent the most frequently applied materials in the construction industrial field: single ply membrane, field-applied coating and asphalt shingle. The protagonist feature of these studied products is their high *albedo*, which is an important focus of the entire work. Even if the chosen product samples represent the most used materials for cool roofing, the *validation* of the bioageing protocol should take into account a wider set of building products. Also the previous ageing standard procedures [124] has been developed and validated considering a large group of flat roofing products.

The number of organism species – In natural ageing, biofilm becomes more complex with the passing of time, and heterotrophic organisms, like fungi, occur on urban surfaces and become integral part of bio-cenosis. Since fungi usually produce a dark pigmentation, as melanin, they can deeply influence the optical features of materials: then it is worth noting this type of organism in a laboratory protocol. Hence, the obtained results through the accelerated biofouling should be considered partial since only the pioneer and photosynthetic species has been evaluated. At the same time, the execution of a biofilm including both phototrophic and heterotrophic organisms, is a not negligible challenge for their different growth medium requirements.

Validation and determination of Reproducibility – Repeatability and uncertainty of the procedure have been evaluated through the results of three repeated test for each material type; this number of repetitions represents the minimum requirement for statistical evaluations. However, the validation of the procedure needs to be performed through a larger number of repeated test, considering more surface types. Afterwards, the reproducibility should be evaluated. It deals with the variability between single test results obtained by different laboratories, applying the same procedure on samples. The reproducibility of the method concerns also to the applicability of the developed bioageing procedure, and this work provides a pre-normative proposal for the standardization of a laboratory exposure practice including biological growth, which could be valuable for future implementations.

8. Future perspectives

At the conclusion of this work, which has tried to understand better the phenomena of biocolonization and biodeterioration of cool building materials and has tried to reproduce them into a laboratory accelerated setup, some implementations should be highlighted in order to prepare the future works and perspective. Most of these are born form the analysis of limitations, which have been discussed in the previous paragraph. The possible future perspectives are described in the next pointed list.

Increasing the set of cool roofing products – The next step of this work should embrace other building materials types in order to include the whole set of currently available roofing products. Increasing the number of material types, might permit also to get a stronger statistical evaluation about the procedure. Moreover, the knowledge of biocolonization rates and the change in solar reflectance over several type of products could enrich the database already available about the physical features of material types (CRRC, EPA). A future validation of the proposed bioaeging protocol should be able to calculate *K* parameter (equation n°1) of other products, estimating their ability to resist to biological aggression.

Modularity of accelerated bioaeging setup – TIS bioreactor system is a scalable and adjustable system where some experimental conditions could be scheduled according to the aim or research needs. This study has developed a final protocol, described in detail in ANNEX I, where each experimental details is defined and should be observed in order to achieve the expected repeatability. However, the device applied as the bioaging chamber leaves the possibility to modify the protocol in order to intensify or mitigate final biocolonization rates. The scalability of the system must regards only the specimen immersion times per day, and the duration of each "*flood and dry*" cycle: these two experimental conditions would influence only the velocity of colonies deposition, but not their shape and/or its color. Other experimental conditions should not be modified without an analysis of relative repeatability and uncertainty. The selection of the species could be modified according to the future out findings or research needs: the number of species could be even increased in order to enlarge the biofilm biodiversity. Moreover, heterotrophic organisms should be involved in the laboratory-accelerated protocol. This future goal should further improve the reliability of the protocol here discussed.

Comparison with natural ageing in hot and humid climates – Partial results from natural ageing which is currently continuing in Modena, would not seem be reproduced by laboratory conditions, which encourages a considerable bio growth on surfaces. The comparison between the natural and laboratory biolcolonization would

not be intended to find out an accurate correlation among aged results obtained through the two different methods, rather to understand the behavior of material against the biofilm growth. The goal should not be focused on the time-correlation among real and accelerated conditions, since the first one is always too unpredictable to be reproduced by the second one. The main reason to validate the experimental results with outdoor ageing is to study how physical changes (as colorimetric parameter and solar reflectance) occurs on the same product type according two different ageing method. The next experimental design, beyond the involvement of more products type, should provide a natural ageing exposure in a hot and humid climate site, where the outdoor conditions are extremely favorable to bio growth.

Scaling-up of TIS bioreactor – After the validation of the procedure, the scaling-up of TIS bioreactor could represent a possible future implementation. The construction of a new prototype of bioageing chamber, would provide the possibility to host larger and more specimen. This could be essential, firstly, in order to couple the laboratory bioageing procedure with standard test method ASTM D7897, where the required specimen sizes are compliant with sample holder of the ageing chamber and the instruments for thermal-physical properties. Secondly, the possibility to expose at the same time more specimen into a bioreactor, would greatly improve the effectiveness of the laboratory work.

Determination of Reproducibility – The reproducibility of the method concerns to the applicability of the developed bioageing procedure. The protocol has been thought in order to provide a further tool to producers and analysis laboratories, which are interested to study the biodeterioration process of surfaces in a fast way. Hence, the procedure should be adequate to be reproduced in other laboratories. The basis to start the evaluation of reproducibility of this bioageing procedure through the involvement of other Laboratories has already been laid. During this PhD work, the preliminary results of this procedure have been presented to the Lawrence Berkeley National Laboratory (LBNL, https://www.lbl.gov/), which is the worldwide reference team and laboratory for cool materials research. LBNL has taken part as the most researches undertaken until now about cool material ageing processes; it shows interest to continue to set a laboratory procedure able to accelerate also biocolonization.

9. Conclusive remarks

Biodeterioration of surfaces is a very complex phenomenon, which depends to too many factors, making its precise and accelerated reproduction into laboratory almost unlikely. The natural progression of biological colonization on different surfaces will continue to change together with climate, micro-climate and all environmental-correlated conditions and parameters. What is certain, however, is that this multifaceted phenomenon occurs everywhere across the outdoor (and indoor) exposed surfaces, through multiple ways, levels and forms. Therefore, this research has studied a procedure to induce, according to a repeatable procedure, the growth of biological colonization on building material products. The experimental procedure does not necessarily reproduces the intricate biocenosis which growth on surfaces with the passing of several years during natural ageing. However, this research gives a draft protocol to study the behavior of different cool surface products when exposed to intensive biological deposition. According to the product's intrinsic characteristics, the level of biocolonization and biodeterioration changes. The group of physical and chemical surface features, which define the primary bioreceptiviy of the product, has been identified through the application of Avrami's model. It makes possible the estimation of the parameter *K*. The results underline the importance to manage and to calibrate each experimental parameter in order to get acceptable values of repeatability. The draft proposal of accelerated bioageing protocol is able to compress intensely the exposure time, giving the possibility to evaluate the behavior of each surface type against biological depositions and bio growth.

The uncertainty (*U%)* calculated on ρ_{sol} values obtained after the bioageing process, remains under the 10% and this represent a sufficient result to consider positively the repeatability of this procedure.

The current challenge for highly reflective material producers concerns the ability to extend as much as possible the high performant surfaces' life. The draft proposal here presented has tried to give a response to this specific industrial need: evaluate the products' durability in a faster and repeatable way in order to improve these features in a rapid way. The urgency of climate crisis, which is gaining great attention from the policies and the citizens, requires each possible effort and available technology aimed to mitigate the environment temperature increase. Among the urban mitigation technologies, reflective materials are able to reduce absorption of solar heat by the city's infrastructures. Therefore, the present work, providing a further tool to analyze and evaluate the durability cool materials, could represent an indirect implementation of their efficiency, providing, as well, to contribute to the urban heat island mitigation.

10. ANNEX I: Bioageing procedure, a draft proposal

Proposal of Standard Practice for Laboratory Biofouling of Roofing Materials to test their resistance to biological aggression

1. Scope

This Procedure is aimed to promote biofilm growth on builidng materials in order to evaluate their resistance to biological aggression, which normally occurs on outdoor exposed surfaces. Biofouling is one of the cause of thermal properties losses and aesthetical appereance degradation, together with deposition and retention of airborne pollutants. At the same time, for its huge variability it is no possible to recreate into the laboratory the same biological dynamics which occurs on surfaces from different geographical areas, since it could involve thousands of organisms species, depending to climate and microclimate conditions. This procedure, then, reports a repeatable setup to accelerate biological growth on builiding material, which not necessarly reproduce what in nature happens on surfaces.

2. Referenced Documents

ASTM C1549 Test Method for Determination of Solar Reflectance Near Ambient Temperature Using a Portable Solar Reflectometer;

ASTM E691 Practice for Conducting an Interlaboratory Study to Determine the Precision of a Test Method;

ASTM D7897 Standard Practice for Laboratory Soiling and Weathering of Roofing Materials to Simulate Effects of Natural Exposure on Solar Reflectance and Thermal Emittance;

3. Terminology

3.1. Solar reflectance—the fraction of incident solar flux reflected by a surface.

3.2. TIS Bioreactor: it consists in a sealed bioageing chamber equipped with a basket to holds material samples, exposed to the bioageing process.

Biological organisms grow into liquid medium which submerges the specimen at regular time intervals.

3.3. *Phototrophic organism:* organisms species which live through photosynthesis and have 5-100 μm diameter cell size.

3.4. *Filter:* polytetrafluoroethylene (PTFE) filters with 0.22 μm pores to ensure that the airflow in and out of the bioreactors is sterile.

3.5. *Growth incubator:* chamber equipped with LED light source and temperature controller.

3.6. *P.A.R.*: Photosyntethically Active Radiation: the amount of light available for photosynthesis, which is light in the 400 to 700 nanometer wavelength range.

3.7. *Precision*: is how close two or more measurements are to each other. Precision could be calculated through the coefficient of variation (*CV*), according to ASTM E691: the ratio of the standard deviation to the mean. The higher the coefficient of variation, the greater the level of dispersion around the mean. It is expressed as a percentage and has no units.

3.8. *Repeatability Coefficient*: it is a precision measure which represents the value below which the absolute difference between two repeated test results may be expected to lie with a probability of 95%. It indicates the precision under repeatability conditions: within-laboratory; same lab, operator, equipment.

4. Summary of the procedure

This practice presents a fast laboratory method to induce biological aggression on building material surface. The practice describes how to encourage biofilm growth on material surfaces, providing al the best growth conditions on surfaces in a repeatable way. The system enables "watering and dry" cycles on material samples simulating the exposure to water availabilty, deposition of organisms colonies and following drying periods. Experimental procedure consists to submerge material samples with a liquid growth medium inoculated with phototrophic organisms (cyanobacteria and green algae) in order to encourage biofilm deposition on surfaces. The "watering and dry" cycle is run two times per day in order to accelerate colonization process.

5. Significance and use

Building material are heavily affected by soiling and weathering processes which reduce their thermo-physical and aesthetical properties. In particular, highly reflective roofs, which can decrease the energy required for building air conditioning helping the

mitigation of the urban heat island, diminish their benefits due to soiling and fouling processes, which reduce solar reflectance.

Biological deposition, which is part of the complete fouling dynamic, represents in hot and humid climates, the major agent of soiling inducing green or dark colored patinas on roofing surfaces. These contribute to change within one or two years the solar reflectance, and other physical properties, of a new building envelope. Current product rating programs require the roofing manufacturers to report values of solar reflectance and thermal emittance measured after three years of natural exposure. To this aim, the standard practice ASTM D7897 provides a rapid laboratory process for soiling and weathering that simulates the three-year-aged radiative properties of roof and other building envelope surface materials. Unfortunately, this standard is mostly focused onto surface soiling and it does not take into proper account the presence and growth of microorganisms. Therefore, the present procedure describe a repeatable way to accelerate biological colonization on material specimens in order to evaluate in a fast way the change of physical properties.

6. Proposal of bioageing procedure: Method and Apparatus

6.1. TIS bioreactor – Pioneer organisms which form a biofilm on surfaces need water and lights availability. At the same time, it is necessary to provide optimal and steady environmental conditions to accelerate biological growth and deposition. To achieve this goal a sealed chamber, not exposed to outsides effects or other contaminants, is provided to induce bioageing. The experimental setup is a Temporary Immersion System (TIS) bioreactor, (example: http://www.plantform.se/pub/, Sweden), used as bioageing chamber. The system consists in a sealed growth vessel made of transparent polycarbonate, with the size of 180 × 160 × 150 mm. The vessel contains a basket with holes of 1 mm in size to holds specimen. A frame with four legs is placed above the basket to avoid the basket to rise when air pres-sure is applied to the bioreactor. The construction and placement of the basket is made so that the specimens on the basket are only immersed into the liquid medium when air pressure is applied to the bioreactor. The bioreactor has three opening holes for medium supply, aeration and ventilation. Specially designed hollow screws provided with silicone seals are fitted tightly within the holes. Connected to these screws are flexible plastic Tygon tubes, with aninner diameter of 3.2 mm, and 0.22 μm polytetrafluoroethylene (PTFE) filters to ensure that the airflow in and out of the bioreactors are sterile. Immersion and ventilation cycles are regulated by two separate air pumps, each connected to a timer and linked with a PTFE filter through the plastic tube (Figure A.1).

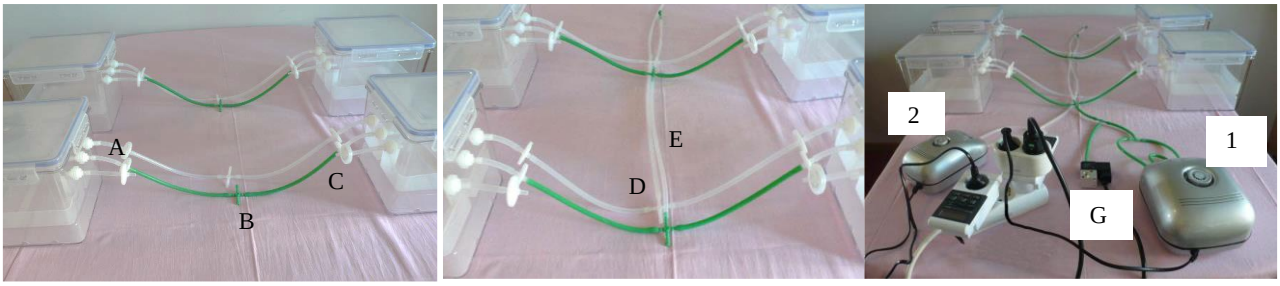

Figure A.1: TIS bioreactor installation

It is possible (not mandatory) to connect more than one bioreactor to the same pump system: green silicon tubes of equal length are placed on the middle filters (A). A green 4-way connectors (B) is attached to the tubes for connection of the bioreactors. White silicon tubes of equal length are placed on the outer filters (C). A white 4-way connectors (D) is attached to the tubes for connection of the bioreactors. Long silicon tubes (E) are used to connect the bioreactors horizontally. The end of the tube from the middle filter of the first bioreactor is connected to a 10W pump (1) and an electrovalve (G) using two 3-way connectors. Both the pump and the electrovalve are then inserted into a 2-way splitter socket attached to a timer. The end of the tube from the outer filter of the first bioreactor is connected to a 5W pump (2) using a 3-way connector and then attached to a second timer. Both timers are then sheduled according to immersion cycles program.

When the pressure induced by the first pump is applied to the middle filter, the nutrient solution is forced to upward and covering the material samples. When pressure is relieved, the nutrients are drained back through the internal basket. In order to facilitate air to go out from the tube connected to the middle filter an electrovalve is applied. This way, materials specimens are only immersed into the liquid medium when air pressure is applied to the bioreactor. Bioreactors must be previuosly autoclaved at 120 °C, 1 atm, for 20 min separately before use.

6.2. Liquid growth medium

The liquid growth medium involved as nutrients source for phototrophic organism is Bold's Basal (PhytoTechnology Laboratories®, USA), specifically formulated for microalgae in vitro growth and stocked into the fridge at 4°C.

The mixture needs to be prepared according commercial instructions: 0.705 g/ L of BBM powder is solved into distilled water and stirred for about 10 minutes to prepare a homogenized solution. Then pH is adjusted, after the adding 1 ml/L of sulfuric acid 0.1%, by KOH solution at 6.6±0.2, reading the value with a calibrated pHmeter. The medium is then inserted into a flasks and autoclaved at 120◦C for 20 min. 600 ml of BBM should be prepared for each bioreactor. In any

case, not less of 500 ml need to be used. When the bioreactor and liquid medium are sterile, liquid BBM is spilled within bioaging chamebr. This operation must be performed under a laminar flow hood to preserve sterility.

6.3. Phototrophic organisms

Organisms species needed for biological growth have been selected according the most common species found in urban enviornment and surfaces and according the large tolerance ranges of coltivation. These species are: *E. mirabilis, K. flaccidum, Gloeaocapsa sp., N. commune*. Each species culture need to be pure and cultivated separatley in sterile growth medium keeping a growth incubator temperature of 24±1°C, with a photoperiod 14 h/day and PAR light intensity of 100±10 μmol/m^2/s photons. Then a specific amount of each species is inoculated into the liquid medium prepared and used to fill each bioreactor. The starting cell concetration into each bioreactor need to be 3*10^2±50 cell/ml. The absorbance of the liquid medium need to be read at 750 nm with UV-Vis Spectrophotometer, after the specific calibration of the instrument. The starting absorbance value requested to start bioaging procedure must remain within the range 0.03-0.07. Then, the adding of organism species volume should be performed gradually, calibrating the absorbance progressively according to the prescribed range. Then, the withdrawn volume of homogenized mother culture of each species, is used for the inoculum into every bioreactor involved in the bioageing procedure. Being sure to insert the same volume of each species into each bioreactor.

6.4. Material specimen preparation

Building material samples are requested to be flat and the minimum thikness should be 4 mm. If the thikness is lower, the specimen is bonded to aluminum plates to provide the adequate material density to avoid flotation during immersion cycles. Samples could be squared or rectangualar shaped, with a minum surface area of 16 cm^2 and maximum one 100 cm^2. In each case, lenght or width must not exceed 10 cm.

Before starting the bioageing procedure, all samples are exposed to a biocidal treatment with UV-C rays (253.8 nm) for at least 30 minutes to each side, using a UV-C Lamp placed at 80 cm over the materials surfaces. Then the specimens are ready to be put on the basket into the biorector: this ooperation is performed under a laminar flow hood to preserve sterility. Depending to the size of the specimens, one or more than one sample could be put into the same TIS vessel.

6.5. Growth incubator

The bioreactors, filled with BBM and inoculated with organisms species and material specimens, are put into growth incubator, which must keep a temperature range of 24±1°C. LED lamps must provide 100±10 μmol/m^2/s photons in homogenous way in each point of the incubator. Th distance between bioreactor and LED lamps must not be low than 25cm and not more than 50 cm otherwise the light intensity provided to the organism is not observed. Light intensity is measured with a certified P.A.R. sensor. As soon as the bioreactors are placed into the incubator, they are connected to the pumps (as described in section 6.1), which are connected to the timers. The timers are automatically activated providing immersion and air cycles. Each timer is set in this way: first timer (linked with the pump, electrovalve and the middle filter) provides one immersion lasting 10 minutes every 12 hours; second timer provides the activation of the second pump, linked with outside filter, and induces 10 minutes of air into the growth chamber. When the second pump is on, the first one must be off and viceversa. In this way two "watering-dry" cycles are provided each day.

7. Procedure

The accelerated bioaging protocol is prepared according the followig steps, as sketched in figure A.2.

Figure A.2. Bioaeging setup procedure

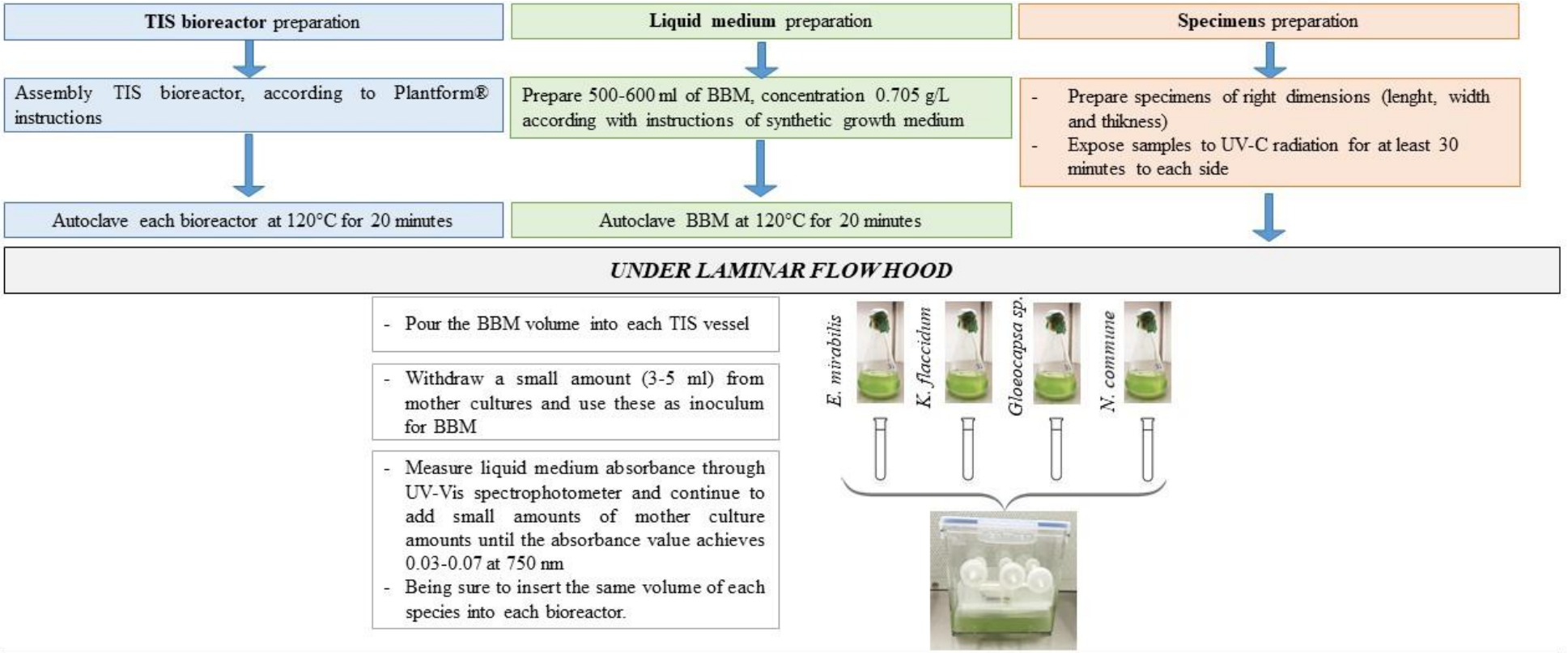

8. Validation, Precision, and Bias

8.1. Measurement of Radiative Properties

The values of aged solar reflectance are measured according to ASTM C1549. The mean error of final solar reflectance calculated on repeated test on three building material type stay withing the range 0.01-0.03. This is translated to a mean coefficient of variation (that is a measure of precision) of 3.3 %. The method precision is evaluated by calculating the repeatability of the accelerated bioageing procedure on solar reflectance of roofing products. Repeatability concerns the variability between independent test results obtained within a single laboratory. The tests performed in each laboratory are conducted by a single operator. The precision of the bioaged surfaces described here is determined by conducting three repeated test on three material types and calculating the data consistency of solar reflectance after accelerated bioaeging exposure, according to Test Method C1549. The repeatability coefficient of the experimental method for solar reflectance is 9.2%

9. Safety instructions

All the steps to prepare the bioreactors to use them as accelerated biological chamber and its contents should be perforemed into a biological laboratory equipped at least with the following instrumentations:

- Analytical balance (d=0.1mg)
- Laminar Flux Hood
- UV-C Lamp: this should be turned on ONLY when it can be shielded with a suitable protective screen
- Autoclave
- UV-Vis Spectrophotometer
- Fridge
- Growth incubator

Personal safety protection devices (SPD) are required according each single instrument and device safety manual of instruction.

References

[1] T. Warscheid and J. Braams, "Biodeterioration of stone: A review," *International Biodeterioration and Biodegradation*, vol. 46, no. 4, pp. 343–368, 2000, doi: 10.1016/S0964-8305(00)00109-8.

[2] P. Berdahl, H. Akbari, R. Levinson, and W. A. Miller, "Weathering of roofing materials - An overview," *Construction and Building Materials*, vol. 22, no. 4, pp. 423–433, 2008, doi: 10.1016/j.conbuildmat.2006.10.015.

[3] P. Berdahl, H. Akbari, R. Levinson, and W. A. Miller, "Construction and Building Materials , February , 2006 Weathering of Roofing Materials-An Overview," 2006.

[4] O. Guillitte, "Bioreceptivity: a new concept for building ecology studies," *Science of the Total Environment*, vol. 167, no. 1–3, pp. 215–220, 1995, doi: 10.1016/0048-9697(95)04582-L.

[5] M. D'Orazio, M. Palladini, L. Aquilanti, and F. Clementi, "Experimental evaluation of the growth rate of mould on finishes for indoor housing environments: Effects of the 2002/91/EC directive," *Building and Environment*, vol. 44, no. 8, pp. 1668–1674, 2009, doi: 10.1016/j.buildenv.2008.11.004.

[6] T. Verdier, M. Coutand, A. Bertron, and C. Roques, "A review of indoor microbial growth across building materials and sampling and analysis methods," *Building and Environment*, vol. 80, pp. 136–149, 2014, doi: 10.1016/j.buildenv.2014.05.030.

[7] C. Gaylarde, M. Ribas Silva, and T. Warscheid, "Microbial impact on building materials: An overview," *Materials and Structures/Materiaux et Constructions*, vol. 36, no. 259, pp. 342–352, 2003, doi: 10.1617/13867.

[8] O. Guillitte and R. Dreesen, "Laboratory chamber studies and petrographical analysis as bioreceptivity assessment tools of building materials," *Science of the Total Environment*, vol. 167, no. 1–3, pp. 365–374, 1995, doi: 10.1016/0048-9697(95)04596-S.

[9] C. C. Gaylarde and P. M. Gaylarde, "A comparative study of the major microbial biomass of biofilms on exteriors of buildings in Europe and Latin America," *International Biodeterioration and Biodegradation*, vol. 55, no. 2, pp. 131–139, 2005, doi: 10.1016/j.ibiod.2004.10.001.

[10] T. H. Tran *et al.*, "Influence of the intrinsic characteristics of mortars on biofouling by Klebsormidium flaccidum," *International Biodeterioration and Biodegradation*, vol. 70, pp. 31–39, 2012, doi: 10.1016/j.ibiod.2011.10.017.

[11] A. Dubosc, G. Escadeillas, and P. J. Blanc, "Characterization of biological stains on external concrete walls and influence of concrete as underlying material," *Cement and Concrete Research*, vol. 31, no. 11, pp. 1613–1617, 2001, doi: 10.1016/S0008-8846(01)00613-5.

[12] W. De Muynck, A. M. Ramirez, N. De Belie, and W. Verstraete, "Evaluation of strategies to prevent algal fouling on white architectural and cellular concrete," *International Biodeterioration and Biodegradation*, vol. 63, no. 6, pp. 679–689, 2009, doi: 10.1016/j.ibiod.2009.04.007.

[13] A. Z. Miller *et al.*, "Bioreceptivity of building stones: A review," *Science of the Total Environment*, vol. 426, pp. 1–12, 2012, doi: 10.1016/j.scitotenv.2012.03.026.

[14] C. Ferrari *et al.*, "Review on the influence of biological deterioration on the surface properties of building materials: Organisms, materials, and methods," *International Journal of Design and Nature and Ecodynamics*, vol. 10, no. 1, pp. 21–39, 2015, doi: 10.2495/DNE-V10-N1-21-39.

[15] S. Manso, G. Mestres, M. P. Ginebra, N. De Belie, I. Segura, and A. Aguado, "Development of a low pH cementitious material to enlarge bioreceptivity," *Construction and Building Materials*, vol. 54, pp. 485–495, 2014, doi: 10.1016/j.conbuildmat.2014.01.001.

[16] S. Manso *et al.*, "Bioreceptivity evaluation of cementitious materials designed to stimulate biological growth," *Science of the Total Environment*, vol. 481, no. 1, pp. 232–241, 2014, doi: 10.1016/j.scitotenv.2014.02.059.

[17] M. L. Coutinho, A. Z. Miller, and M. F. Macedo, "Biological colonization and biodeterioration of architectural ceramic materials: An overview," *Journal of Cultural Heritage*, vol. 16, no. 5, pp. 759–777, 2015, doi: 10.1016/j.culher.2015.01.006.

[18] M. Sleiman *et al.*, "Soiling of building envelope surfaces and its effect on solar reflectance - Part II: Development of an accelerated aging method for roofing materials," *Solar Energy Materials and Solar Cells*, vol. 122, pp. 271–281, 2014, doi: 10.1016/j.solmat.2013.11.028.

[19] C. C. Lin and W. Y. Chen, "Effect of paint composition, nano-metal types and substrate on the improvement of biological resistance on paint finished building material," *Building and Environment*, vol. 117, pp. 49–59, 2017, doi: 10.1016/j.buildenv.2017.02.013.

[20] G. Santunione, C. Ferrari, C. Siligardi, A. Muscio, and E. Sgarbi, "Accelerated biological ageing of solar reflective and aesthetically relevant building materials," *Advances in Building Energy Research*, vol. 13, no. 2, pp. 264–281, 2019, doi: 10.1080/17512549.2018.1488616.

[21] E. Di Giuseppe, 2013, Nearly Zero Energy Buildings and Proliferation of Microorganisms: a Current Issue for Highly Insulated and Airtight Building Envelopes In: Springer (Eds), pp. 3-27.

[22] O. Ortega-Morales, J. L. Montero-Muñoz, J. A. Baptista Neto, I. B. Beech, J. Sunner, and C. Gaylarde, "Deterioration and microbial colonization of cultural heritage stone buildings in polluted and unpolluted tropical and subtropical climates: A meta-analysis," *International Biodeterioration and Biodegradation*, vol. 143, no. June, 2019, doi: 10.1016/j.ibiod.2019.104734.

[23] T. H. Tran, "Influence of the intrinsic characteristics of mortars on their biofouling by pigmented organisms: Comparison between laboratory and fieldscale experiments." .

[24] B. Prieto, B. Silva, and O. Lantes, "Biofilm quantification on stone surfaces: Comparison of various methods," *Science of the Total Environment*, vol. 333, no. 1–3, pp. 1–7, 2004, doi: 10.1016/j.scitotenv.2004.05.003.

[25] J. J. Ortega-Calvo, X. Ariño, M. Hernandez-Marine, and C. Saiz-Jimenez, "Factors affecting the weathering and colonization of monuments by phototrophic microorganisms," *Science of the Total Environment*, vol. 167, no. 1–3, pp. 329–341, 1995, doi: 10.1016/0048-9697(95)04593-P.

[26] P. Berdahl, H. Akbari, and L. S. Rose, "Aging of reflective roofs : soot deposition," vol. 41, no. 12, pp. 2355–2360, 2002.

[27] L. Tomaselli, G. Lamenti, M. Bosco, and P. Tiano, "Biodiversity of photosynthetic micro-organisms dwelling on stone monuments," *International Biodeterioration & Biodegradation*, vol. 46, no. 3, pp. 251–258, Oct. 2000, doi: 10.1016/S0964-8305(00)00078-0.

[28] K. C. Marshall and J. Wiley, "The world of biofilms- quantified," *Biofilms*, vol. 9, no. May, pp. 1991–1991, 1991.

[29] H. Barberousse, R. J. Lombardo, G. Tell, and A. Couté, "Factors involved in the colonisation of building façades by algae and cyanobacteria in France," *Biofouling*, vol. 22, no. 2, pp. 69–77, 2006, doi: 10.1080/08927010600564712.

[30] C. C. Gaylarde, L. H. G. Morton, K. Loh, and M. A. Shirakawa, "Biodeterioration of external

architectural paint films - A review," *International Biodeterioration and Biodegradation*, vol. 65, no. 8, pp. 1189–1198, 2011, doi: 10.1016/j.ibiod.2011.09.005.

[31] H. K. Tanaca, C. M. R. Dias, C. C. Gaylarde, V. M. John, and M. A. Shirakawa, "Discoloration and fungal growth on three fiber cement formulations exposed in urban, rural and coastal zones," *Building and Environment*, vol. 46, no. 2, pp. 324–330, 2011, doi: 10.1016/j.buildenv.2010.07.025.

[32] P. Fernandes, "Applied microbiology and biotechnology in the conservation of stone cultural heritage materials," *Applied Microbiology and Biotechnology*, vol. 73, no. 2, pp. 291–296, 2006, doi: 10.1007/s00253-006-0599-8.

[33] C. G. H. G. Morton, "Deterogenic biofilm on Building and their control: a Review." Biofouling, pp. Vol14; 59–74, 1999.

[34] P. M. Gaylarde, C. C. Gaylarde, P. Cx, and P. Alegre, "Algae and cyanobacteria on painted buildings in Latin America PDF created with FinePrint pdfFactory trial version http://www.fineprint.com PDF created with FinePrint pdfFactory trial version http://www.fineprint.com," vol. 46, no. June, 2000.

[35] C. A. Crispim and C. C. Gaylarde, "Cyanobacteria and biodeterioration of cultural heritage: A review," *Microbial Ecology*, vol. 49, no. 1, pp. 1–9, 2005, doi: 10.1007/s00248-003-1052-5.

[36] J. J. Ortega-Calvo, M. Hernandez-Marine, and C. Saiz-Jimenez, "Biodeterioration of building materials by cyanobacteria and algae," *International Biodeterioration*, vol. 28, no. 1–4, pp. 165–185, 1991, doi: 10.1016/0265-3036(91)90041-O.

[37] M. A. Shirakawa, C. C. Gaylarde, P. M. Gaylarde, V. John, and W. Gambale, "Fungal colonization and succession on newly painted buildings and the effect of biocide," *FEMS Microbiology Ecology*, vol. 39, no. 2, pp. 165–173, 2002, doi: 10.1016/S0168-6496(01)00214-8.

[38] M. Romani *et al.*, "Current and future chemical treatments to fight biodeterioration of outdoor building materials and associated biofilms: Moving away from ecotoxic and towards efficient, sustainable solutions," *Science of the Total Environment*, vol. 802, p. 149846, 2022, doi: 10.1016/j.scitotenv.2021.149846.

[39] C. Saiz-Jimenez, "Biodeterioration vs biodegradation: The role of microorganisms in the removal of pollutants deposited on historic buildings," *International Biodeterioration and Biodegradation*, vol. 40, no. 2–4, pp. 225–232, 1997, doi: 10.1016/S0964-8305(97)00035-8.

[40] R. Mitchell and J. Gu, "Changes in the bioÿlm micro ora of limestone caused by atmospheric pollutants," vol. 46, no. 2000, pp. 299–303, 2001.

[41] A. Stechmann and T. Cavalier-Smith, "Rooting the eukaryote tree by using a derived gene fusion," *Science*, vol. 297, no. 5578, pp. 89–91, 2002, doi: 10.1126/science.1071196.

[42] W. F. Vincent, "Cyanobacteria," *Elsevier*, pp. 48–67, 2009, doi: 10.1037/14768-003.

[43] B. A. Whitton, "Diversity, Ecology, and Taxonomy of the Cyanobacteria," *Photosynthetic Prokaryotes*, pp. 1–51, 1992, doi: 10.1007/978-1-4757-1332-9_1.

[44] S. Scheerer, O. Ortega-Morales, and C. Gaylarde, *Chapter 5 Microbial Deterioration of Stone Monuments-An Updated Overview*, 1st ed., vol. 66, no. 08. Elesvier Inc., 2009.

[45] E. I. Friedmann, "Endolithic microorganisms in the Antarctic cold desert," *Science*, vol. 215, no. 4536, pp. 1045–1053, 1982, doi: 10.1126/science.215.4536.1045.

[46] P. T. S. Pereira, A. Zille, E. Micheletti, P. Moradas-Ferreira, R. De Philippis, "Complexity of cyanobacterial exopolysaccharides: composition, structures, inducing factors and putative genes iinvolved in theri biosynthesis and assembly," vol. 33, pp. 917–941, 2009.

[47] H. Bin Wang, S. J. Wu, and D. Liu, "Preparation of polysaccharides from cyanobacteria Nostoc commune and their antioxidant activities," *Carbohydrate Polymers*, vol. 99, pp. 553–555, 2014, doi: 10.1016/j.carbpol.2013.08.066.

[48] S. Jensen, B. O. Petersen, S. Omarsdottir, B. S. Paulsen, J. O. Duus, and E. S. Olafsdottir, "Structural characterisation of a complex heteroglycan from the cyanobacterium Nostoc commune," *Carbohydrate Polymers*, vol. 91, no. 1, pp. 370–376, 2013, doi: 10.1016/j.carbpol.2012.08.063.

[49] I. B. Beech and C. C. Gaylarde, "Microbial polysaccharides and corrosion," *International Biodeterioration*, vol. 27, no. 2, pp. 95–107, 1991, doi: 10.1016/0265-3036(91)90002-9.

[50] M. F. Macedo, A. Z. Miller, A. Dionísio, and C. Saiz-Jimenez, "Biodiversity of cyanobacteria and green algae on monuments in the Mediterranean Basin: An overview," *Microbiology*, vol. 155, no. 11, pp. 3476–3490, 2009, doi: 10.1099/mic.0.032508-0.

[51] G. Gómez-Alarcón, M. L. Muñoz, and M. Flores, "Excretion of organic acids by fungal strains isolated from decayed sandstone," *International Biodeterioration and Biodegradation*, vol. 34, no. 2, pp. 169–180, 1994, doi: 10.1016/0964-8305(94)90006-X.

[52] A. Z. Miller, L. Laiz, A. Dionísio, M. F. Macedo, and C. Saiz-Jimenez, "Growth of phototrophic biofilms from limestone monuments under laboratory conditions," *International Biodeterioration and Biodegradation*, vol. 63, no. 7. pp. 860–867, 2009, doi: 10.1016/j.ibiod.2009.04.004.

[53] A. F. Bravery, "Biodeterioration of Paint—a State-of-the-Art Comment," *Biodeterioration 7*, pp. 466–485, 1988, doi: 10.1007/978-94-009-1363-9_63.

[54] P. T. S. Pereira, A. Zille, E. Micheletti, P. Moradas-Ferreira, R. De Philippis, "Complexity of cyanobacterial exopolysaccharides: composition, structures, inducing factors and putative genes involved in their biosynthesis and assembly," *Microbiologiy Reviews*, vol. 33, pp. 917–941, 2009.

[55] H. H. E. Schlichting, "Some subaerial algae from ireland," *British Phycological Journal*, vol. 10, no. 3, p. 267, 1975, doi: 10.1080/00071617500650251.

[56] Y. C. Wee, "Growth of algae on exterior painted masonry surfaces," *International Biodeterioration*, vol. 24, no. 4–5, pp. 367–371, 1988, doi: 10.1016/0265-3036(88)90022-X.

[57] C. Urzì and M. Realini, "Colour changes of Noto's calcareous sandstone as related to its colonisation by microorganisms," *International Biodeterioration and Biodegradation*, vol. 42, no. 1, pp. 45–54, 1998, doi: 10.1016/S0964-8305(98)00045-6.

[58] A. Danin and G. Caneva, "Deterioration of limestone walls in Jerusalem and marble monuments in Rome caused by cyanobacteria and cyanophilous lichens," *International Biodeterioration*, vol. 26, no. 6, pp. 397–417, 1990, doi: 10.1016/0265-3036(90)90004-Q.

[59] F. E. W. Eckhardt, U. Kiel, D.- Kiel, and W. Germany, "I. Drever (ed.), The Chemistry of Weathering, 161-173. © 1985 by D. Reidel Publishing Company.," no. 4, pp. 161–173, 1985.

[60] R. P. George, S. Ramya, D. Ramachandran, and U. Kamachi Mudali, "Studies on Biodegradation of normal concrete surfaces by fungus Fusarium sp.," *Cement and Concrete Research*, vol. 47, pp. 8–13, 2013, doi: 10.1016/j.cemconres.2013.01.010.

[61] K. Sterflinger and H. Prillinger, "Molecular taxonomy and biodiversity of rock fungal communities in an urban environment (Vienna, Austria)," *Antonie van Leeuwenhoek, International Journal of General and Molecular Microbiology*, vol. 80, no. 3–4, pp. 275–286, 2001, doi: 10.1023/A:1013060308809.

[62] J. D. Gu, T. E. Ford, N. S. Berke, and R. Mitchell, "Biodeterioration of concrete by the fungus

Fusarium," *International Biodeterioration and Biodegradation*, vol. 41, no. 2, pp. 101–109, 1998, doi: 10.1016/S0964-8305(98)00034-1.

[63] I. B. Beech, "Corrosion of technical materials in the presence of biofilms - Current understanding and state-of-the art methods of study," *International Biodeterioration and Biodegradation*, vol. 53, no. 3, pp. 177–183, 2004, doi: 10.1016/S0964-8305(03)00092-1.

[64] E. S. Jacobson, "Pathogenic roles for fungal melanins," *Clinical Microbiology Reviews*, vol. 13, no. 4, pp. 708–717, 2000, doi: 10.1128/CMR.13.4.708-717.2000.

[65] M. A. de la Torre, G. Gomez-Alarcon, C. Vizcaino, and T. T. Garcia, "Biochemical mechanisms of stone alteration carried out by filamentous fungi living in monuments," *Biogeochemistry*, vol. 19, no. 3, pp. 129–147, 1992, doi: 10.1007/BF00000875.

[66] H. Annuk and A. P. Moran, *Microbial Biofilm-Related Polysaccharides in Biofouling and Corrosion*, First edit. Elsevier Inc., 2010.

[67] D. J. Giannantonio, J. C. Kurth, K. E. Kurtis, and P. A. Sobecky, "Effects of concrete properties and nutrients on fungal colonization and fouling," *International Biodeterioration and Biodegradation*, vol. 63, no. 3, pp. 252–259, 2009, doi: 10.1016/j.ibiod.2008.10.002.

[68] D. J. Giannantonio, J. C. Kurth, K. E. Kurtis, and P. A. Sobecky, "Molecular characterizations of microbial communities fouling painted and unpainted concrete structures," *International Biodeterioration and Biodegradation*, vol. 63, no. 1, pp. 30–40, 2009, doi: 10.1016/j.ibiod.2008.06.004.

[69] X. Liu, R. J. Koestler, T. Warscheid, Y. Katayama, and J. D. Gu, "Microbial deterioration and sustainable conservation of stone monuments and buildings," *Nature Sustainability*, vol. 3, no. 12, pp. 991–1004, 2020, doi: 10.1038/s41893-020-00602-5.

[70] H. Akbari and R. Levinson, "Evolution of Cool-Roof Standards in the US," vol. 2, pp. 1–32, doi: 10.3763/aber.2008.0201.

[71] H. Akbari, M. Pomerantz, and H. Taha, "Cool surfaces and shade trees to reduce energy use and improve air quality in urban areas," *Solar Energy*, vol. 70, no. 3, 2001, doi: 10.1016/S0038-092X(00)00089-X.

[72] A. L. Pisello, *High-albedo roof coatings for reducing building cooling needs*. Elsevier Ltd., 2015.

[73] ASTM C1549 - 09, "Standard test method for determination of solar reflectance near ambient temperature using a portable solar reflectometer," *American Society for Testing Materials*, vol. 04, no. Reapproved 2014, pp. 6–9, 2014, doi: 10.1520/C1549-09R14.2.

[74] C. Ferrari, A. Libbra, A. Muscio, and C. Siligardi, "Influence of the irradiance spectrum on solar reflectance measurements," *Advances in Building Energy Research*, vol. 7, no. 2, pp. 244–253, 2013, doi: 10.1080/17512549.2013.865563.

[75] ASTM and 98 C 1371, "Standard Test Method for Determination of Emittance of Materials Near Room Temperature Using Portable Emissometers," vol. 04, no. Reapproved 2010, pp. 1–8, 2010, doi: 10.1520/C1371-15.2.

[76] R. Levinson, P. Berdahl, A. Asefaw Berhe, and H. Akbari, "Effects of soiling and cleaning on the reflectance and solar heat gain of a light-colored roofing membrane," *Atmospheric Environment*, vol. 39, no. 40, pp. 7807–7824, 2005, doi: 10.1016/j.atmosenv.2005.08.037.

[77] R. Levinson *et al.*, "Methods of creating solar-reflective nonwhite surfaces and their application to residential roofing materials," vol. 91, no. 2007, pp. 304–314, 2008, doi: 10.1016/j.solmat.2006.06.062.

[78] H. Akbari and D. Kolokotsa, "Three decades of urban heat islands and mitigation technologies research," *Energy and Buildings*, vol. 133, pp. 834–842, 2016, doi:

10.1016/j.enbuild.2016.09.067.

[79] H. Akbari, H. D. Matthews, and D. Seto, "The long-term effect of increasing the albedo of urban areas," 2012, doi: 10.1088/1748-9326/7/2/024004.

[80] A. L. Pisello, "State of the art on the development of cool coatings for buildings and cities," *Solar Energy*, vol. 144, pp. 660–680, 2017, doi: 10.1016/j.solener.2017.01.068.

[81] A. Synnefa, A. Dandou, M. Santamouris, M. Tombrou, and N. Soulakellis, "On the use of cool materials as a heat island mitigation strategy," *Journal of Applied Meteorology and Climatology*, vol. 47, no. 11, pp. 2846–2856, 2008, doi: 10.1175/2008JAMC1830.1.

[82] M. Santamouris, A. Synnefa, and T. Karlessi, "Using advanced cool materials in the urban built environment to mitigate heat islands and improve thermal comfort conditions," *Solar Energy*, vol. 85, no. 12, 2011, doi: 10.1016/j.solener.2010.12.023.

[83] L. Zhao, X. Lee, R. B. Smith, and K. Oleson, "Strong contributions of local background climate to urban heat islands," *Nature*, vol. 511, no. 7508, pp. 216–219, 2014, doi: 10.1038/nature13462.

[84] T. R. Oke, G. T. Johnson, D. G. Steyn, and I. D. Watson, "Simulation of surface urban heat islands under 'ideal' conditions at night part 2: Diagnosis of causation," *Boundary-Layer Meteorology*, vol. 56, no. 4, pp. 339–358, 1991, doi: 10.1007/BF00119211.

[85] M. Santamouris *et al.*, "Passive and active cooling for the outdoor built environment – Analysis and assessment of the cooling potential of mitigation technologies using performance data from 220 large scale projects," *Solar Energy*, vol. 154, pp. 14–33, 2017, doi: 10.1016/j.solener.2016.12.006.

[86] M. Santamouris, "Recent progress on urban overheating and heat island research. Integrated assessment of the energy, environmental, vulnerability and health impact. Synergies with the global climate change," *Energy and Buildings*, vol. 207, p. 109482, 2020, doi: 10.1016/j.enbuild.2019.109482.

[87] A. Pyrgou, P. Hadjinicolaou, and M. Santamouris, "Urban-rural moisture contrast: Regulator of the urban heat island and heatwaves' synergy over a mediterranean city," *Environmental Research*, vol. 182, no. May 2019, p. 109102, 2020, doi: 10.1016/j.envres.2019.109102.

[88] A. Gasparrini *et al.*, "Projections of temperature-related excess mortality under climate change scenarios," *The Lancet Planetary Health*, vol. 1, no. 9, pp. e360–e367, 2017, doi: 10.1016/S2542-5196(17)30156-0.

[89] J. Paravantis, M. Santamouris, C. Cartalis, C. Efthymiou, N. Kontoulis, "Mortality Associated with High Ambient Temperatures, Heatwaves, and the Urban Heat Island in Athens, Greece." *Sustainability*, vol. 9(4), 606, doi: doi.org/10.3390/su9040606.

[90] H. Akbari, R. Levinson, and L. Rainer, "Monitoring the energy-use effects of cool roofs on California commercial buildings," *Energy and Buildings*, vol. 37, no. 10, 2005, doi: 10.1016/j.enbuild.2004.11.013.

[91] C. Romeo and M. Zinzi, "Impact of a cool roof application on the energy and comfort performance in an existing non-residential building. A Sicilian case study," *Energy and Buildings*, vol. 67, pp. 647–657, 2013, doi: 10.1016/j.enbuild.2011.07.023.

[92] A. Synnefa, M. Santamouris, and H. Akbari, "Estimating the effect of using cool coatings on energy loads and thermal comfort in residential buildings in various climatic conditions," *Energy and Buildings*, vol. 39, no. 11, 2007, doi: 10.1016/j.enbuild.2007.01.004.

[93] H. Akbari, S. Menon, and A. Rosenfeld, "Global cooling: Increasing world-wide urban

albedos to offset CO 2," *Climatic Change*, vol. 94, no. 3–4, pp. 275–286, 2009, doi: 10.1007/s10584-008-9515-9.

[94] H. Akbari and H. D. Matthews, "Global cooling updates : Reflective roofs and pavements," *Energy & Buildings*, vol. 55, pp. 2–6, 2012, doi: 10.1016/j.enbuild.2012.02.055.

[95] R. Paolini *et al.*, "Effects of soiling and weathering on the albedo of building envelope materials: Lessons learned from natural exposure in two European cities and tuning of a laboratory simulation practice," *Solar Energy Materials and Solar Cells*, vol. 205, no. September 2019, p. 110264, 2020, doi: 10.1016/j.solmat.2019.110264.

[96] R. Levinson, H. Akbari, S. Konopacki, and S. Bretz, "Inclusion of cool roofs in nonresidential Title 24 prescriptive requirements," *Energy Policy*, vol. 33, no. 2, 2005, doi: 10.1016/S0301-4215(03)00206-4.

[97] M. Sleiman *et al.*, "Soiling of building envelope surfaces and its effect on solar reflectance - Part I: Analysis of roofing product databases," *Solar Energy Materials and Solar Cells*, vol. 95, no. 12, pp. 3385–3399, 2011, doi: 10.1016/j.solmat.2011.08.002.

[98] P. Munafò, G. B. Goffredo, and E. Quagliarini, "TiO2-based nanocoatings for preserving architectural stone surfaces: An overview," *Construction and Building Materials*, vol. 84, pp. 201–218, 2015, doi: 10.1016/j.conbuildmat.2015.02.083.

[99] Z. Zhang *et al.*, "Biofouling resistance of titanium dioxide and zinc oxide nanoparticulate silane/siloxane exterior facade treatments," *Building and Environment*, vol. 59, pp. 47–55, 2013, doi: 10.1016/j.buildenv.2012.08.006.

[100] O. F. T. H. E. Council, "Regulation (EU) No 524/2013 of the European Parliament and of the Council," *Fundamental Texts On European Private Law*, pp. 1–123, 2020, doi: 10.5040/9781782258674.0009.

[101] D. Kolokotsa, C. Diakaki, S. Papantoniou, and A. Vlissidis, "Numerical and experimental analysis of cool roofs application on a laboratory building in Iraklion, Crete, Greece," *Energy and Buildings*, vol. 55, pp. 85–93, 2012, doi: 10.1016/j.enbuild.2011.09.011.

[102] R. Arreche and P. Vázquez, "Green biocides to control biodeterioration in materials science and the example of preserving World Heritage Monuments," *Current Opinion in Green and Sustainable Chemistry*, vol. 25, p. 100359, 2020, doi: 10.1016/j.cogsc.2020.100359.

[103] L. Graziani, E. Quagliarini, A. Osimani, L. Aquilanti, F. Clementi, and M. D'Orazio, "The influence of clay brick substratum on the inhibitory efficiency of TiO2 nanocoating against biofouling," *Building and Environment*, vol. 82, pp. 128–134, 2014, doi: 10.1016/j.buildenv.2014.08.013.

[104] M. R. Fidanza and G. Caneva, "Natural biocides for the conservation of stone cultural heritage: A review," *Journal of Cultural Heritage*, vol. 38, pp. 271–286, 2019, doi: 10.1016/j.culher.2019.01.005.

[105] M. D. Cheng, W. Miller, J. New, and P. Berdahl, "Understanding the long-term effects of environmental exposure on roof reflectance in California," *Construction and Building Materials*, vol. 26, no. 1, pp. 516–526, 2012, doi: 10.1016/j.conbuildmat.2011.06.052.

[106] M. D. Cheng *et al.*, "Surface reflectance degradation by microbial communities," *Journal of Building Physics*, vol. 40, no. 3, pp. 263–277, 2016, doi: 10.1177/1744259115611866.

[107] G. Beata, "The use of -omics tools for assessing biodeterioration of cultural heritage: A review," *Journal of Cultural Heritage*, vol. 45, pp. 351–361, 2020, doi: 10.1016/j.culher.2020.03.006.

[108] T. Dornieden, A. A. Gorbushina, and W. E. Krumbein, "Biodecay of cultural heritage as a

space/time-related ecological situation - An evaluation of a series of studies," *International Biodeterioration and Biodegradation*, vol. 46, no. 4, pp. 261–270, 2000, doi: 10.1016/S0964-8305(00)00107-4.

[109] X. Li, D. Liu, and J. Yao, "Aerosolization of fungal spores in indoor environments," *Science of The Total Environment*, vol. 820, p. 153003, 2022, doi: 10.1016/j.scitotenv.2022.153003.

[110] E. Cheek, V. Guercio, C. Shrubsole, and S. Dimitroulopoulou, "Portable air purification: Review of impacts on indoor air quality and health," *Science of the Total Environment*, vol. 766, p. 142585, 2021, doi: 10.1016/j.scitotenv.2020.142585.

[111] A. Nevalainen, M. Täubel, and A. Hyvärinen, "Indoor fungi: Companions and contaminants," *Indoor Air*, vol. 25, no. 2, pp. 125–156, 2015, doi: 10.1111/ina.12182.

[112] K. C. Dannemiller, J. F. Gent, B. P. Leaderer, and J. Peccia, "Influence of housing characteristics on bacterial and fungal communities in homes of asthmatic children," *Indoor Air*, vol. 26, no. 2, pp. 179–192, 2016, doi: 10.1111/ina.12205.

[113] A. Hoisington, J. P. Maestre, K. A. Kinney, and J. A. Siegel, "Characterizing the bacterial communities in retail stores in the United States," *Indoor Air*, vol. 26, no. 6, pp. 857–868, 2016, doi: 10.1111/ina.12273.

[114] R. I. Adams *et al.*, "Ten questions concerning the microbiomes of buildings," *Building and Environment*, vol. 109, pp. 224–234, 2016, doi: 10.1016/j.buildenv.2016.09.001.

[115] K. F. Nielsen, G. Holm, L. P. Uttrup, and P. A. Nielsen, "Mould growth on building materials under low water activities. Influence of humidity and temperature on fungal growth and secondary metabolism," *International Biodeterioration and Biodegradation*, vol. 54, no. 4, pp. 325–336, 2004, doi: 10.1016/j.ibiod.2004.05.002.

[116] A. M. Madsen, "Effects of Airflow and Changing Humidity on the Aerosolization of Respirable Fungal Fragments and Conidia of Botrytis cinerea," *Applied and Environmental Microbiology*, vol. 78, no. 11, pp. 3999–4007, 2012, doi: 10.1128/AEM.07879-11.

[117] R.A. Sharpe, N. Bearman, C.R. Thornton, K. Husk, N.J. Osborne "Indoor fungal diversity and asthma: a meta-analysis and systematic review of risk factors." *Journal of Allergy and Clinical Immunology*, vol. 135(1), pp. 110-22, 2015, doi: 10.1016/j.jaci.2014.07.002.

[118] N. M. Sham, N. I. Ahmad, M. A. Pahrol, and Y. H. Leong, "Fungus and mycotoxins studies in hospital environment: A scoping review," *Building and Environment*, vol. 193, no. November 2020, p. 107626, 2021, doi: 10.1016/j.buildenv.2021.107626.

[119] P. Krijgsheld *et al.*, "Development in aspergillus," *Studies in Mycology*, vol. 74, pp. 1–29, 2013, doi: 10.3114/sim0006.

[120] A. H. A. Awad *et al.*, "Indoor air fungal pollution of a historical museum, Egypt: a case study," *Aerobiologia*, vol. 36, no. 2, pp. 197–209, 2020, doi: 10.1007/s10453-019-09623-w.

[121] M. Sleiman *et al.*, "Soiling of building envelope surfaces and its effect on solar reflectance - Part III: Interlaboratory study of an accelerated aging method for roofing materials," *Solar Energy Materials and Solar Cells*, vol. 143, pp. 581–590, 2015, doi: 10.1016/j.solmat.2015.07.031.

[122] ANSI, "ANSI / CRRC S100 (2016) Standard Test Methods for Determining Radiative Properties of Materials," vol. 100, 2016.

[123] ASTM, "ASTM G7/G7M Standard Practice for Atmospheric Environmental Exposure Testing of Nonmetallic Materials," pp. 1–7, 1995, doi: 10.1520/G0007.

[124] A. D7897, "Standard Practice for Laboratory Soiling and Weathering of Roofing Materials to Simulate Effects of Natural Exposure on Solar Reflectance," pp. 1–11, 2019, doi: 10.1520/D7897-18.2.

[125] O. Favez, H. Cachier, A. Chabas, P. Ausset, and R. Lefevre, "Crossed optical and chemical evaluations of modern glass soiling in various European urban environments," *Atmospheric Environment*, vol. 40, no. 37, pp. 7192–7204, 2006, doi: 10.1016/j.atmosenv.2006.06.022.

[126] M.-D. D. Cheng, S. M. Pfiffner, W. A. Miller, and P. Berdahl, "Chemical and microbial effects of atmospheric particles on the performance of steep-slope roofing materials," *Building and Environment*, vol. 46, no. 5, pp. 999–1010, 2011, doi: http://dx.doi.org/10.1016/j.buildenv.2010.10.025.

[127] H. Takebayashi *et al.*, "Experimental examination of solar reflectance of high-reflectance paint in Japan with natural and accelerated aging," *Energy and Buildings*, vol. 114, pp. 173–179, 2016, doi: 10.1016/j.enbuild.2015.06.019.

[128] Dornelles, "Natural weathering of cool coatings and its effect on solar reflectance of roof surfaces." *Energy Procedia*, vol. 78, 1587 – 1592, 2015, doi: 10.1016/j.egypro.2015.11.216 .

[129] E. Mastrapostoli, M. Santamouris, D. Kolokotsa, P. Vassilis, D. Venieri, and K. Gompakis, "On the ageing of cool roofs: Measure of the optical degradation, chemical and biological analysis and assessment of the energy impact," *Energy and Buildings*, vol. 114, pp. 191–199, 2016, doi: 10.1016/j.enbuild.2015.05.030.

[130] A. L. Pisello, V. L. Castaldo, G. Pignatta, F. Cotana, and M. Santamouris, "Experimental in-lab and in-field analysis of waterproof membranes for cool roof application and urban heat island mitigation," *Energy and Buildings*, vol. 114, 2016, doi: 10.1016/j.enbuild.2015.05.026.

[131] S. Kültür and N. Türkeri, "Assessment of long term solar reflectance performance of roof coverings measured in laboratory and in field," *Building and Environment*, vol. 48, no. 1, pp. 164–172, 2012, doi: 10.1016/j.buildenv.2011.09.004.

[132] H. Barberousse, B. Ruot, C. Yéprémian, and G. Boulon, "An assessment of façade coatings against colonisation by aerial algae and cyanobacteria," *Building and Environment*, vol. 42, no. 7, pp. 2555–2561, 2007, doi: 10.1016/j.buildenv.2006.07.031.

[133] H. M. Künzel, M. Krus, C. Fitz, W. Hofbauer, C. Scherer, and K. Breuer, "Accelerated Test Procedure to Assess the Microbial Growth Resistance of Exterior Finishes," *12th International Conference on Durability of Building Materials and Components*, pp. 1–8, 2011, [Online]. Available: http://www.ibp.fraunhofer.de/content/dam/ibp/de/documents/Publikationen/Konferenzbeitraege/Englisch/Accelerated Test Procedure to Assess the Microbial Growth Resistance of Exterior Finishes.pdf.

[134] M. Avrami, "Kinetics of phase change. I: General theory," *The Journal of Chemical Physics*, vol. 7, no. 12, pp. 1103–1112, 1939, doi: 10.1063/1.1750380.

[135] M. Avrami, "Kinetics of phase change. II Transformation-time relations for random distribution of nuclei," *The Journal of Chemical Physics*, vol. 8, no. 2, pp. 212–224, 1940, doi: 10.1063/1.1750631.

[136] M. Avrami, "Granulation, phase change, and microstructure kinetics of phase change. III," *The Journal of Chemical Physics*, vol. 9, no. 2, pp. 177–184, 1941, doi: 10.1063/1.1750872.

[137] E. Quagliarini *et al.*, "Effect of temperature and relative humidity on algae biofouling on different fired brick surfaces," *Construction and Building Materials*, vol. 199, pp. 396–405, 2019, doi: 10.1016/j.conbuildmat.2018.12.023.

[138] T. H. Tran *et al.*, "Avrami's law based kinetic modeling of colonization of mortar surface by alga Klebsormidium flaccidum," *International Biodeterioration and Biodegradation*, vol. 79, pp. 73–80, 2013, doi: 10.1016/j.ibiod.2012.12.012.

[139] L. Graziani, E. Quagliarini, and M. D'Orazio, "TiO2-treated different fired brick surfaces for biofouling prevention: Experimental and modelling results," *Ceramics International*, vol. 42, no. 3, pp. 4002–4010, 2016, doi: 10.1016/j.ceramint.2015.11.069.

[140] L. Graziani, E. Quagliarini, and M. D'Orazio, "The role of roughness and porosity on the self-cleaning and anti-biofouling efficiency of TiO2-Cu and TiO2-Ag nanocoatings applied on fired bricks," *Construction and Building Materials*, vol. 129, pp. 116–124, 2016, doi: 10.1016/j.conbuildmat.2016.10.111.

[141] L. Graziani and E. Quagliarini, "On the modelling of algal biofouling growth on nano-TiO2 coated and uncoated limestones and sandstones," *Coatings*, vol. 8, no. 2, 2018, doi: 10.3390/coatings8020054.

[142] E. Quagliarini, L. Graziani, D. Diso, A. Licciulli, and M. D'Orazio, "Is nano-TiO2 alone an effective strategy for the maintenance of stones in Cultural Heritage?," *Journal of Cultural Heritage*, vol. 30, pp. 81–91, 2018, doi: 10.1016/j.culher.2017.09.016.

[143] M. Welander, J. Persson, H. Asp, and L. H. Zhu, "Scientia Horticulturae Evaluation of a new vessel system based on temporary immersion system for micropropagation," *Scientia Horticulturae*, vol. 179, pp. 227–232, 2014, doi: 10.1016/j.scienta.2014.09.035.

[144] J. K. Smith, J. D. Parry, J. G. Day, and R. J. Smith, "A PCR technique based on the Hip1 interspersed repetitive sequence distinguishes cyanabacterial species and strains," *Microbiology*, vol. 144, no. 10, pp. 2791–2801, 1998, doi: 10.1099/00221287-144-10-2791.

[145] F. Wilhem, *Anatomie, Physiologie und Systemkund*, vol. 3, no. 2. 1843.

[146] T. Darienko, L. Gustavs, and T. Pröschold, "Species concept and nomenclatural changes within the genera Elliptochloris and Pseudochlorella (Trebouxiophyceae) based on an integrative approach," *Journal of Phycology*, vol. 52, no. 6, pp. 1125–1145, 2016, doi: 10.1111/jpy.12481.

[147] P. C. Silva, K. R. Mattox, and W. H. Blackwell, "the Generic Name Hormidium As Applied To Green Algae," *Taxon*, vol. 21, no. 5–6, pp. 639–645, 1972, doi: 10.2307/1219167.

[148] Q. Li, B. Zhang, Z. He, and X. Yang, "Distribution and diversity of bacteria and fungi colonization in stone monuments analyzed by high-throughput sequencing," *PLoS ONE*, vol. 11, no. 9, pp. 1–17, 2016, doi: 10.1371/journal.pone.0163287.

[149] C. C. Gaylarde, "Influence of Environment on Microbial Colonization of Historic Stone Buildings with Emphasis on Cyanobacteria," *Heritage*, vol. 3, no. 4, pp. 1469–1482, 2020, doi: 10.3390/heritage3040081.

[150] C. A. Crispim, C. C. Gaylarde, and P. M. Gaylarde, "Biofilms on church walls in Porto Alegre, RS, Brazil, with special attention to cyanobacteria," *International Biodeterioration and Biodegradation*, vol. 54, no. 2–3, pp. 121–124, 2004, doi: 10.1016/j.ibiod.2004.03.001.

[151] G. Escadeillas, A. Bertron, P. Blanc, and A. Dubosc, "Accelerated testing of biological stain growth on external concrete walls. Part 1: Development of the growth tests," *Materials and Structures/Materiaux et Constructions*, vol. 40, no. 10, pp. 1061–1071, 2007, doi: 10.1617/s11527-006-9205-x.

[152] C. Kitzing and U. Karsten, "Effects of UV radiation on optimum quantum yield and sunscreen contents in members of the genera Interfilum, Klebsormidium, Hormidiella and Entransia (Klebsormidiophyceae, Streptophyta)," *European Journal of Phycology*, vol. 50, no. 3, pp. 279–287, 2015, doi: 10.1080/09670262.2015.1031190.

[153] M. Chioccioli, B. Hankamer, and I. L. Ross, "Flow cytometry pulse width data enables rapid and sensitive estimation of biomass dry weight in the microalgae Chlamydomonas

reinhardtii and Chlorella vulgaris," *PLoS ONE*, vol. 9, no. 5, pp. 1–12, 2014, doi: 10.1371/journal.pone.0097269.

[154] H. K. Lichtenthaler, "Chlorophylls and Carotenoids: Pigments of Photosynthetic Biomembranes," *Plant Cell Membranes*, vol. 148, pp. 350–382, 1987.

[155] M. Performance *et al.*, "Standard Test Method for Solar Absorptance , Reflectance , and Transmittance of Materials Using Integrating Spheres 1," vol. 03, pp. 1–9, 1996, doi: 10.1520/E0903-20.2.

[156] R. Levinson, H. Akbari, and P. Berdahl, "Measuring solar reflectance-Part II: Review of practical methods," *Solar Energy*, vol. 84, no. 9, 2010, doi: 10.1016/j.solener.2010.04.017.

[157] R. Levinson, H. Akbari, and P. Berdahl, "Measuring solar reflectance-Part I: Defining a metric that accurately predicts solar heat gain," *Solar Energy*, vol. 84, no. 9, 2010, doi: 10.1016/j.solener.2010.04.018.

[158] P. P. a I. Molding and E. Materials, Standard Classification System for," *Society*, vol. 06, no. Reapproved 1992, pp. 1–6, 1994.

[159] M. E. Callow *et al.*, "Microtopographic cues for settlement of zoospores of the green fouling alga Enteromorpha," *Biofouling*, vol. 18, no. 3, pp. 237–245, 2002, doi: 10.1080/08927010290014917.

[160] G. Escadeillas, A. Bertron, E. Ringot, P. J. Blanc, and A. Dubosc, "Accelerated testing of biological stain growth on external concrete walls. Part 2: Quantification of growths," *Materials and Structures/Materiaux et Constructions*, vol. 42, no. 7, pp. 937–945, 2009, doi: 10.1617/s11527-008-9433-3.

[161] U. N. I. EN 15976, "Determinazione dell'emissività," 2012.

[162] E177-04e1, "Standard Practice for Use of the Terms Precision and Bias in ASTM Test Methods," *ASTM Book of Standards*, pp. 1–9, 2016, doi: 10.1520/E0177-14.2.

[163] ISO, "Evaluation of measurement data — Guide to the expression of uncertainty in measurement," *International Organization for Standardization Geneva ISBN*, vol. 50, no. September, p. 134, 2008, [Online]. Available: http://www.bipm.org/en/publications/guides/gum.html.

[164] L. Håkanson, "The role of characteristic coefficients of variation in uncertainty and sensitivity analyses, with examples related to the structuring of lake eutrophication models," *Ecological Modelling*, vol. 131, no. 1, pp. 1–20, 2000, doi: 10.1016/S0304-3800(00)00219-2.

[165] M. A. Borowitzka, *Biology of microalgae*, no. 1998. Elsevier Inc., 2018.

[166] F. Khajepour, S. A. Hosseini, R. Ghorbani Nasrabadi, and G. Markou, "Effect of Light Intensity and Photoperiod on Growth and Biochemical Composition of a Local Isolate of Nostoc calcicola," *Applied Biochemistry and Biotechnology*, vol. 176, no. 8, pp. 2279–2289, 2015, doi: 10.1007/s12010-015-1717-9.

[167] W. D. J. Kaewmaneesuk, C. Ariyadet, M. Thirabunyanon, S. Jaturonglumlert, "Influence Of Led Red-Light Intensity On Phycocyanin Accumulation In The Cyanobacterium Nostoc Commune Vaucher," *Journal of Fundamental and Applied Sciences*, vol. 4, no. 1, pp. 9–10, 2018, [Online]. Available: http://dx.doi.org/10.4314/jfas.v10i1s.7.

[168] Y. Nuhoglu *et al.*, "The accelerating effects of the microorganisms on biodeterioration of stone monuments under air pollution and continental-cold climatic conditions in Erzurum, Turkey," *Science of the Total Environment*, vol. 364, no. 1–3, pp. 272–283, 2006, doi: 10.1016/j.scitotenv.2005.06.034.

[169] G. Muhetaer *et al.*, "Effects of light intensity and exposure period on the growth and stress responses of two cyanobacteria species: Pseudanabaena galeata and Microcystis aeruginosa," *Water (Switzerland)*, vol. 12, no. 2, 2020, doi: 10.3390/w12020407.

[170] R. Singh, A. K. Upadhyay, D. V. Singh, J. S. Singh, and D. P. Singh, "Photosynthetic performance, nutrient status and lipid yield of microalgae Chlorella vulgaris and Chlorococcum humicola under UV-B exposure," *Current Research in Biotechnology*, vol. 1, pp. 65–77, 2019, doi: 10.1016/j.crbiot.2019.10.001.

[171] M. Ehling-Schulz, W. Bilger, and S. Scherer, "UV-B-induced synthesis of photoprotective pigments and extracellular polysaccharides in the terrestrial cyanobacterium Nostoc commune," *Journal of Bacteriology*, vol. 179, no. 6, pp. 1940–1945, 1997, doi: 10.1128/jb.179.6.1940-1945.1997.

[172] C. Paliwal *et al.*, "Abiotic stresses as tools for metabolites in microalgae," *Bioresource Technology*, vol. 244, pp. 1216–1226, 2017, doi: 10.1016/j.biortech.2017.05.058.

[173] M. R. Gauthier, G. N. A. Senhorinho, and J. A. Scott, "Microalgae under environmental stress as a source of antioxidants," *Algal Research*, vol. 52, no. March, p. 102104, 2020, doi: 10.1016/j.algal.2020.102104.

[174] R. Paolini, M. Zinzi, T. Poli, E. Carnielo, and A. G. Mainini, "Effect of ageing on solar spectral reflectance of roofing membranes: Natural exposure in Roma and Milano and the impact on the energy needs of commercial buildings," *Energy and Buildings*, vol. 84, pp. 333–343, 2014, doi: 10.1016/j.enbuild.2014.08.008.

[175] M. A. Shirakawa, K. Loh, V. M. John, M. E. S. Silva, and C. C. Gaylarde, "Biodeterioration of painted mortar surfaces in tropical urban and coastal situations: Comparison of four paint formulations," *International Biodeterioration and Biodegradation*, vol. 65, no. 5, pp. 669–674, 2011, doi: 10.1016/j.ibiod.2011.03.004.

[176] M. D. Orazio, "NZEB e il Degrado Biologico Delle Superfici,"CIL, pp. 50–54, 2018.

[177] P. pei Han *et al.*, "Proteomic profiling of Nostoc flagelliforme reveals the common mechanism in promoting polysaccharide production by different light qualities," *Biochemical Engineering Journal*, vol. 132, pp. 68–78, 2018, doi: 10.1016/j.bej.2017.12.006.

[178] S. P. Singh and P. Singh, "Effect of temperature and light on the growth of algae species: A review," *Renewable and Sustainable Energy Reviews*, vol. 50, pp. 431–444, 2015, doi: 10.1016/j.rser.2015.05.024.

[179] E. Gallego-Cartagena *et al.*, "A comprehensive study of biofilms growing on the built heritage of a Caribbean industrial city in correlation with construction materials," *International Biodeterioration and Biodegradation*, vol. 147, no. August 2019, p. 104874, 2020, doi: 10.1016/j.ibiod.2019.104874.

[180] H. A. Viles and A. A. Gorbushina, "Soiling and microbial colonisation on urban roadside limestone: A three year study in Oxford, England," *Building and Environment*, vol. 38, no. 9–10, pp. 1217–1224, 2003, doi: 10.1016/S0360-1323(03)00078-7.

[181] D. Giovannacci *et al.*, "Algal colonization kinetics on roofing and façade tiles: Influence of physical parameters," *Construction and Building Materials*, vol. 48, pp. 670–676, 2013, doi: 10.1016/j.conbuildmat.2013.07.034.

[182] R. Schumann, N. Häubner, S. Klausch, and U. Karsten, "Chlorophyll extraction methods for the quantification of green microalgae colonizing building facades," *International Biodeterioration and Biodegradation*, vol. 55, no. 3, pp. 213–222, 2005, doi: 10.1016/j.ibiod.2004.12.002.

[183] "Microalgal culture," *Biotechnology and applied phycology*, 2004.

[184] A. Maadane *et al.*, "Antioxidant activity of some Moroccan marine microalgae: Pufa profiles, carotenoids and phenolic content," *Journal of Biotechnology*, vol. 215, pp. 13–19, 2015, doi: 10.1016/j.jbiotec.2015.06.400.

[185] F. Jia, M. Kacira, and K. L. Ogden, "Multi-wavelength based optical density sensor for autonomous monitoring of microalgae," *Sensors (Switzerland)*, vol. 15, no. 9, pp. 22234–22248, 2015, doi: 10.3390/s150922234.

[186] J. D. Gu, "Microbial biofilms, fouling, corrosion, and biodeterioration of materials," *Handbook of Environmental Degradation Of Materials: Third Edition*, pp. 273–298, 2018, doi: 10.1016/B978-0-323-52472-8.00014-9.

[187] H. Akbari, R. Levinson, and S. Stern, "Procedure for measuring the solar reflectance of flat or curved roofing assemblies," *Solar Energy*, vol. 82, no. 7, 2008, doi: 10.1016/j.solener.2008.01.001.

[188] R. Paolini, T. Poli, M. Zinzi, A. G. Mainini, A. Speroni, and A. Zani, "Invecchiamento e sporcamento di cool materials : esposizione naturale e accelerata."

[189] M. Owczarek-Kościelniak, B. Krzewicka, J. Piątek, Ł. M. Kołodziejczyk, and P. Kapusta, "Is there a link between the biological colonization of the gravestone and its deterioration?," *International Biodeterioration and Biodegradation*, vol. 148, no. December 2019, 2020, doi: 10.1016/j.ibiod.2019.104879.

[190] Brown, "Airborne Algae:," vol. 264, no. 1949, pp. 583–585, 1963.

[191] R. Stancheva *et al.*, "Phylogenetic position of Zygogonium ericetorum (Zygnematophyceae, Charophyta) from a high alpine habitat and ultrastructural characterization of unusual aplanospores," *Journal of Phycology*, vol. 50, no. 5, pp. 790–803, 2014, doi: 10.1111/jpy.12229.

[192] F. Rindi, M. D. Guiry, and J. M. López-Bautista, "Distribution, morphology, and phylogeny of Klebsormidium (Klebsormidiales, Charophyceae) in urban environments in Europe," *Journal of Phycology*, vol. 44, no. 6, pp. 1529–1540, 2008, doi: 10.1111/j.1529-8817.2008.00593.x.

[193] F. Rindi and M. D. Guiry, "Composition and distribution of subaerial algal assemblages in Galway City, western Ireland," *Cryptogamie, Algologie*, vol. 24, no. 3, pp. 245–267, 2003.

[194] A. Miller, A. Dionísio, and M. F. Macedo, "Primary bioreceptivity: A comparative study of different Portuguese lithotypes," *International Biodeterioration and Biodegradation*, vol. 57, no. 2, pp. 136–142, 2006, doi: 10.1016/j.ibiod.2006.01.003.

[195] M. Thornbush and H. Viles, "Changing patterns of soiling and microbial growth on building stone in Oxford, England after implementation of a major traffic scheme," *Science of the Total Environment*, vol. 367, no. 1, pp. 203–211, 2006, doi: 10.1016/j.scitotenv.2005.11.022.

[196] B. Moroni, L. Pitzurra, and G. Poli, "Microbial growth and air pollutants in the corrosion of carbonate building stone: Results of laboratory and outdoor experimental tests," *Environmental Geology*, vol. 46, no. 3–4, pp. 436–447, 2004, doi: 10.1007/s00254-004-1045-9.

[197] C. Ferrari, G. Santunione, A. Libbra, A. Muscio, and E. Sgarbi, "How accelerated biological aging can affect solar reflective polymeric based building materials," *Journal of Physics: Conference Series*, vol. 923, no. 1, 2017, doi: 10.1088/1742-6596/923/1/012046.

[198] C. M. Grossi, R. M. Esbert, F. Díaz-Pache, and F. J. Alonso, "Soiling of building stones in urban environments," *Building and Environment*, vol. 38, no. 1, pp. 147–159, 2003, doi: 10.1016/S0360-1323(02)00017-3.

[199] L. Pitzurra, B. Moroni, A. Nocentini, G. Sbaraglia, G. Poli, and F. Bistoni, "Microbial growth and air pollution in carbonate rock weathering," *International Biodeterioration and*

Biodegradation, vol. 52, no. 2, pp. 63–68, 2003, doi: 10.1016/S0964-8305(02)00175-0.

[200] C. Guo, S. Lv, Y. Liu, and Y. Li, "Biomarkers for the adverse effects on respiratory system health associated with atmospheric particulate matter exposure," *Journal of Hazardous Materials*, vol. 421, no. July 2021, p. 126760, 2022, doi: 10.1016/j.jhazmat.2021.126760.

[201] A. Holzinger and M. Pichrtová, "Abiotic stress tolerance of charophyte green algae: New challenges for omics techniques," *Frontiers in Plant Science*, vol. 7, no. MAY2016, pp. 1–17, 2016, doi: 10.3389/fpls.2016.00678.

[202] M. Kumar and P. Ralph, "Systems biology of marine ecosystems," *Systems Biology of Marine Ecosystems*, pp. 1–351, 2017, doi: 10.1007/978-3-319-62094-7.

[203] K. Goiris, K. Muylaert, I. Fraeye, I. Foubert, J. De Brabanter, and L. De Cooman, "Antioxidant potential of microalgae in relation to their phenolic and carotenoid content," *Journal of Applied Phycology*, vol. 24, no. 6, pp. 1477–1486, 2012, doi: 10.1007/s10811-012-9804-6.

[204] T. Lu *et al.*, "Evaluation of the toxic response induced by azoxystrobin in the non-target green alga Chlorella pyrenoidosa," *Environmental Pollution*, vol. 234, pp. 379–388, 2018, doi: 10.1016/j.envpol.2017.11.081.

[205] A. Udayan, M. Arumugam, and A. Pandey, "Nutraceuticals From Algae and Cyanobacteria," *Algal Green Chemistry: Recent Progress in Biotechnology*, pp. 65–89, 2017, doi: 10.1016/B978-0-444-63784-0.00004-7.

[206] D. M. Hodges, J. M. DeLong, C. F. Forney, and R. K. Prange, "Improving the thiobarbituric acid-reactive-substances assay for estimating lipid peroxidation in plant tissues containing anthocyanin and other interfering compounds," *Planta*, vol. 207, no. 4, pp. 604–611, 1999, doi: 10.1007/s004250050524.

[207] R. L. Heath and L. Packer, "Photoperoxidation in isolated chloroplasts," *Archives of Biochemistry and Biophysics*, vol. 125, no. 1, pp. 189–198, 1968, doi: 10.1016/0003-9861(68)90654-1.

[208] M. Axelsson and F. Gentili, "A single-step method for rapid extraction of total lipids from green microalgae," *PLoS ONE*, vol. 9, no. 2, pp. 17–20, 2014, doi: 10.1371/journal.pone.0089643.

[209] M. Altunoz, G. Montevecchi, F. Masino, L. Zanasi, and A. Antonelli, "Biodiesel properties of Neochloris oleoabundans grown in sludge waste," *Cleaner Engineering and Technology*, vol. 5, 2021, doi: 10.1016/j.clet.2021.100295.

[210] J. Hadj Saadoun *et al.*, "Lipid profile and growth of black soldier flies (Hermetia illucens, Stratiomyidae) reared on by-products from different food chains," *Journal of the Science of Food and Agriculture*, vol. 100, no. 9, pp. 3648–3657, 2020, doi: 10.1002/jsfa.10397.

[211] F. Masino, A. Ulrici, and A. Antonelli, "Extraction and quantification of main pigments in pesto sauces," *European Food Research and Technology*, vol. 226, no. 3, pp. 569–575, 2008, doi: 10.1007/s00217-007-0572-5.

[212] A. S. Fernandes, F. C. Petry, A. Z. Mercadante, E. Jacob-Lopes, and L. Q. Zepka, "HPLC-PDA-MS/MS as a strategy to characterize and quantify natural pigments from microalgae," *Current Research in Food Science*, vol. 3, pp. 100–112, 2020, doi: 10.1016/j.crfs.2020.03.009.

[213] C. Niemi, S. Lage, and F. G. Gentili, "Comparisons of analysis of fatty acid methyl ester (FAME) of microalgae by chromatographic techniques," *Algal Research*, vol. 39, no. November 2018, p. 101449, 2019, doi: 10.1016/j.algal.2019.101449.

[214] Q. Béchet, A. Shilton, and B. Guieysse, "Modeling the effects of light and temperature on

algae growth: State of the art and critical assessment for productivity prediction during outdoor cultivation," *Biotechnology Advances*, vol. 31, no. 8, pp. 1648–1663, 2013, doi: 10.1016/j.biotechadv.2013.08.014.

[215] L. Wang *et al.*, "Analysis of algae growth mechanism and water bloom prediction under the effect of multi-affecting factor," *Saudi Journal of Biological Sciences*, vol. 24, no. 3, pp. 556–562, 2017, doi: 10.1016/j.sjbs.2017.01.026.

[216] A. Arnold, "An Assessment of the Asphalt Shingle Roofing Process for Residential Buildings," *Procedia Engineering*, vol. 145, pp. 760–765, 2016, doi: 10.1016/j.proeng.2016.04.099.

[217] E. Quagliarini, F. Bondioli, G. B. Goffredo, A. Licciulli, and P. Munafò, "Self-cleaning materials on Architectural Heritage: Compatibility of photo-induced hydrophilicity of TiO2 coatings on stone surfaces," *Journal of Cultural Heritage*, vol. 14, no. 1, pp. 1–7, 2013, doi: 10.1016/j.culher.2012.02.006.

[218] R. Zarzuela, M. Carbú, M. L. A. Gil, J. M. Cantoral, and M. J. Mosquera, "Ormosils loaded with SiO2 nanoparticles functionalized with Ag as multifunctional superhydrophobic/biocidal/consolidant treatments for buildings conservation," *Nanotechnology*, vol. 30, no. 34, 2019, doi: 10.1088/1361-6528/ab1ff0.

[219] L. K. Herrera and H. A. Videla, "The importance of atmospheric effects on biodeterioration of cultural heritage constructional materials," *International Biodeterioration and Biodegradation*, vol. 54, no. 2–3, pp. 125–134, 2004, doi: 10.1016/j.ibiod.2004.06.002.

[220] R. Paolini, A. Zani, T. Poli, F. Antretter, and M. Zinzi, "Natural aging of cool walls: Impact on solar reflectance, sensitivity to thermal shocks and building energy needs," *Energy and Buildings*, vol. 153, pp. 287–296, 2017, doi: 10.1016/j.enbuild.2017.08.017.

[221] D. Roodvoets, W. Miller, and A.O. Desjarlais, "Long term reflective performance of roof membranes," *Proceedings of the 19th*, no. January 2004, 2004, [Online]. Available: http://www.kuleuven.ac.be/bwf/projects/annex41/protected/data/ORNL May 2004 Paper A41-T3-US-04-3.pdf.

[222] M. Kottek, J. Grieser, C. Beck, B. Rudolf, and F. Rubel, "World map of the Köppen-Geiger climate classification updated," *Meteorologische Zeitschrift*, vol. 15, no. 3, pp. 259–263, 2006, doi: 10.1127/0941-2948/2006/0130.

[223] M. Boccolari, "2013_Boccolari_Changes in temperature and precipitation extremes observed inModena, Italy.pdf." 2013.

[224] M. Boccolari, P. Frontero, and L. Lombroso, "CLIMATE OF MODENA (ITALY):," no. December 2014, 1998.

[225] T. D. Mitchell, T. R. Carter, P. D. Jones, M. Hulme, and M. New, "A comprehensive set of high-resolution grids of monthly climate for Europe and the globe : the observed record (1901-2000) and 16 scenarios (2001-2100)." *Geography*, vol. 55, no. July, p. 30, 2004, [Online]. Available: http://www.ipcc-data.org/docs/tyndall_working_papers_wp55.pdf.

[226] V. Wiktor, F. De Leo, C. Urzì, R. Guyonnet, P. Grosseau, and E. Garcia-Diaz, "Accelerated laboratory test to study fungal biodeterioration of cementitious matrix," *International Biodeterioration and Biodegradation*, vol. 63, no. 8, pp. 1061–1065, 2009, doi: 10.1016/j.ibiod.2009.09.004.

[227] F. Gladis and R. Schumann, "Influence of material properties and photocatalysis on phototrophic growth in multi-year roof weathering," *International Biodeterioration and Biodegradation*, vol. 65, no. 1. pp. 36–44, 2011, doi: 10.1016/j.ibiod.2010.05.014.

[228] B. Ji, W. Zhang, N. Zhang, J. Wang, G. A. Lutzu, and T. Liu, "Biofilm cultivation of the oleaginous microalgae Pseudochlorococcum sp.," *Bioprocess and Biosystems Engineering*, vol. 37, no. 7, pp. 1369–1375, 2014, doi: 10.1007/s00449-013-1109-x.

[229] S. F. Li, A. Fanesi, T. Martin, and F. Lopes, "Biomass production and physiology of Chlorella vulgaris during the early stages of immobilized state are affected by light intensity and inoculum cell density," *Algal Research*, vol. 59, no. August, p. 102453, 2021, doi: 10.1016/j.algal.2021.102453.

[230] B. Prieto, D. Vázquez-Nion, E. Fuentes, and A. G. Durán-Román, "Response of subaerial biofilms growing on stone-built cultural heritage to changing water regime and CO2 conditions," *International Biodeterioration and Biodegradation*, vol. 148, no. December 2019, p. 104882, 2020, doi: 10.1016/j.ibiod.2019.104882.

[231] P. Sanmartín, F. Villa, F. Cappitelli, S. Balboa, and R. Carballeira, "Characterization of a biofilm and the pattern outlined by its growth on a granite-built cloister in the Monastery of San Martiño Pinario (Santiago de Compostela, NW Spain)," *International Biodeterioration and Biodegradation*, vol. 147, no. December 2019, p. 104871, 2020, doi: 10.1016/j.ibiod.2019.104871.